SEQUENCED COPOLYMERS WITH CONTROLLED MOLECULAR WEIGHTS PREPARED VIA ENTROPY-DRIVEN RING-OPENING METATHESIS POLYMERIZATION

by

Amy Lynn Short

B.S. Xavier University, 2008

M.S. University of Pittsburgh, 2014

Submitted to the Graduate Faculty of the

Kenneth P. Dietrich School of Arts and Sciences in partial fulfillment

of the requirements for the degree of

Doctor of Philosophy

University of Pittsburgh

2016

UNIVERSITY OF PITTSBURGH

Dietrich School of Arts and Sciences

This dissertation was presented

by

Amy Lynn Short

It was defended on

May 27, 2016

and approved by

Dennis P. Curran, Distinguished Service Professor of Chemistry and Bayer Professor, Department of Chemistry

Barry Gold, Professor and Department of Pharmaceutical Sciences Chair, Co-director of the Drug Discovery Institute

W. Seth Horne, Assistant Professor, Department of Chemistry

Dissertation Advisor: Tara Y. Meyer, Associate Professor, Department of Chemistry and McGowan Center for Regenerative Medicine

SEQUENCED COPOLYMERS WITH CONTROLLED MOLECULAR WEIGHTS PREPARED VIA ENTROPY-DRIVEN RING-OPENING METATHESIS POLYMERIZATION

Amy Lynn Short, Ph.D.

University of Pittsburgh, 2016

A segmer-based approach towards monomer synthesis was successfully carried out to produce a series of linear α,ω-diolefinic species with varying linker lengths. Ring-closing metathesis (RCM) using a *cis*-selective ruthenium catalyst yielded a large strainless macrocycle that then underwent entropy-driven ring-opening metathesis polymerization (ED-ROMP). When compared to the same polymerization carried out with the complementary *trans*-monomer, the ED-ROMP of *cis*-monomer demonstrated a significantly higher degree of molecular weight control. The narrow dispersity exhibited by this process suggests that a new regime of selectivity enhanced ED-ROMP (SEED-ROMP) has been achieved. Reaction kinetics for this process were probed and the process was compared to alternative polymerization methods. Finally, the high degree of control was exemplified in a series of chain extension and block copolymerization experiments. Ultimately, SEED-ROMP represents a novel method to obtain well-defined copolymers of precise molecular weights.

TABLE OF CONTENTS

LIST OF TABLES

LIST OF FIGURES

LIST OF SCHEMES

LIST OF ABBREVIATIONS

A	Acrylic acid subunit
Ac	Acyl
AcOH	Acetic acid
ACS	Accelerated Cell Senescence
ADMET	Acyclic diene metathesis
B	Butenoic acid subunit
Bn	Benzyl
CH_2Cl_2	Dichloromethane
CDP	Cyclodepolymerization
Đ	Polydispersity index, PDI
DCC	*N,N′*-dicyclohexylcarbodiimide
DCE	1,2-Dichloroethane
DED-ROMP	Deactivation entropy-driven ring-opening metathesis polymerization
DIC	*N,N′*-Diisopropylcarbodiimide
DIPEA	*N,N′*-Diisoprophylethylamine, Hünig's base
DMSO	Dimethyl sulfoxide
DP	Degree of polymerization
DPTS	4-(dimethylamino)pyridinium 4-toluenesulfonate
EI	Electron ionization
ED-ROMP	Entropy-driven ring-opening metathesis polymerization
Eg	Ethylene glycol
equiv	Equivalent
ESI	Electrospray ionization
Et	Ethyl
EtOAc	Ethyl acetate
EVE	Ethyl vinyl ether
FT	Fourier transform
G	Glycolic acid subunit
GPC	Gel permeation chromatography
h	Hour
IR	Infrared spectroscopy
L	Lactic acid subunit
M	Molar
MCO	Macrocyclic oligomers
MD	Molecular dynamics
Me	Methyl

mL	Milliliter
M_n	Number average molecular weight
MS	Mass spectroscopy
M_w	Weight average molecular weight
Mol	Mole
NEt_3	Triethylamine
NHC	*N*-heterocyclic carbene
NMR	Nuclear magnetic resonance
P	Pentenoic acid subunit
PDI	Polydispersity index, Đ
PEG	Polyethylene glycol
Ph	Phenyl
PS	Polystyrene
RCM	Ring-closing metathesis
ROMP	Ring-opening metathesis polymerization
ROP	Ring-opening polymerization
rt	Room temperature
SAP	Segmer assembly polymerization
sec	Second
SEC	Size exclusion chromatography
segmer	Sequenced oligomer
Si	Silyl protecting group (TBS or TBDPS)
TASF	Tris-(dimethylamino)sulfonium difluorotrimethylsilicate
TBAF	tetrabutylammonium fluoride
TBS	*tert*-Butyl dimethylsilyl
TBDPS	*tert*-Butyl dimethylsilyl
T_g	Glass transition temperature
THF	Tetrahydrofuran

ACKNOWLEDGEMENTS

I would like to extend my sincere appreciation to the many people that have inspired and encouraged me along my journey. First and foremost, I would like to thank Professor Tara Meyer for providing me with the opportunity to work in her laboratory. I am incredibly grateful for her training, critiques, encouragement, stimulating conversation and honesty. To my other educators – my Bethany teachers and my high school chemistry teacher Adele Salerno – who gave me direction and helped me to find my place in the world. To Rick Mullins, especially, for his ongoing support of an absentminded undergrad that started out with a 39% and ended up with straight A's and a PhD. Xavier is very lucky to have you around. To Professors Kaz Koide and Billy Day, for the time they invested and the constructive feedback that helped me to improve during my time at Pitt. To my various committee members Kay Brummond, Seth Horne, Kabirul Islam, Steve Weber and especially Barry Gold and Dennis Curran, who both made significant efforts to help me obtain my Masters degree and transition smoothly into my PhD project. To all of my past and current lab members that I have had the privilege of working with: Ryan, Jeff, Shaopeng, Mike, Jamie, Colin, Jordan, Emily, Dan, Sara, Prema, Lee, Jielu, Austin, Yuta, Tim, Kate, John, Sami, Yanping, Basu, Yang, Shin, Mike, Evan, Dandan, Xiaoge, Fengling, Michael and Leke.

To the Lovelies and to all my friends, who are really good sports when I start talking about science things. You have all helped me to maintain my sanity and my perspective over the

past few years and have always been willing to lend a hand when I have needed it the most! We may not be related, but we might as well be. I'd also like to acknowledge some of the others who have been great company these past few years: Vonnegut, García Márquez, Austen, Tolkien, Kay, Calvino, Hobb, Eco, Sedaris, Adams, Bryson, Le Guin, Clavell, Doyle, Pratchett, Gaiman, Russell, McMurtry, Haldeman, Atwood, Herbert, Cornwell, Erikson, Martin, Sanderson, Abercrombie, Lynch, Miéville, Stephenson, and Plascencia. *The road goes ever on and on…*

To my family, who have loved me unconditionally along the way, even though it has taken so long for me to get here. To Julie, who taught me early on to stand up for myself and for whom I have so much love. To Jack, who, like me, loves challenges that can be solved through excessive tinkering. We are all so lucky to have you in our lives. To Callie, Andrew, Karen and Brian, and to all of the Fisher-Short clan who have accepted me without question as one of the family. You are the greatest in-laws that a person could ask for! An especially big thanks to Mom, who recognized early on that I marched to the beat (and time) of my own drum and gave me so much love. For all of the "why" questions she patiently answered. For all of the books she stayed up reading with me at bedtime. For the limitless phone hugs which can absolutely be felt if you just try hard enough. For always encouraging me and for being my champion even when things in her own life were challenging. I am who I am today because of you and I will never be able to thank you enough. Finally, I need to thank the supremely patient, ever supportive, effusively loving, tightly squeezing, hilariously dancing handsomeface of my life, Timothy. I'll love you 'til the day I die.

1.0 INTRODUCTION

1.1 SEQUENCED COPOLYMER SYNTHESIS

Monomer sequences contained within engineered and naturally occurring polymers impart unique physical and chemical properties to the bulk material. Biopolymers such as proteins, for example, have behaviors and morphologies wholly dependent on their constitutive amino acid sequences.[1-3] The profound complexity of naturally occurring biopolymers is difficult to reproduce synthetically, and as such, far fewer and less rigorous studies have been carried out on non-biological polymers.[4] One of our primary goals is to explore the interplay between sequence and properties using bioassimilable engineered materials. Ultimately, the results of this project and others in our research group have demonstrated unequivocally that control over monomer sequence is not only possible, but that it leads to polymers with properties that are predictable and customizable.

In this dissertation, we will begin first with an overview of the principles and limitations governing sequenced and living polymerization methods, focusing specifically on entropy-driven ring-opening metathesis polymerization (ED-ROMP). Next, we will describe the preparation of sequenced macrocyclic monomers containing either *cis*- or *trans*-internal olefins from α,ω-diolefin precursors. We will then discuss the development of a method to produce sequenced copolymers with defined molecular weights through ED-ROMP, selectivity enhanced ED-

ROMP (SEED-ROMP), and deactivation ED-ROMP (DED-ROMP). Specifically, molecular weights and dispersities of the polymers obtained through these methods will be investigated and compared. Finally, we will demonstrate the application of this method in the formation of block copolymers through a one-pot sequential ED-ROMP − ROMP protocol.

1.1.1 PLGA as an ideal system to explore, elaborate and optimize

Poly (lactic-*co*-glycolic acids) (PLGAs) are some of the most successfully implemented polymers for medicinal applications.[5,6] They typically are comprised of a random sequence of lactic (**L**) and glycolic (**G**) units that are bioassimilable upon hydrolytic degradation.[6-8] Relative amounts of **L** or **G** can be adjusted to improve stability or to tailor the polymer's physical properties for specific purposes. Applications of PLGAs are diverse and include FDA- and EMA-approved microparticle formulations and biomedical devices used for such purposes as drug delivery and stem cell scaffolding for regenerative medicine.[7,9-14] Scheduled degradation over short periods of time is useful in applications such as drug delivery. PLGAs that degrade over much longer periods of time are well suited to applications such as temporary implants and stem cell scaffolds. Importantly, very few options for scaffolding materials exist in regenerative medicine applications, and fewer afford the customization ability of sequenced PLGAs. Because lactic and glycolic acids are physiologically benign, there are innumerable opportunities for growth in this area of biomedical science.

1.1.2 Segmer-based approach used by Meyer group

Traditionally, PLGAs are synthesized through the condensation of lactic acid and glycolic acid or the ring-opening polymerization (ROP) of lactide and glycolide (Scheme 1A). Both of these methods result in a random assembly of **L** and **G** monomers and no degree of sequence control is observed. PLGA copolymers are fairly simple to obtain, but tradeoffs with regards to efficiency and versatility often need to be made when targeting higher levels of sequence fidelity.[4]

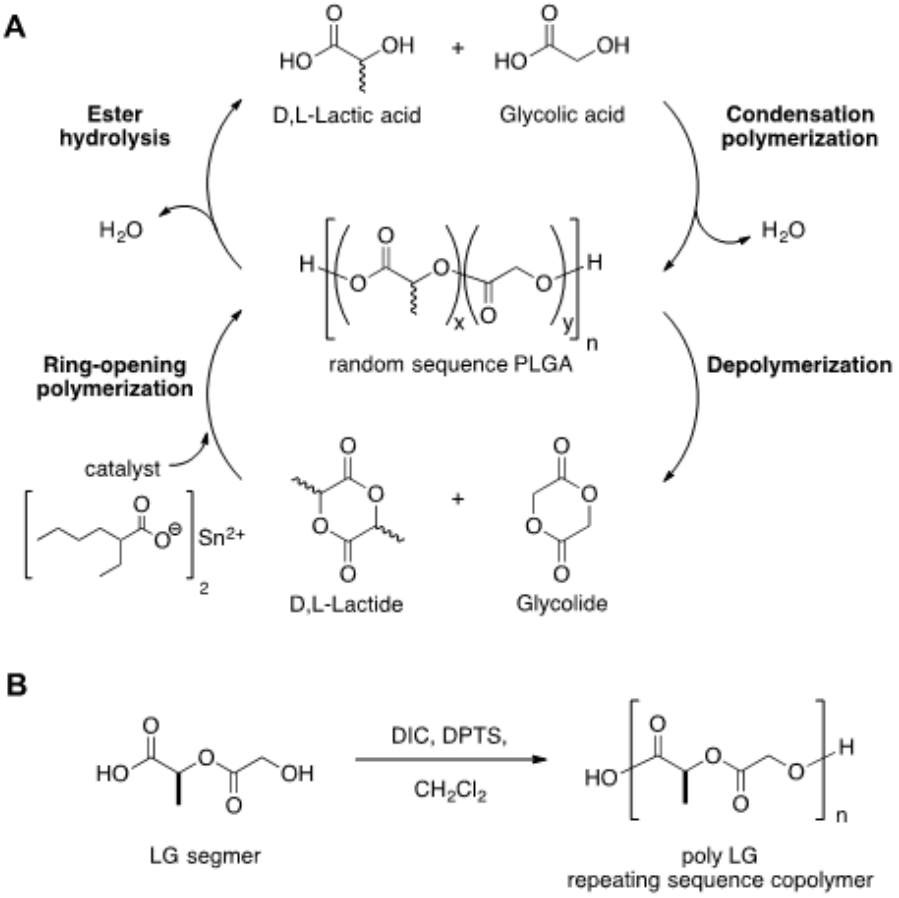

Scheme 1. A. Randomly sequenced PLGAs assembled through condensation or ring-opening polymerization; B. Repeating sequence copolymers constructed through SAP.

In recent years, our group has developed the Segmer Assembly Polymerization (SAP), an iterative and mild approach for producing polymers with tunable monomer sequences (Scheme 1B).[15-17] SAP improves on traditional methods by pre-assembling short templates of precisely sequenced **L** and **G** monomers. These sequenced oligomers, called segmers, can be comprised of any length or combination of **L** and **G** units. Syntheses of these segmers are straightforward and iterative, involving sequential deprotection and coupling until the desired segmer is obtained. Segmers can then be polymerized through a standard ester condensation protocol to yield repeating sequence copolymers with perfect stereocontrol for the **L**-components.

Traditional condensation polymerization and SAP can incorporate an incredible range of α-hydroxy acids beyond just **L** and **G**.[18] The resulting polymers will have wholly unique properties, as established by the ratios, sequences, and stereochemistry of their respective constituent monomers.. Although there is a synthetic tradeoff that is accepted in the production of segmers, SAP offers an unparalleled degree of sequence refinement that is otherwise unachievable through ROP methods (Figure 1). Using an orthogonal protecting group strategy, iterative deprotection and coupling steps are carried out until the desired unprotected segmer is obtained. This strategy can be used to obtain a large library of segmers combinations in a convergent manner. The segmer can then be subjected to condensation polymerization to yield a repeating sequence copolymer.

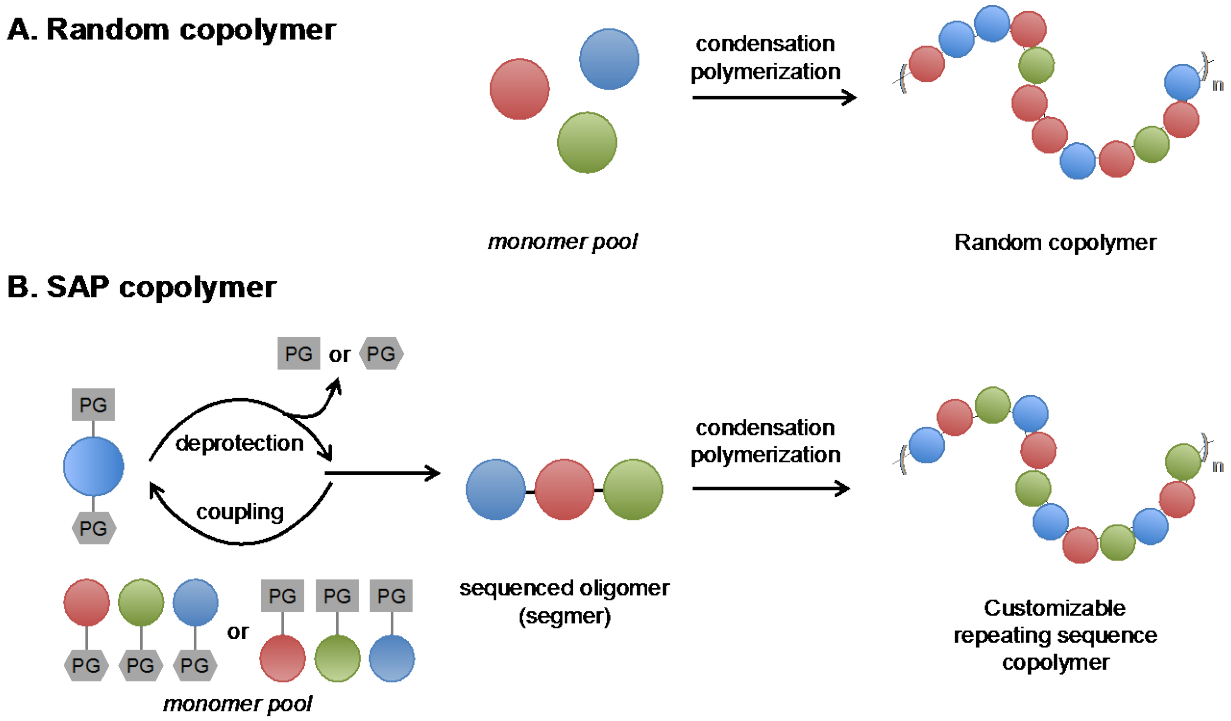

Figure 1. Comparison of traditional condensation polymerization (A) and SAP (B) as methods to obtain random or repeating sequence copolymers from a pool of α-hydroxy acids.

The diversity in method and monomer options gives rise to a naming convention whereby critical information about the polymerization method along with ratios and stereochemistry of monomers can be provided (i.e., **R-ROP-PLGA-75** refers to random ring-opening polymerization to form PL*L*GA with 75% stereopure **L***L* and 25% **G** content). In cases where the method is defined previously, emphasis on sequence fidelity can be made simply by naming the segmer used, as in **poly LG**, which describes a perfectly sequenced polymer of repeating **LG** segmers. Sequenced oligomers are named in order of C side to O side, as demonstrated in Scheme 1B.

In solution, sequenced PLGAs have microstructures that are highly dependent on sequence and stereochemistry, resulting in NMR spectra that are surprisingly well resolved and

differentiable. Although there are limitations to NMR analysis of PLGAs constructed through SAP, we have observed up to octad level spectral resolution corresponding to stereocenters 31 atoms apart.[17] Further evidence that SAP produces polymers without discernable sequence scrambling can be found by inspecting their MALDI spectra.[19] For instance, the masses of the chains present in **poly LG** correspond to incremental decreases of segmer mass (130 amu) and minor peaks corresponding to **L** (72 amu) or **G** (58 amu) loss (Figure 2).

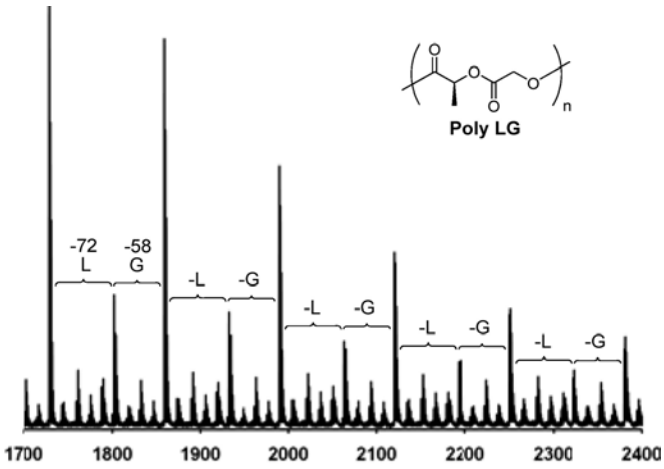

Figure 2. MALDI TOF analysis confirms the sequence fidelity of **poly LG** following SAP.
Image reprinted with permission from The American Chemical Society, Ref. 17, copyright 2010.

1.1.3 Influence of sequence on physical properties of polymers

Former group members Dr. Ryan Stayshich and Dr. Jian Li have recently demonstrated the unique ability to manipulate the hydrolytic susceptibility and degradation mechanism of sequenced PLGAs through adjustments to the monomer sequence.[15-17,20] In an exhaustive study currently underway, we are investigating further the complex interplay between monomer

sequence and physical attributes of PLGAs. Microparticle morphology and degradation properties in particular have been found to be incredibly dependent on the order and frequency of lactic and glycolic repeat units (Figure 3). By manipulating the sequence and stereopurity of PLGAs, the duration and mechanism of polymer degradation can be successfully customized.[20,21] Sequenced PLGAs are viable for bioengineering applications requiring a narrow but variable interval over which decomposition should occur.[15]

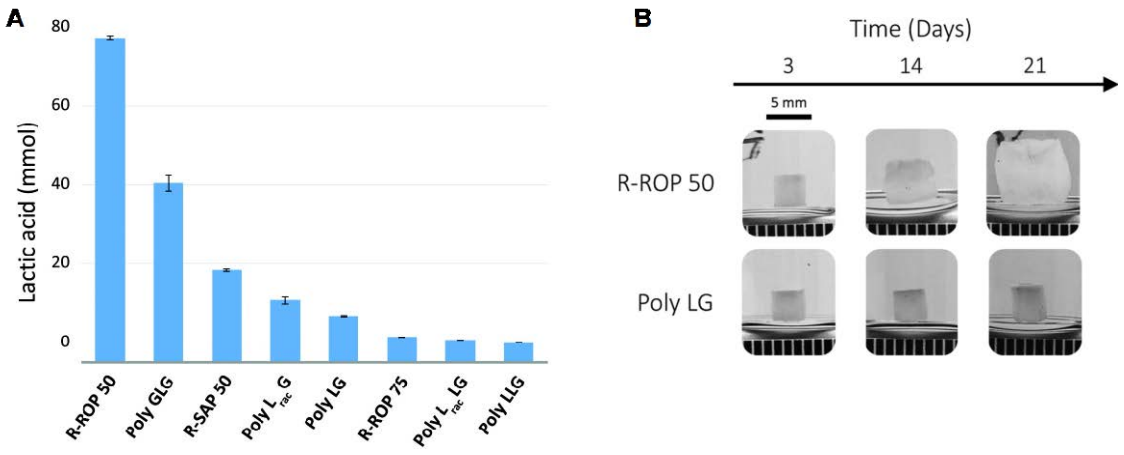

Figure 3. The influence of sequence on degradation (A) and swelling (B) of PLGAs.
Images reprinted with permission from The American Chemical Society, Ref. 20, copyright 2014.

The most significant conclusions from these physical properties studies thus far have been:

a) Racemic PLGAs degrade faster than stereopure PLGAs.

b) Random PLGAs degrade rapidly compared to sequenced PLGAs, which have more linear degradation rates.

c) Longer G-block lengths lead to faster degradation. Conversely, increased numbers of L-L linkages slow degradation.

d) The mechanism of structural failure for polymeric materials depends greatly on sequence.

These findings have been further demonstrated in ongoing studies focused on the structural features and mechanism of degradation (stereocomplex formation, lactic acid and drug release, swelling and erosion, two-photon and SEM visualization of pellet morphologies during decomposition) as well as the investigation of physical and mechanical properties (stress/strain and modulus, contact angle, fiber production via electrospinning).[15,16,19,21,22]

1.1.4 Limitations of SAP-condensation method to obtain sequenced PLGAs

The SAP method has been of great use in enabling access to custom sequence PLGAs, but suffers from lack of reproducibility with respect to polymer molecular weights. Typically, molecular weights (M_ns) for our SAP-produced PLGAs fall in the range of 20-40 kDa with dispersities (Đ) of 1.2-1.6, but an increased degree of control over molecular weight would make these materials much more robust for industrial and biological applications. Our group therefore set out to explore methods that would enable us to target particular molecular weights without sacrificing sequence control.

1.2 CONTROLLED POLYMERIZATIONS AND ENTROPY-DRIVEN RING-OPENING METATHESIS POLYMERIZATION

The ultimate goal of this research project was to improve our SAP method in order to obtain polymers with predetermined molecular weights and monodisperse molecular weight distributions. Use of an equilibrium-based polymerization such as ED-ROMP would eliminate the possibility of achieving a truly living polymerization. However, we hypothesized that a highly controlled polymerization would be possible through modulation of key reaction parameters.

Matyjaszewski defines controlled polymerization as one that exhibits characteristics of a living polymerization, but where nonproductive chain-breaking events like termination or secondary metathesis undoubtedly occur.[23-26] The occurrence of these chain-breaking processes is negligible compared to propagation and therefore does not significantly affect the outcome of the polymerization. Degree of "livingness" in these pseudo-ideal reactions is not only subjective but also can be misleading because factors such as chain lengthening often lead to further deviation. The most important characteristic of controlled polymerizations is the simultaneous growth of chains, leading to desirable features including:

A) Predictable molecular weights that are proportional to monomer conversion and tuned through adjustments of the monomer to initiator ratio.

B) Linear first-order kinetic behavior where the rate constant of chain propagation (k_{pr}) can be related to monomer concentration ([M]) as a function of time (t) such that:

$$k_{pr} = \frac{\ln\frac{[M]_0}{[M]_t}}{t} \qquad \text{(Equation 1)}$$

C) Poisson molecular weight distributions indicated by molecular weight dispersities (calculated by M_w/M_n) close to 1.

1.2.1 Principles governing the mechanism and outcomes of ROMP and ED-ROMP

ROMP is a powerful and versatile tool that harnesses the inherent reactivity of strained cyclic monomers. The mechanism for ruthenium-catalyzed olefin metathesis, originally proposed by Chauvin, begins with an initiation step in which a transition metal alkylidine coordinates to a cyclic olefin.[27-31] Subsequent [2+2]-cycloaddition yields a metallocyclobutane intermediate that can undergo cycloreversion and then elaboration through further propagation steps. Because the reactivity of the new chain end is similar to that of the initiating species, propagation continues until equilibrium is achieved or the reaction is terminated (Scheme 2). The driving force of ROMP is the enthalpic release of ring strain, although minor entropic penalties counteract this to a small degree.[32]

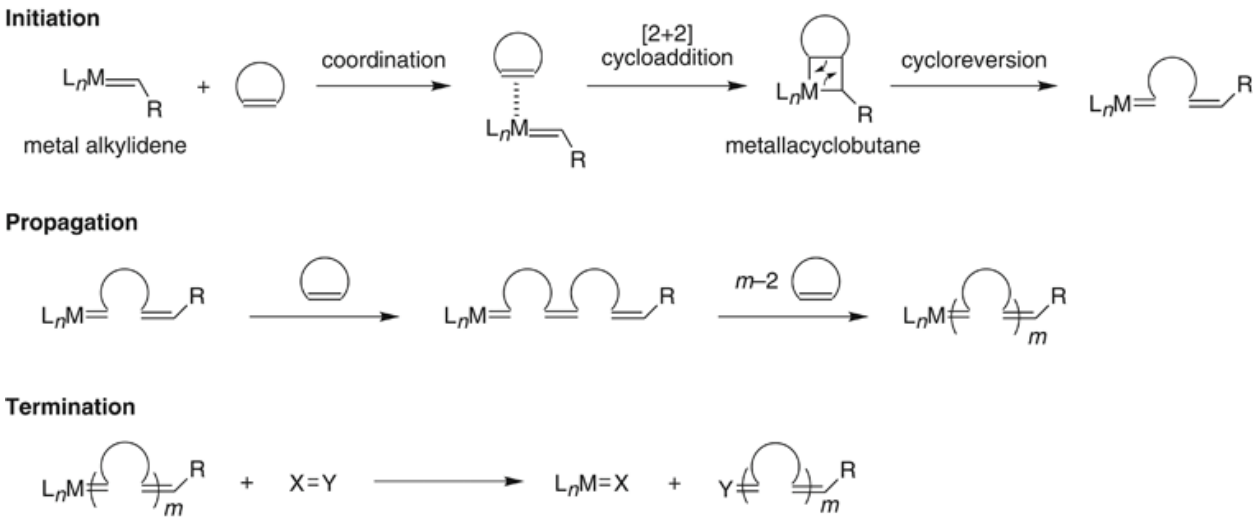

Scheme 2. Mechanism of ring-opening metathesis polymerization.
Reprinted with permission from Macmillan Publishers Ltd: Ref. 33, copyright 2010.

While mechanistically similar, ED-ROMP is quite distinct from ROMP because the macrocyclic monomers are inherently strainless. With ring sizes greater than 14 atoms, release of ring strain (ΔH) is negligible and the reaction is instead driven forward by the influence of increased translational and conformational entropy (ΔS). Reaction parameters governing ED-ROMP behavior can be understood by applying the Gibb's free energy equation:

$$\Delta G_p = \Delta H_p - T\Delta S_p \qquad \text{(Equation 2)}$$

with the understanding that $\Delta H_{ED\text{-}ROMP}$ is far closer to zero than the ΔH_{ROMP}. Factors that enhance the entropic contribution to ΔG_p, such as monomer concentration and temperature, therefore, become much more influential. It is not uncommon for ED-ROMP to be carried out in 0.1-5 M solutions or even neat conditions. Although there are many early examples of its use, very few of those resulted in high yields or thorough polymer characterization.[34-43] More recently, the generality of ED-ROMP has been demonstrated through incorporation of a variety

of backbones including esters, amides, aromatic rings, polyethylene glycol (PEG) and rotaxanes.[44]

A prominent feature of ROMP and ED-ROMP is the propensity of growing polymer chains towards undesired secondary metathesis events like intramolecular backbiting and intermolecular chain transfer (Scheme 3).[33,45] In intermolecular chain transfer, the active metal alkylidine of one polymer chain intercepts an internal olefin of another polymer chain. The number of active chains in solution remains constant, but these chains will now have redistributed molecular weights. In intramolecular chain transfer, also known as backbiting, the active chain end reacts with itself, leading to a macrocyclic oligomer (MCO) and a truncated polymer chain. These competing metathetical pathways do not deactivate polymer chains to further growth, but are typically undesired because they increase the heterogeneity of polymer chain lengths obtained.

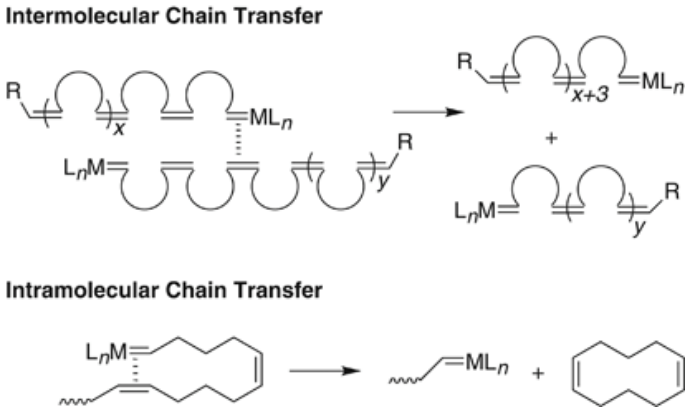

Scheme 3. Intermolecular and intramolecular secondary metathesis.
Reprinted with permission from Macmillan Publishers Ltd: Ref. 33, copyright 2010.

Strategies have been employed to minimize the degree of secondary metathesis that occurs during ROMP, including the use of specialized catalysts with higher catalyst initiation

rates,[46] solvents that exhibit increased coordination to catalyst,[47] addition of competitive ligands such as PCy_3 or PPh_3,[48,49] and manipulation of substrate to increase monomer reactivity.[45] Similar efforts to curb secondary metathesis have not been extensively investigated for ED-ROMP reactions. Although secondary metathesis broadens the dispersity of resulting polymers, it does not lead to sequence scrambling. It is therefore anticipated that even if an ED-ROMP is poorly controlled with respect to molecular weight, polymeric products will retain their desired sequences.

1.2.2 Ring-chain equilibrium in ED-ROMP

According to the Jacobson-Stockmayer theory of ring-chain equilibrium, the formation of MCOs during ED-ROMP is inevitable (Figure 4, top).[50-52] Assuming a catalytic amount of active chains are present, monomer initially will be incorporated into the growing polymer chain. However, at a late stage in the polymerization, a critical monomer concentration will be approached where backbiting and polymerization are predicted to occur at equal rates.[41-43] The dispersity of the sample, as determined by M_w/M_n, is theoretically predicted to approach 2 at equilibrium.

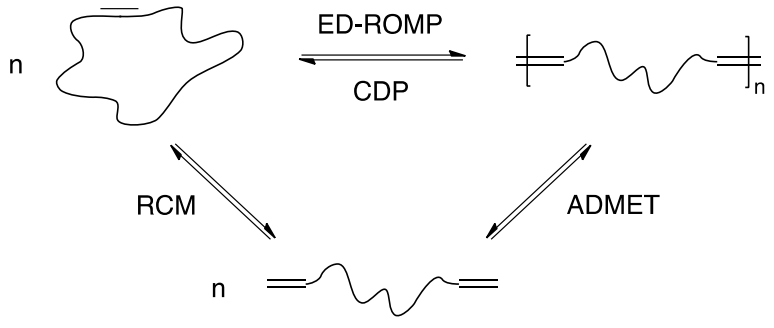

Figure 4. Metathetical equilibrium between cyclic, linear and polymer species.

Additionally, this phenomenon can be taken advantage of in order to recycle polymer through a process known as cyclodepolymerization (CDP; Figure 4, top).[53,54] Here, high dilution conditions entropically favor polymer degradation into a mixture of cyclic monomer and MCOs. Condensation polymers that can be recycled in this way are of incredible interest for industrial purposes and include polyesters,[55-60] polycarbonates,[56,61,62] polyamides,[60] and high-performance aromatic polymers.[63,64] Although CDP is not always viable, it is seen an incredible advantage to be able to successfully recycle polymers into their respective MCOs through ring-chain equilibrium manipulation.[58]

CDP can also serve as a high yielding and efficient means of obtaining MCO starting materials for ED-ROMP.[56,65-67] Monomers that cannot be obtained through ring-closing metathesis (RCM) or suffer from contamination with adventitious linear oligomers are excellent candidates for this method. Polymeric species can be first obtained from linear α,ω-diolefins through acyclic diene metathesis polymerization (ADMET, Figure 4, right). The condensation polymerization can be facilitated through vacuum removal of the ethylene byproduct in a way similar to RCM (Figure 4, left). When the purified polymer is exposed to additional catalyst under dilute conditions, ring-chain equilibrium leads to degradation of the material into a mixture of corresponding MCOs that can then be subjected to ED-ROMP.

The interconnected relationship between RCM, CDP, ED-ROMP and ADMET enables access to polymer through multiple routes. While ADMET is an attractive option for certain purposes, it simply does not allow controlled molecular weight polymers to be obtained on a reasonable scale without rigorous optimization for each new oligomeric sequence.[68] Step growth processes such as ADMET are inherently time dependent and suffer from diminishing

concentrations of reactive end groups as the reaction progresses. Further, it is incredibly difficult to predict polymeric molecular weights for a particular segmer without extensive trial and error.

ED-ROMP is significantly less dependent on time, tolerant of many functional groups, and produces polymers whose molecular weights are inherently related to reagent stoichiometry and concentration.[69,70] In examples where both ADMET and ED-ROMP were carried out on analogous monomers, ED-ROMP consistently gave higher molecular weight polymers.[40,55,71-73] In this precedent, minimal methodological optimization for ED-ROMP was required regardless of functional groups contained therein. The comprehensive nature of the method was identified as an attractive complement for our group's PLGA studies, where a large variety of monomer sequences would be subjected to standardized polymerization conditions.

2.0 DEVELOPMENT OF A SELECTIVITY-ENHANCED ENTROPY-DRIVEN RING-OPENING METATHESIS POLYMERIZATION

2.1 PROJECT RATIONALE

In an effort to harness the untapped potential of sequenced copolymers, we set out to exploit the advantageous sequence control possible during ED-ROMP while working towards an improved molecular weight profile. ED-ROMP benefits from many characteristics ideal for this research project: generality and functional group tolerance, sequence fidelity, scalability, and the potential for molecular weights that are determined by monomer to initiator ratios. Despite this, several challenges would need to be overcome in order to make this a successful and viable alternative to the SAP method. Molecular weight and dispersity control were anticipated to be the primary means of achieving our goals.

As previously mentioned, the SAP method produces PLGAs with a broad range of molecular weights and dispersities. Segmers requiring G-G couplings during condensation (GLG, GLLG, etc.) were much more resistant to high conversions and typically only achieved molecular weights ~20 kDa.[17] It was not uncommon, however, for other "well-behaved" segmers to produce polymers with highly variable molecular weights, even when carried out by the same researcher. Both ED-ROMP and SAP would necessarily provide polymeric materials with good sequence control, but it was our hope that ED-ROMP would allow us to achieve what we could

not with SAP in terms of consistent and predictable molecular weight profiles. In addition to developing a method to obtain *pseudo*-PLGAs via ED-ROMP using standard conditions, we also wanted to expand the current art for improving molecular weight control during copolymer synthesis. Finally, we wanted to identify synthetic steps that would be ideal for diversification in future stages of the project.

2.1.1.1 Selectivity-enhanced ED-ROMP

To the best of our knowledge, no study of ED-ROMP has been carried out with the purpose of improving molecular weight control, lowering dispersities and accessing block copolymers. In order to achieve this, we hypothesized that application of an additional kinetic driving force to the polymerization would be necessary. We believed that as in ROMP, an increase in the rate of propagation (k_{pr}) would mitigate the rate of secondary metathesis (k_{tr}) to further improve molecular weight control during polymerization (Scheme 4). While the ring-chain equilibrium would prevent a completely living system with no chain breaking events, a polymerization with unparalleled living character would certainly be achieved. Overall, the result would be a selectivity-enhanced ED-ROMP, which we have termed SEED-ROMP. Importantly, SEED-ROMP would enable the polymerization to enter a more living regime where block architectures would be possible.

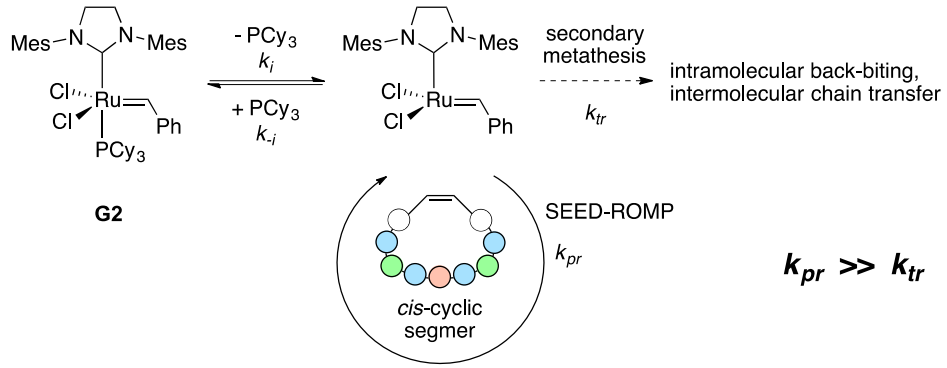

Scheme 4. Proposed rate enhancement during SEED-ROMP would curb secondary metathesis.

Reactivity differences between *cis*- and *trans*-olefins have been widely utilized in smaller ring systems where enthalpic contributions to ring strain dominate. For instance, the ring strain observed in *cis*-cyclooctene (COE) is 7.4 kcal/mol whereas the ring strain of *trans*-COE is 16.7 kcal/mol.[74] Although ROMP of either monomer will deliver polycyclooctene, the ROMP of *trans*-COE has more inherently living character due to its elevated reactivity.[45,75] In a strainless macrocyclic system such as ours, analogous considerations of *cis/trans* reactivity differences are not possible.

In SEED-ROMP, we speculated that a combination of kinetic and thermodynamic improvements would lead to a significant improvement in control for the polymerization (Figure 5). Steric bias would likely increase catalyst accessibility for the *cis*-monomer. The degree of this enhancement might depend on factors such as conformational flexibility, size of the macromonomer and steric demands of the existing catalyst ligands. This trend has been reported in other systems, where *Z*-olefins had greater access than *E*-olefins to sterically encumbered catalysts.[76-79] Further, this effect would be responsible for decreasing k_{tr} in SEED-ROMP relative to ED-ROMP because the bulky polymerized chain responsible for secondary metathesis would contain *trans*-olefins.[80] An enthalpic driving force would also be anticipated for the reaction due

to the *cis*-to-*trans* conversion of olefinic material during polymerization, further favoring the metathesis of macromonomer over polymerized material.[81,82]

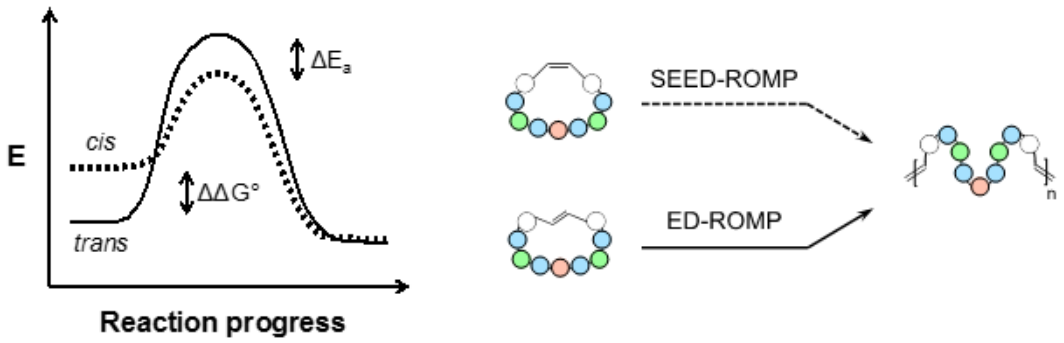

Figure 5. SEED-ROMP benefits from both a kinetic and thermodynamic advantage during polymerization.

Ultimately, an increase in k_{pr} along with a decrease in k_{tr} would have the potential to significantly improve the degree of molecular weight control observed in the system.[45,46,83] We predicted that if we were able to achieve this, we would likely observe the following:

A) In early stages of polymerization, molecular weights would increase rapidly due to high monomer concentration and rapid propagation. Though dispersities might be elevated at the earliest time points due to delays in catalyst initiation and subsequent chain introduction, they would shortly thereafter decrease and remain low as a result of the kinetic bias of propagation over secondary metathesis.

B) In late stages of polymerization, molecular weight growth would stall as remaining monomer is depleted. Only at very long reaction times would k_{tr} surpass k_{pr}, leading to increased dispersities and decreased molecular weights.

C) A linear relationship would be observed when comparing molecular weights with different monomer:catalyst ratios, assuming prohibitive viscosity increases did not result in poor mixing.

2.1.1.2 Deactivation ED-ROMP

Fast-initiating ruthenium species such as Grubbs' third generation catalyst (**G3**, Figure 6) are frequently utilized to achieve a more controlled ROMP.[69,84] This catalyst features a strongly ligating NHC group and also weakly coordinating bromopyridines that dissociate more rapidly than the phosphine ligands of Grubbs first and second generation catalysts (**G1** and **G2**, Figure 6).[85] The result is a k_{pr} that is somewhat larger than that of **G2** but a k_i that is more than 10,000 times higher.[86,87] The relatively high k_i/k_{pr} as well as the short lifetime of this catalyst mitigates secondary metathesis events.

With negligible chain transfer, backbiting, or chain termination, monodisperse polymers are possible even when using monomers typically susceptible to secondary metathesis such as norbornene.[46] The degree of control achieved with **G3** is demonstrated through its linear relationship between molecular weight and monomer to catalyst ratio. Despite the advantage of increased access to polymers of targeted molecular weights and narrow dispersities, this catalyst has a significantly truncated lifetime that may preclude sequential reactions.[88] It therefore represents a short-lived alternative to **G2** mediated ED-ROMP and exists as a distinct form of polymerization that we have termed deactivation ED-ROMP (DED-ROMP).

2.1.1.3 Summary

The SAP method developed within our group allows for an extraordinary degree of sequence control, but is associated with challenges in accessing higher molecular weight polymers and

achieving molecular weight control. ED-ROMP offers a means to bypass these obstacles in a mechanistically orthogonal way. It enables the synthesis of sequenced copolymers with increased opportunities for tunable molecular weights and specialty reactions such as block copolymerization (Table **1**).

Table 1. **Comparing the attributes of SAP and proposed ED-ROMP methods**.

Polymerization method	Acronym	Sequence fidelity	Sequence complexity	Scalability	Generality	Average M_n	Control of M_n	Reduced Đ	Block copoymers
Segmer assembly polymerization	SAP								
Entropy-driven ROMP	ED-ROMP								
Selectivity-enhanced ED-ROMP	SEED-ROMP								
Deactivation ED-ROMP	DED-ROMP								

excellent — poor

Our research plan was to first assess the generality of ED-ROMP using a variety of macromonomers containing internal *trans-olefins*. The results from these polymerizations, carried out by Ryan Weiss, will be briefly summarized herein.[22] Then, using a well-performing sequence from this preliminary study, we would carry out SEED-ROMP with the corresponding *cis*-macromonomer. The results from the preliminary ED-ROMP study would enable us to compare the degree of selectivity enhancement encountered during subsequent SEED-ROMP experiments. If the SEED-ROMP resulted in a substantial improvement in living character for the polymerization, we would further probe the limits of polymeric architectures achievable through chain extension and block copolymer experiments. Finally, we wanted to compare

molecular weights and dispersities for polymers constructed through SEED-ROMP and DED-ROMP.

2.2 DESIGN AND SYNTHESIS OF CYCLIC PLGA-INSPIRED MONOMERS

2.2.1 Synthetic Plan for ED-ROMP studies of *cis*- and *trans*-macromonomers

In an effort to make a convergent and diversifiable scheme, we developed a synthesis following the SAP philosophy of segmer assembly. Late-stage RCM would allow for a highly efficient route to obtain macromonomers necessary for ED-ROMP and SEED-ROMP studies. Each step could conceivably be scaled up to obtain gram-quantities of material. RCM requires dilute conditions to prevent intermolecular metathesis (<0.01 M), and would therefore be the most limiting step with respect to scale. With compounds as large as our linear segmers, even more dilute conditions would likely be required. Overall, the iterative nature of this route makes it extremely tolerant of sequence modifications and highly general; requirements include formation of an α,ω-diolefin prior to RCM and a functionally benign backbone that will not interfere with metathesis (Scheme 5).

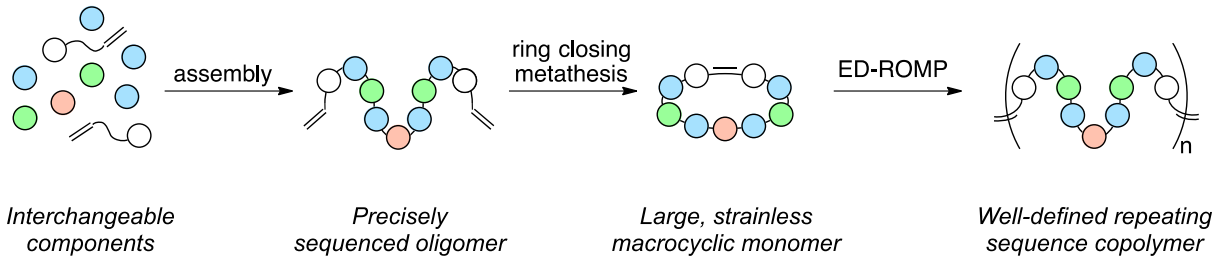

Scheme 5. Proposed route for the convergent synthesis of sequenced copolymers via ED-ROMP.

2.2.2 Catalyst selection for RCM and ED-ROMP reactions

We proposed that through judicious selection of catalysts, we would be able to achieve our goals in a highly convergent manner. We benefitted from the substantial pioneering work of others like Grubbs, Schrock, and Hoveyda in the field of organometallic chemistry and had access to many suitable commercially available options.[80,89,90] As mentioned previously, Grubbs' third generation catalyst (**G3**, Figure 6) is ideal for DED-ROMP studies due to its relatively high k_i/k_{pr}. Use of this catalyst would lead to rapid polymer formation and abrupt catalyst deactivation prior to late-stage secondary metathesis.

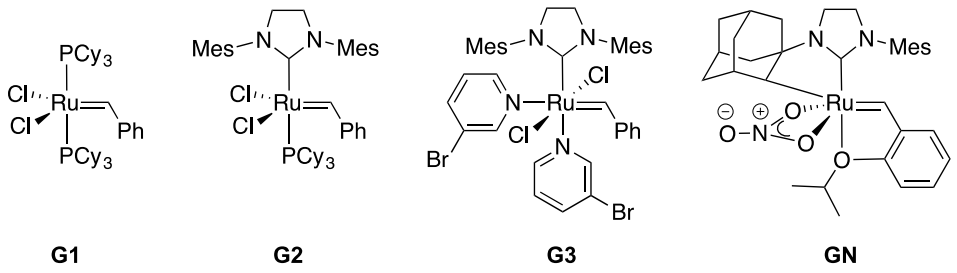

Figure 6. Grubbs' 1st (**G1**) and 2nd generation (**G2**), *cis*-selective nitrato-type Grubbs (**GN**) and Grubbs' 3rd generation (**G3**) catalysts selected to facilitate ED-ROMP studies.

Grubbs' robust second generation catalyst (**G2,** Figure 6) would be used to obtain *trans*-olefins through RCM and also to carry out ED-ROMP reactions. These applications were highly precedented using a variety of ring sizes and peripheral functionality.[57,91] CH_2Cl_2 would be used as a reaction solvent with appropriate levels of dilution or concentration to manipulate ring chain equilibrium and stabilize polar intermediates during catalyst initiation.[87] Conveniently, when using **G2**, saturation conditions can be assumed for the polymerization, as described in great detail by Grubbs and coworkers.[87] **G2** experiences a reduced phosphine ligand dissociation rate

(k_1) when compared to catalysts like **G1**, but a comparatively improved dissociative substitution rate (k_2) with incoming olefin. The apparent rate of propagation for polymerizations carried out with **G2** could be expressed as:

$$\frac{-\mathrm{d}[\mathrm{M}]}{\mathrm{d}t} = k_p[\text{Ru activated chains}] = \ln\frac{[\mathrm{M}]_0/[\mathrm{M}]_\mathrm{t}}{\mathrm{t}} \qquad \text{Equation (3)}$$

As the key step to obtaining the SEED-ROMP macromonomers, we required a *cis*-selective catalyst capable of carrying out RCM with high selectivity and compatible functional group tolerance. We turned to Grubbs and coworkers' very recent work in *cis*-selective catalyst development. Though there were few examples of its use in literature, we were intrigued by the group's C-H activated ruthenium catalyst **GN** (Figure 6).[92-96] The catalyst features a bidentate X-type nitrato ligand, adamantyl chelate, NHC carbene and Hoveyda-type styrenyl ligand and was shown to deliver products with high Z-selectivity due to its proposed side-bound mechanism.[97,98] In this mechanism, transition states leading to *E*-products are disfavored due to electronic destabilization and constrained ligand geometry that reinforces steric interactions between the metallocyclobutane substituents and the mesityl ring of the NHC ligand (Scheme 6).[99]

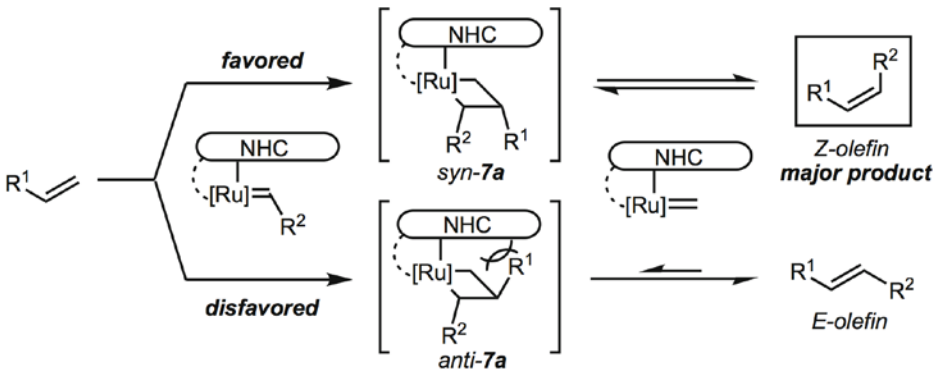

Scheme 6. Proposed steric interactions for various ruthenacycle confromations of **GN**.
Reprinted with permission from Springer: Ref. 99, copyright 2014.

Of great interest to us, a series of RCM experiments have been carried out by Grubbs and coworkers to produce minimally functionalized macrocycles 13-20 atoms in size with 30-75% yields and >75% *Z*-selectivity.[96] Use of this catalyst had not yet been fully explored in literature, and so we recognized this as an exceptional opportunity to expand the current scope of reactions possible. We also acknowledged that uncertainties with respect to functional group and substrate intolerance were a significant potential pitfall, but we nonetheless moved forward with plans for alternate routes if *cis*-selective RCM could not be achieved.[100-104]

2.2.3 Biological and chemical significance of selected ED-ROMP monomers

Segmer components for ED-ROMP were selected to mimic the PLGA system while incorporating necessary olefinic functionality for metathesis. We anticipated that these *pseudo*-PLGAs would have differing physical properties from the PLGAs previously synthesized by our group.[17,105,106] The olefinic component would likely lower the glass transition temperature (T_g) by increasing conformational flexibility and by interrupting polymeric associations. Slightly offsetting this, the palindromic nature of the sequences would generate even numbers of carbon atoms spanning these ester groups following hydrogenation, a factor known to encourage crystallinity.[107,108] While PLGA is a solid at room temperature, we were uncertain what the morphology of these polymers would be. Hydrolytic byproducts were also of interest to us. Lactic and glycolic monomers would be used along with ethylene glycol and an additional olefinic tether group (containing C_8, C_6, and C_4 alkenyl groups). Hydrolytic byproducts from these components (lactic acid, glycolic acid, ethylene glycol, suberic acid, adipic acid and

succinic acid, respectively) are bioassimilable or have very low associated toxicity and can be eliminated through normal metabolic pathways.[6-8]

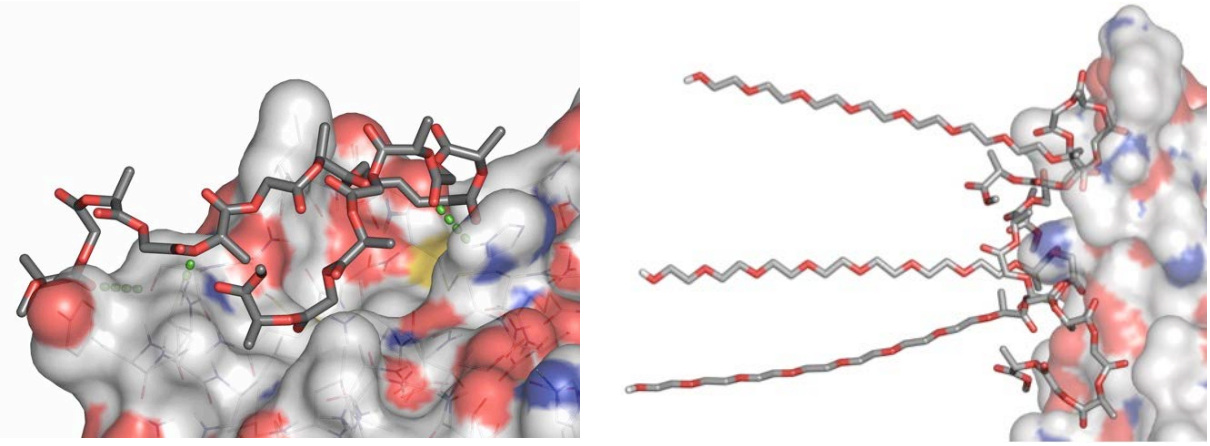

Figure 7. Graphical depiction of H-bonding opportunities (left) and a partial micellar array (right) of PEG-terminated ED-ROMP polymers and human insulin.

Preliminary models were constructed to graphically demonstrate the potential interaction of these *pseudo*-PLGAs in applications such as encapsulating micelles. Our goal was to qualitatively depict favorable associations between *pseudo*-PLGA models and biomaterials such as proteins. In these experiments, truncated sequences of *pseudo*-PLGA were terminated with a short block of polyethylene glycol (PEG), a typical strategy to reinforce micellar structure. A crystal structure of human insulin was obtained from the Protein Data Bank and imported into MacPyMol for analysis (PDB ID 1BEN).[109] Rapid virtual screening was carried out with MM2 energy minimization, removal of non-polar hydrogens, selection of rotatable bonds and predictive docking analysis using AutoDock Vina 1.1.2 and the MGL Tools 1.5.6 suite from the Scripps Research Institute.[110-113] Representative binding conformations are shown in Figure 7. We recognized the significant limitations of this method, especially with respect to polymeric

sequence, size and bond rotation, and so quantitative predictions of binding affinity were not taken into account. Observable in all models were the favorable H-bonding interactions possible between the *pseudo*-PLGA and the protein and also the predictable preference of PEG chains to point outward. While the biocompatibility of polymer fragments was of general interest to us in the planning stages of this project, physical, mechanical and biological properties studies of these materials is not our primary focus at this stage of the research program.

2.2.4 Synthesis of linear Eg-(LGL-X)$_2$ segmers

ED-ROMP segmers were designed to incorporate alternating lactic and glycolic pairs with specific consideration for regioregularity. A lack of regiospecificity is typical in metathesis reactions (Figure 8).[60] In recent ED-ROMP studies of linear-sequence monomers, Jamie Nowalk found a statistical distribution of head-tail, tail-tail, and head-head polymeric linkages were incorporated into the copolymer (representative outcome: 49%, 25% and 26%, respectively).[114] Substrate-modification approaches have been successfully implemented in ROMP to achieve high head-to-tail regioregularity, as demonstrated by the work of Hillmyer, Gutekunst and Hawker.[115-117] These existing solutions are not possible in ED-ROMP systems where macromonomers do not have inherent ring strain and therefore not as high of reactivity or where incorporation of ancillary functionality is required.

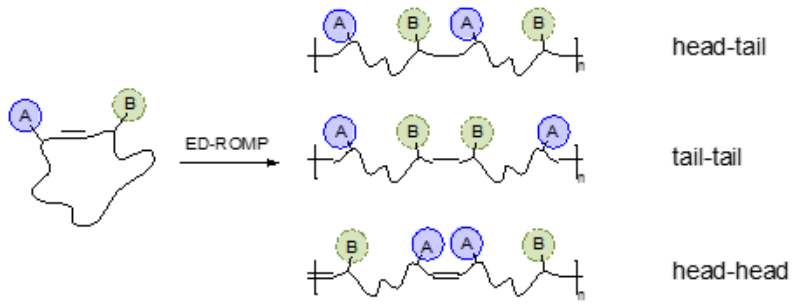

Figure 8. Linkage types observed following ED-ROMP with asymmetric macromonomer sequences.

Palindromic sequences were developed to bypass this challenge and to eliminate spectral ambiguity during segmer assembly and polymerization. Conveniently, we found that this alteration significantly improved our ability to monitor reaction progress with respect to conversion and isomeric ratios. Macromonomer ring sizes for the desired library varied from 26-32 atoms, which was well above the threshold necessary for ED-ROMP. Requisite internal olefins were incorporated with various alkenoate ester moieties (**X**), and an ethylene glycol (**Eg**) subunit reminiscent of **G** served as a symmetric center. Once polymerized, the material had a sequence of $[\text{-X-LGL-Eg-LGL-X-}]_n$ with the length of the alkyl chain in **X** varying from 0-2 (Figure 9).

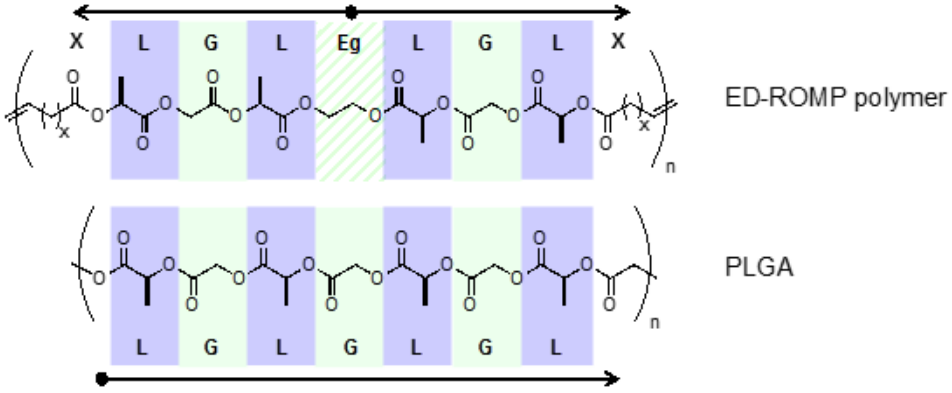

Figure 9. Palindromic sequence of ED-ROMP polymers compared to PLGA.
Lactic acid, L = blue; glycolic acid, G = green, ethylene glycol, Eg = striped green.

Sequenced oligomers were constructed using the segmer assembly method that had proved to be so robust in our group's previous studies.[17,22] The symmetric nature of the macromonomers allowed for a highly convergent approach to be used. Coupling with alkenoate esters and RCM were carried out at a late stage to enable facile library diversification through extensions in the alkyl chain length and incorporation of either *cis*- or *trans*-internal olefins.

Efforts began with synthetic optimization and large-scale production of the RCM precursors. The complete synthesis of **Eg-(LGL)$_2$** was carried out multiple times on a 10-30 g scale with respect to final isolated product, resulting in a substantial improvement in yield compared to previous efforts. A carbodiimide-promoted coupling strategy was employed to join **G**, **L**, **Eg** and **X** (**X** = pentenoate, **P**; butenoate, **B**; or acrylate, **A**) scaffolds and proved to be both mild and consistently high-yielding.[17,118,119] Two additional analogues prepared by Ryan Weiss incorporated an acidic subunit reminiscent of the commercially ubiquitous caprolactone (heptenoic acid, **C**) to form **Eg-(LC-P)$_2$** and **Eg-(LLC-P)$_2$** segmers.[22]

Starting with **Me-L-Si**, saponification to **L-Si** was immediately followed by carbodiimide-promoted coupling with **Bn-G** to form **Bn-GL-Si** (Scheme 7). Hydrogenolysis of the benzyl protecting group and subsequent coupling to **Bn-L** produced **Bn-LGL-Si**. Further hydrogenolysis yielded **LGL-Si**, which was then coupled to either side of ethylene glycol to give the symmetric **Eg-(LGL-Si)$_2$**. The entire process was carried out over 6 steps with 64% overall yield. When required, purifications were facile owing to the disparate polarities of starting material and products at each stage. Reactions were highly scalable, with similar outcomes whether on a 50 mg or a 50 g scale.

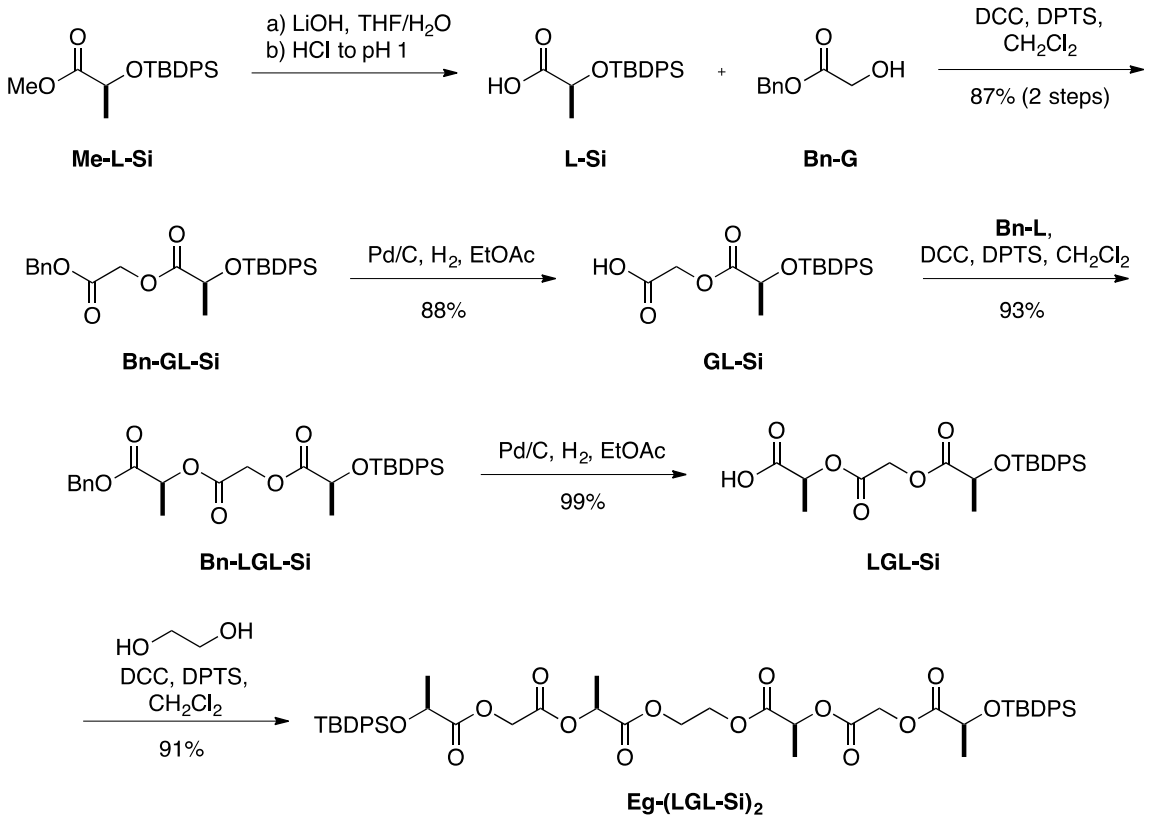

Scheme 7. Scalable and high-yielding synthesis of **Eg-(LGL-Si)$_2$**.

Double silyl deprotection of **Eg-(LGL-Si)$_2$** was unexpectedly challenging considering the ease with which the reaction was carried out on similar mono-protected species in our group. The reaction itself proceeded in a nearly stepwise fashion and could be monitored easily by TLC; R_f values for starting material, mono-deprotected intermediate, and product were easily distinguishable and the compounds themselves were separable during purification. However, it proved to be suprisingly sensitive, frequently generating oligomers and hydrolytic byproducts that co-eluted with product during purification. These byproducts remained inseparable in later steps, and so optimization at this stage was prioritized. The most common contaminants during deprotection included those resulting from asymmetric single deprotection or compounds like **L-Eg-L** that resulted from cleavage at the site of the centermost **G-L** linkage. **G-L** bond lability in this reaction correlates well with ongoing degradation studies in our group where increased hydrolytic susceptibility of **-G-** linkages is observed.

Multiple strategies were employed to minimize the potential for unwanted side reactions, including use of an AcOH buffer, changes in concentration of TBAF and use of alternative deprotection reagents (Table 2). Large equivalents of AcOH slowed the reaction prohibitively (entries 5, 6) but also suppressed the formation of oligomeric species. When reactions under these conditions were allowed to proceed over multiple days (entries 7, 8), quantitative yields were possible. Unfortunately, these same conditions periodically resulted in small amounts of oligomer formation and the lack of reproducibility was unacceptable for our purposes. Concerned that different outcomes were achieved with different bottles of commercial TBAF, we attempted deprotection with the crystalline tris-(dimethylamino)sulfonium difluorotrimethylsilicate (TASF), a less basic fluoride source (entries 9, 10).[120] Complete conversion was achieved, but the product mixture had significant oligomer contamination. We

therefore turned back to TBAF, but focused efforts on minimizing the basic contaminants produced through contact with water. Gratifyingly, pre-drying all freshly-purchased reagents successfully suppressed undesired side reactions and consistently delivered pure **Eg-(LGL)$_2$** with excellent yields on a multigram scale.

Table 2. Representative outcomes for the deprotection of **Eg-(LGL-Si)$_2$**.

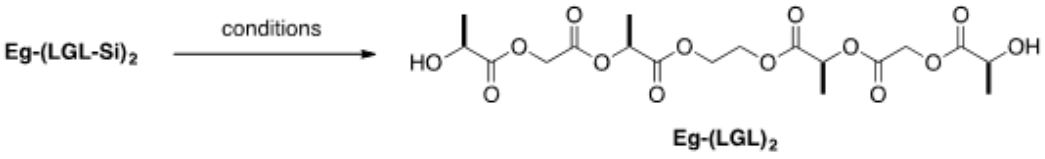

Eg-(LGL)$_2$

Entry	Conditions[‡]	Result
1	TBAF (3.5), AcOH (5), THF (0.1 M), rt 1h	48% with formation of oligomers
2	---------- THF (0.05 M), rt 1h	n.d., mixture of SM, mono, oligomers
3	---------- THF (0.05 M), rt 30 min	n.d., mixture of SM, mono, oligomers
4	---------- THF (0.05 M), 0 °C to rt 1h	n.d., mixture of SM, mono, oligomers
5	TBAF (3), AcOH (16), THF (0.05 M), 0 °C, 30 min	SM and trace mono
6	---------- THF (0.05 M), rt 30 min	SM and trace mono
7	---------- THF (0.05 M), 0 °C 6 h, rt 40h	[†] Quantitative (370 mg scale)
8	---------- THF (0.05 M), 0 °C 20 h, rt 3d	[†] Quantitative (3.1 g scale)
9	TASF (5), THF (0.1 M), 0 °C to rt, 2h	Mixture of product and oligomers
10	---------- H_2O (7), rt, 2h	Mixture of product and oligomers
11	TBAF (3), AcOH (8), pre-dried, THF (0.04 M), 4h	89 % yield

[‡]Equivalents of each reagent shown in parentheses, dashed lines indicate same equivalents as previous entry; n.d. = not determined; SM = starting material; mono = mono-deprotected intermediate; [†] this is the best result achieved but was not consistently reproducible; all reported oligomer mixtures were inseparable through column chromatography.

It is worth noting that the optimization series for the deprotection of **E$_g$-(LGL-Si)$_2$** also resulted in the establishment of a method to cleanly obtain mono-deprotected material, **Si-LGL-E$_g$-LGL** (Table 2, entry 8, modified with truncated reaction times). Asymmetric segmer architectures could be accessed using this route, as demonstrated through the coupling of **LGL-**

Eg-LGL-Si to 3-butenoic acid to form **B-LGL-Eg-LGL-Si** (Scheme 8). Though beyond the scope of the current project, this strategy would be ideal in systems where asymmetric monomer was desired. For instance, incorporation of a group capable of post-functionalization after polymerization would enable attachment of cleavable drug, fluorophore, or RGD group in a 1:1 rather than a 2:1 ratio of pendant group to segmer. Due to the incredible functional group tolerance of ED-ROMP, we would expect polymerization of this modified compound to proceed similarly to the others.[22] Control over degree of polymerization (DP) would translate to control over amount of this pendant group contained in polymer and, significantly, would solve an ongoing problem encountered with formulating drug-loaded PLGAs.[8] Use of this asymmetric pathway to control head-tail ratios during the polymerization of non-palindromic sequences may not be ideal for our purposes because any reduction in k_{pr} would necessarily decrease molecular weight control during ED-ROMP.

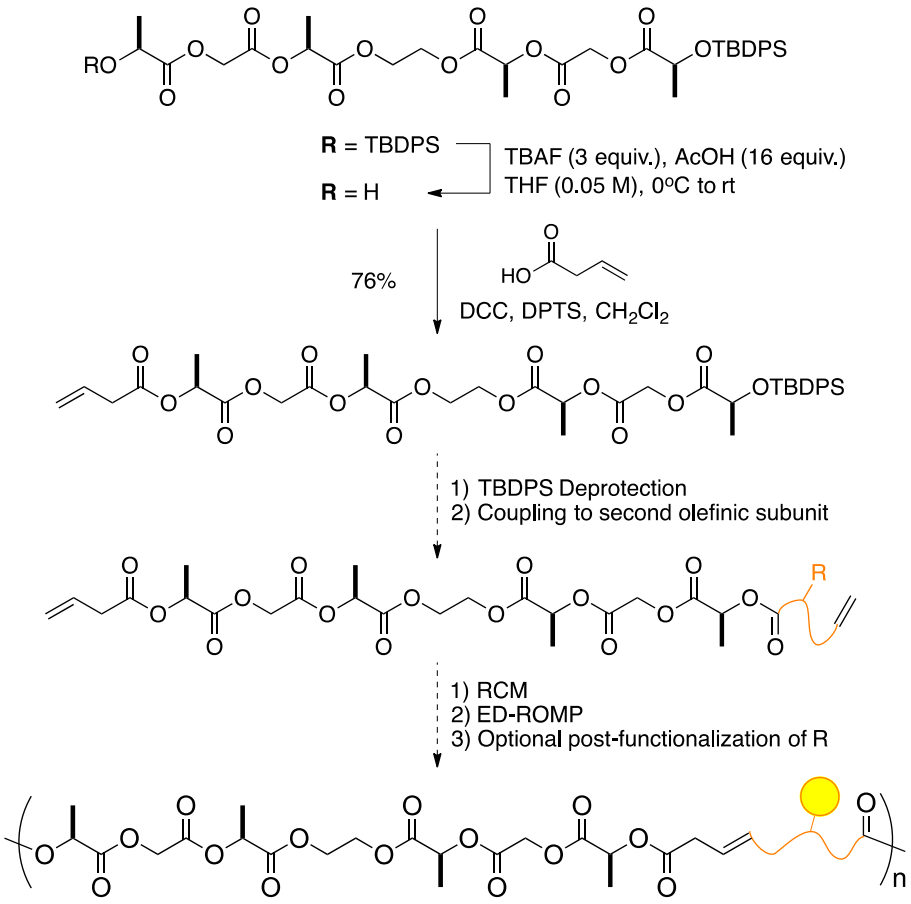

Scheme 8. Possible mono-deprotection route to incorporate pendant group for biomaterials applications.

Once the diol **Eg-(LGL)$_2$** was obtained, each side could be coupled to form the corresponding C_3, C_4, or C_5 alkenoate ester **Eg-(LGL-X)$_2$** (Scheme 9). The double couplings that provided **Eg-(LGL-B)$_2$** and **Eg-(LGL-P)$_2$** went smoothly on multigram scales by adjusting the standard conditions for mono-esterification. More mild reaction conditions were required for the formation of **Eg-(LGL-A)$_2$**, which proved to be more sensitive to our standard coupling procedures. To improve reaction outcomes, conditions were adjusted to increase dilution, shorten reaction times, lower temperature, and facilitate coupling with a mild base and DMAP. After

encountering difficulties with **Eg-(LGL-A)$_2$** in later metathesis reactions, no further experiments were carried out on this substrate.

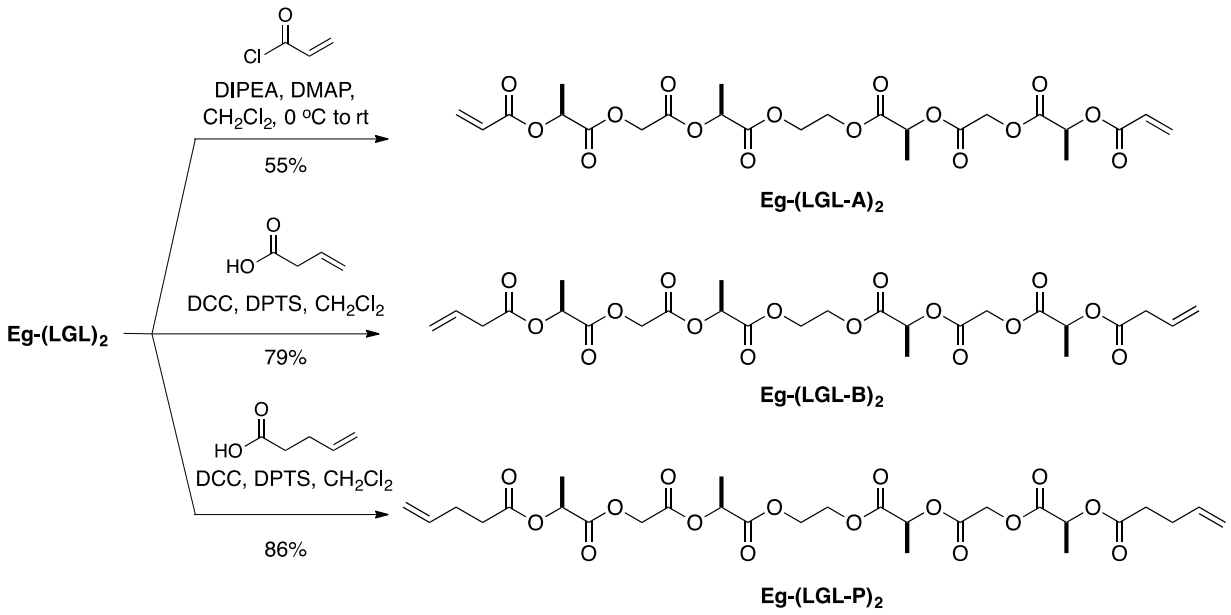

Scheme 9. Coupling of **Eg-(LGL)$_2$** to form **Eg-(LGL-X)$_2$**.

2.2.5 *Trans*-selective RCM with G2 to form *trans*-cyclic-Eg-(LGL-P)$_2$

With the linear α,ω-diolefin segmers in hand, RCM was carried out to produce the cyclic monomers needed for ED-ROMP. Use of catalyst **G2** and dilute conditions (0.001 M) delivered ***trans-cyclic*-Eg-(LGL-P)$_2$** in 93% yield with 84% *trans*-olefin selectivity (Scheme 10). Regardless of scale, conversion of starting material was complete after stirring overnight, and the increased polarity of the cyclic species made purification efforts straightforward. As in other stages, ^{1}H-NMR proved valuable due to the loss of terminal olefin peaks at ~5.8 ppm, the formation of internal olefin peaks at ~5.5 ppm, and the decreased distance between **G**-methylene

peaks at ~4.8-4.7 ppm (Figure 10). Ryan Weiss performed similar RCM experiments to successfully obtain ***trans-cyclic*-Eg-(LGL-B)$_2$** and ***trans-cyclic*-Eg-(LC-P)$_2$** for the project's initial ED-ROMP studies.[22] Efforts to perform RCM on **Eg-(LGL-A)$_2$** were unsuccessful, likely due to the decreased reactivity of the electron deficient olefin.[121-123] Gram-scale reactions could be carried out on **Eg-(LGL-P)$_2$**, **Eg-(LGL-B)$_2$,** and **Eg-(LC-P)$_2$** in >80% yield. Tolerance of exposure to air and significant humidity in the laboratory when preparing stock solutions was also noted. Significant increases in scale would therefore only be limited by the dilute conditions necessary to inhibit intermolecular oligomerization.

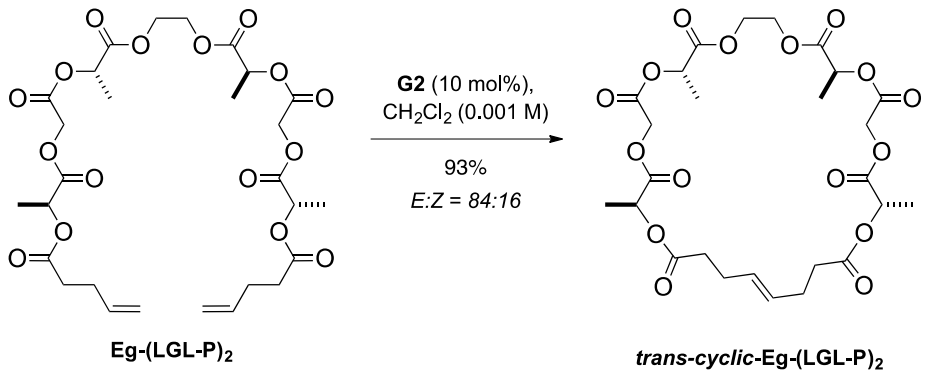

Scheme 10. Ring-closing metathesis to form ***trans-cyclic*-Eg-(LGL-P)$_2$**.

2.2.6 *Cis*-selective RCM with GN to form *cis*-cyclic-Eg-(LGL-P)$_2$

Nine steps in the synthesis of the *cis*-selective **GN** catalyst (Figure 6) had already been carried out in high yield when it serendipitously became commercially available. With a reliable supply of catalytic material, our efforts shifted from catalyst synthesis to the ring closing itself. Surprisingly, it appears that usage of this catalyst has only been reported from the Grubbs group thus far. Only two substrate types have undergone **GN**-catalyzed RCM,[94,96,124,125] but it has also

been used to catalyze homodimerization and cross metathesis,[92,124,125] ROMP,[93] and ethenolysis.[96,126]

An allylbenzene homodimerization was first carried out as a control experiment to compare the reactivity of the commercially available catalyst to that observed by Grubbs and coworkers.[92] Though it was noted that the catalyst was more stable than others in the series, we also wanted to establish that our glovebox conditions would be sufficient for carrying out the RCM successfully. Early studies of **GN** noted that steric interactions with the NHC, while enhancing *cis*-selectivity, also could lead to a decrease in productive catalyst turnovers.[96,97] In order to manipulate ring-chain equilibrium and discourage oligomerization, dilute conditions, elevated temperatures and vacuum were required.

The reaction was successfully monitored over time in an NMR tube equipped with a controlled atmosphere valve. THF-d_8 solvent was used so progress could be directly monitored for conversion and % *cis*-isomer observed. A **GN** stock solution was prepared and directly added to a solution of **1** in the glovebox (Scheme 11). The reaction tube was frequently evacuated to remove ethylene byproduct and drive the reaction equilibrium forward. After letting the reaction go overnight, conversion had increased to 70%, with negligible *trans* isomer observed. Consistent with what has been previously observed, the reaction stalled if not frequently evacuated but would continue again once vacuum was applied.[127-130] The rather small volume of headspace in the reaction tube likely magnified this effect. Additional time and evacuation of the reaction vessel led to increased conversion at the cost of *Z*-selectivity, with a final sample having 87% conversion and 83% *cis*-isomer. Satisfied in the reaction outcome, we proceeded with our synthesis.

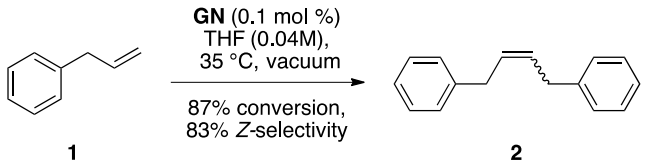

Scheme 11. Homodimerization of allylbenzene.

The homodimerization reaction highlighted for us the delicate balance that can exist between temperature, concentration, vacuum efficiency and reaction time with this catalyst. Understanding that we would have to optimize the RCM of monomers for conversion and *Z*-selectivity, we set out to probe key reaction parameters. Concentration and solvent choice were an immediate concern, as dilution would discourage undesired intermolecular reactions and solvent adjustment has been known to bring about beneficial conformational changes during RCM.[94] Preliminary RCM reactions were carried out with the C_4-alkenoate to form ***cis-cyclic*-Eg-(LGL-B)$_2$.** Dissolution in 1,2-dichloroethane (DCE) was found to produce fewer byproducts when compared to THF (not shown), so further experiments were exclusively run in DCE. DCE in this case may encourage conformational coiling, increasing proximity of chain ends. Additionally, freeze-pump-thaw cycles did not appear to substantially influence reaction outcomes so commerically available solvent was used without degassing or distilling. Important findings and representative examples are shown below in Table 3.

Table 3. Representative results of *cis*-selective RCM experiments.

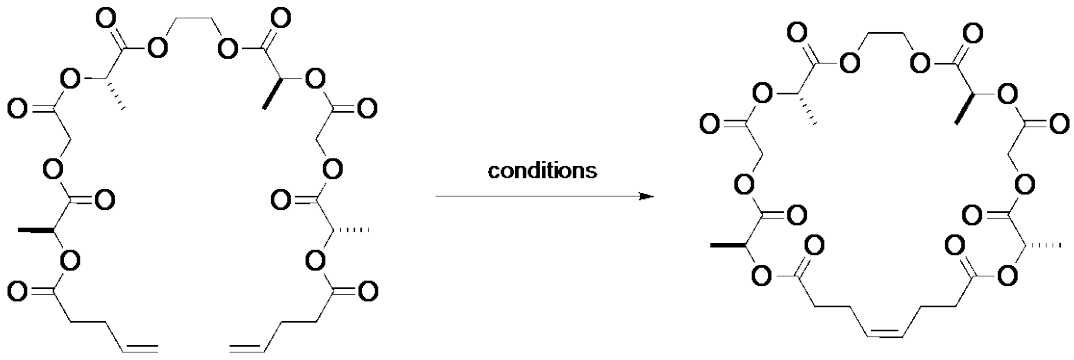

Eg-(LGL-P)$_2$ **_cis-cyclic_-Eg-(LGL-P)$_2$**

Entry	Conditions	% *Z*-selectivity	% yield
1	GN (10 mol%), DCE (0.03 M), 60°C, periodic evacuation, 23 h	n.d.	≤ 10[†]
2	GN (10 mol%), DCE (0.005 M), 60°C, slight vacuum, 24 h	88	49
3	GN (2×10 mol%), DCE (0.005 M), 60°C, slight vacuum, 26 h	78	89
4	GN (10 mol%), DCE (0.005 M), 60°C, reflux with vacuum, 26 h	88	88

n.d. = not determined; [†] Percent conversion value, determined by crude NMR.

Constant vacuum conditions proved to be the parameter most responsible for reaction success. Initially, the RCM of **Eg-(LGL-P)$_2$** was carried out in oversized vessels with frequent evacuation to account for ethylene generation, but long reaction times made this protocol impractical (Entry 1). The reactions stalled and oligomeric byproducts contaminated the sample, falling closely in line with our homodimerization results and those by Grubbs and coworkers.[96] When a very slight active vacuum was applied, the yield improved modestly and *Z*-selectivity reached 88% (Entry 2). Wanting to encourage further product formation, the same reaction was carried out, but with a second aliquot of 10 mol% catalyst added (Entry 3). The yield was successfully increased to 89%, but at the cost of 10% *Z*-selectivity. Our primary concern was

optimizing the reaction to minimize oligomer formation increase *Z*-selectivity. High conversion was less of a priority due to the ease of isolating unreacted starting material.

Looking to efficiently remove ethylene, a more elaborate apparatus was designed to allow moderate vacuum to be established. This increased vacuum allowed the solution to reflux, which would further encourage solvated ethylene removal. The modification resulted in both high yield (88%) and high *Z*-selectivity (88%, Entry 4). The reaction was reproducible and scalable, being carried out on up to a 1.4 g scale while maintaining an 87-90% *Z*-selectivity. In these cases, the color of the catalyst solution often was markedly different than the pale purple of reaction solutions containing active catalyst. Conveniently, oligomeric byproducts were not observed using these conditions and unreacted starting material could be easily isolated during purification to raise yields to >90% BRSM.

Although the ^{1}H-NMR spectrum for ***cis-cyclic*-Eg-(LGL-P)$_2$** was very similar to that of the *trans*-isomer, it was possible to differentiate them (Figure 10). The resonances corresponding to internal alkene protons (~5.4 ppm) and **G**-methylene protons (~4.8 ppm) were shifted upfield by 0.1 ppm and 0.02 ppm, respectively, compared to *trans*-cyclic species. It is interesting to note when comparing the NMRs of **LGL-B** and **LGL-P** variants that the relative position of peaks corresponding to internal olefins reverses, with the *cis*-ring peak appearing farther downfield. Due to the active vacuum of the reaction apparatus, monitoring conversion of starting material to product mid-reaction was difficult. After reaction conditions had been optimized, it was not necessary to disrupt the vacuum and backfill with active nitrogen to remove aliquots for NMR or TLC.

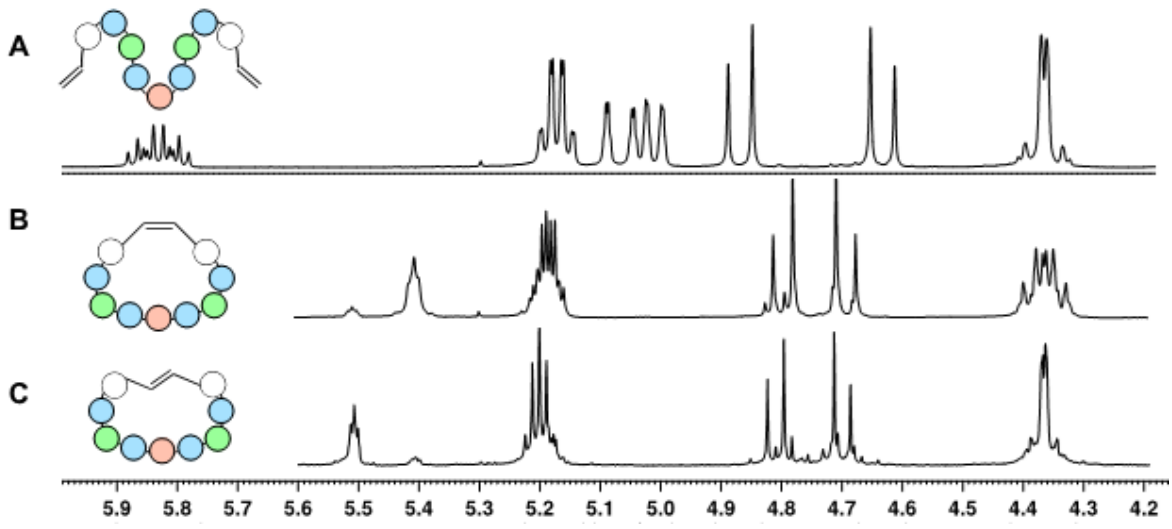

Figure 10. Comparing the chemical shifts of linear segmer (A) with *cis- and trans*-cyclic segmers (B and C).

Once the RCM had been sufficiently optimized for the substrate, we continued on with the SEED-ROMP studies. In the course of synthesizing additional monomer in later stages of the project, we unexpectedly encountered two additional points of interest regarding this monomer. First, the extreme base sensitivity observed for **Eg-(LGL-Si)$_2$** and **Me-GL-TBS** was not observed for ***cis-cyclic*-Eg-(LGL-P)$_2$**. In studies probing the stability of macromonomer, no decomposition was observed even when exposed to up to 30 equivalents LiOH at room temperature (Scheme 12). Decomposition would be certain in aqueous solutions over extended periods of time, but this degree of hydrolytic resistance was unexpected.

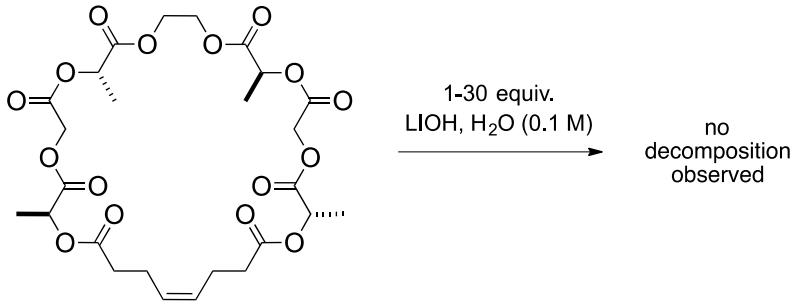

Scheme 12. The macromonomer is stable when exposed to aqueous basic conditions.

In the course of determining the ideal vacuum strength for the reaction, a higher concentration RCM was carried out. NMR and MS of the crude reaction mixture confirmed 82% conversion of the starting material to the linear dimer ***cis*-$\mathbf{P_p}$-(LGL-Eg-LGL-P)$_2$,** where $\mathbf{P_p}$ stands for the C_8 diester resulting from the metathesis of two P groups (Scheme 13). The result, while clearly not desired for this aspect of the project, is interesting nonetheless as it relates to planned future studies on the relationship between ring size and reactivity during SEED-ROMP. ED-ROMP monomers are inherently unstrained and so we hypothesize that reactivity trends will not be affected by ring size.[55,60] This homodimer can undergo either a *cis*- or a *trans*-selective RCM to produce a cyclic dimer for ED-ROMP. In a substrate containing two *cis*-olefins, SEED-ROMP results for varying ring sizes can be directly compared. In a substrate containing one *cis*-olefin and one *trans*-olefin, reactivity differences between each olefin can be studied with more control. In a non-palindromic sequence, this *cis*-*trans*-dimer approach could also be used to influence head-tail ratios due to the increased reactivity of the *cis*-olefin. While this route has not pursued further at this time, intentional oligomer formation is nonetheless a means to explore the SEED-ROMP of larger rings at a later date.

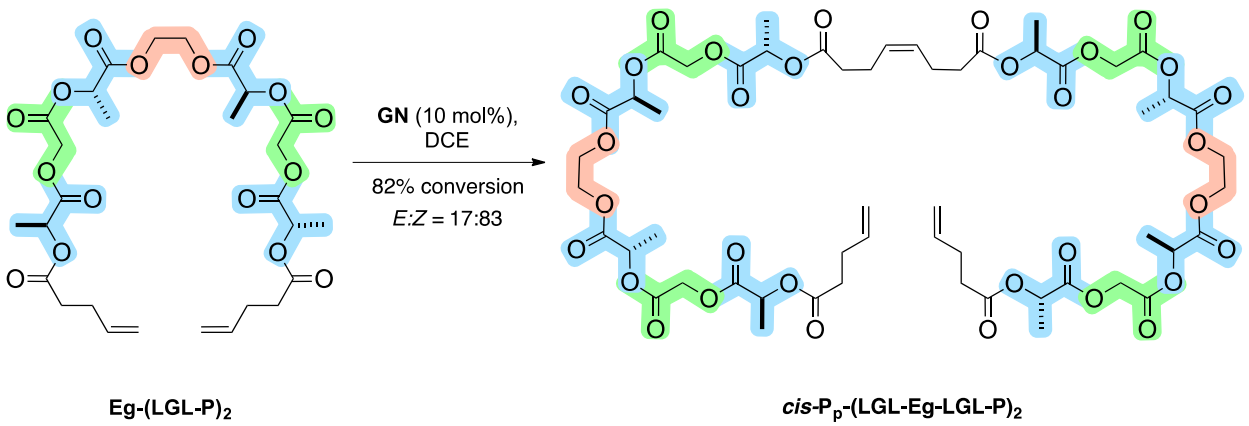

Scheme 13. *Cis*-selective homodimerization of **Eg-(LGL-P)$_2$**.

Shortly after the optimization series was undertaken, Grubbs and coworkers published examples of *cis*-selective cross metathesis and RCM of more functionally complex peptidomimetics.[94] They noted that cross-metathesis reactions occurred best at higher concentrations (0.1-0.4 M) and provided materials with 60% conversion, nicely paralleling what was observed in our incidental homodimerization reaction. In their hands, resin-bound 21-membered peptidomimetics were obtained through RCM with good conversions (70-80%) and *Z*-selectivities (>90%) when 10 mol% or 2×10 mol% catalyst were used. Both our results and those of the Grubbs group demonstrate clearly that high functional group tolerance and *Z*-selectivity can be expected with catalyst **GN**, even when carrying out reactions on large and bulky oligomeric material.

2.2.7 Use of scavenger resin to remove quenched ruthenium species

The macromonomer samples obtained through RCM were of excellent purity for the ED-ROMP and SEED-ROMP projects described herein. However, we foresaw that later stages of this

research project would necessarily involve microparticle fabrication and *in vivo* histology studies similar to the ongoing SAP-PLGA project. In an effort to address the presence of heavy metals in metathesis samples, we sought out an efficient purification method. Oral absorption of Ru is low (up to 3.5% in rats) and acute and genetic toxicity studies suggest that it is less toxic than platinum species such as the chemotherapeutic cisplatin.[131] For pharmaceutical purposes, the FDA limits ruthenium in excipients and drug substances orally (5 ppm, 100 μg permitted daily exposure) and parenterally (0.5 ppm, 10 μg permitted daily exposure).[132] With good solubility in CH_2Cl_2 and high catalyst contamination (10 mol%), we decided that this would be the ideal stage for targeted Ru removal. True to our synthetic approach, we desired a highly general and scalable method to achieve this. Though crude material was subjected to column chromatography after RCM, there was often a distinguishable Ru contamination in the otherwise colorless samples on large scales. Further purifications decreased the residual Ru, but this process is highly inefficient with regards to time cost and solvent waste.

We selected the mercaptopropyl QuadraSil®MP resin, which was reported to sequester >99% residual Grubbs catalyst (< 5 ppm Ru) and to be easily removed by filtration.[133] Resin was added (50 equiv with respect to catalyst) to a solution of unpurified RCM material in CH_2Cl_2 (0.01 M) and vigorously stirred overnight. All sequestered Ru contaminants settled to the bottom of the vial and could be easily removed by passage through a pre-rinsed syringe filter (Figure 11D). Resulting samples were colorless. Use of this resin in such proportions may be cost prohibitive with multi-gram scale RCM, but carrying out the same protocol with even 5 equiv. of resin resulted in a dramatic reduction of Ru content (Figure 11C). Once concentrated, crude samples could then be purified by column prior to polymerization.

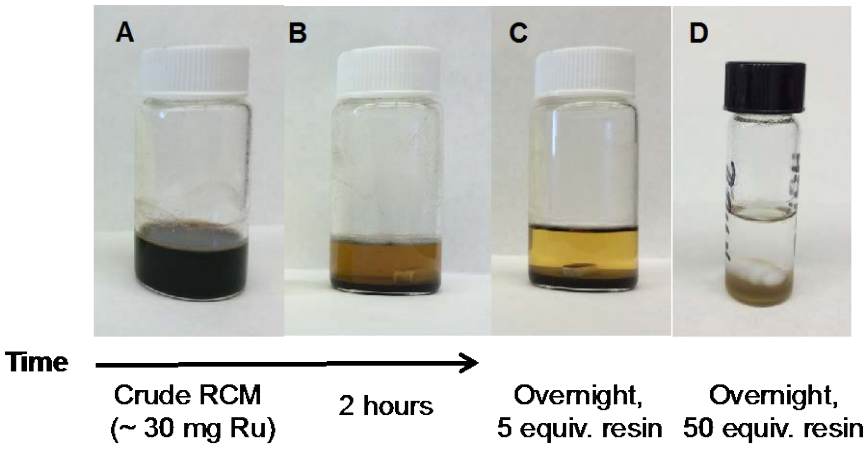

Figure 11. Use of resin to sequester Ru contaminants over time following RCM.

2.3 SELECTIVITY-ENHANCED ENTROPY-DRIVEN RING-OPENING METATHESIS POLYMERIZATION

ED-ROMP of the ring-closed macrocycle was of great interest to us and proved highly successful with both *cis*- and *trans*-macromonomers. This section will first explain how reactions were monitored and analyzed during polymerization. Then we will describe the ED-ROMP studies carried out in our group, starting with a brief summary of results for the ED-ROMP of *trans*-macromonomers carried out by Ryan Weiss.[22] Finally, a thorough examination will be detailed for the unprecedented SEED-ROMP behavior observed when ***cis-cyclic*-Eg-(LGL-P)$_2$** was used.

2.3.1 Monitoring reaction outcomes during ED-ROMP

Reaction progress could successfully be monitored during the course of ED-ROMP experiments through aliquot removal and a subsequent ethyl vinyl ether (EVE) quench.[87] A significant challenge for polymeric analysis by NMR is that conformational flexibility, high viscosity, and sequence scrambling often leads to substantial peak broadening. As discussed previously, sequenced PLGAs have well-resolved spectra as a result of conformational bias in polymer microstructures. Conformational bias is extended to these ED-ROMP materials despite the palindromic sequence modification and alkyl chain incorporation.

As in prior PLGA studies, the peaks corresponding to **G**-methylene protons were essential for examining reaction progress. While this method provides a good estimate of monomer depletion, it should be noted that MCO formation due to ring-chain equilibrium confounds the analysis, as larger MCOs have peaks that overlap with those of the polymer. Therefore, % conversion values calculated in this way are better understood as a comparison of the relative amounts of unreacted monomer to polymer and large MCOs. When the polymer was exposed to catalyst in high dilution conditions to maximize MCO formation, it was estimated that the monomer was by far the most stable compound and represented 93% of the mixture at equilibrium. The deviation for conversion calculations due to the contribution from large MCOs is therefore minimal. This outcome is discussed in further detail in Section 2.3.6. Estimated conversion and *E:Z* ratios of macromonomer were determined at each stage of the polymerization as shown below in Figure 12.

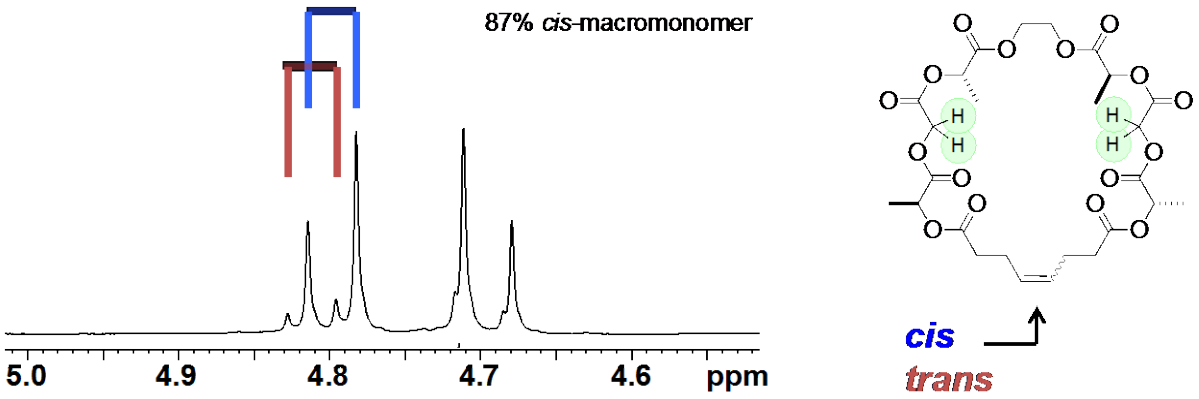

Figure 12. Macromonomer *cis*-to-*trans* ratios can be determined by comparing **G**-methylene ^{1}H-NMR peaks.

As in previous PLGA studies, polymeric samples also gave easily identifiable NMR spectra. Individual peaks were sharp and resolved without any additional purification following the polymerization. A crude NMR following the SEED-ROMP of ***cis-cyclic*-Eg-(LGL-P)$_2$** is shown below in Figure 13. Ratios of the *cis*-to-*trans* isomer ratio in polymer samples were determined by examining olefinic peaks g (5.4-5.5 ppm) because **G**-methylene peaks for these isomers had coalesced. Polymerizations had such large DPs that end groups could not be observed by NMR.

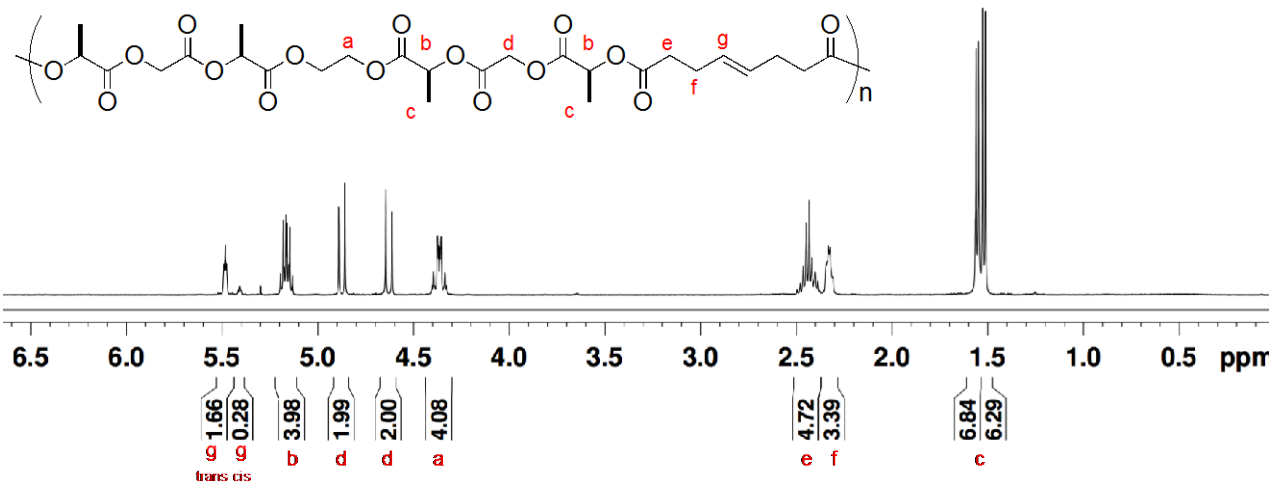

Figure 13. ^{1}H-NMR of unpurified polymer following the SEED-ROMP of ***cis-cyclic*-Eg-(LGL-P)$_2$**.

Molecular weights and dispersities were determined using gel permeation chromatography (GPC), a form of size exclusion chromatography that separates components based on their hydrodynamic volumes. Earlier elution times correspond to higher molecular weight materials, and narrow peak widths correspond to decreased dispersity. Conversion of monomer to polymer was also apparent in each sample. An example is shown below, where the polymerization of ***cis-cyclic*-Eg-(LGL-P)$_2$** over time can be clearly observed (Figure 14).

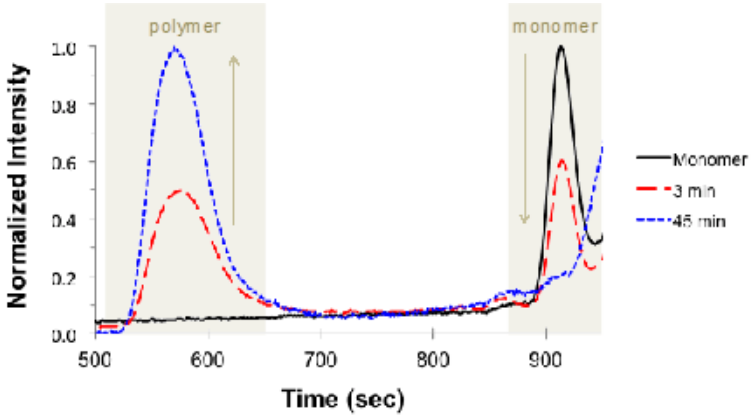

Figure 14. Representative GPC curves demonstrating SEED-ROMP progress.

2.3.2 Summary of results for the ED-ROMP of *trans*-macromonomers

Initial polymerization studies were carried out by Ryan Weiss and involved the ED-ROMP of *trans*-macromonomers prepared through the **G2**-mediated RCM described above. These experiments clearly demonstrated outcomes that we had predicted, and in some respects exceeded our expectations for polymerization control.[22] Polymeric sequences were retained in all examples (**LGL-P**, **LGL-B**, **LC-P**, **LLC-P** variations) and functional group tolerance for all

sequences was apparent. Standard conditions of 1.25 mol% **G2** catalyst and 0.7 M CH_2Cl_2 were used to obtain polymers with M_n 26-50 kDa and dispersities of 1.3-1.4. Following polymerization, hydrogenation over Pd/C reduced internal olefins to yield completely saturated alkyl chains between repeating units. A representative example for the ED-ROMP of ***trans-cyclic*-Eg-(LGL-P)$_2$**, is shown below in Scheme 14 with each component of the segmer shaded for clarity.

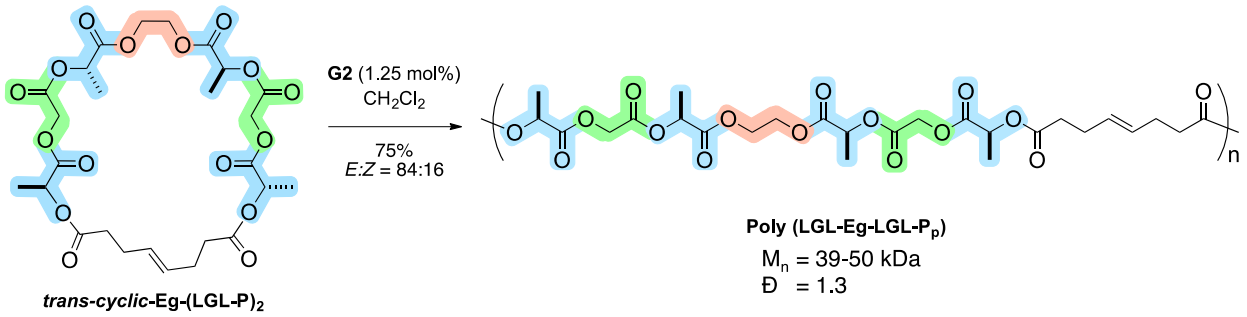

Scheme 14. ED-ROMP of ***trans-cyclic*-Eg-(LGL-P)$_2$**.

As theoretically predicted, monomer conversion increased rapidly at the onset of the reaction and a ring-chain equilibrium point was reached after 2 h (Figure 15). Molecular weights also rose rapidly at the early stages of the polymerization, but suffered as the reaction continued due to apparent increase of secondary metathesis. For instance, in the ED-ROMP of ***trans-cyclic*-Eg-(LGL-P)$_2$**, molecular weights peaked at 50 kDa after 30 min when monomer conversion was at 53%. After that point, secondary metathesis began to compete more aggressively with propagation and M_n decreased. Concurrently to this, Đ increased from 1.15 to 1.29, reflecting a more heterogeneous population of chain lengths. Despite this increase, dispersities remained well below the theoretical value of 2 and significantly lower than many previously reported

experiments.[44] Reactions were stopped once maximum conversion had been maintained for 2-3 hours to maintain lower dispersity samples. Additionally, the lifetime of **G2** is presumably too short for the time required to achieve equilibrium.

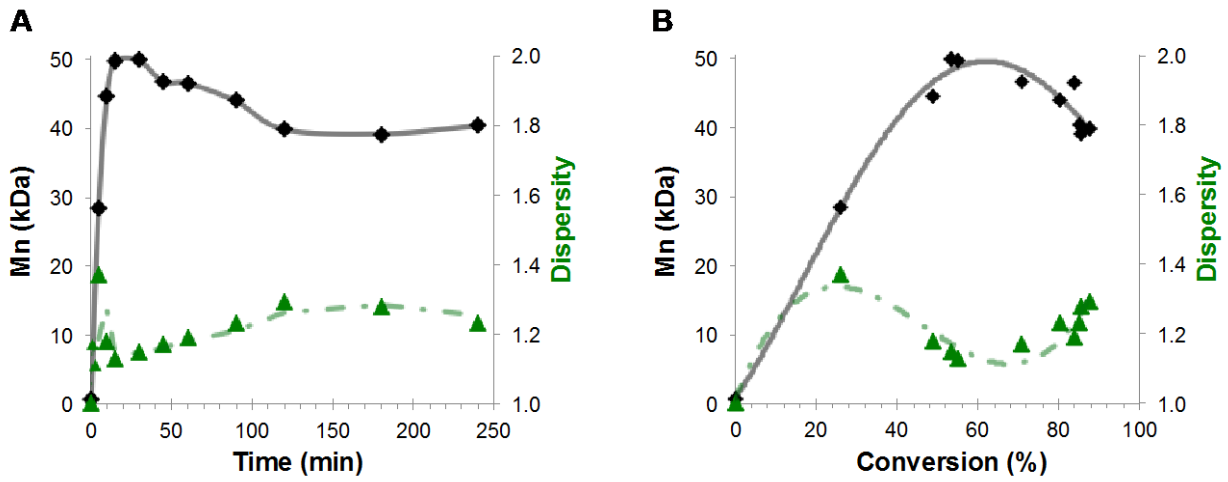

Figure 15. Molecular weight (solid black) and dispersity (dashed green) as a function of time (A) and % conversion (B) for the ED-ROMP of ***trans-cyclic*-Eg-(LGL-P)$_2$**.

A degree of molecular weight control was observed when [M]/[cat] ratios were adjusted at four intervals across a range of 20-125 in the ED-ROMP of ***trans-cyclic*-Eg-(LLC-P)$_2$**, but deviations from theoretical molecular weights were clearly apparent (Figure 16). In a perfectly living system, for instance, one would expect a doubling of [M]/[cat] to result in a doubling of polymer molecular weight. We are uncertain at this time as to the cause of non-linear deviations from predicted M_ns when [M]/[cat] ratios are adjusted. The phenomenon appears to be independent of secondary metathesis as dispersities for the polymers were consistent (~1.3) for all of the experiments. The deviation, wherein molecular weights are higher than theoretically

predicted at high catalyst loadings and lower than theoretically predicted at lower catalyst loading has also been previously observed by other groups during ED-ROMP.[88]

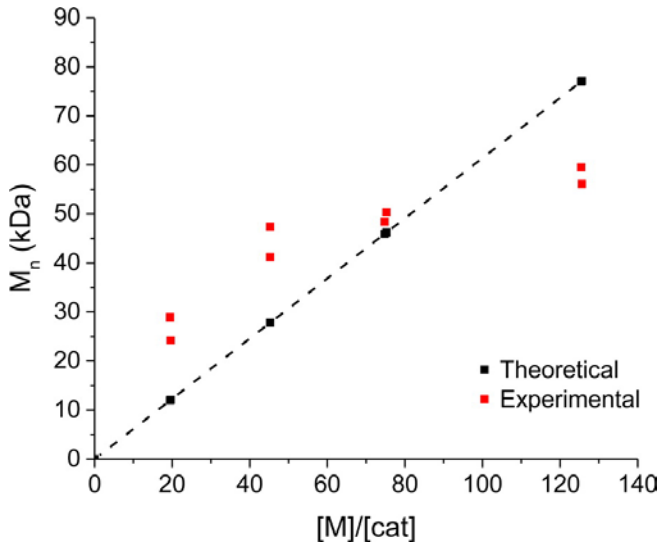

Figure 16. Adjusting monomer to catalyst ratios influences molecular weights obtained during ED-ROMP. *Reprinted with permission from The American Chemical Society, Ref. 22, copyright 2015.*

Overall, these preliminary ED-ROMP experiments yielded polymers with moderate control of molecular weights and complete sequence retention. Most importantly, they demonstrated the generality of the method; results were highly reproducible and ED-ROMP was successful regardless of alkene tether length or variations in scale or macrocycle ring size. Dispersities were comparable to those obtained in the SAP method, but we now were able to consistently access a higher molecular weight regime for our polymeric materials.

We also saw that there was significant potential for improvement through use of SEED-ROMP. ED-ROMP of *trans*-macromonomers did not produce polymers with as much molecular weight control as was ideal. The non-linear [M]/[cat] plot demonstrated that targeted molecular

weights may not be possible in new sequences without prior [M]/[cat] studies. Further, improvements in dispersity would enable polymerization to block architectures.

2.3.3 Low concentration manipulation of ring-chain equilibrium during ED-ROMP

Prior to carrying out SEED-ROMP experiments, a NMR scale competition experiment was devised for a 50:50 mixture of ***cis-cyclic*-Eg-(LGL-P)$_2$** and ***trans-cyclic*-Eg-(LGL-P)$_2$**. An automated time course experiment was developed using a custom delay schedule spanning a 5h period. Our goal was to monitor consumption of monomer in the initial stages of the reaction to gauge reactivity differences between *cis*- and *trans*-isomers. The dilute solution required for NMR analysis would slow reaction kinetics at crucial early stages of the reaction. We understood that the effects of ring-chain equilibrium and secondary metathesis at such dilution would highly favor oligomer formation rather than polymer. Experiments carried out by Gross and coworkers showed that oligomers predominated in ED-ROMPs carried out with their samples in concentrations <0.05 M.[88] Whether polymer or oligomer formed was not an immediate concern for this experiment, though, as bias towards *cis*-macromonomer consumption would likely still be evident.

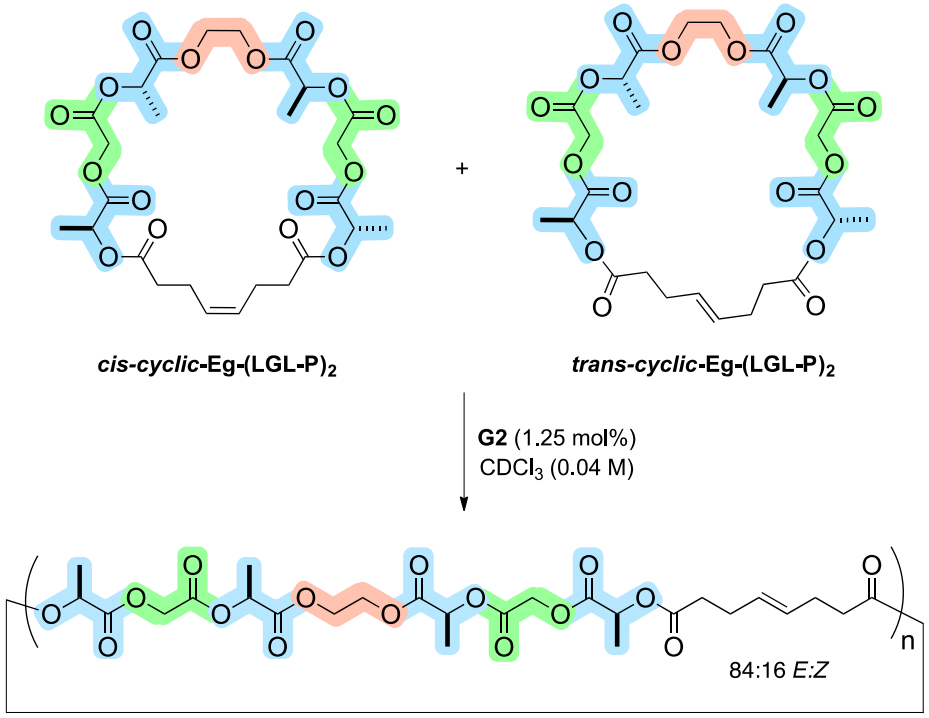

Scheme 15. Competition experiment using *cis*- and *trans*-macromonomers.

As expected, the *cis*-fused macrocycle reacted quickly and equilibrium was established after 1h to yield a mixture of metathesis products with ~16% *cis*-olefin content. While *cis*-monomer consumption could be directly observed through the reaction, *trans*-monomer peaks were unfortunately not differentiable from those of the products (Figure 17). We would expect **G**-methylene peaks for a highly unconstrained system (i.e. those of larger MCOs) to be set far apart, as seen in the homodimerized material and the polymer. Indeed, small peaks in that region did appear at longer reaction times. We were uncertain at what threshold in MCO size (n in Scheme 15) this peak shift would occur. The results of this experiment nonetheless showed that the significant preference in MCO size is very small when ring-chain equilibrium dominates. While it did not give us a clear determination of *cis*/*trans* reactivity differences as we had hoped, it corroborated later cyclodepolymerization experiments in which the ring-chain equilibrium was

manipulated in the opposite direction. Later MALDI analysis of samples that had reached ring-chain equilibrium showed that the overwhelming preference in MCO ring size was n = 1. What we had likely achieved in this preliminary reaction was therefore simply a ring-opening followed by a *trans*-selective ring-closing reaction along with a statistical distribution of MCOs with n>1.

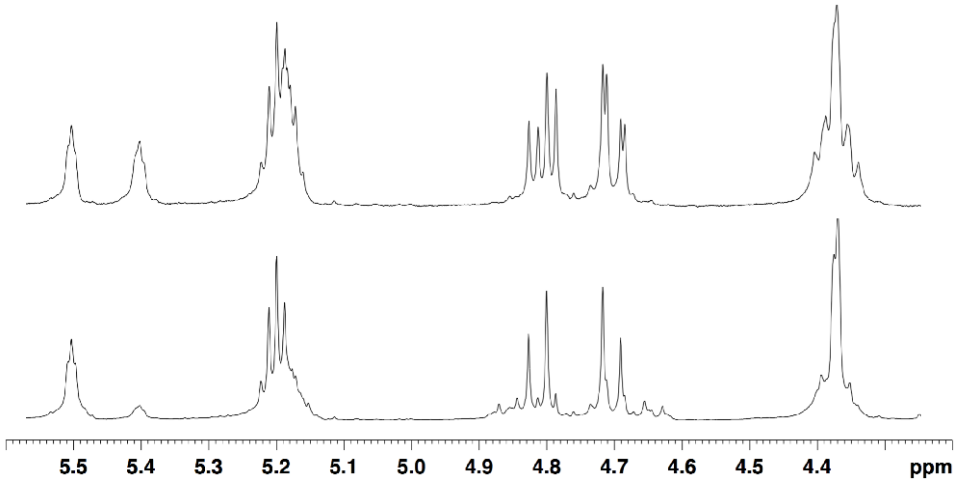

Figure 17. Reaction of a ~50:50 isomeric mixture of macromonomers (top) when exposed to **G2** in dilute conditions (bottom).

2.3.4 Kinetics study of selectivity enhanced ED-ROMP

With the *cis*-macromonomer in hand, we examined its behavior when exposed to 1.25 mol% **G2** at high concentration (0.7 M). Excitingly, the polymerization under these conditions appeared to enter a selectivity-enhanced regime as we had hypothesized. Visual inspection alone showed a dramatic improvement in the rate of polymerization when ***cis-cyclic*-Eg-(LGL-P)$_2$** was used. The reaction solution became an immobile gel after just 2 min and conversion reached 89% after only 10 min (Figure 18). This change in physical appearance was in stark contrast to the *trans*-macromonomer experiments, where 1 h was required for similar viscosity changes to be

observed and 2 h were required for 88% conversion to be achieved. Direct overlays of reaction outcomes for ED-ROMP and SEED-ROMP are shown in the following section.

Figure 18. Sample mixtures became gelled within 2 min of SEED-ROMP.

Examination of very early and very late time points for SEED-ROMP gave us insight into the respective degree of kinetic and thermodynamic enhancement of this reaction. As we had hoped, the increased rate of propagation appeared to decrease the incidence of secondary metathesis in the course of the reaction. Dispersity was maintained at 1.1 and molecular weights exceeding 60 kDa (Table 4). When the polymerization was allowed to continue for 4 h, conversion exceeded 95%, M_n was maintained at 60.0 kDa, and dispersity was an unprecedentedly low 1.11. To the best of our knowledge, this represents the highest degree of living character that has ever been observed in an ED-ROMP.

Table 4. Results for the SEED-ROMP of ***cis-cyclic*-Eg-(LGL-P)$_2$** at selected time intervals.

Entry	Time (min)	% conversion	M_n (kDa)	M_w (kDa)	DP	Đ
–	0	0	0.603	0.603	1	1.0
1	1	25.1	51.4	60.1	85	1.20
2	3	66.8	61.8	68.8	103	1.11
3	5	71.7	61.6	68.9	102	1.12
4	10	88.8	65.8	72.0	109	1.10
5	15	87.2	60.5	67.3	100	1.11
6	20	90.7	59.4	66.4	99	1.12
7	30	91.8	62.2	69.0	103	1.11
8	45	93.2	61.4	68.7	102	1.12
9	60	87.5	57.7	64.1	96	1.11
10	90	94.9	57.1	64.4	95	1.13
11	120	95.5	57.6	64.0	96	1.11
12	180	95.8	55.3	62.0	92	1.12
13	240	95.8	60.0	66.8	100	1.11

Visualization of data from this kinetics study shows just how profoundly the performance of ED-ROMP was improved (Figure 19). Molecular weights increased rapidly at the earliest stages of the reaction and only suffered ~6 kDa of mass reduction by the time the reaction was quenched at 4 h (Figure 19A, B). Dispersity increases were not observed at prolonged reaction times as in previous experiments, which is suggestive of minimal secondary metathesis (Figure 19A and B, green). GPC peaks remained monodisperse over all time points although fluctuations in molecular weights could easily be seen (Figure 19E). An aliquot left for 2 days prior to quenching displayed additional deterioration with respect to molecular weight and dispersity (54.4 kDa, 1.12, Figure 19E purple). The catalyst lifetime had certainly been eclipsed during

such a long reaction period, but the continued reaction compared with the 4 h time point suggests that total loss of catalyst activity was not the reason for observed secondary metathesis evasion.

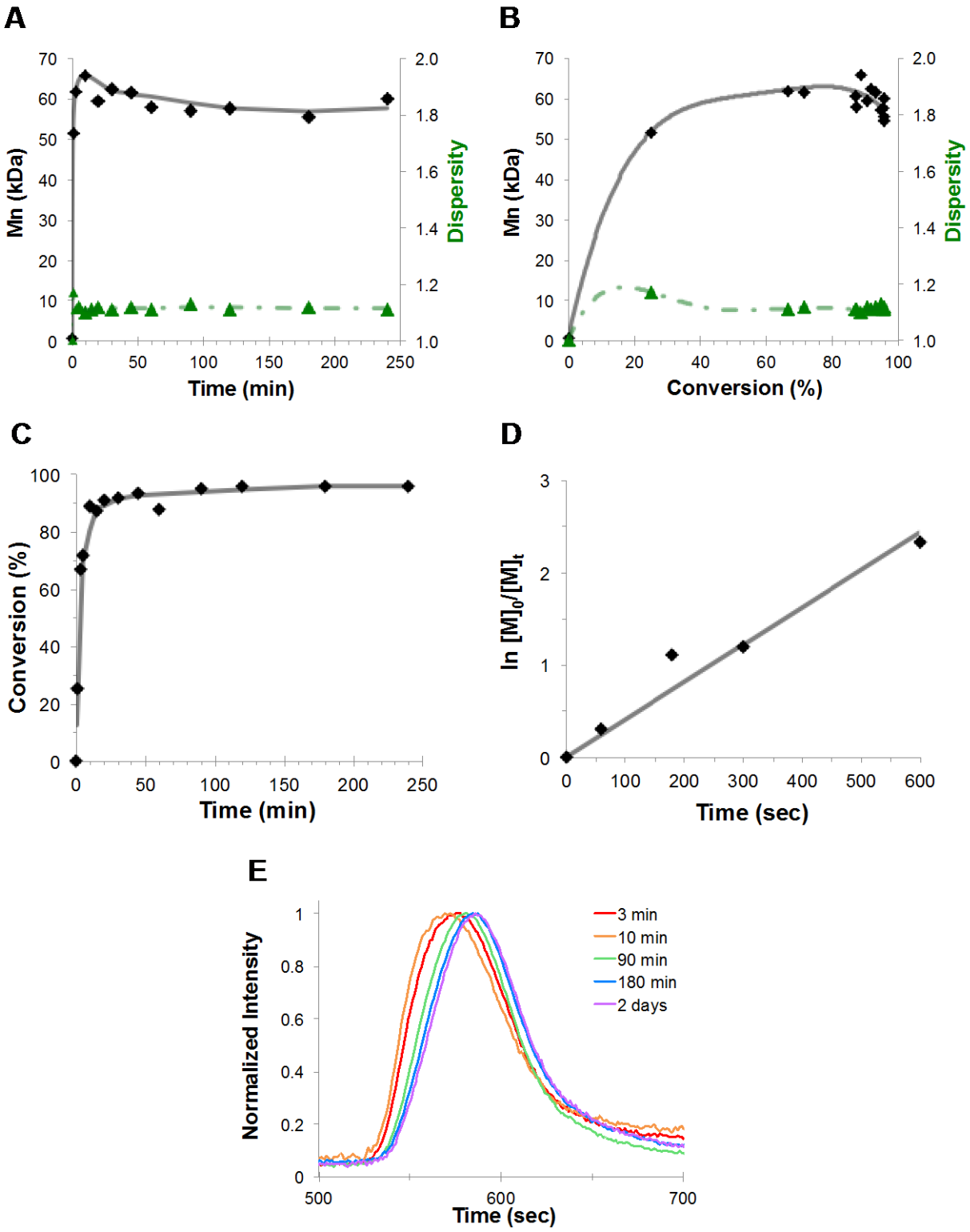

Figure 19. Visualizing SEED-ROMP data; M_n (solid black) and Đ (dashed green) vs. time (A) and % conversion (B); % conversion vs. time (C); rate law determination (D); overlay of GPC traces for selected time points.

Conversion was high but incomplete, owing to the equilibrium processes that are unavoidable during ED-ROMP. We expected a slightly lower conversion due to the ring-chain equilibrium, especially when compared to the ED-ROMP of the *trans*-macromonomer. At this time, it is uncertain why monomer depletion is so complete in this reaction. The rate of reaction is certainly faster, which would work to stymie secondary metathesis and encourage monomer conversion. However, the polymer formed through SEED-ROMP and ED-ROMP is identical, and should be subjected to the same ring chain equilibrium that would convert polymer to MCOs. Early catalyst deactivation is a possibility, although as noted above, the polymerization did continue in some capacity at longer reaction times.

Rapid chain propagation followed first order kinetics (Figure 19D). The rate of propagation for the reaction, 4.1×10^{-3} s^{-1}, was determined using Equation 3 to plot $ln\left(\frac{[M]_0}{[M]_t}\right)$ over time (Figure 19D). A linear correlation was observed until monomer became too depleted at 89% conversion (t = 600s). The rate obtained is within a range expected for ED-ROMP, and is an order of magnitude less than for that of the ROMP of strained rings such as cyclooctene and norbornene, which have ring strain.[33,44,59,88,134,135]

Additional analysis of monomer consumption during SEED-ROMP revealed significant reactivity differences between ***cis-cyclic*-Eg-(LGLP)$_2$** and ***trans-cyclic*-Eg-(LGLP)$_2$**. All SEED-ROMP reactions were carried out with monomer having at least 87:13 *cis*- to *trans*-olefin ratios. The ^{1}H-NMR peaks correlating to **G**-methylene and olefinic protons were differentiable enough to compare isomeric ratios in the samples (Figure 12, Figure 19). In this reaction, the rate of *cis*-macromonomer consumption far exceeded that of *trans*-macromonomer in the starting mixture. So, although the monomer sample began with a *cis*-to-*trans* ratio of 87:13, the ratio had reversed to 35:65 after 10 min, becoming enriched in *trans*-isomer at higher conversions (Figure 20).

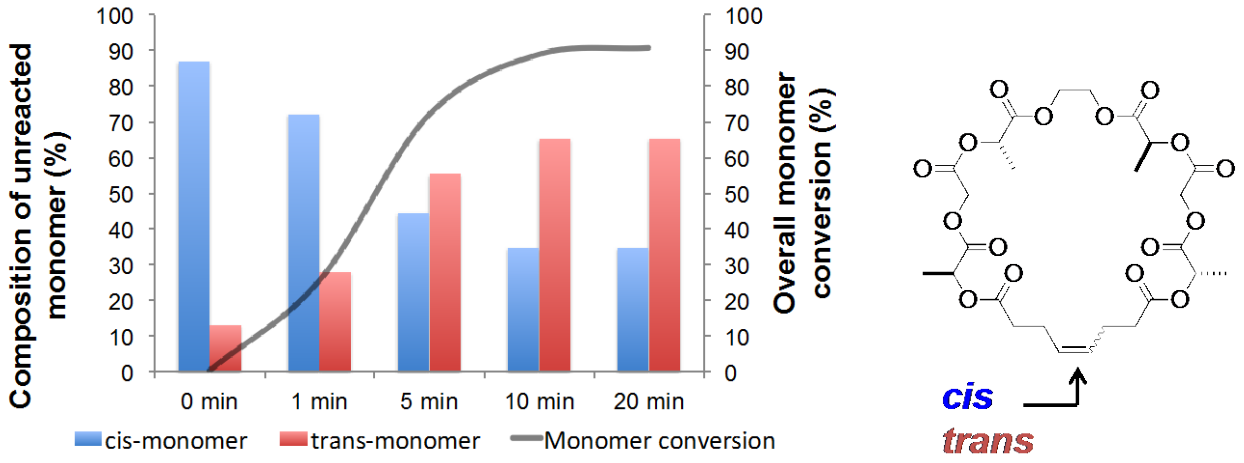

Figure 20. Remaining macromonomer becomes enriched in *trans*-isomer as conversion increases.

Ultimately in this project, we hoped to achieve molecular weight control in a range suitable for our group's ongoing PLGA studies (30-50 kDa). We and others had seen a non-linear relationship when catalyst amounts were altered during ED-ROMP, and we were curious what the molecular weight limitations of SEED-ROMP would be. In the ensuing SEED-ROMP experiments, molecular weight control was found to be linear over an extended range of catalyst loading, enabling M_ns between 40-75 kDa to be targeted. This result would only be expected in a highly controlled system with a number of active chain ends proportional to catalyst.[136] Molecular weights above theoretically predicted values suggest that the number of propagating chains is fewer than the moles of catalyst added. A sustained linear relationship for all experiments implies an unparalleled degree of molecular weight control can be expected across an expansive range of [M]/[cat]. The consistent deviation from theoretical values also suggests that a predictable fraction of catalyst is active in the initial stage of SEED-ROMP when the majority of monomer is consumed. Access to even greater molecular weights would likely be

relatively straightforward, but is beyond the needs of our group and the detection limits of the GPC and so was not pursued further.

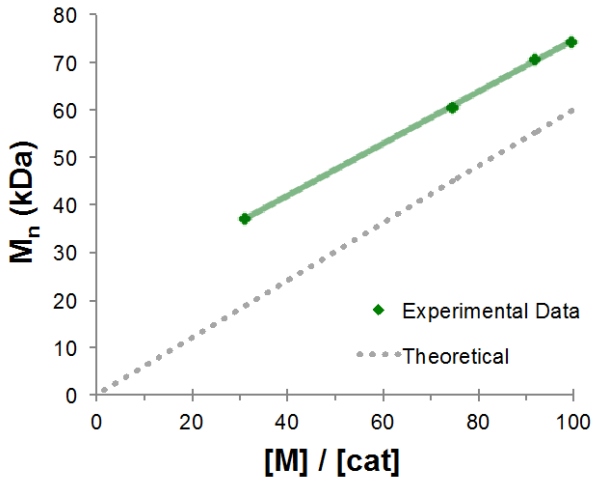

Figure 21. Predictable relationship observed when mol% catalyst was varied.

To further investigate the degree of livingness and the role of secondary metathesis in the polymerization, chain extension experiments were carried out. Dispersity values remained low throughout SEED-ROMP polymerizations, even at long reaction times. As noted above, letting the reaction continue after 4 h resulted in slight degradation of polymeric materials, seen through broadening dispersity and decreasing M_n. This continued reactivity showed that at least some of the initially activated chains remained active at longer periods of time. However, we wanted to unequivocally determine whether the lack of significant dispersity increases at longer reaction times was due to inherent bias of the SEED-ROMP system or if a significant number of active chains had been deactivated in earlier stages of the reaction.

Chain extension experiments would mimic block copolymerization, in which an initial monomer sample was allowed to polymerize for a period before a second batch of monomer was

added to the mixture (Scheme 16). In this case, the monomer used in both additions would be the same. The result of the experiment would be a lengthening of the active chains by an amount determined by the moles of monomer supplied in the second addition. If, for example, half of the active chains were quenched after the initial stages of the polymerization, then they would no longer be able to participate in SEED-ROMP when the second batch of monomer was added. The result would be a mixture containing two populations of polymer, each with narrow dispersities: one of M_n correlating to the monomer-to-catalyst ratio of the first addition, and one with a significantly higher M_n to account for the additional monomer provided. Ideally, a monodisperse population of chains at elevated molecular weights would be obtained instead. If this was the case, we could conclude that the high degree of living character in the system was the reason for the incredibly low maintained dispersities.

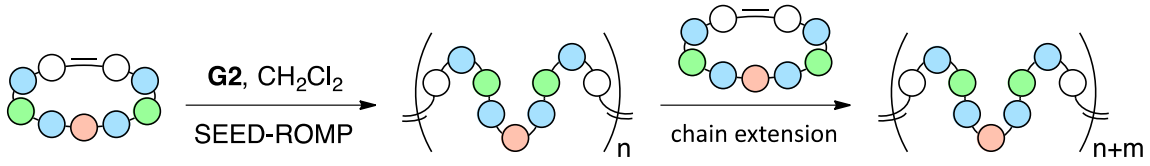

Scheme 16. Chain extension experiments lengthen chains by providing additional monomer for SEED-ROMP.

Initial ED-ROMP reactions were carried out with 1.25 mol% **G2** at 0.7 M CH_2Cl_2. After 10 or 30 min, an additional aliquot of monomer in 0.7 M CH_2Cl_2 was added to the reaction solution and allowed to stir for an additional 10 or 30 min. The experiment was first carried with only 10 min allowed for each phase of polymerization, but this resulted in incomplete conversion of monomer during chain extension. The polymer that resulted had a M_n of 74.3 kDa, which, when adjusted for monomer conversion, was only 0.4 kDa away from the experimentally

predicted M_n of Figure 21. The experiment was subsequently repeated using 30 min for each stage of the polymerization to encourage conversion of monomer. Allowing the monomer additional time to react during increased conversion to 91%. The molecular weight of the polymeric sample unfortunately fell into a range that is not well-resolved using currently available columns. The GPC peak remained monomodal following polymerization, with dispersities of 1.11 maintained in both experiments. A GPC overlay for the chain extension of **poly (LGL-Eg-LGL-P_p)** is shown below, demonstrating the increase in molecular weight without change in dispersity (Figure 22). These chain extension experiments support our claim of living character for the polymerization, they corroborate the catalyst variation experiments, and they also provide an alternate method to obtain high molecular weight polymers or copolymers.

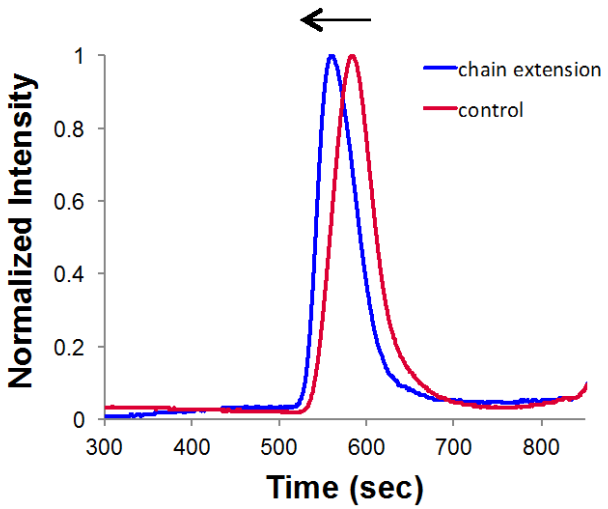

Figure 22. Molecular weight increases and dispersity is maintained during chain extension experiments.

The results from SEED-ROMP improve greatly on prior experiments of ED-ROMP using *trans*-macromonomers. Conversion of monomer during the reaction was rapid and molecular weights were obtained in a highly predictable manner based on monomer conversion and

[M]/[cat] ratios across an expansive molecular weight range. Linear first-order kinetic behavior was observed and the rate constant of chain propagation (k_{pr}) is in the range expected for an ED-ROMP. Very low dispersity polymers were obtained in all experiments regardless of scale, catalyst loading, method of monomer addition or conversion. Molecular weights diminished and dispersity increased over longer reaction periods by a very small amount, as would be expected, but these effects were not significant. Finally, polymers were well-defined and showed no signs of sequence scrambling by ^{1}H-NMR.

2.3.5 Comparison of ED-ROMP outcomes when using *cis*- or *trans*-macromonomer.

Although specific points of comparison have already been addressed in the previous section, we thought it would be beneficial to see a visual comparison of data obtained when *cis*- or *trans*-macromonomer was used. Presented here are plots overlaying data regarding the molecular weight, conversion, dispersity and initial rate of SEED-ROMP and ED-ROMP (Figure 23). In these figures, the profound level of kinetic bias introduced into the reaction is clearly visible.

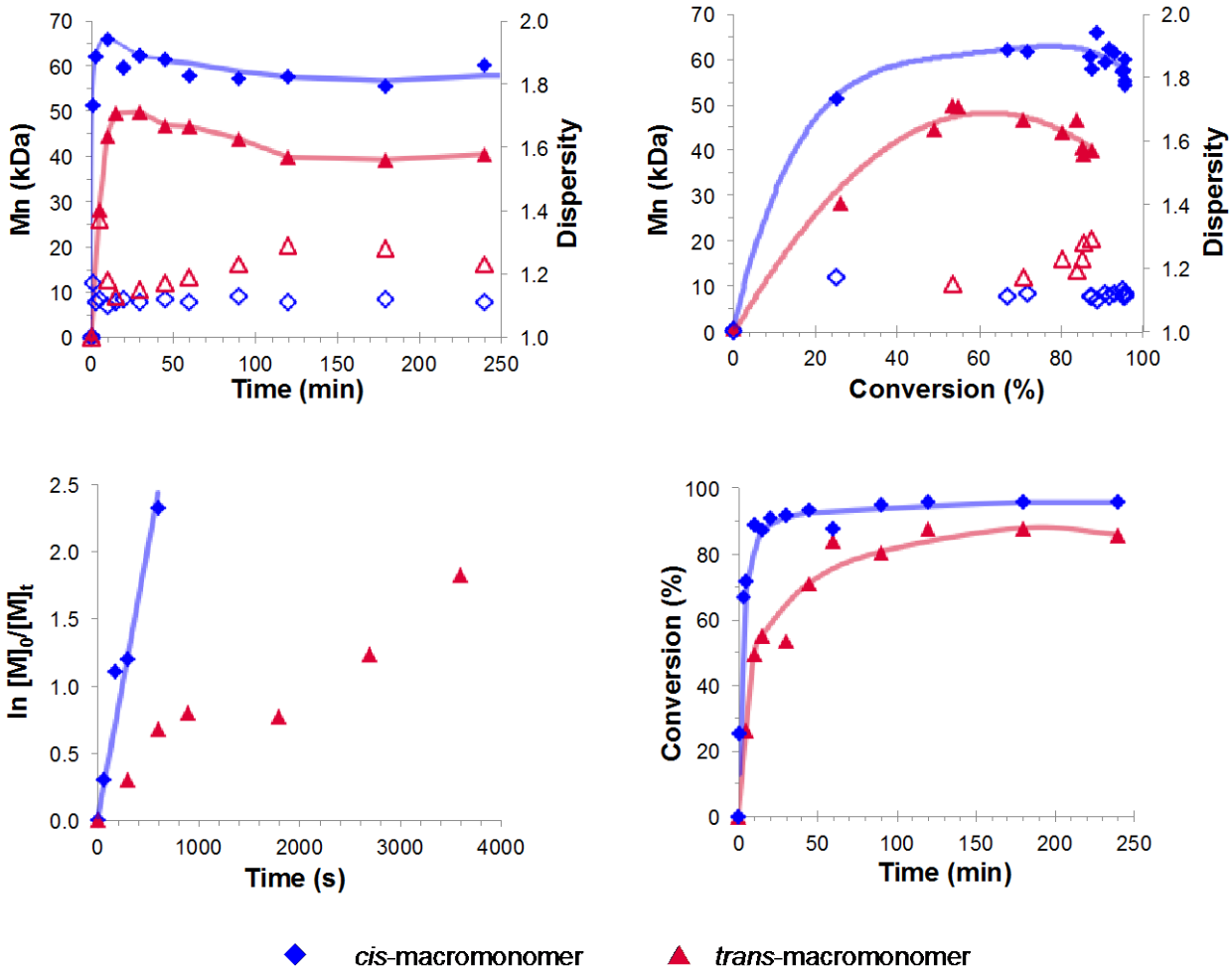

Figure 23. Comparison of SEED-ROMP and ED-ROMP when using *cis*- and *trans*-macromonomers, respectively.

2.3.6 Manipulating the metathetical equilibrium through ADMET and CDP.

We next moved to compare the sequential RCM and ED-ROMP method to alternative pathways and methodologies for obtaining sequenced copolymers. Our goal was to perform preliminary experiments to gauge the reactivity of **Eg-(LGL-P)$_2$** under ADMET conditions and to determine whether polymeric materials could be recycled back to monomer through CDP (Figure 4).

Starting from the open chain α,ω-diolefin **Eg-(LGL-P)$_2$**, one can envision direct formation of **poly (LGL-Eg-LGL-P$_p$)** through ADMET (Scheme 17).

As mentioned previously, in those few examples where ADMET and ED-ROMP were both used, ED-ROMP gave access to higher molecular weight polymers.[40,55,71] Additionally, ADMET often requires more extensive optimization for every substrate to reach the desired conversion, dispersity, and molecular weight. It is a step growth polymerization that engages in continuous cross-metathesis, average molecular weight increases slowly relative to conversion so high conversions are required to obtain longer chain lengths. Similar to ED-ROMP, ADMET suffers from weak thermodynamic driving force for polymerization due to its enthalpically neutral bond formation. Elevated temperatures and ethylene removal can be used, but there is a significant barrier to higher molecular weight polymers without extensive optimization.

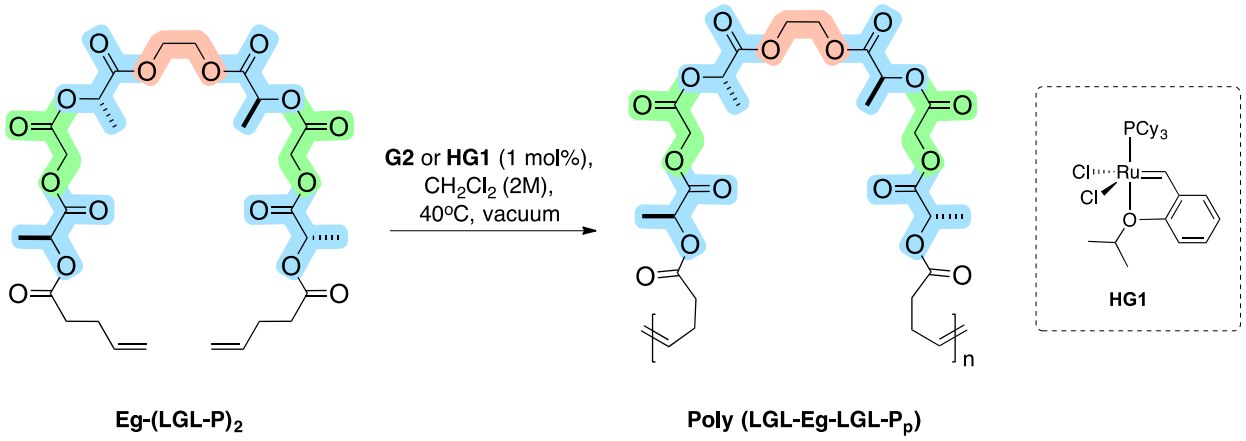

Scheme 17. ADMET of **Eg-(LGL-P)$_2$** using **HG1** or **G2**.

Hoveyda Grubbs 1st generation catalyst (**HG1**) has previously been used to obtain moderate molecular weight polymers through ADMET and was selected for the study.[137] In the early stages of the synthesis of **GN**, we had prepared **HG1** from **G1**, and so had access to large

quantities of that catalyst. A second reaction using **G2** would be carried out, although we noted that in some cases, increased olefin isomerization of monomeric and polymeric materials has been noted.[138-140] **Eg-(LGL-P)$_2$** was subjected to 1 mol% of either **HG1** or **G2** at high concentration in a sealed tube. Vacuum was applied to the vessel and the mixture was heated to 40 °C while stirring to encourage ethylene removal.[141] After quenching the reactions with EVE, the product mixtures were analyzed.

We found that a significant population of smaller chain sizes (DP 2, 3, 6) still predominated when either **GH1** or **G2** were used, indicating a very sluggish reaction. The reaction appeared slower when **G2** was used, and internal olefin isomerization was also observed. To counter the low reactivity of the monomer, longer reaction times and use of a higher boiling solvent could be used. Higher molecular weight chains represented only a very small fraction of the mixture and had an M_n of 43.1 kDa and Đ of 1.12, suggesting that optimization of the reaction could conceivably lead to an alternate route of access to **poly (LGL-Eg-LGL-P$_p$)**. Based on literature precedent, we would expect that moderate molecular weights and low dispersities would not be possible without significant optimization, and even then may not compare to that observed with ED-ROMP.[40,57,71,72] The most attractive use of ADMET for our purposes is as a tool to access macrocyclic monomers that are resistant to RCM conditions via CDP.

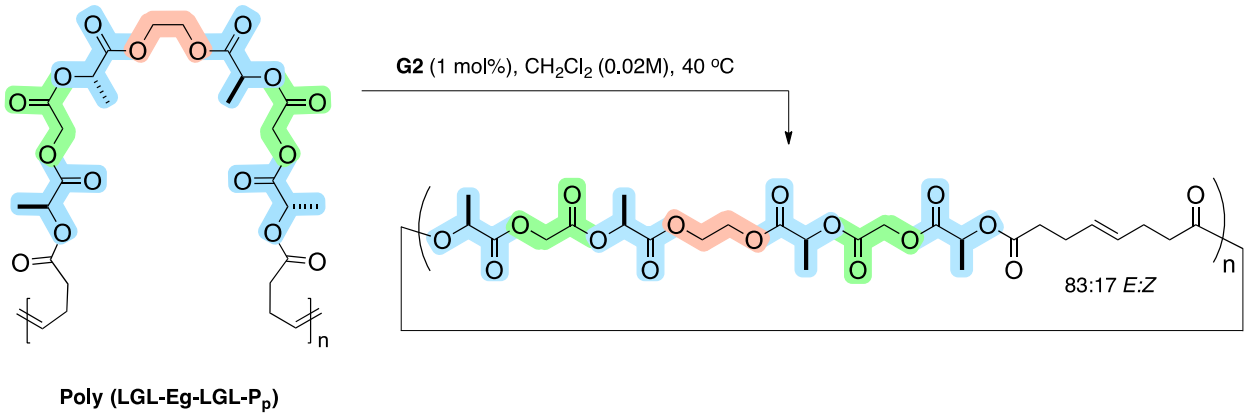

Poly (LGL-Eg-LGL-P_p)

Scheme 18. Cyclodepolymerization of **poly (LGL-Eg-LGL-P_p)** to produce a mixture of MCOs.

CDP allows for both the recycling of polymeric and oligomeric species back to their respective MCOs.[55,58,142] Assuming the CDP is complete, the product mixture will contain MCOs with little contamination by adventitious linear olefins. This would be ideal in a situation where RCM was impossible or where it yielded an inseparable mixture of α,ω-diolefin precursor and ring-closed product. Using a sample of **poly (LGL-Eg-LGL-P_p)** from earlier ED-ROMP studies, a dilute mixture was prepared using CH_2Cl_2 (0.02 M) and 1 mol% **G2**. The solution was allowed to stir at 40 °C for 8 h prior to quenching with EVE. The resulting NMR mirrored that of the dilute *cis-trans* competition experiment previously conducted, suggesting that equilibrium had been established (Figure 17, Figure 24).

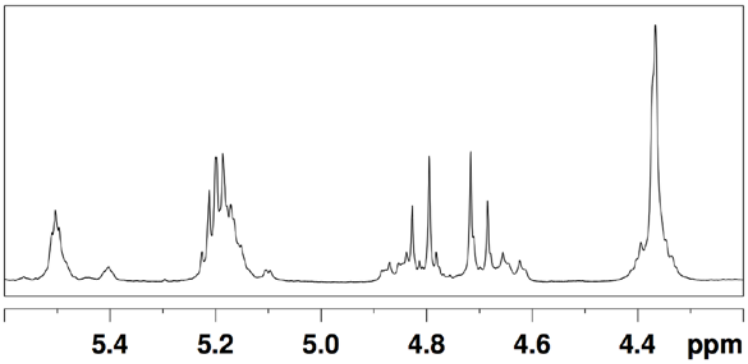

Figure 24. NMR of MCO mixture following cyclodepolymerization with **G2**.

The product mixture had a 83:17 ratio of *E:Z* products, which was also consistent with previous findings. Analysis of the ESI-MS shows that the masses of MCOs present in the product mixture heavily favor the macrocyclic species where n=1. Ratios of detected intensities for the peaks corresponding to n=1, n=2, and n=3 were approximately 93 : 7 : < 1. This strategy of recycling polymerized materials is ideal in situations where *trans*-macromonomer is desired, but it is not possible at this time to access the *cis*-macromonomer using this method. When CDP was carried out in the presence of up to 15 mol% **GN** in DCE at 60 °C, ***cis-cyclic*-Eg-(LGL-P)$_2$** was not obtained. This result is expected, given the steric constraints of the catalyst, which is known to have negligible reactivity with internal *trans*-olefins.[96,126,143]

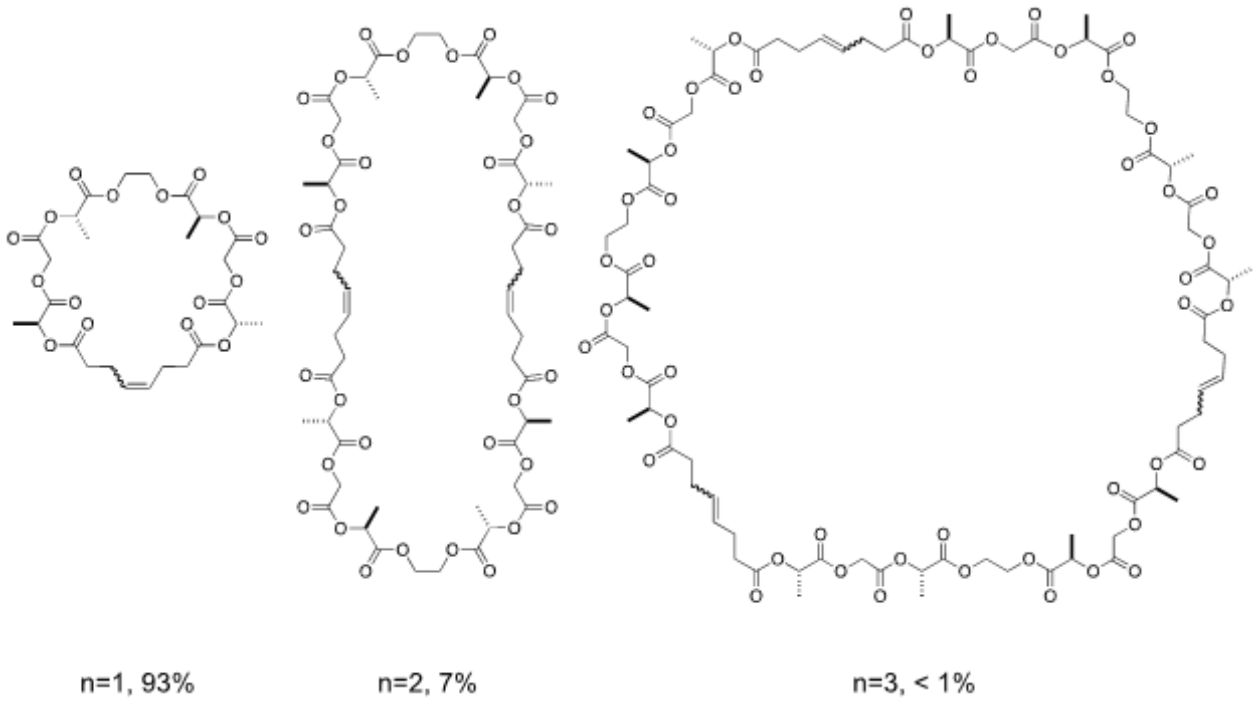

Figure 25. Cyclodepolymerization favors the formation of small MCOs.

2.3.7 Deactivation ED-ROMP using fast-initiating Grubbs' third generation catalyst

Following the ED-ROMP studies of ***trans-cyclic*-Eg-(LGLP)$_2$** and ***cis-cyclic*-Eg-(LGLP)$_2$**, we wanted to compare the results to those obtained when using DED-ROMP conditions. The unprecedented level of control we were able to achieve during SEED-ROMP led us to hypothesize that we had entered into the regime of molecular weight control typically only seen when using **G3** in ROMP. Specifically, the low dispersity and apparently linear relationship between molecular weight and monomer to catalyst ratio were similar to what would be expected in DED-ROMP, as discussed previously.

Exposure of ***cis-cyclic*-Eg-(LGLP)$_2$** to **G3** resulted in polymer with molecular weight and dispersity comparable to those observed in SEED-ROMP (58.2 kDa and 1.16, compare to Table

4). The polymerization occurred rapidly as anticipated, with the sample viscosity increasing to prevent stirring after only 2 min. Complete conversion was observed when the polymerization was quenched after 2 h. As in previous experiments, the molecular weight obtained was over 10 kDa higher than that predicted by monomer to catalyst ratio. Further molecular weight control studies were not performed, although a linear trend could be expected as described above. The final polymer resulting from DED-ROMP contained 86% *trans*-olefin, similar to ED-ROMP and SEED-ROMP polymers. When ***trans-cyclic*-Eg-(LGL-P)$_2$** was exposed to the same conditions, similarly high conversions and *trans*-olefin content were observed, although sample viscosity appeared to increase at a slower rate.

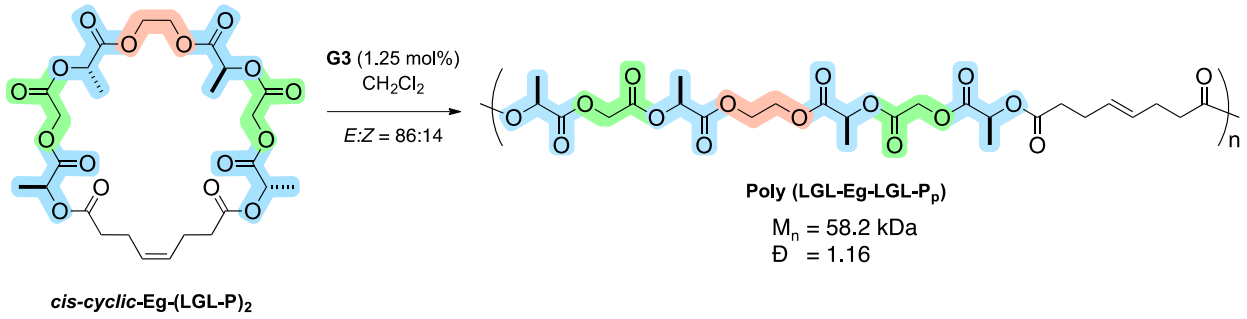

Scheme 19. DED-ROMP of ***cis-cyclic*-Eg-(LGL-P)$_2$** using **G3**.

Due to the nature of the catalysts used to perform SEED-ROMP and DED-ROMP, the mechanism of formation for these polymers is necessarily distinct. The high reactivity and selectivity of SEED-ROMP is founded on principles of kinetic and thermodynamic enhancement induced by the macrocyclic *cis*-olefin. Conversely, high reactivity and selectivity in DED-ROMP is primarily due to improvements in the ratio of k_i to k_{pr} for the catalyst itself. NMRs obtained mid-polymerization for these two distinctive reactions demonstrate this significant difference. As

shown in Figure 26, the consumption of *cis*-monomer is more rapid than *trans* during SEED-ROMP. As the reaction progresses, *trans*-monomer begins to dominate the remaining monomer pool. In DED-ROMP, *cis*-monomer depletion does not occur to such a degree, with 65% *cis*-monomer remaining at 86% conversion.

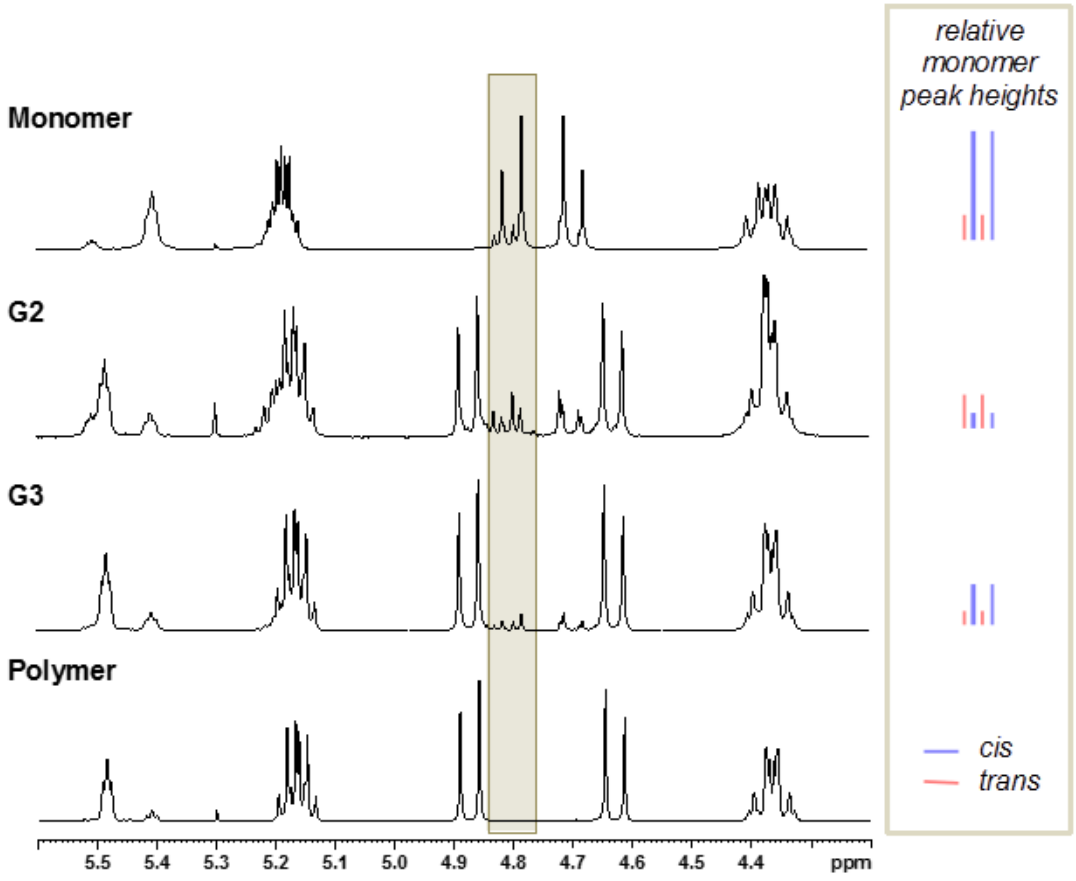

Figure 26. Conversion of *cis*-monomer is more rapid during SEED-ROMP than DED-ROMP. Monomer and final polymer samples are shown at top and bottom, respectively; NMRs corresponding to aliquots removed prior to complete conversion during SEED-ROMP (**G2**) and DED-ROMP (**G3**) are shown in the middle; relative peak heights corresponding to **G**-methylene protons are illustrated at right.

2.3.8 Rationalizing the selectivity enhancement observed during SEED-ROMP

The underlying source of selectivity enhancement that occurs during SEED-ROMP is presumably related to the improved ability of the *cis*-macromonomer to access the propagating catalyst.[83] In a collaborative effort with Dr. Peng Liu and Cheng Fang, we set out to computationally investigate and rationalize the phenomena. We compiled a series of model compounds, shown below in Figure 27, to enable comparison of both *cis*- and *trans*-macromonomers of varying sizes. This collaborative effort is still ongoing and therefore only preliminary findings are summarized in brief herein.

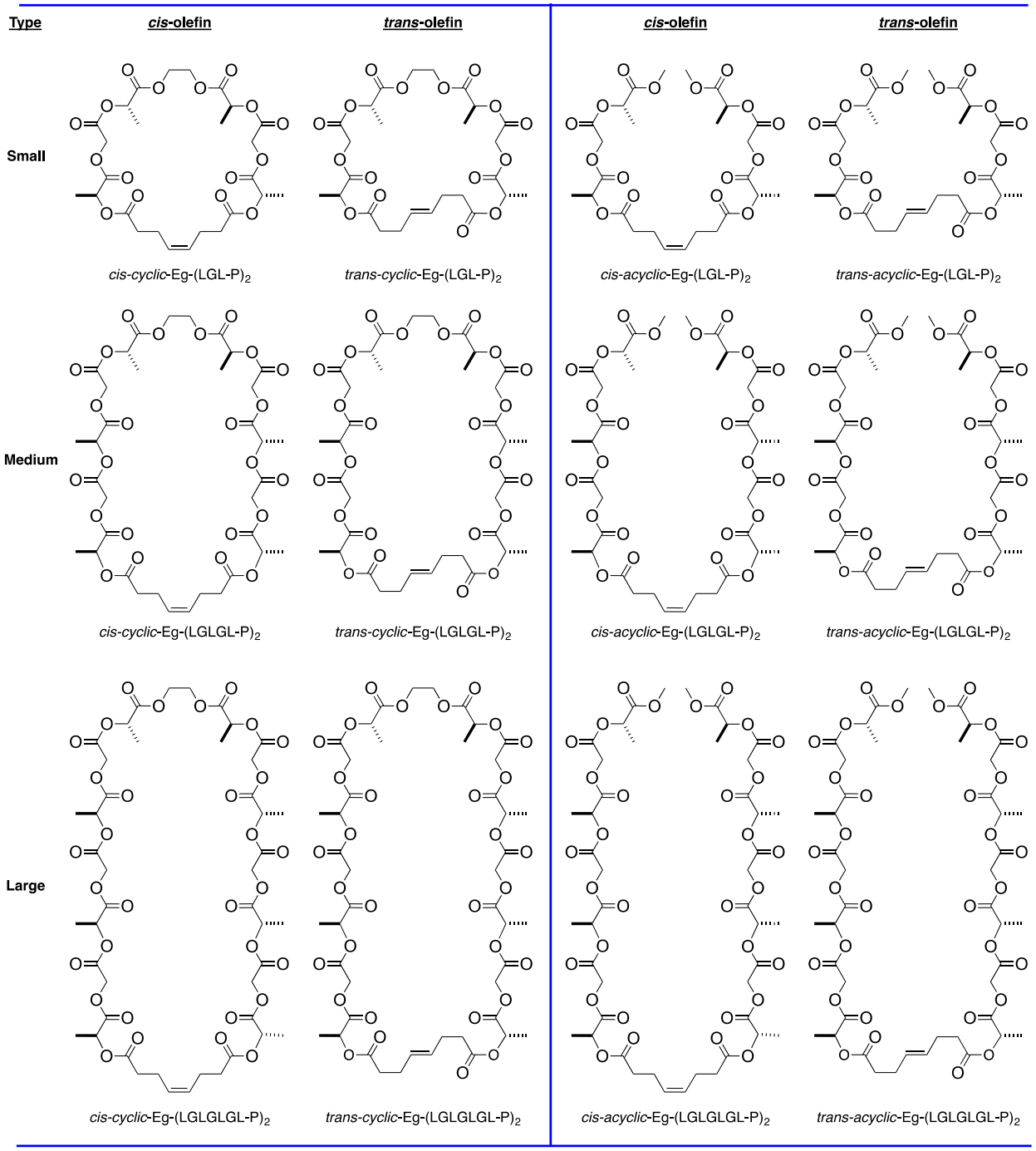

Figure 27. Monomer library for the computational analysis of ED-ROMP kinetics. Left: cyclic, right: acyclic.

Computational studies carried out by Dr. Liu and Mr. Fang suggest that the reactivity enhancement observed for ***cis*-cyclic-Eg-(LGL-P)$_2$** is due to the increased likelihood of the macromonomer to exist in a conformationally active state. The constrained nature of the

macromonomers in energy-minimized conformations limits the accessibility of internal olefins during metathesis, which necessarily has a significant effect on their respective abilities to engage in chain propagation. Further investigations confirmed that the activation energy required for [2+2] cycloaddition was highly dependent on the dihedral angle of the two C-C bonds adjacent to the olefin. It appears that increased populations of *cis*-macromonomers exist in metathesis-active conformations required for polymerization. More complete details regarding these findings will be published in the near future.

2.4 SEQUENTIAL ED-ROMP—ROMP BLOCK COPOLYMERIZATION

Once we had established the highly living character of SEED-ROMP, we next expanded the scope of our studies to include the formation of defined block copolymers. Block copolymer architectures are typically only accessible during living polymerizations because successful integration of both block components requires controlled chain extension.[84] Copolymerizations of non-living ED-ROMP scaffolds have been carried out previously but did not provide access to well-defined block copolymers. In their work to synthesize long chain polyesters, Duchateau and coworkers performed a tandem ED-ROMP—ROMP but obtained polymers with dispersities >2 and with little sequence control.[106] Contrary to previous efforts, we envisioned a one-pot ED-ROMP—ROMP protocol could be used to yield well-defined block microstructures controlled through the sequential addition of monomer components (Scheme 20).

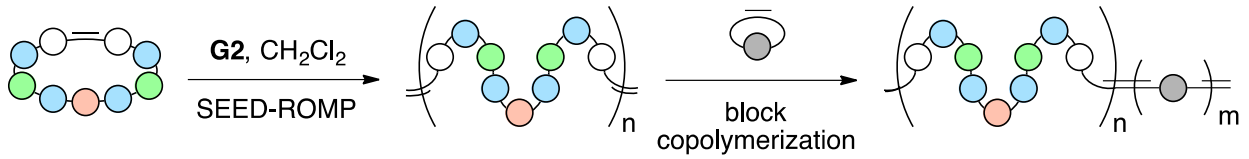

Scheme 20. Block copolymers formed through successive SEED-ROMP and ROMP.

ROMP was a mechanistically ideal pairing for the SEED-ROMP protocol because the two reactions could conceivably be carried out in one pot. In this process, SEED-ROMP would be allowed to occur prior to addition of a more reactive strained monomer for ROMP. Concentrations and catalyst loadings for the two reactions are highly compatible. Sequential addition would limit the opportunity for gradient copolymers to form, as might be the case if both monomers were exposed to catalyst simultaneously.[144] Relative ratios of each monomer incorporated into the copolymer backbone could be adjusted simply by altering feed ratios. As before, final molecular weights would be proportional to the amount of catalyst used (i.e. number of chains possible) and amounts of monomer added (i.e. DP possible for each block).

We had already demonstrated through chain extension experiments that a second polymerization reaction was possible following an initial SEED-ROMP with **G2**. If the second phase of metathesis polymerization was highly controlled, as in our chain extension experiments, a low dispersity "co" polymer would be produced. We could foreseeably use this strategy to carry out ED-ROMP reactions with two types of *pseudo*-PLGAs to make a true copolymer with tailored degradation patterns or cleavable pendant groups. In this preliminary study, we wanted to demonstrate that this principle could effectively be applied to monomers other than our *pseudo*-PLGAs. Typically, **G3** is used to obtain ROMP block copolymers due to the secondary metathesis that can be prevalent when using **G2**.[46,83,84,145] Because we had already shown that

molecular weight control could be maintained with a second addition of monomer, we did not prioritize low dispersity as much in these block copolymerizations as we had in previous experiments.

We proposed the use of norbornene (NBE) as a model system for ROMP due to its immense popularity and potential for functional group diversification. While we would be using nonfunctionalized NBE for these proof-of-concept experiments, its pharmaceutical applicability when fully functionalized has been well documented.[33,69,145-148] For instance, NBE polymers appended with a tripeptide arginine-glycine-aspartic acid (RGD) motif showed higher activity than the corresponding peptide in cancer-associated fibroblast inhibition.[149-151] Additionally, solubility properties can be tailored for copolymers through the use of NBE functionalized with a polyethylene glycol (PEG) chain.[152,153] Amphiphilic copolymers incorporating NBE-PEG and other polar groups have been shown to self-assemble into micelles with great success for applications such as drug delivery.[154,155] The significant precedent for appending groups such as a fluorophore, solubility-enhancing group, or cleavable drug to NBE makes this substrate highly attractive for our purposes (Figure 28).

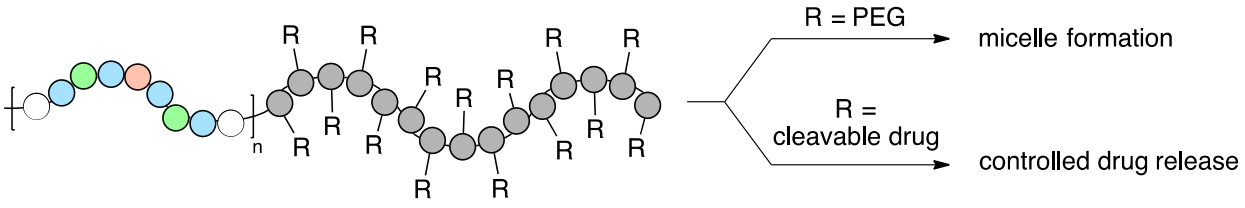

Figure 28. Copolymer with a ROMP block functionalized to incorporate drug or to enhance solubility properties.

Block copolymerization using a sequential SEED-ROMP—ROMP protocol was successful when ROMP occurred for short reaction times. Preliminary ROMP

homopolymerization experiments demonstrated that at longer reaction times, molecular weights plummeted and dispersities approached 2 as secondary metathesis took hold. Block copolymerizations were started with SEED-ROMP, which was carried out by exposing ***cis-cyclic*-Eg-(LGL-P_p)$_2$** to 1.25 mol% **G2** in 0.7 M CH_2Cl_2. After 10 min, 25 equivalents NBE in 0.7 M CH_2Cl_2 were added to the polymerization mixture. The ROMP was allowed to proceed for either 1 min or 5 min prior to quenching with EVE. An excess of monomer was added to encourage preferential block formation over secondary metathesis, and unreacted NBE could later be removed *in vacuo* due to its relatively low boiling point (96 °C). A control experiment was quenched after the initial 10 min SEED-ROMP and delivered **poly (LGL-Eg-LGL-P_p)** with molecular weight and dispersity consistent with previous kinetics and chain extension experiments (M_n 60.4 and Đ of 1.1). Block architectures could be successfully accessed upon NBE addition, producing copolymers with elevated M_ns (Scheme 21).

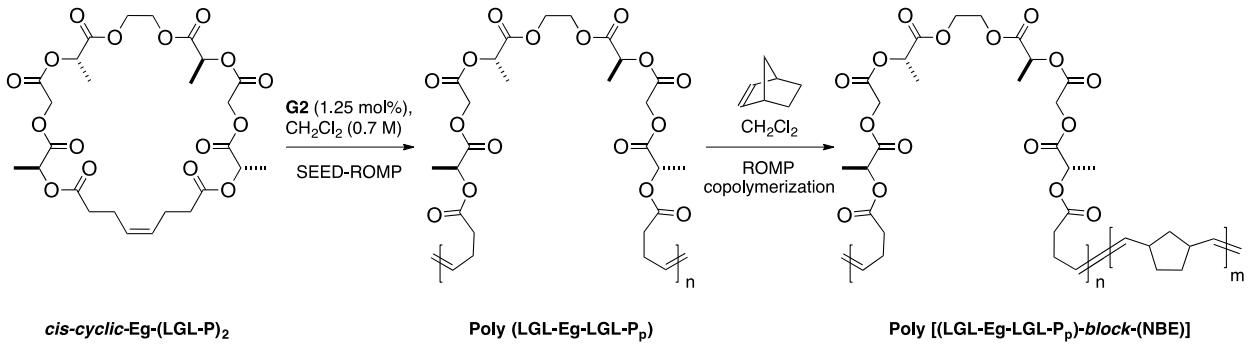

Scheme 21. Block copolymerization through sequential SEED-ROMP—ROMP.

Molecular weight changes for the copolymers at different reaction times were as expected, with an initial increase in M_n with the onset of ROMP (Figure 29, green) and later

decrease at longer reaction times (Figure 29, blue). The propensity of NBE to engage in secondary metathesis was evident as time progressed, and dispersities would be expected to increase further if longer times for ROMP were permitted.[145] Molecular weights increased approximately 11 kDa during the ROMP phase of the reaction even with truncated reaction times. The 6.4-fold difference in monomer molecular weight leads to smaller contributions to overall polymer molecular weight for NBE at similar DPs. The polymer obtained after polymerization had a molecular weight of 71 kDa, representing a $DP_{SEED\text{-}ROMP}$ of 100 and DP_{ROMP} of 117. Thermal properties for block copolymers were not determined, although visual inspection shows that the T_g of the of block copolymers is certainly above that of **poly (LGL-Eg-LGL-P_p)**.[156]

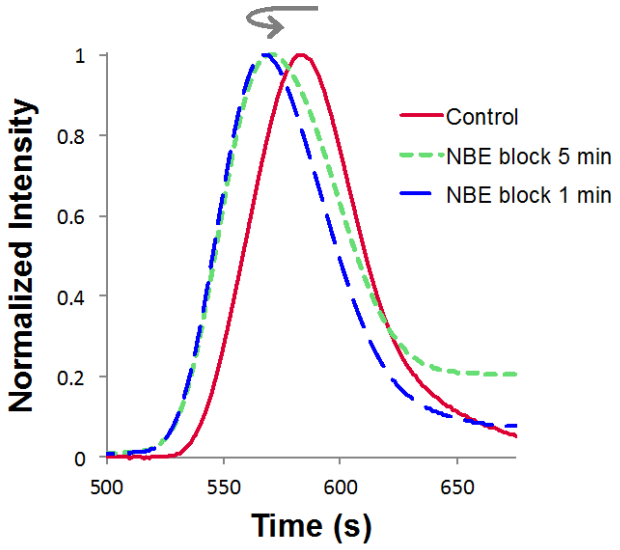

Figure 29. GPC overlay for control (red) and block copolymerization (blue and green, dashed) experiments.

As expected, NMR analysis of block copolymers was complicated by the atactic nature of the polymer, but nonetheless correlated well with what was anticipated.[157] Olefinic linkages in

the polynorbornene block occurred with 59-64% *cis*-selectivity in block copolymerizations and preliminary ROMP homopolymerization experiments. Resonances associated with protons and carbons at vinyl (5.2, 5.4 and 134, 133 ppm) and allylic (2.8, 2.4 and 39, 43 ppm) positions could be evaluated for *cis*- and *trans*-linkages, respectively. A representative NMR is shown below comparing the block copolymer with those of homopolymers **poly (LGL-Eg-LGL-P_p)** and **poly (NBE)** (Figure 30).

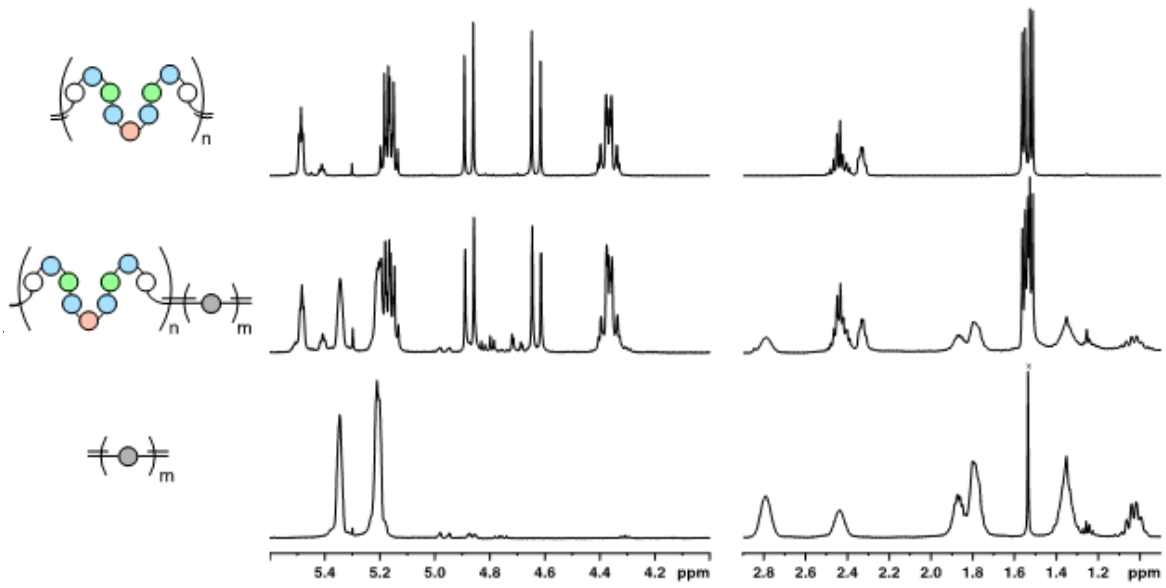

Figure 30. Comparison of ^{1}H-NMR spectra for homopolymers and SEED-ROMP—ROMP block copolymer.

Improvements could certainly be made with regards to monomer incorporation during this preliminary study. Although NBE has a large degree of ring strain (27.2 kcal/mol), it also suffers from decreased propagation rates due to steric hindrance impeding the formation of the Ru-olefin metallocyclobutane.[74] It is uncertain at this time what DP_{ROMP} would be targeted in

future efforts within our group, but secondary metathesis certainly limits the DP_{ROMP} achievable while maintaining a controlled block copolymerization when non-functionalized NBE is used.[158] Poor control over the ROMP would likely not prevent future applications where NBE-PEG was utilized to improve water solubility. However, control over DP_{ROMP} would certainly be necessary if the aim was to append drug or fluorophore. Chain transfer reagents or labile coordinating ligands like PPh_3 have been used in the past to improve the k_i/k_{pr} for the reaction and allow access to a higher DP_{ROMP}.[48,145] Preliminary ROMP homopolymerization reactions also suggested conducting the ROMP at 0 °C would result in decreased secondary metathesis. An alternative to this approach would be to simply use **G3** as long as reactions could be completed within the catalyst lifetime.[46] The success of these proof-of-concept block copolymerizations suggests that this method will be viable in applications with more complex block architectures in future studies.

3.0 SUMMARY AND FUTURE DIRECTIONS

3.1.1 Summary

In this thesis, we have demonstrated that a highly living regime of ED-ROMP is possible for sequenced oligomers when the macromonomer contains an endocyclic *cis*-olefin. This powerful reaction has enabled us to produce sequenced copolymers with unprecedented levels of control over a broad range of molecular weights. Sequenced α,ω-diolefins were synthesized according to the efficient and scalable segmer assembly method. They were then subjected to RCM, mediated by either the *trans*-selective **G2** or the *cis*-selective **GN**. Both reactions proved to be high yielding and highly selective. This the first time that successful use of **GN** has been reported outside of the Grubbs group, and has certainly expanded the scope of reactions possible for this new catalyst.

Selectivity enhancement and the living character of SEED-ROMP were probed in a series of kinetics and chain extension experiments. All polymerization reactions could be precisely analyzed using standard NMR spectroscopy and SEC methods. Molecular weights and conversion increased rapidly during the reaction, and dispersity was maintained even at long reaction times. A linear correlation between [M]/[cat] and M_n was established, a characteristic that is typically only observed during a living polymerization. Compared to the ED-ROMP of the corresponding *trans*-macromonomer, significant improvements in rate of propagation and

molecular weight control were observed. Further, cyclodepolymerization was shown as a viable method to recycle polymerized material back to a mixture of MCOs. Polymer chains could be extended once initial monomer had been consumed through the addition of more monomer or the highly strained bicyclic NBE. These polymerizations demonstrate the potential for the incorporation of property-modulating groups through a sequential SEED-ROMP—ROMP protocol. They also provide the opportunity to access significantly higher M_n sequenced copolymers in future studies.

3.1.2 Future Directions

SEED-ROMP represents a new method to obtain well-defined sequenced copolymers with a high degree of molecular weight control. It is a clear improvement over our SAP approach in terms of molecular weight control, and more extensive physical properties analysis of these polymers are currently underway. Our primary focus moving forward is the exploration of the physical and morphological properties of ED-ROMP materials, with an emphasis on practical applicability. We specifically want to know whether the interesting properties displayed by SAP-PLGAs will also be observed with these polymers.

One goal of further properties studies of ED-ROMP materials is to gain an understanding how each component of the segmer contributes to the overall properties of the corresponding polymer. For instance, we have found that the olefin tether of the ED-ROMP material can easily be reduced following polymerization, but its inherent flexibility is disruptive to lattice formation.[22] The ED-ROMP polymers discussed herein have a high degree of PLGA character, but have been tuned to enable the metathetical formation of palindromic sequenced polymers.

When possible, we intentionally designed requisite sequence modifications to minimize divergence from PLGA. Two groups, the ethylene glycol and the olefinic tether, have been specifically incorporated for this to occur. Now that we have demonstrated that ED-ROMP is possible for a range of polyester sequences, we will work to study how these two groups affect properties such as microparticle degradation and how their influence can be minimized.

In order to study the property-directing role of non-**L** or **G** groups in the ED-ROMP polymers, we are currently investigating the limits of influence that tether and linker groups can have. One phase of this project will be devoted to increasing the amount of **L** and **G** character in a non-palindromic macromonomer, which would likely align the properties of the resulting polymer more closely to those of SAP-PLGAs. We also are concerned with situations in which ancillary groups modify the polymer properties significantly. Sequence-controlled polymers are often obtained at the cost of incorporation of property directing groups.[4,116,117,144,159] We believe that ED-ROMP enables the formation of sequence-controlled polymers with comparatively diminished impact on the polymeric backbone. We have therefore begun an additional phase of the ED-ROMP study in order to gain insight into the property-directing role of alternate linker groups. Preliminary experiments have been carried out to facilitate this second study, and are briefly summarized below.

Using a convergent strategy, we will substitute the ethylene glycol subunit in ED-ROMP macromonomers with a variety of endocyclic linker groups. As in our current synthetic method, coupling to the linker group will precede RCM. Linker groups to be incorporated include alkyl, ethylene glycol, sulfide, and urea and will eventually be expanded further (Scheme 22).

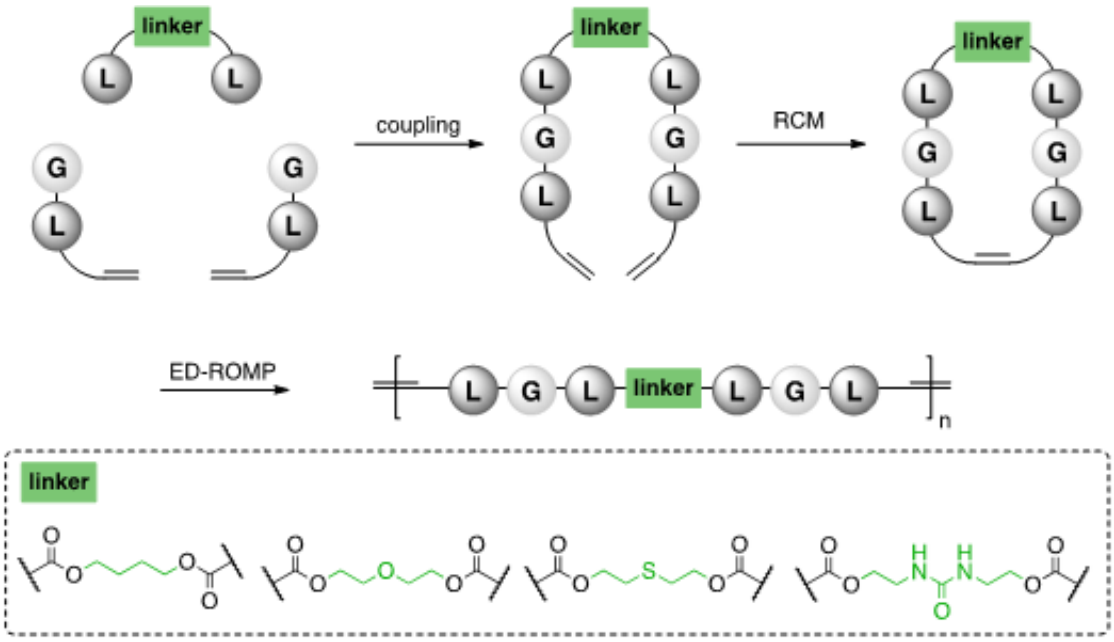

Scheme 22. General route to obtain ED-ROMP materials with linker variation for physical properties studies.

Synthesis of the most stable precursors to **Linker-(LGL-B)$_2$** formation have been carried out on multi-gram scale. Linker fragment synthesis began with the hydrolysis of **Me-L-Si** as previously discussed. Double coupling of alkyl, ethylene glycol, sulfide, and urea diols to **L-Si** delivered **9-12**, with the most significant byproduct resulting from single coupling. A first year graduate student, Jordan Swisher, conducted the purification of sulfide and PEG analogues, finding that unreacted monomer and asymmetric intermediate were isolable during purification. Deprotection of **7** went smoothly, providing **L-alkyl-L** (10) in high yield when the conditions previously developed for **Eg-(LGL-TBDPS)$_2$** were used. This unprotected diol was stable at low temperature over several months, but analogues **10-12** were maintained at the protected intermediate to avoid potential decomposition.

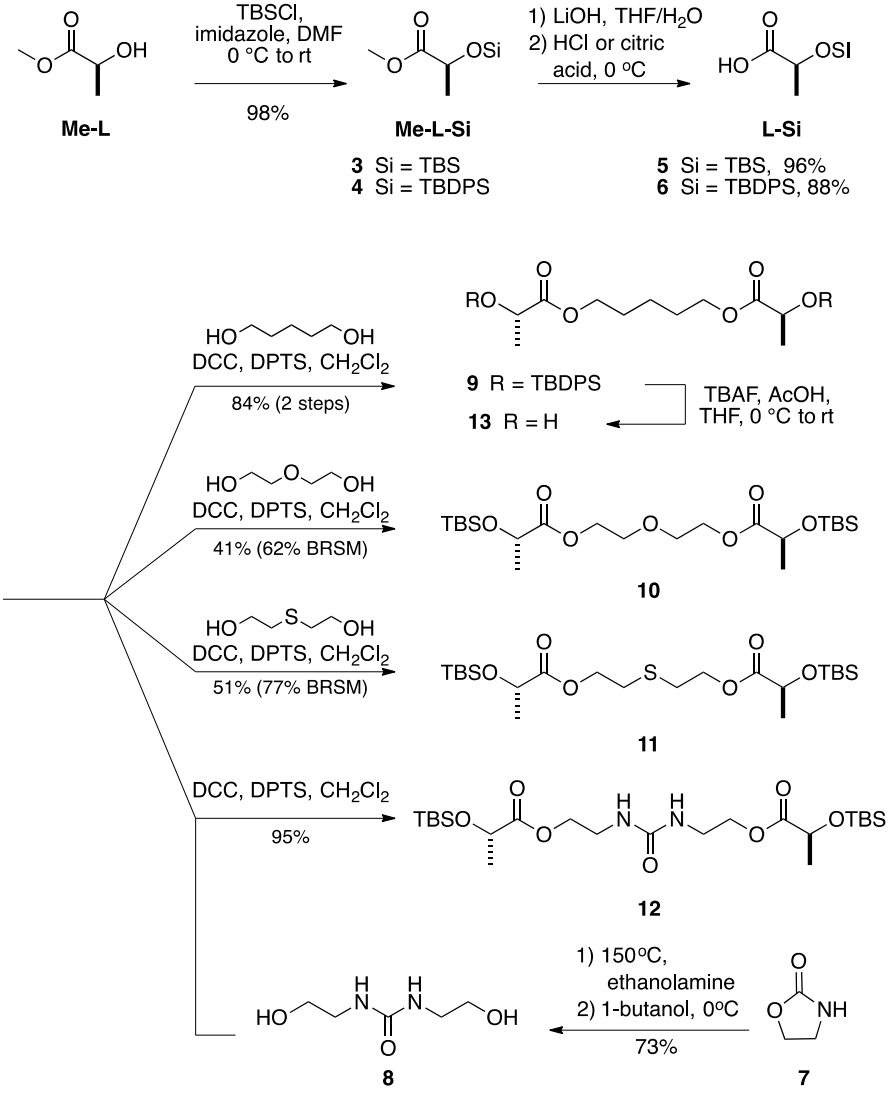

Scheme 23. Synthesis of **L-linker-L** fragments **8-11**.

Multigram synthesis of the second fragment was carried out according the segmer assembly method, stopping at the most stable advanced intermediate, **Me-GL-B** (**18**) (Scheme 24). As above, **Me-L-Si** saponification yielded **L-Si**, which was immediately coupled to **Bn-G** to yield **Bn-GL-Si**. Protecting group strategies were adjusted slightly to enable facile **G**-deprotection at a later stage in the presence of a terminal olefin. The benzyl protecting group was replaced with methyl, affording **Me-GL-TBDPS** in two steps with 88% yield. Deprotection of

the silane delivered **Me-GL,** which could then be coupled to 3-butenoic acid to form **Me-GL-B** in 75% over two steps. The efficiency of this scheme could certainly be improved by establishing desired protecting groups prior to the initial **L-G** coupling reaction. These preliminary studies were carried out with stock materials that we had in hand, with ease of access being prioritized over stepwise efficiency. In future development of this project, this process will certainly be streamlined. Once the linker is incorporated into the segmer, RCM will lead to the desired macromonomer that can then be polymerized via ED-ROMP or SEED-ROMP.

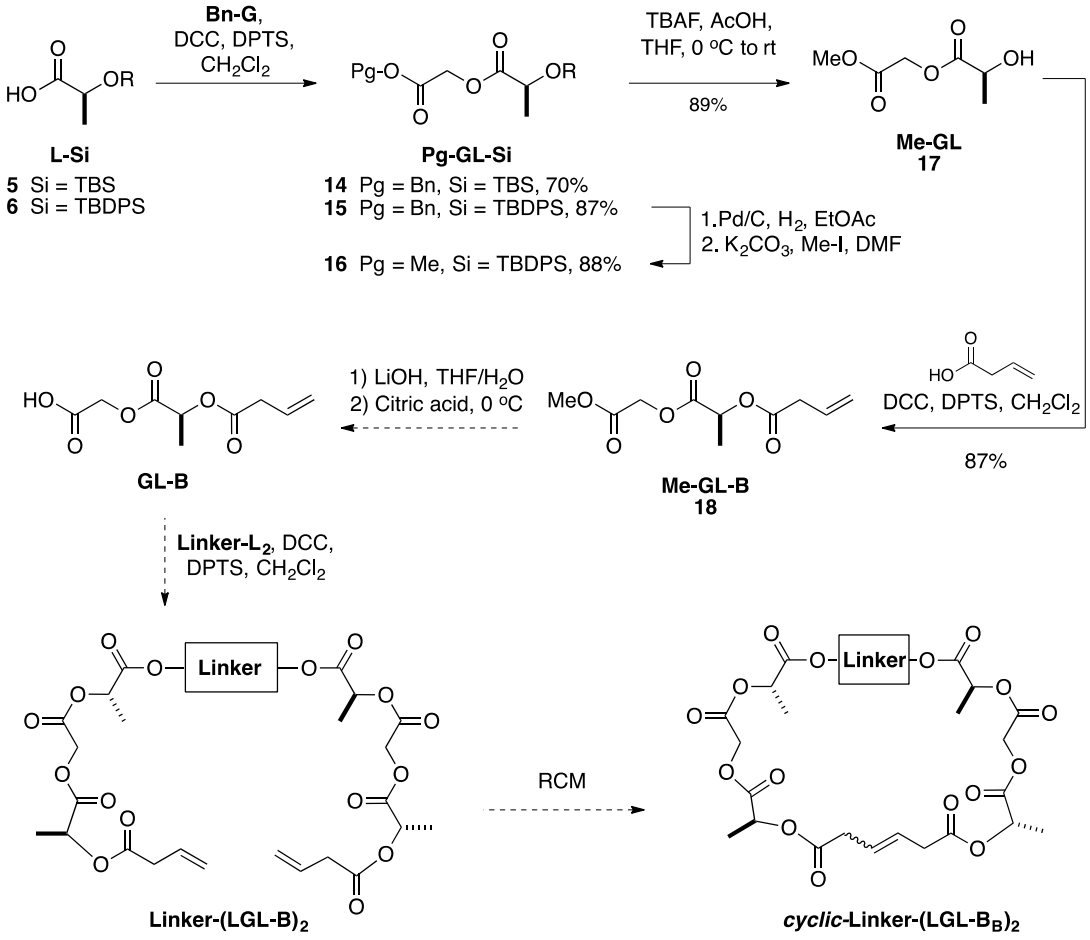

Scheme 24. Progress towards the synthesis of cyclic linker analogues.

4.0 EXPERIMENTAL

Modeling Experimental

Substrates for preliminary docking studies were constructed using ChemDraw Ultra 12.0. The geometrically optimized conformations were obtained from MM2 energy minimization before being converted to .mol format using Chem3D Pro 12.0. PyMOL was used for further rendering and visualization of models. Removal of non-polar hydrogens, selection of rotatable bonds and predictive docking analysis were carried out using AutoDock Vina 1.1.2 and the MGL Tools 1.5.6 suite from the Scripps Research Institute.[110-113]

Synthesis Experimental

All reactions were performed under an inert atmosphere of N_2 gas in oven-dried glassware using anhydrous solvents, unless otherwise noted. Methylene chloride (CH_2Cl_2, Fisher), ethyl acetate (EtOAc, Sigma Aldrich) and tetrahydrofuran (THF) were purified by a solvent dispensing system by J. C. Meyer and passed over two columns of neutral alumina. All other anhydrous solvents were purchased from Sigma-Aldrich. Reactions were monitored by thin–layer chromatography (TLC) carried out on 0.25 mm EMD silica gel plates (60F–254) using heat or UV light (254 nm) for visualization and $KMnO_4$ stain as a developing agent. TSI silica gel (230–400 mesh) was used for flash chromatography. ^{1}H- and ^{13}C-NMR spectra were recorded on a

Bruker Avance II Ultrashield Plus equipped with a cryoprobe at 600 and 150 MHz, 500 and 125 MHz, or 400 and 100 MHz, respectively. Chemical shift values are in ppm relative to residual solvent signal. The following abbreviations are used to indicate the multiplicities: s = singlet, d = doublet, t = triplet, q = quartet, m = multiplet, br = broad. HRMS data was obtained on a LC/Q-TOF instrument. Low-resolution mass spectra were obtained on an Applied Biosciences API 2000 ESI- triple quadrupole mass spectrometer with a Shimadzu UFLC inlet system. Molecular weights and dispersities were obtained on a Waters GPC (THF, 0.5 mL/min flow rate) with Jordi 500, 1000, and 10000 Å divinyl benzene columns, and refractive index detector (Waters) was calibrated to polystyrene standards.

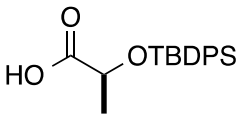

Preparation of L-TBDPS (6).

To a stirring solution of **Me-L-Si** (**4**, 37.8 g, 110 mmol) in THF (500 mL) at 0 ºC was slowly added a solution of LiOH (18.5 g, 442 mmol) in H_2O (500 mL). Once the addition was complete, the solution was allowed to warm to rt and stirred for an additional 3 h. The reaction solution was concentrated to half volume, diluted with brine (100 mL) and extracted with Et_2O (3 × 200 mL). The aqueous layer was acidified to pH < 1 with 3M HCl. The mixture was then extracted with Et_2O (5 × 100 mL), dried over $MgSO_4$, filtered, and concentrated *in vacuo* to provide the crude product as a colorless oil (32.0 g, 88%). The oil had identical spectral properties to those

found in literature[17] and was used in subsequent reactions without further purification; ^{1}H NMR (400 MHz, $CDCl_3$) δ 7.68 (m, 4 H), 7.43 (m, 6 H), 4.35 (q, *J* = 6.8 Hz, 1 H), 1.34 (d, *J* = 7.2 Hz, 3 H), 1.12 (s, 9 H).

Representative protocol: ALS-1015

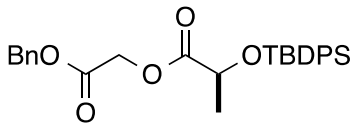

Preparation of Bn-GL-TBDPS (15).

To a stirring solution of **Bn-G** (17.8 g, 107.3 mmol) and **L-TBDPS** (**6**, 32.0 g, 97.5 mmol) in CH_2Cl_2 (1000 mL) was added DPTS (5.741 g, 19.5 mmol). Once the DPTS had dissolved, DCC (22.1 g, 107 mmol) was added and the solution stirred overnight. The reaction mixture was then filtered, concentrated to approximately 250 mL, diluted with hexanes, and filtered again. This concentration and filtration cycle was repeated one additional time whereupon the solution was concentrated *in vacuo*. The crude material was purified by flash chromatography (SiO_2, 2.5-10% EtOAc in hexanes) to provide the product as a colorless oil (46.48 g, 87%); ^{1}H NMR (500 MHz, $CDCl_3$) δ 7.67 (m, 4H), 7.44 (m, 11H), 5.8 (s, 2H), 4.61 (d, *J* = 16.0 Hz, 1H), 4.46 (d, *J* = 15.6 Hz, 1H), 4.39 (q, *J* = 6.8 Hz, 1H), 1.38 (d, *J* = 6.8 Hz, 3H), 1.07 (s, 9H).

Representative protocol: ALS-1016

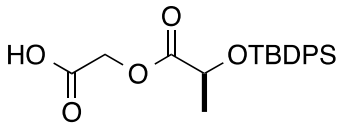

Preparation of GL-TBDPS.

To a stirring solution of **Bn-GL-TBDPS** (34.1 g, 71.4 mmol) in EtOAc (700 mL) under N_2 was added 10% Pd/C (3.41 g, 10% w/w). The reaction vessel was then purged twice with a H_2 balloon and allowed to stir overnight under 1 atm H_2. Once the reaction had completed, the vessel was evacuated and filled with N_2 and the mixture was filtered over celite and concentrated *in vacuo*. The crude material was purified by flash chromatography (SiO_2, 2.5-25% EtOAc in hexanes) to provide the product as a colorless liquid (27.6 g, 88%); ^{1}H NMR (400 MHz, $CDCl_3$) δ 11.03 (br s, 1H), 7.68 (m, 4H), 7.46 (m, 6H), 4.62 (d, J = 16.4 Hz, 1H), 4.51 (d, J = 16.4 Hz, 1H), 4.42 (q, J = 6.8 Hz, 1H), 1.42 (d, J = 6.8 Hz, 3H), 1.10 (s, 9H); ^{13}C NMR (100 MHz, $CDCl_3$) δ 173.03, 172.79, 135.89, 135.73, 133.39, 132.89, 129.84, 127.67, 127.61, 68.60, 59.98, 26.77, 21.23, 19.21; HRMS (ESI) $[M-H]^+$ calc mass 385.14713, found 385.14768.[22]

Representative protocol: Sequence-controlled copolymers prepared via entropy-driven ring-opening metathesis polymerization.[22]

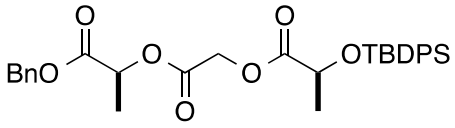

Preparation of Bn-LGL-TBDPS.

To a stirring solution of **Bn-L** (11.6 g, 64.2 mmol) and **GL-TBDPS** (22.6 g, 58.4 mmol), in CH_2Cl_2 (290 mL) was added DPTS (13.3 g, 64.2 mmol). Once the mixture became

homogeneous, DCC (13.3 g, 64.2 mmol) was added and the reaction was allowed to stir overnight. The solution was filtered and the filtrate was concentrated *in vacuo*. The crude material was purified by flash chromatography (SiO_2, 2.5-25% EtOAc in hexanes) to provide the product as a colorless liquid (32.0 g, 93%); ^{1}H NMR (400 MHz, $CDCl_3$) δ 7.70 (m, 4H), 7.46 (m, 11H), 5.18 (q, *J* = 7.2 Hz, 1H), 5.18 (d, *J* = 14.0 Hz, 1H), 5.17 (d, *J* = 14.0 Hz, 1H), 4.70 (d, *J* = 16.0 Hz, 1H), 4.47 (d, *J* = 16.0 Hz, 1H), 4.41 (d, *J* = 6.8 Hz, 1H), 1.50 (d, *J* = 6.8 Hz, 3H), 1.44 (d, *J* = 6.8 Hz, 3H), 1.08 (s, 9H); ^{13}C NMR (100 MHz, $CDCl_3$) δ 173.15, 170.06, 167.01, 136.05, 135.88, 135.30, 133.57, 133.11, 129.97, 128.77, 128.60, 128.30, 127.81, 127.76, 69.43, 68.76, 67.32, 60.45, 26.94, 21.43, 19.37, 16.96; HRMS (ESI) $[M+NH_4]^+$ calc mass 566.2574, found 566.2578.

Representative protocol: ALS-1018.

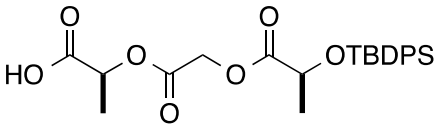

Preparation of LGL-TBDPS.

To a stirring solution of **Bn-LGL-TBDPS** (29.8 g, 54.2 mmol) in EtOAc (540 mL) under N_2 was added 10% Pd/C (10 % w/w, 5.42 g). The reaction vessel was evacuated and purged three times with a 1 atm H_2 balloon. The reaction was allowed to stir 1 day under 1 atm H_2. The vessel was placed under N_2, filtered over celite, and concentrated *in vacuo*. The crude material was purified by flash chromatography (SiO_2, 5-100% EtOAc in hexanes) to provide the product as a colorless liquid (25.0 g, 99%); ^{1}H NMR (400 MHz, $CDCl_3$) δ 11.13 (br s, 1H), 7.66-7.64 (m, 4H), 7.43-

7.32 (m, 6H), 5.16 (q, J = 7.2 Hz, 1H), 4.65 (d, J = 16 Hz, 1H), 4.42 (d, J = 16 Hz, 1H), 4.36 (q, J = 6.8 Hz, 1H), 1.50 (d, J = 7.2 Hz, 3H), 1.40 (d, J = 6.8 Hz, 3H), 1.07 (s, 9H); ^{13}C NMR (100 MHz, $CDCl_3$) δ 174.96, 173.08, 166.82, 135.89, 135.72, 133.38, 132.93, 129.82, 127.65, 127.60, 68.70, 68.59, 60.23, 26.77, 21.26, 19.20, 16.67; HRMS (ESI) $[M+H]^+$ calc mass 457.16771, found 457.16838.[22]

Representative protocol: ALS-1023

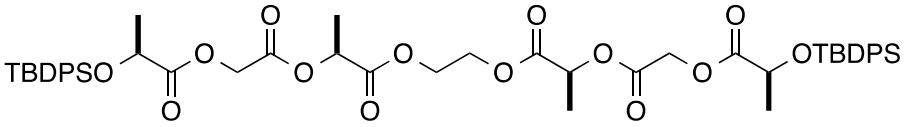

Preparation of Eg-(LGL-Si)$_2$.

To a stirring solution of ethylene glycol (1.84 mL, 32.5) and **LGL-Si** (24.9 g, 54.2) in CH_2Cl_2 (120 mL) was added DPTS (1.43 g, 4.85 mmol). Once the mixture became homogeneous, DCC (5.45 g, 26.4 mmol) was added and the reaction was allowed to stir overnight. The solution was filtered and the filtrate was concentrated *in vacuo*. The crude material was purified by flash chromatography (SiO_2, 7.5-20% EtOAc in hexanes) to provide the product as a colorless liquid (11.3 g, 98.3%); ^{1}H NMR (400 MHz, $CDCl_3$) δ 7.68 (m, 8H), 7.46-7.34 (m, 12H), 5.17 (q, J = 6.8 Hz, 2H), 4.68 (d, J = 16.0 Hz, 2H), 4.46 (d, J =15.6 Hz, 2H), 4.40 (q, J = 6.8 Hz, 2H), 4.34 (m, 4H), 1.48 (d, J = 7.2 Hz, 6H), 1.40 (d, J = 6.8 Hz, 6H), 1.07 (s, 18H); ^{13}C NMR (100 MHz, $CDCl_3$) δ 172.98, 169.75, 166.82, 135.88, 135.71, 133.38, 132.95, 129.81, 127.65, 127.59, 69.09, 68.58, 62.69, 60.24, 26.77, 21.26, 19.20, 16.70; HRMS (ESI) $[M+NH_4]^+$ calc mass 960.4022, found 960.4017.[22]

Representative protocol: Sequence-controlled copolymers prepared via entropy-driven ring-opening metathesis polymerization.[22]

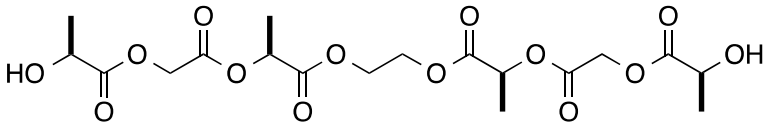

Preparation of Eg-(LGL)$_2$.

To a stirring solution of **Eg-(LGL-TBDPS)$_2$** (3.16 g, 3.33 mmol) in THF (83 mL) at 0 ^{o}C under N_2 was slowly added acetic acid (3.0 mL, 53 mmol) and then TBAF (1.0 M in THF, 10.0 mL). The reaction was stirred at 0 ^{o}C overnight, then the ice bath was removed and stirring continued at rt for an additional day. After cooling the reaction mixture to 0 ^{o}C, brine (150 mL) was added. The resulting aqueous layer was extracted with CH_2Cl_2 (3 × 150 mL), the combined organic layers were washed with aqueous saturated sodium bicarbonate solution (150 mL), dried over $MgSO_4$ and then concentrated *in vacuo*. The concentrate was then chromatographed over silica using 25-75% EtOAc in hexanes as the eluent to provide the product as a white solid (1.55 g, quantitative). *Note: although this particular experiment was the highest yielding of all attempts, the conditions described above did not lead to consistent reaction outcomes. An optimized procedure is also included here with a typical yield.* To a stirring solution of **Eg-(LGL-TBDPS)$_2$** (0.114 g, 0.12 mmol) in THF at 0 ^{o}C was added AcOH (55 μL, 0.97 mmol) that had been pre-dried over 3 Å molecular sieves prior to use. TBAF (1.0 M in THF, 363 μL, 0.36 mmol) was added dropwise and the resulting solution was stirred at rt 4 h. The solution was then cooled to 0 ^{o}C, diluted with EtOAc (5 mL) and pH 7.4 buffer (5 mL) was added. The aqueous layer was

extracted with EtOAc (3 × 5 mL), the combined organic layers were dried over Na_2SO_4, filtered, and concentrated *in vacuo* to give the crude product as a faintly yellow oil. The residue was purified by chromatography on SiO_2 (35−100% EtOAc in hexanes) to provide the product as a colorless liquid (89%; R_f = 0.10, 50% EtOAc in hexanes); ^{1}H NMR (500 MHz, $CDCl_3$) δ 5.22 (q, *J* = 7.0 Hz, 2H), 4.85 (d, *J* = 16.0 Hz, 2H), 4.76 (d, *J* = 16.0 Hz, 2H), 4.44 (m, 6H), 2.89 (s, 1H), 2.88 (s, 1H), 1.54 (d, *J* = 7.0 Hz, 6H), 1.50 (d, *J* = 6.8 Hz, 6H); ^{13}C NMR (125 MHz, $CDCl_3$) δ 175.01, 169.89, 166.90, 69.58, 66.91, 62.96, 61.02, 20.40, 16.87; HRMS (ESI) $[M+NH_4]^+$calc mass 484.1666, found 484.1627.

Representative protocol: ALS-1094.

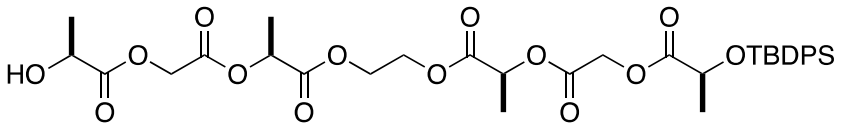

Preparation of LGL-Eg-LGL-TBDPS.

Monodeprotected **LGL-Eg-LGL-TBDPS** could be obtained as the major product by using the above deprotection method, but stopping the reaction prior to completion. The time required depended significantly on the scale of the reaction, but deprotection occurred in a stepwise manner and could be easily monitored by TLC **(**R_f 0.34, 50% EtOAc in hexanes); ^{1}H NMR (500 MHz, $CDCl_3$) δ 7.68 (m, 4H), 7.45 (m, 6H), 5.18 (q, *J* = 7.0 Hz, 1H), 5.17 (q, *J* = 7.0 Hz, 1H), 4.84 (d, *J* = 16 Hz, 1H), 4.74 (d, *J* = 16 Hz, 1H), 4.68 (d, *J* = 16 Hz, 1H), 4.47 (d, *J* = 16 Hz, 1H), 4.43 (m, 6H), 2.76 (d, *J* = 5.5 Hz, 1H), 1.52 (d, *J* = 7.0 Hz, 3H), 1.49 (d, *J* = 7.0 Hz, 6H), 1.42 (d, *J* = 7.0 Hz, 3H), 1.09 (s, 9H); ^{13}C NMR (125 MHz, $CDCl_3$) δ 175.01, 173.17, 169.99, 169.82,

167.04, 166.78, 136.05, 135.88, 133.55, 133.14, 129.98, 127.82, 127.76, 69.53, 69.27, 68.76, 66.86, 62.93, 62.87, 61.01, 60.44, 26.94, 21.42, 20.46, 19.37, 16.86.

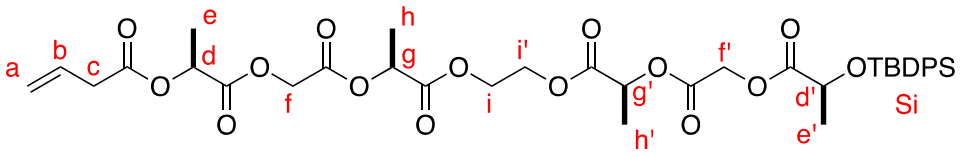

Preparation of **B-LGL-Eg-LGL-TBDPS**.

To a stirring solution of **LGL-Eg-LGL-TBDPS** (89 mg, 0.13 mmol) and vinyl acetic acid (18 µL, 0.16 mmol) in CH_2Cl_2 (1.4 mL) was added DPTS (8.4 mg, 0.28 mmol) and then DCC (32 mg, 0.16 mmol). The mixture was allowed to stir 19 h, then additional vinyl acetic acid (5 µL, 0.044 mmol) in CH_2Cl_2 (0.2 mL) was added. After 1.5 h, hexanes were added (2 mL) and the mixture was filtered. The filtrate was washed with 1M HCl (0.5 mL) and sat. aq. $NaHCO_3$ (0.5 mL), then the combined aqueous layers were extracted with CH_2Cl_2 (2 mL). The combined organic layers were washed with brine (2 mL) and concentrated *in vacuo* to give the crude product as a colorless oil. The residue was purified by chromatography on SiO_2 (15−20% EtOAc in hexanes) to provide the product as a colorless liquid (76 mg, 76%); ^{1}H NMR (500 MHz, $CDCl_3$) δ 7.68 (m, 4H; *ArH*), 7.45 (m, 6H; *ArH*), 5.94 (ddt, *J* = 17.0, 10.5, 7.0 Hz, 1H; *b*), 5.22 (m, 5H; *a,d,g,g'*), 4.87 (d, *J* = 16.0 Hz, 1H; *f*), 4.68 (d, *J* = 16.0 Hz, 1H; *f*), 4.64 (d, *J* = 16.0 Hz, 1H; *f'*), 4.47 (d, *J* = 16.0 Hz, 1H; *f'*), 4.40 (m, 4H; *i,i'*), 4.38 (q, *J* = 7.0 Hz, 1H; *d*), 3.19 (m, 2H; *c*), 1.57 (d, *J* = 7.0 Hz, 3H; *h,h' or e*), 1.51 (d, *J* = 7.0 Hz, 3H; *h,h' or e*), 1.49 (d, *J* = 7.0 Hz, 3H; *h,h' or e*), 1.42 (d, *J* = 7.0 Hz, 3H; *e'*), 1.09 (s, 9H; *SiCH*$_3$); ^{13}C NMR (125 MHz, $CDCl_3$) δ 173.14, 170.97, 170.24, 169.93, 169.85, 167.00, 166.73, 136.05, 135.88, 133.57, 133.14, 129.98,

129.77, 127.82, 127.76, 119.09, 69.42, 69.26, 68.76, 68.56, 62.92, 62.85, 60.86, 60.42, 38.72, 26.94, 21.42, 19.37, 16.95, 16.87, 16.86.

Representative protocol: ALS-2047.

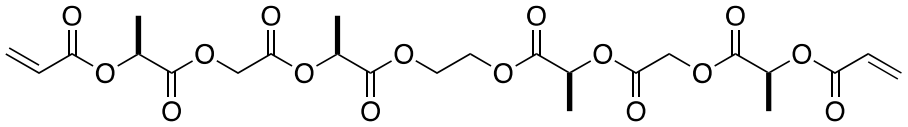

Preparation of Eg-(LGL-A)$_2$.

To a stirring solution of **Eg-(LGL)$_2$** (55 mg, 0.118 mmol) in CH_2Cl_2 (1.2 mL) at 0 °C was added DIPEA (82 μL, 0.472 mmol), DMAP (6 mg, 0.0472 mmol), and then a solution of acryloyl chloride (38 μL, 0.472 mmol) in CH_2Cl_2 (0.7 mL) dropwise. The solution was stirred for 30 min, and then allowed to warm to room temperature and stirred for an additional 1.5 h. Once the reaction was completed by TLC, it was cooled to 0 °C, diluted with CH_2Cl_2 (5 mL), and quenched with sat. aq. $NaHCO_3$ (5 mL). The resulting aqueous layer was extracted with CH_2Cl_2 (3 □5 mL), the combined organic layers were washed with brine (5 mL), dried with Na_2SO_4, filtered, and concentrated *in vacuo* to give the crude product as a faintly yellow oil. The residue was purified by chromatography on SiO_2 (5−25% EtOAc in hexanes) to provide the product as a colorless liquid (68 mg, 55 %); ^{1}H NMR (400 MHz, $CDCl_3$) δ 6.51 (dd, J = 17.6, 1.2 Hz, 2 H), 6.22 (dd, J = 17.2, 10.4 Hz, 2 H), 5.92 (dd, J = 10.4, 0.8 Hz, 2 H), 5.27 (q, J = 6.8 Hz, 2 H), 5.20 (q, J = 7.2 Hz, 2 H), 4.89 (d, J = 16.0, 2H), 4.68 (q, J = 16.0 Hz, 2H), 4.40 (m, 4H), 1.62 (d, J = 7.2 Hz, 6H), 1.53 (d, J = 6.8 Hz, 6H); ^{13}C NMR (100 MHz, $CDCl_3$) δ 170.24, 169.84, 166.73,

165.41, 132.22, 127.60, 69.38, 68.48, 62.88, 60.83, 17.01, 16.83; HRMS $[M+H]^+$ calc mass 575.1612, found 575.1582.

Representative protocol: ALS-1068.

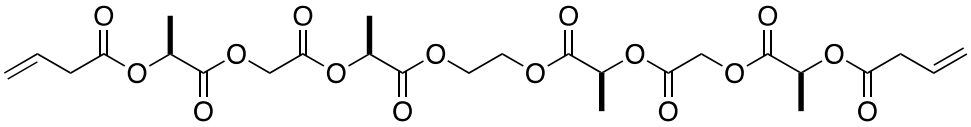

Preparation of Eg-(LGL-B)$_2$.

To a stirring solution of **Eg-(LGL)$_2$** (0.113 g, 0.243 mmol), 3-butenoic acid (0.05 mL, 0.588 mmol) in CH_2Cl_2 (2.4 mL) was added DPTS (0.029 g, mmol). Once the mixture became homogeneous, DCC (0.112 g, 0.542 mmol) was added and the reaction was allowed to stir overnight. The reaction was filtered to and the filtrate was diluted with CH_2Cl_2 (50 mL), washed with 1 M HCl (50 mL), and washed with saturated aqueous $NaHCO_3$ (50 mL). The aqueous layer was then extracted with CH_2Cl_2 (2 × 25 mL), the organic layers were combined, dried over $MgSO_4$, and concentrated *in vacuo*. The crude material was purified by flash chromatography (SiO_2, 17.5-20% EtOAc in hexanes) to provide the product as a colorless liquid (0.116 g, 79.2%); ^{1}H NMR (400 MHz, $CDCl_3$) δ 5.98 (ddt, *J* = 17.2, 10.4, 6.8 Hz, 2H), 5.22 (m, 8H), 4.89 (d, *J* = 16.0 Hz, 2H), 4.61 (d, *J* = 16.0 Hz, 2H), 4.39 (m, 4H), 3.23 (m, 4H), 1.58 (d, *J* = 7.2 Hz, 6H), 1.53 (d, *J* = 7.2 Hz, 6H); ^{13}C NMR (100 MHz, $CDCl_3$) δ 170.82, 170.08, 169.69, 166.57, 129.59, 118.94, 69.24, 68.38, 62.73, 60.69, 38.55, 16.78, 16.69; HRMS (ESI) $[M+H]^+$ calc mass 603.19251, found 603.19073.[22]

Representative protocol: Sequence-controlled copolymers prepared via entropy-driven ring-opening metathesis polymerization.[22]

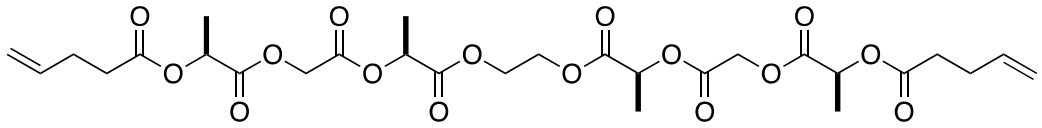

Preparation of Eg-(LGL-P)$_2$.

To a stirring solution of **Eg-(LGL)$_2$** (0.980 g, 2.10 mmol), 3-butenoic acid (0.47 mL, 4.62 mmol) in CH_2Cl_2 (42 mL) was added DPTS (0.247 g, 0.840 mmol). Once the mixture became homogeneous, DCC (0.954 g, 4.62 mmol) was added and the reaction was allowed to stir overnight. The reaction was concentrated to half volume and then filtered. The filtrate was washed with 1 M HCl (10 mL), and washed with saturated aqueous $NaHCO_3$ (10 mL). The aqueous layer was then extracted with CH_2Cl_2 (10 mL), the organic layers were combined, washed with brine (15 mL), dried over Na_2SO_4, and concentrated *in vacuo*. The crude material was purified by flash chromatography (SiO_2, 15-20% EtOAc in hexanes) to provide the product as a colorless liquid (1.13 g, 86%); ^{1}H NMR (400 MHz, $CDCl_3$) δ 5.89 (ddt, *J* = 16.8, 10.4, 6.4 Hz, 2H), 5.200 (q, *J* = 7.2 Hz, 2H), 5.197 (q, *J* = 7.2 Hz, 2H), 5.09 (dd, *J* = 16.8, 1.2 Hz, 2H), 5.02 (dd, *J* = 10.4, 1.2 Hz, 2H), 4.89 (d, *J* = 16.0 Hz, 2H), 4.65 (d, *J* = 16.0 Hz, 2H), 4.41 (m, 4H), 2.56 (m, 4H), 2.44 (m, 4H), 1.57 (d, J = 7.2 Hz, 6H), 1.53 (d, *J* = 7.2 Hz, 6H); ^{13}C NMR (100 MHz, $CDCl_3$) δ 172.51, 170.39, 169.87, 166.77, 136.55, 115.78, 69.40, 68.32, 62.90, 60.82, 33.23, 28.78, 17.00, 16.87; HRMS (ESI) $[M+H]^+$ calc mass 631.22326, found 631.2225.[22]

Representative protocol: ALS-1084.

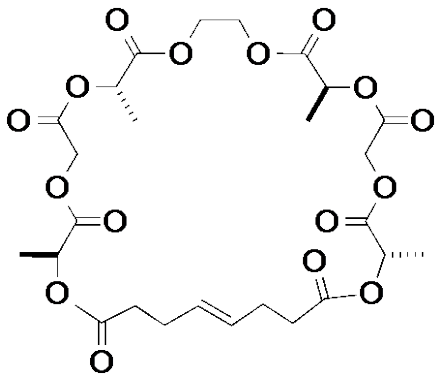

Preparation of *trans-cyclic*-Eg-(LGL-P)$_2$.

To a stirring solution of **Eg-(LGL-P)$_2$** (17 mg, 27 μmol) in CH_2Cl_2 (27 μL) was added a solution of catalyst **G2** (2.3 mg, 2.7 μmol) in CH_2Cl_2 (1 mL). The resulting solution was stirred for 18 h before being quenched through the addition of ethyl vinyl ether (0.2 mL). Once concentrated, the crude oil was purified by chromatography on SiO_2 (10–20% EtOAc in hexanes) to afford ***trans-cyclic*-Eg-(LGL-P)$_2$** (17 mg, 93% yield, 84% *trans*) as a colorless oil. ^{1}H NMR (500 MHz, $CDCl_3$) δ 5.54 (m, *trans*) and 5.41 (m, *cis*) (2H), 5.23 (m, 4H), 4.83 (d, J = 16 Hz, 2H), 4.72 (d, J = 16 Hz, 2H), 4.41 (m, 4H), 2.47 (m, 4H), 2.36 (m, 4H), 1.55 (d, J = 7.0 Hz, 6H), 1.53 (d, J = 7.0 Hz); ^{13}C NMR (125 MHz, $CDCl_3$) δ 172.37, 170.35, 169.92, 166.77, 129.49 (*trans*), 129.14 (*cis*), 69.51, 68.26, 62.87, 60.94, 33.79, 27.72, 17.02, 16.85; HRMS (ESI) $[M+H]^+$ calc mass 603.19251, found 603.19028.[22]

Representative protocol: ALS-1069.

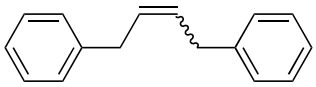

2

Preparation of 2 through allylbenzene homodimerization.

In the glovebox, a solution of **GN** (949 µg, 1.5 µmol) in THF-d_6 (0.1 mL) was added to an NMR tube equipped with a controlled atmosphere valve. Allylbenzene (**1**, 0.177 g, 1.5 mmol) in THF-d_6 (0.4 mL) was then added, the tube was sealed, removed from the glovebox, evacuated and heated to 35 °C. The tube was periodically evacuated, and NMRs were taken for 2 days prior to quenching the reaction mixture with EVE (0.5 mL) and concentrating *in vacuo*. After 2 days, 87% conversion from **1** to **2** was observed, with 83% *cis*-olefin selectivity. For clarity, peak integrals are provided as if the mixture contained a 50:50 ratio of **1**:**2**. ^{1}H NMR (500 MHz, $CDCl_3$) δ 7.29 (m, 10H; **2**), 7.24 (m, 10H; **1**), 6.02 (ddt, J = 17.2, 10.4, 6.8 Hz, 2H; **1**), 5.75 (m, 2H; **2**), 5.39 (s, ethylene), 5.11 (m, 2H; **1**), 3.57 (d, J = 5.6 Hz, 4H; **2**), 3.39 (d, J = 6.4 Hz, 2H; **1**). Data for the remaining time points is shown below.

Representative protocol: ALS-1017.

Table 5. Homodimerization of allylbenzene with **GN.**

Time (h)	% Conversion	% *cis*
0.75	35	nd
2	35	nd
5	61	nd
22	70	nd
28	70	nd
48	87	82.6

nd: not observed or quantified; stagnant % conversions indicate periods with no evacuation

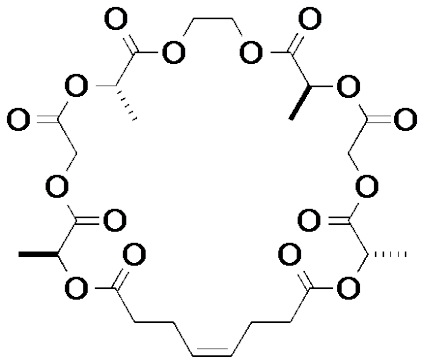

Preparation of *cis-cyclic*-Eg-(LGL-P)$_2$.

In the glovebox, a solution of ruthenium catalyst **GN** (69 mg, 0.1094 mmol) in DCE (20 mL) was added to a stirring solution of **Eg-(LGL-P)$_2$** (690 mg, 1.094 mmol) in DCE (200 mL). The vessel was immediately removed from the glovebox and stirred at 60 °C under a constant low vacuum (photo of apparatus follows protocol). After 26 h of stirring, the reaction solution was cooled to rt, ethyl vinyl ether (2 mL) was added, and the solution was stirred for an additional 30 min before being concentrated. The crude product was purified by chromatography on SiO_2 (10–25% EtOAc in hexanes) to afford ***cis-cyclic*-Eg-(LGL-P)$_2$** (0.578 g, 88% yield, 95 % BRSM, 12:88 *E:Z*) as a colorless oil; ^{1}H NMR (500 MHz, $CDCl_3$) δ 5.51 (m, *trans*) and 5.43 (m, *cis*)(2H), 5.23 (m, 4H), 4.83 (d, *J* = 16.0 Hz, 2H, *trans*), 4.81 (d, *J* = 16.0 Hz, 2H, *cis*), 4.40 (m, 4 H), 2.48 (m, 8H), 1.55 (d, *J* = 7.0 Hz, 6H), 1.53 (d, *J* = 7.0 Hz, 6H); ^{13}C NMR (125 MHz, $CDCl_3$) δ 172.44, 170.32, 169.92, 166.77, 129.47 (*trans*), 129.12 (*cis*), 69.52, 68.34, 62.81, 60.96, 33.96, 22.91, 16.94, 16.80; HRMS (ESI) calc. mass 603.1920, found 603.1940.

Representative protocol: ALS-2061.

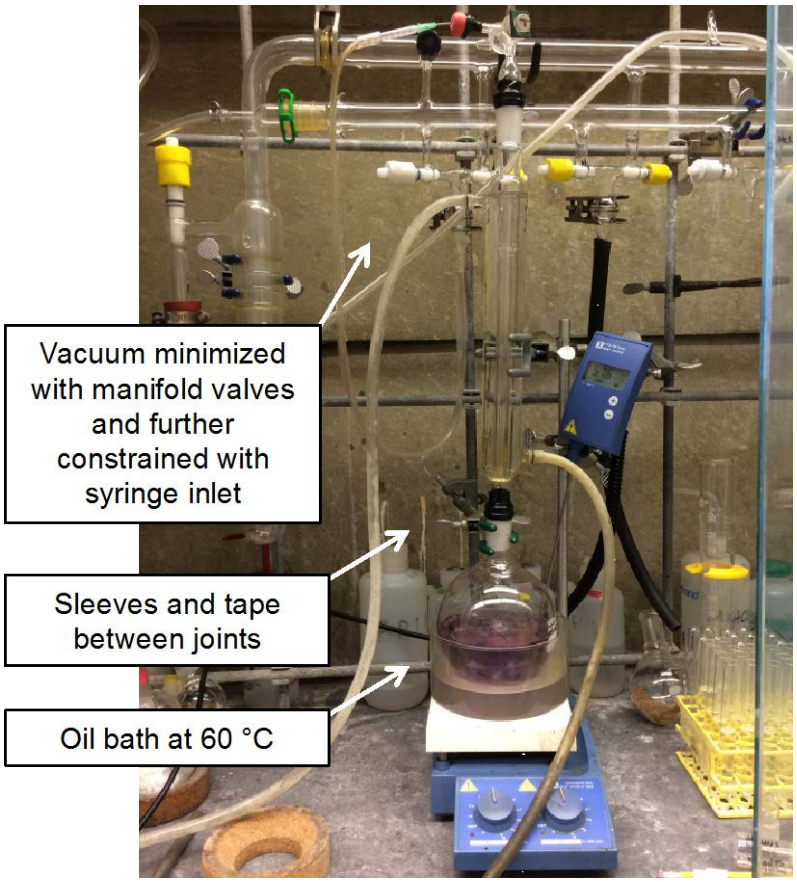

Figure 31. Apparatus setup for RCM using *cis*-selective catalyst **GN**.

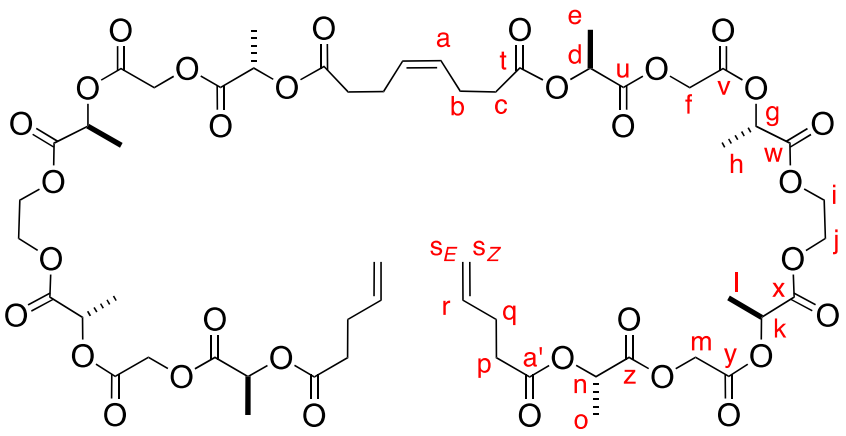

Preparation of homodimer P_p-(LGL-Eg-LGL-P)$_2$.

Prepared as above, but solvent was removed by vacuum overnight, providing a mixture of starting material and homodimer in a 18:82 ratio (80%, 83% *cis*-internal olefin). ^{1}H NMR (500 MHz, $CDCl_3$) δ 5.87 (ddt, *J* = 17.0, 10.5, 6.5, 2H; *r*), 5.49 (m, 0.17 rel. H; *trans-a*), 5.44 (m, 0.83 rel. H; *cis-a*), 5.193 (q, *J* = 7.0 Hz, 4H; *n* & *k* or *g* & *d*), 5.190 (q, *J* = 7.0 Hz, 4H; *n* & *k* or *g* & *d*), 5.09 (dd, *J* = 17.0, 1.5 Hz, 2H; s_Z), 5.02 (dd, *J* = 10.5, 1.5 Hz, 2H; s_E), 4.88 (d, *J* = 16.0 Hz, 1H; *f*), 4.88 (d, *J* = 16.0 Hz, 1H; *m*), 4.65 (d, *J* = 16.5 Hz, 1H; *m*), 4.65 (d, *J* = 16.0 Hz, 1H; *f*), 4.40 (m, 8H; *i & j*), 2.55 (m, 4H; *c & p*), 2.47 (m, 4H; *b & q*), 1.56 (d, *J* = 7.0 Hz, 12H; *e* & *o*), 1.52 (d, *J* = 7.0 Hz, 12 H; *h & l*); ^{13}C NMR (125 MHz, $CDCl_3$) δ 172.49, 170.38, 169.87, 166.77, 136.57 (*r*), 129.48 *(trans-a)*, 129.03 (*cis-a*), 115.77 (*s*), 69.41 (*g & k*), 68.36 (*d* or *n*) 68.33 (*d* or *n*), 62.91 (*i & j*), 60.84 (*f & m*), 33.84 (*c*), 33.26 (*p*), 28.78 (*q*), 22.66 (*b*), 17.00 (*e & o*) 16.87 (*h & l*); HRMS (ESI) $[M+H]^+$ calc mass 1233.4085, found 1233.4086.

Representative protocol: ALS-2051, 0.1 M concentration suggested for further investigations.[94]

ED-ROMP competition experiment between *cis* and *trans-cyclic*-Eg-(LGL-P)$_2$.

A pre-mixed solution of ***trans-cyclic*-Eg-(LGL-P)$_2$** (6.2 mg, 10.2 μmol) and ***cis-cyclic*-Eg-(LGL-P)$_2$** (5.8 mg, 9.6 μmol) in $CDCl_3$ (315 μmol) was added to an NMR tube equipped with a controlled atmosphere valve. A solution of **G2** (220 μg, 0.25 μmol) in $CDCl_3$ (160 μL) was then added under N_2 and the tube was inserted into a 600 MHz NMR for further analysis as the reaction progressed. 20 ^{1}H NMR spectra were acquired over the course of 4 hours, with particular attention being paid to the G-methylene peak region 4.65-4.85 ppm. A final ratio of

cis:*trans* observed for the quenched solution was 0.20 to 1, corresponding to 17% *cis*-monomer remaining. Data for the remaining time points is shown below.

Representative protocol: ALS-1080.

Table 6. Amount of *cis-cyclic*-Eg-(LGL-P_p) remaining during ED-ROMP at various time points.

Time (min)	Adjusted % *cis*
0	50.0
5	47.8
9	43.4
11	40.9
13	40.1
15	36.1
17	34.3
20	32.9
27	26.6
32	24.8
37	21.7
47	20.3
57	19.7
67	19.0
87-240	16.8

Removal of ruthenium contaminants using metal scavenger resin.

To a solution of unpurified *cis-cyclic*-Eg-(LGL-P)$_2$ (Ru contamination: 30 mg, 0.05 mmol) was in CH_2Cl_2 (5 mL) was added QuadraSil®MP thiol resin (5-50 equiv). The resulting mixture was vigorously stirred for 18-24 h and the insoluble material was then removed through a pre-rinsed syringe filter. The filtrate was concentrated *in vacuo,* then the crude material was subjected to purification by chromatography on SiO_2 as described above.

Representative protocols: ALS-2078 (50 equiv resin) and ALS-2080 (5 equiv resin).

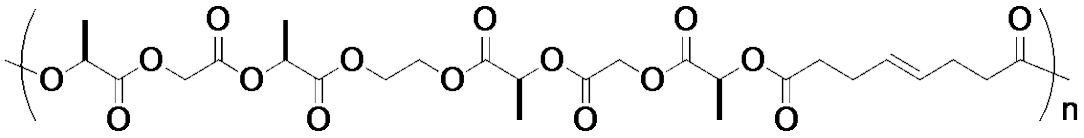

Preparation of poly (LGL-Eg-LGL-P_p).

Poly (LGL-Eg-LGL-P_p) was synthesized using a variety of methods, detailed below. Representative spectral data is as follows: ^{1}H NMR (500 MHz, $CDCl_3$) δ 5.49 (m, 1.7 H; *trans*), 5.42 (m, 0.3H, *cis*), 5.20 (q, *J* = 7.5 Hz, 2H), 5.18 (q, *J* = 7.0 Hz, 2H), 4.89 (d, *J* = 16.5 Hz, 2H), 4.65 (d, *J* = 16.5 Hz, 2H), 4.41 (m, 4H), 2.50 (m, 4H), 2.35 (m, 4H), 1.56 (d, *J* = 7.0 Hz, 6H), 1.53 (d, *J* = 7.5 Hz, 6H); ^{13}C NMR (125 MHz, $CDCl_3$) δ 172.39, 170.27, 169.75, 166.66, 129.35, 69.27, 68.17, 62.79, 60.69, 33.69, 27.58, 16.88, 16.74; DSC: Tg = 18 °C.

SEC (THF) for ED-ROMP experiments: M_n = 33.4 kDa, M_w = 46.0 kDa, Đ = 1.40.[22]

SEC (THF) for SEED-ROMP experiments: M_n = 60.4 kDa, M_w = 67.3 kDa, Đ = 1.11. *ALS-2002*

SEC (THF) for DED-ROMP experiments: M_n = 58.2 kDa, M_w = 67.6 kDa, Đ = 1.16. *ALS-3069*

SEED-ROMP kinetics study.

To a stirring solution of ***cis-cyclic*-Eg-(LGL-P)$_2$** (72 mg, 120 μmol) and CH_2Cl_2 (121 μL) was added a solution of catalyst **G2** (1.3 mg, 1.5 μmol) in CH_2Cl_2 (50 μL). Aliquots were removed via pipette at the specified time points over the course of 2 days and added to a GC vial containing a solution of ethyl vinyl ether in order to quench the catalyst. Samples were diluted

with CH_2Cl_2, passed through a celite plug and concentrated. The *cis*-to-*trans* ratio of monomer was approximated by comparing peak integrations at 4.85-4.75 ppm (Figure 32). Total conversion was approximated by comparing peak integrations at 4.9-4.75 ppm (Figure 13). The *E:Z* ratio of polymeric materials, as determined by peak integrations at 5.6-5.3 ppm, was 85:15.

Representative protocol: ALS-2002.

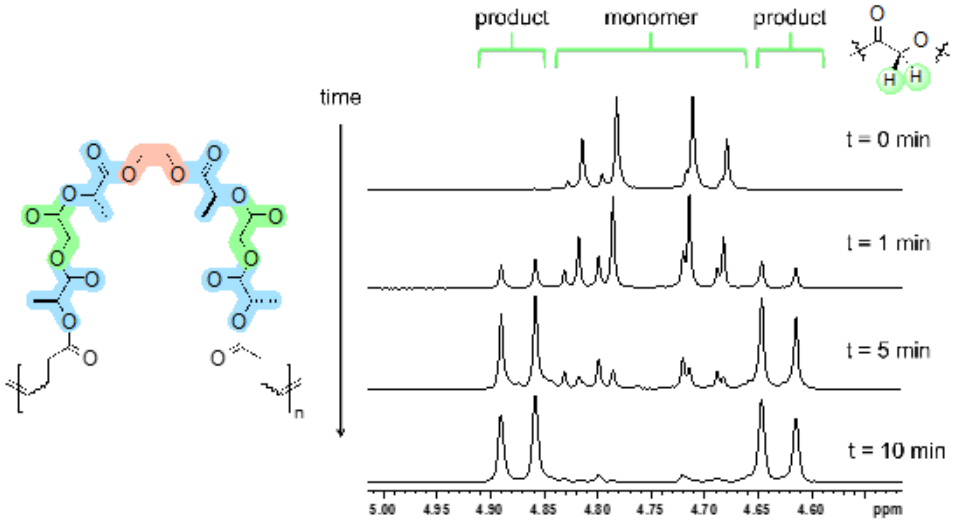

Figure 32. Monitoring *cis*- and *trans*-macromonomer consumption during SEED-ROMP.

Table 7. Analysis of polymerization samples during SEED-ROMP kinetics studies.

Aliquot #	time (min)	% conversion	M_n (kDa)	M_w (kDa)	Đ	DP	% cis in SM remaining	% trans in SM remaining	% Mcis	% Mtrans
—	0		0.603	–	1.0	1	86.9	13.1	86.9	13.1
1	1	25	51.4	60.1	1.2	85	72.1	27.9	53.3	20.6
2	3	67	61.8	68.8	1.11	103	36.97	63.0	12.20	20.80
3	5	72	61.6	68.9	1.12	102	44.55	55.4	13.50	16.80
4	10	89	65.8	72.0	1.10	109	34.69	65.3	3.40	6.40
5	15	87	60.5	67.3	1.11	100	36.07	63.9	4.40	7.80
6	20	91	59.4	66.4	1.12	99	34.74	65.3	3.30	6.20
7	30	92	62.2	69.0	1.11	103	–	–	–	–
8	45	93	61.4	68.7	1.12	102	–	–	–	–
9	60	88	57.7	64.1	1.11	96	–	–	–	–
10	90	95	57.1	64.4	1.13	95	–	–	–	–
11	120	96	57.6	64.0	1.11	96	–	–	–	–
12	180	96	55.3	62.0	1.12	92	–	–	–	–
13	240	96	60.0	66.8	1.11	100	–	–	–	–

Molecular weight control study.

A solution of catalyst **G2** (1-3 mol%) in CH_2Cl_2 (~0.5 M) was added to a vial containing ***cis-cyclic*-Eg-(LGL-P)$_2$** in CH_2Cl_2 (final concentration 0.7 M). Reaction mixtures were shaken for 2 h, quenched with EVE (0.5 mL), and shaken an additional 30 min. The mixture was dissolved in CH_2Cl_2 and concentrated *in vacuo* to yield **poly (LGL-Eg-LGL-P$_p$)** with varying molecular weights. Results are summarized in the table below. Entry 4, corresponding to the results of a chain extension experiment, has also been included.

Representative protocols: ALS-2008, 2028, 3083, 3085.

Table 8. Molecular weight control study of SEED-ROMP at various catalyst loadings.

Entry	mol % cat	% conversion	Theo. MW (kDa)	Adj. theo. MW (kDa)	M_n (kDa)	M_w (kDa)	PDI	Adj. [M]	[cat]	Adj. [M]/[cat]
monomer	-	-	-	-	602.54	602.54	1.00	-	-	-
1	1	92	60.3	55.3	70.7	83.2	1.17	0.642	0.007	91.7
2	1.25	93	48.4	45.0	60.4	67.3	1.12	0.651	0.008712	74.7
3	3	94	20.1	18.9	36.9	48.8	1.32	0.657	0.0212	31.0
4	0.625	68	88.4	60.0	74.3	82.4	1.1	0.0	0.00011	99.6

Chain extension experiment of poly (LGL-Eg-LGL-P_p).

A solution of catalyst **G2** (0.18 mg, 0.22 μmol) in CH_2Cl_2 (10 μL) was added to a pre-mixed solution of ***cis-cyclic*-Eg-(LGL-P)$_2$** (10.5 mg, 17.4 μmol) in CH_2Cl_2 (15 μL). After shaking for 20 min, a second aliquot of ***cis-cyclic*-Eg-(LGL-P)$_2$** (10.5 mg, 17.4 μmol) in CH_2Cl_2 (25 μL) was added. The polymerization was quenched through the addition of EVE (0.5 mL) and allowed to shake for 30 min. The mixture was dissolved in CH_2Cl_2 and passed through a celite plug before concentrating *in vacuo* to yield a viscous residue (18.4 mg, 90.6% conversion, 31% *cis*-olefin in unreacted starting material). Spectral data matched that previously reported for p**oly (LGL-Eg-LGL-P_p)**. SEC (THF): molecular weights too high to be determined; Đ ≈ 1.11. *Note: when each phase of polymerization was allowed to stir for only 10 min, polymer was obtained with 68% conversion, adjusted theo. M_n = 60.0 kDa, actual M_n = 74.3 kDa, M_w = 82.5 kDa, Đ = 1.11. Representative protocol: ALS-2030.*

ADMET of poly (LGL-Eg-LGL-P_p) with HG1.

A solution of catalyst **HG1** (0.585 mg, 0.974 μmol) in CH_2Cl_2 (9 μL) was added to a pre-mixed solution of **Eg-(LGL-P)$_2$** (61 mg, 97.4 μmol) in CH_2Cl_2 (40 μL) in a sealed tube. The tube was backfilled with N_2 and then evacuated before stirring at 40 °C. The tube was periodically evacuated over the course of the reaction, then quenched with EVE (1 mL) and stirred for 10 min before concentrating *in vacuo* to provide a mixture of oligomers (n=2-6 observed by SEC) and

poly (LGL-Eg-LGL-P_p) with DPs ranging from 2 to 71 (58 mg, 64% *trans*-internal olefin in product mixture).

Representative protocol: ALS-3063.

Cyclodepolymerization of poly (LGL-Eg-LGL-P_p).

A solution of catalyst **G2** (0.23 mg, 0.27 μmol) in CH_2Cl_2 (200 μL) was added to a pre-mixed solution of **poly (LGL-Eg-LGL-P_p)** (16 mg, 26.6 μmol) in CH_2Cl_2 (1.12 mL). The reaction was stirred at 40 °C under N_2 for 8h then quenched with EVE (2 mL) and stirred for an additional 30 min. It was then concentrated *in vacuo* to provide ***cyclic*-Eg-(LGL-P)$_2$** and oligomers with size n as a viscous oil (16 mg, 83% *trans*-olefin in product mixture); in each of the three peak regions (n = 1-3), peaks corresponding to $[M+H]^+$ (minor), $[M+Na]^+$ (major) and $[M+K]^+$ (minor) were observed:

n = 1: HRMS $[M+Na]^+$ calc mass 625.1745, found 625.1746, detected intensity 8.4×10^8

n = 2: HRMS $[M+Na]^+$ calc mass 1227.3592, found 1227.3595, detected intensity 6.24×10^7

n = 3: HRMS $[M+Na]^+$ calc mass 1807.5613, found 1807.5617, detected intensity 1.97×10^6

Representative protocol: ALS-3051.

DED-ROMP of *cis-cyclic*-Eg-(LGL-P)$_2$ catalyzed by G3.

A solution of catalyst **G3** (0.196 mg, 0.222 μmol) in CH_2Cl_2 (10 μL) was added to a pre-mixed solution of ***cis-cyclic*-Eg-(LGL-P)$_2$** (10.7 mg, 17.8 μmol) in CH_2Cl_2 (15 μL) and shaken for 2h. The reaction was quenched through the addition of EVE (0.5 mL), allowed to stir for an additional 30 min, then concentrated *in vacuo* to yield crude **poly (LGL-Eg-LGL-P$_p$)** (10.1 mg, 94%, 86% *trans*-olefin). Trace amounts of unreacted monomer were observed by ^{1}H NMR but were too small to be quantified. SEC (THF): M_n = 58.2 kDa, M_w = 67.6 kDa, Đ = 1.16.

Representative protocol: ALS-3069.

DED-ROMP of *trans-cyclic*-Eg-(LGL-P)$_2$ catalyzed by G3.

A solution of catalyst **G3** (0.352 mg, 0.398 μmol) in CH_2Cl_2 (20 μL) was added to a pre-mixed solution of ***trans-cyclic*-Eg-(LGL-P)$_2$** (19.2 mg, 31.9 μmol) in CH_2Cl_2 (26 μL) and shaken for 2h. The reaction was quenched through the addition of EVE (0.5 mL), allowed to stir for an additional 30 min, then concentrated *in vacuo* to yield crude **poly (LGL-Eg-LGL-P$_p$)** (18 mg, 94%, 87% *trans*-olefin). Trace amounts of unreacted monomer were observed by ^{1}H NMR but were too small to be quantified. SEC (THF): unable to be obtained by GPC at this time due to instrument repairs.

Representative protocol: ALS-3071.

ROMP of strained monomers to form homopolymers at various temperatures.

Representative protocols: ALS-2035-2046.

Preliminary ROMP experiments were conducted using the same conditions as block experiments but without initial addition of ED-ROMP monomer. Note that lack of monomer and overall dilution with respect to total molecule concentration necessarily brings about differences for ROMP and ROMP paired with ED-ROMP—ROMP. The results from this set of experiments do not therefore reflect precise outcomes expected for the ROMP phase of the sequential reaction. Two strained monomers were used in these control studies, NBE and COE. Sample protocols and a table of results are detailed below:

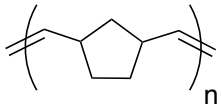

A. ROMP of norbornene to form poly(NBE).

A solution of **G2** (180 μg, 0.212 μmol) in CH_2Cl_2 (25 μL) was added to a pre-mixed solution of NBE (40 mg, 423 μmol) in CH_2Cl_2 (25 μL) at room temperature. The vial was shaken for 1 min, then EVE was added and the mixture was diluted with additional CH_2Cl_2 (0.3 mL) with manual stirring. The quenched solution was passed through a celite plug with CH_2Cl_2 rinsing and concentrated *in vacuo* to provide crude **poly(NBE)** as a white solid (4.7 mg, 50 μmol, 12% conversion, 54% *cis*-olefin incorporation); ^{1}H NMR (500 MHz, $CDCl_3$) δ 5.38 (m, *trans*) and 5.23 (m, *cis*) (2H), 2.79 (br s, *cis*) and 2.44 (br s, *trans*) (2H), 1.88 (br m, 1.1H), 1.80 (br m, 2H),

1.35 (br m, 2H), 1.09 (m, 1H); ^{13}C NMR (125 MHz, $CDCl_3$) δ 134.17, 134.10, 134.00, 133.93, 133.33, 133.18, 133.05, 43.58, 43.29, 42.91, 42.25, 38.83, 38.57, 33.28, 33.09, 32.53, 32.36.

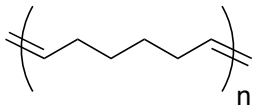

B. ROMP of *cis*-cyclooctene to form poly(COE).

A solution of **G2** (180 μg, 0.212 μmol) in CH_2Cl_2 (10 μL) was added to a pre-mixed solution of *cis*-COE (47 mg, 425 μmol) in CH_2Cl_2 (40 μL) at room temperature. The vial was shaken for 5 min at 0 °C, then EVE was added and the mixture was diluted with additional CH_2Cl_2 (0.3 mL) with manual stirring. The quenched solution was passed through a celite plug with CH_2Cl_2 rinsing and concentrated *in vacuo* to provide crude **poly(COE)** as a white solid (10.8 mg, 98 μmol, 23% conversion, 34% *cis*-olefin incorporation); ^{1}H NMR (500 MHz, $CDCl_3$) δ 5.41 (m, *trans*) and 5.35 (m, *cis*) (2H), 2.02 (m, *cis*) and 1.99 (m, *trans*) (4H), 1.33 (m, 8H).

Table 9. Homopolymerization of NBE and COE in preliminary ROMP experiments.

	NBE rt, 1 min	NBE rt, 5 min	NBE 0 °C, 1 min	NBE 0 °C, 5 min	COE rt, 1 min	COE rt, 5 min	COE 0 °C, 1 min	COE 0 °C, 5 min
Mn (kDa)	48	23	11*	77*	69	nd	53	89
Mw (kDa)	63	47	12	85	86	nd	63	102
Đ	1.3	2.1	1.1	1.1	1.2	nd	1.2	1.1
% conversion (by mass)	6.5	30	12	6.5	75	81	37	23
DP_{theo} [M]/[cat]	2000	2000	2000	2000	2000	2000	2000	2000
DP_{actual} (Mn/monomer)	507	243	116	814	626	nd	476	811

nd. This polymer was insoluble in THF and not analyzed further by SEC.

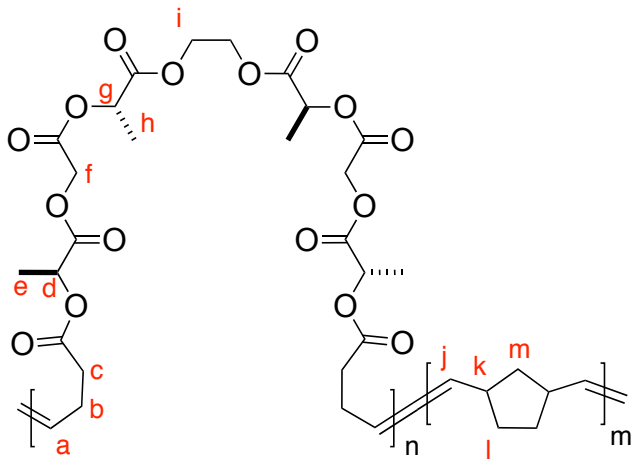

Sequential SEED-ROMP—ROMP: preparation of poly [(LGL-Eg-LGL-P_p)-*block*-(NBE)].

Representative protocols: ALS-2006-2011.

SEED-ROMP—ROMP reactions were carried out sequentially, with SEED-ROMP occurring for 10 min prior to NBE addition. ROMP was allowed to continue for either 1 min or 5 min. Control experiments were quenched after the SEED-ROMP phase of the reaction. A sample protocol is detailed below:

A solution of **G2** (0.18 mg, 0.218 μmol) in CH_2Cl_2 (10 μL) was added to a pre-mixed solution of ***cis-cyclic*-Eg(LGL-P_p)** (10.5 mg, 17.4 μmol) in CH_2Cl_2 (15 μL) and allowed to shake for 10 min before a pre-mixed solution of NBE (41 mg, 435 μmol) in CH_2Cl_2 (25 μL) was added at room temperature. The vial was shaken for 1 min, and EVE was added and was shaken for an additional 10 min. The mixture was diluted to a pre-weighed vial after diluting with CH_2Cl_2 (0.3 mL) and concentrated *in vacuo* to provide crude **poly [(LGL-Eg-LGL-P_p)-*block*-(NBE)]** as a solid (18.5 mg, 93% SEED-ROMP monomer conversion, 64% *cis*-olefin incorporation in **poly(NBE)**; based on DP, composition is 46 mol% block A (**poly (LGL-Eg-LGL-P_p)**, DP 100) and 54 mol% block B (**poly(NBE)**, DP 117). To add clarity to integration numbers presented

herein, a 50:50 ratio of A:B has been assigned, and a 50:50 *cis:trans* ratio has been assigned for the NBE block. ^{1}H NMR (500 MHz, $CDCl_3$) δ 5.51 (m, a_{trans}) and 1.42 (m, a_{cis}) (2H), 5.35 (br s, 1H, j_{trans}) and 5.21 (m, 5H, *dg* & j_{cis}), 4.89 (d, *J* = 16.0 Hz, 2H, *f*), 4.65 (d, *J* = 16.5 Hz, 2H, *f*), 4.41 (m, 4H, *i*), 2.85 (br s, 2H, k_{cis}), 2.50 (m, 5H, *c* and k_{trans}), 2.33 (m, 4H, *b*), 1.87 (m, 1H, m_1), 1.80 (m, 2H, l_1) 1.55 (d, *J* = 6.0 Hz, 6H, *e*), 1.53 (d, *J* = 7.0 Hz, 6H, *h*) 1.35 (m, 2H, l_2), 1.09 (m, 1H, m_2); ^{13}C NMR (125 MHz, $CDCl_3$) δ 172.49 (*A*), 170.38 (*A*), 169.86 (*A*), 166.78 (*A*), 134.14 (*B*), 134.07 (*B*), 134.03 (*B*), 133.99 (*B*), 133.90 (*B*), 133.28 (*B*), 133.15 (*B*), 133.00 (*B*), 129.49 (*A*), 129.154 (*B*), 129.04 (*B*), 69.41 (*A*), 68.36 (*A*), 68.30 (*A*), 62.92 (*A*), 60.83 (*A*), 43.56 (*B*), 43.27 (*B*), 42.90 (*B*), 42.24 (*B*), 38.81 (*B*), 38.56 (*B*), 33.84 (*A*), 33.25 (*B*), 33.07 (*B*), 32.52 (*B*), 32.36 (*B*), 27.72 (*A*), 17.02 (*A*), 16.88 (*A*); SEC (THF): M_n = 71.4 kDa, M_w = 78.8 kDa, Đ = 1.10.

Representative protocol: ALS-2006 to 2011.

Table 10. Sequential ED-ROMP—ROMP Block copolymerization

Conditions	**1**	**2**	**3**
Time ED-ROMP (min)	10	10	10
Time ROMP (min)	--	1	5
Mn	60.4	71.4	66.6
Mw	67.3	78.8	75
Đ	1.11	1.10	1.13

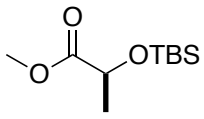

Preparation of Me-L-TBS (3).

To a mixture of **Me-L (**104 g, 1.0 mol) and imidazole (68.1 g, 1 mol) in DMF (60 mL) at 0 ^{o}C was added TBSCl (158 g, 1.05 mol) in 3 portions. After stirring 24 h, the reaction mixture was diluted with brine (250 mL) and extracted with Et_2O (3 × 500 mL). The combined organic layers were then washed with brine (300 mL), dried with $MgSO_4$, filtered, and concentrated *in vacuo* to give the crude product as a colorless oil (214 g, 98%). The residue had identical spectral properties to those found in literature[160] and was used in subsequent reactions without further purification; ^{1}H NMR (500 MHz, $CDCl_3$) δ 4.35 (q, *J* = 5.2 Hz, 1 H), 3.72 (s, 3 H), 1.40 (d, *J* = 5.6 Hz), 0.90 (s, 9 H), 0.10 (s, 3 H), 0.07 (s, 3 H); ^{13}C NMR (125 MHz, $CDCl_3$) δ 174.69, 68.55, 51.98, 25.86, 21.50, -4.84, -5.13.

Representative protocol: ALS-2089.

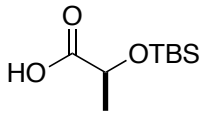

Preparation of L-TBS (5).

A solution of LiOH (77 mg, 1.85 mmol) in H_2O (4.6 mL) was added dropwise to a pre-cooled solution of **Me-L-TBS** (**3**, 101 mg, 0.463 mmol) in THF (4.6 mL). Once addition was complete and the starting material was gone by TLC, the THF was concentrated *in vacuo*, brine was added (5 mL), and the aqueous layer was extracted with Et_2O (2 × 10 mL). The aqueous layer was acidified until pH ~4 with 1 M HCl, then immediately extracted with Et_2O (3 × 10 mL), dried over $MgSO_4$, filtered, and concentrated *in vacuo* to give the crude product as a colorless oil (90 mg, 96%). This compound was unstable at room temperature and used shortly after its

preparation. It had identical spectral properties to those found in literature[161] and was used in subsequent reactions without further purification; *The following protocol modifications can be made: (a) if the reaction is incomplete by TLC, a preliminary wash with organic solvent can be carried out to isolate unreacted starting material; (b) on larger scales, acidification should be carried out carefully but rapidly at 0 °C and 0.5-1 M citric acid can be used in place of HCl to avoid decomposition at pH < 3.* ^{1}H NMR (500 MHz, $CDCl_3$) δ 9.30 (br s, 1 H), 4.39 (q, *J* = 6.6 Hz, 1 H), 1.47 (d, *J* = 6.6 Hz, 3 H), 0.94 (s, 9 H), 0.159 (s, 3 H), 0.155 (s, 3 H); ^{13}C NMR (125 MHz, $CDCl_3$) δ 174.01, 68.96, 25.77, 21.20, -4.41, –5.16.

Representative protocol: ALS-3029

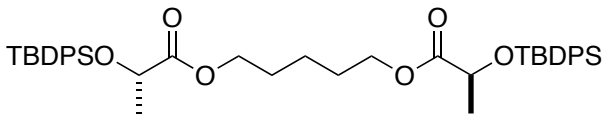

Preparation of alkyl-(L-TBDPS)$_2$ (9)

1,5-pentanediol (0.91 mL, 8.4 mmol), DCC (3.66 g, 17.7 mmol) and DPTS (0.993 g, 3.38 mmol) were sequentially added to a solution of **L-TBDPS** (**6**, 5.82 g, 17.7 mmol) in CH_2Cl_2 (84 mL). The mixture was stirred for 16 h, then was concentrated to 25% volume, diluted with hexanes (30 mL) and filtered. The filtrate was concentrated *in vacuo* to give the crude product as a yellow oil then purified by flash chromatography on SiO_2 (10−40% EtOAc in hexanes) to provide the product as a colorless oil (5.136 g, 84%) with trace contamination with unreacted **6**; ^{1}H NMR (500 MHz, $CDCl_3$) δ 7.73 (m, 8H), 7.44 (m, 12H), 4.29 (q, *J* = 6.5 Hz, 2H), 3.95 (m, 4H), 1.50

(p, J = 7.0 Hz, 4H), 1.36 (d, J = 7.0 Hz, 6H), 1.31 (m, 2H), 1.09 (s, 18H); HRMS (ESI) $[M+NH_4]^+$ calc mass 742.3954, found 742.3944.

Representative protocol: ALS-2058.

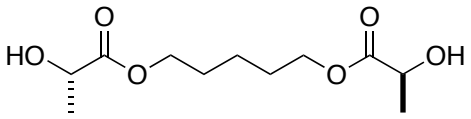

Preparation of L-alkyl-L (13).

To a stirring solution of **9** (5.10 g, 7.04 mmol) in THF (70 mL) at 0 °C was slowly added pre-dried AcOH (1.0 mL, 17.6 mmol) and TBAF (4.1 mL, 15.5 mmol). The ice bath was removed and the reaction was stirred at rt for 2 h, when the solution was cooled to 0 °C and additional TBAF (11.4 mL) was added. The solution was stirred for another 1.5 h, then was quenched with the addition of brine (100 mL) after cooling to 0 °C. The THF was concentrated and the solution was diluted with Et_2O and separated. The aqueous layer was extracted with Et_2O (3 × 100 mL), the combined organic layers were washed with sat. aq. NH_4Cl (50 mL) and dried over $MgSO_4$. The solution was concentrated *in vacuo* and purified by flash chromatography on SiO_2 (15−50% EtOAc in hexanes) to provide the product as a colorless oil (5.14 g, 84%); ^{1}H NMR (500 MHz, $CDCl_3$) δ 4.30 (dq, J = 6.5, 5.0 Hz, 2H), 4.24 (m, 4H), 2.77 (d, J = 5.0 Hz, 2H), 1.75 (p, J = 6.5 Hz, 4H), 1.47 (m, 2H), 1.43 (d, J = 6.5 Hz, 6H); ^{13}C NMR (125 MHz, $CDCl_3$) δ 175.90, 66.89, 65.42, 28.28, 22.37, 22.37, 20.58; HRMS (ESI) $[M+H]^+$ calc mass 249.1333, found 249.1333.

Representative protocol: ALS-2058.

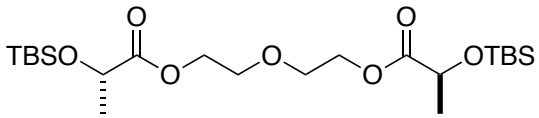

Preparation of PEG-(L-TBS)$_2$ (10).

To a stirring solution of diethylene glycol (1.11 g, 10.5 mmol) and **L-TBS** (**3**, 4.49 g, 22.0 mmol) in CH_2Cl_2 (105 mL) was added DPTS (1.23 g, 4.18 mmol) and DCC (4.53 g, 22.0 mmol). The solution was stirred 24 h, then concentrated to 25% volume, diluted with hexanes (50 mL) and filtered. The filtrate was concentrated *in vacuo* then purified by chromatography on SiO_2 (10−100% EtOAc in hexanes) to provide the product as a colorless oil with minor contamination with **3** and mono-coupled intermediate (2.03 g, 41%, 62% BRSM); ^{1}H NMR (500 MHz, $CDCl_3$) δ 4.37-4.21 (m, 6H), 3.70 (t, J = 5.0 Hz, 4H), 1.41 (d, J = 8.5 Hz, 6H), 0.90 (s, 18H), 0.10 (s, 6H), 0.07 (s, 6H); ^{13}C NMR (125 MHz, $CDCl_3$) δ 174.21, 69.12, 68.45, 63.83, 25.86, 21.49, 18.45, -4.80, -5.14; HRMS (ESI) $[M+NH_4]^+$ calc mass 479.2855, found 479.2842.

Representative protocol: ALS-3027.

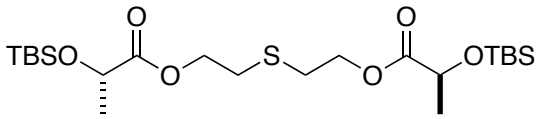

Preparation of sulfide-(L-TBS)$_2$ (11).

To a stirring solution of 2,2'-thiodethanol (1.26 g, 10.3 mmol) and **L-TBS** (**3**, 4.43 g, 21.7 mmol) in CH_2Cl_2 (103 mL) was added DPTS (1.21 g, 4.13 mmol) and DCC (4.47 g, 21.7 mmol). The

solution was stirred 23 h, then concentrated to 25% volume, diluted with hexanes (50 mL) and filtered. The filtrate was concentrated *in vacuo* then purified by chromatography on SiO_2 (10−100% EtOAc in hexanes) to provide the product as a colorless oil with trace contamination with **3** and mono-coupled **Si-L-sulfide** intermediate (2.60 g, 51%, 78% BRSM); ^{1}H NMR (500 MHz, $CDCl_3$) δ 4.36-4.25 (m, 6H), 2.82 (t, *J* = 6.8 MHz, 2H), 1.41 (d, *J* = 6.8 MHz, 6H), 0.90 (s, 18H), 0.10 (s, 6H), 0.07 (s, 6H); ^{13}C NMR (125 MHz, $CDCl_3$) δ 174.01, 68.45, 63.59, 35.07, 30.76, 25.86, 21.52, -4.76, -5.10; HRMS (ESI) $[M+NH_4]^+$ calc mass 512.2892, found 512.2898.

Representative protocol: ALS-3025.

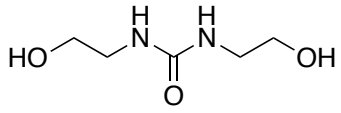

Preparation of 1,3-bis(hydroxymethyl)urea (8).

A solution of oxazolidinone (**7**, 10.0 g, 115 mmol) and ethanolamine (7.0 mL, 117 mmol) were stirred at 150 °C for 3.5 h, then the mixture was allowed to cool to rt. 1-butanol (20 mL) was added with manual stirring, and the mixture was let to stand at 0 °C for 17h. After warming to rt, the solid product was collected by vacuum filtration with washing by hexanes (20 mL). The collected solid was diluted with acetone (100 mL) and stirred 1h before filtering again. The white solid (12.4 g, 73%) had identical spectral properties to those found in literature[162] and was used in subsequent reactions without further purification; ^{1}H NMR (500 MHz, DMSO-d_6) δ 6.02 (t, *J*

= 5.5 Hz, 2 H; *NH*), 4.68 (t, *J* = 5.5 Hz, 2 H; *OH*), 3.41 (q, *J* = 5.5 Hz, 4 H; HO-*CH*$_2$), 3.09 (q, *J* = 5.5 Hz, 4 H; NH-*CH*$_2$); ^{13}C NMR (125 MHz, DMSO-d$_6$) δ 159.32, 61.76, 43.01.

Representative protocol: ALS-2083.

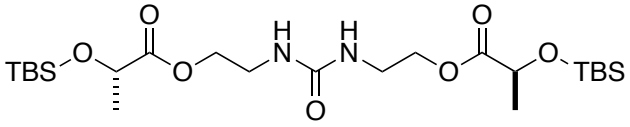

Preparation of Urea-(L-TBS)$_2$ (12)

To a stirring solution of **8** (0.928 g, 6.26 mmol) and **L-TBS** (**5**, 2.69 g, 13.2 mmol) in CH_2Cl_2 (63 mL) was added DPTS (0.737 g, 2.51 mmol) and DCC (2.71 g, 13.2 mmol). The solution was stirred 18 h, then concentrated to 25% volume, diluted with hexanes (50 mL) and filtered. The filtrate was concentrated *in vacuo* and isolated as a crude solid that was used without further purification (2.94 g, 95%); ^{1}H NMR (500 MHz, $CDCl_3$) δ 4.75 (t, *J* = 5.5 Hz, 2H, N<u>H</u>), 4.35 (q, *J* = 6.5 Hz, 2H, CH), 4.25 (m, 4H, O-*CH*$_2$), 3.50 (m, 4H, N-*CH*$_2$), 1.40 (d, *J* = 7 Hz, 6H, *CH*$_3$), 0.90 (s, 18H, ^{t}Bu-*CH*$_3$), 0.09 (s, 6H, Si-*CH*$_3$), 0.07 (s, 6H, Si-*CH*$_3$); HRMS (ESI) $[M+H]^+$ calc mass 521.3073, found 521.3077.

Representative protocol: ALS-3023.

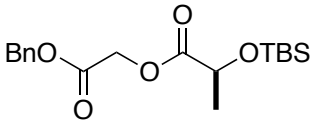

Preparation of Bn-GL-TBS (16).

To a stirring solution of **Bn-G** (12.0 g, 72.4 mmol) and **L-TBS** (**5**, 12.3 g, 60.3 mmol) in CH_2Cl_2 (600 mL) was added DPTS (3.56 g, 12.1 mmol). Once the DPTS had dissolved, DCC (14.9 g, 72.4 mmol) was added and the solution stirred 21 h. The reaction mixture was then filtered, concentrated to approximately 50 mL, diluted with 50% Et_2O in hexanes (200 mL), and filtered. The filtrate was concentrated *in vacuo* and the crude yellow oil was purified by flash chromatography (SiO_2, 2.5% EtOAc in hexanes) to provide the product as a colorless oil (14.8 g, 70%); ^{1}H NMR (500 MHz, $CDCl_3$) δ 7.39 (m, 5 H), 5.19 (s, 2 H), 4.74 (d, J = 16.0 Hz, 1 H), 4.68 (d, J = 16.0 Hz, 1 H), 4.46 (q, J = 6.5 Hz, 1 H), 1.45 (d, J = 7.0 Hz, 3 H); 0.90 (s, 9 H), 0.10 (s, 3 H), 0.08 (s, 3 H); ^{13}C NMR (125 MHz, $CDCl_3$) δ 173.63, 167.54, 135.19, 128.79, 128.71, 128.59, 68.28, 67.28, 60.92, 25.85, 21.49, 18.44, -4.81, -5.19; HRMS (ESI) $[M+K]^+$ calc mass 359.2686, found 359.2041.

Representative protocol: ALS-3053.

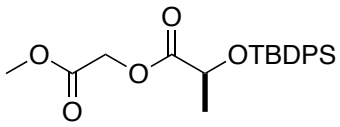

Preparation of Me-GL-TBDPS (18).

To a solution of **GL-TBDPS** (1.03 g, 2.66 mmol) in DMF (9.9 mL) were added K_2CO_3 (1.84 g, 13.3 mmol) and CH_3I (0.835 mL, 13.3 mmol) dropwise. After stirring for 18 h, the reaction mixture was filtered with EtOAc rinsing. The filtrate was partitioned between EtOAc (40 mL) and H_2O (40 mL) and the resulting organic layer was washed with H_2O (2 × 30 mL), sat. aq.

$NaHCO_3$ (30 mL), $Na_2S_2O_3$ (30 mL) and brine (30 mL). Unreacted starting material was isolated by acidifying the combined aqueous layers with 1 M HCl and extracting with EtOAc (3 × 10 mL). The organic layer that contained product was dried over Mg_2SO_4, filtered, and concentrated *in vacuo* to provide the product as a colorless oil (0.633 g, 86%). The crude compound contained a silyl ether impurity and was used in the subsequent step without further purification. ^{1}H NMR (500 MHz, $CDCl_3$) δ 7.73 (m, 4H), 7.46 (m, 6H), 4.59 (d, J = 15.6 Hz, 1H), 4.46 (d, J = 16.0 Hz, 1H), 4.42 (q, J = 6.8 Hz, 1H), 3.73 (s, 3H), 1.43 (d, J = 6.8 Hz, 3H), 1.10 (s, 9H) (silyl contaminant observed at 7.73, 7.46, 1.07); ^{13}C NMR (125 MHz, $CDCl_3$) δ 173.24, 168.06, 136.06, 135.89, 133.63, 133.15, 129.96, 127.81, 127.76, 68.83, 60.66, 52.32, 26.94, 21.41, 19.38 (silyl contaminant observed at 135.34, 134.94, 129.80, 127.87, 26.71, 19.36); HRMS (ESI) calc mass 418.2044, found 418.2048.

Representative protocol: ALS-2055.

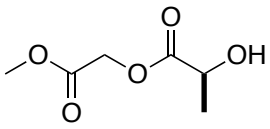

Preparation of Me-GL (19).

To a stirring solution of **Me-GL-TBDPS** (**16**, 0.536 g, 1.37 mmol) in THF (13.7 mL) at 0 °C was slowly added AcOH (0.310 mL, 5.49 mmol) and then TBAF (2.75 mL, 2.75 mmol) that had been pre-dried over 3 Å MS. The reaction solution was allowed to warm to rt by removing the ice bath. After stirring for an additional 2 h, a solution of sat. aq. NaCl (5 mL) was added, the THF was concentrated under reduced pressure and the solution was diluted with Et_2O (20 mL). The

aqueous layer was extracted with Et_2O (2 × 5 mL), and the combined organic layers were washed with sat. aq. NH_4Cl (10 mL), dried over $MgSO_4$, filtered and concentrated *in vacuo* to give the crude product as a colorless oil (0.193 g, 89%); ^{1}H NMR (500 MHz, $CDCl_3$) δ 4.77, (d, J = 16.0 Hz, 1H), 4.69 (d, J = 16.0 Hz), 4.44 (m, 1H), 3.78 (s, 3H), 2.78 (m, 1H), 1.50 (d, 3H); ^{13}C NMR (125 MHz, $CDCl_3$) δ 175.17, 167.81, 66.90, 61.24, 52.54, 20.47; LRMS $[M+H]^+$ calc mass 385, found 385.

Representative protocol: ALS-2057.

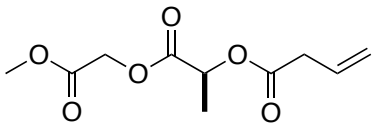

Preparation of Me-GL-B (20).

Protocol: To a stirring solution of **Me-GL** (96 mg, 0.593 mmol) in CH_2Cl_2 (5.9 mL) was added vinyl acetic acid (57 µL, 0.652 mmol), DPTS (35 mg, 0.119 mmol) and DCC (135 mg, 0.652 mmol). The resulting solution was stirred 18 h, and then additional vinyl acetic acid (43 µL, 0.533 mmol) was added. This reaction solution was concentrated *in vacuo* after stirring 4 h and re-dissolved in a solution of 75% hexanes in CH_2Cl_2 (5 mL). The precipitate was removed by filtration. The filtrate was washed with $NaHCO_3$ (5 mL), the aqueous layer was extracted with CH_2Cl_2 (2 × 5 mL) and dried over Na_2SO_4, filtered, and concentrated *in vacuo* to give the crude product as a faintly yellow oil. The residue was purified by chromatography on SiO_2 (5−40% EtOAc in hexanes) to provide the product as a colorless liquid (119 mg, 87%); ^{1}H NMR (500 MHz, $CDCl_3$) δ 5.98 (ddt, J = 17.0, 10.5, 7.0 Hz, 1H), 5.23 (dd, J = 10.5, 1.5 Hz, 1H), 5.19 (dd, J = 17.0, 1.5 Hz, 1H), 5.21 (q, J = 7.2 MHz, 1H), 4.79 (d, J = 4.79 Hz, 1H), 4.61 (d, J = 16.0 Hz,

1H), 3.23 (m, 2H), 1.59 (d, J = 7.0 Hz, 3H); ^{13}C NMR (125 MHz, $CDCl_3$) δ170.97, 170.28, 167.74, 129.74, 119.06, 68.60, 61.03, 51.44, 38.71, 16.92; HRMS (ESI) $[M+H]^+$ calc mass 231.086, found 232.0864.

Representative protocol: ALS-2060.

APPENDIX

EXPERIMENTAL SPECTRA

L-TBDPS
OTBDPS
HO
O
7.728
7.724
7.709
7.704
7.675
7.672
7.655
7.651
7.633
7.616
7.613
7.497
7.494
7.490
7.486
7.479
7.472
7.464
7.460
7.457
7.453
7.430
7.421
7.411
7.406
7.403
7.394
7.391
7.386
7.382
4.356
4.339
4.322
4.305
1.314
1.297
1.116
ppm
1
2
3
4
5
6
7
8
9
10
9.37
3.00
1.01
6.40
4.22

Bn-GL-TBDPS
BnO
OTBDPS
ppm
9.38
3.00
1.01
1.00
1.00
2.00
11.15
4.14
1.074
1.225
1.243
1.261
1.367
1.384
2.028
4.079
4.097
4.115
4.133
4.339
4.356
4.373
4.390
4.418
4.457
4.567
4.607
5.113
5.145
5.177
7.240
7.288
7.295
7.298
7.302
7.315
7.323
7.327
7.332
7.336
7.342
7.343
7.348
7.351
7.354
7.354
7.359
7.373
7.375
7.379
7.387
7.393
7.397
7.401
7.408
7.412
7.415
7.422
7.430
7.433
7.437
7.634
7.638
7.644
7.646
7.651
7.654
7.658
7.663
7.667
7.670

GL-TBDPS
OTBDPS
HO
O
O
O
O
7.681
7.672
7.665
7.662
7.657
7.455
7.437
7.417
7.397
7.377
7.355
7.337
4.615
4.574
4.507
4.466
4.417
4.400
4.383
4.366
2.046
1.424
1.408
1.092
ppm
1
2
3
4
5
6
7
8
9
10
9.09
3.03
1.02
1.01
1.00
6.17
4.05

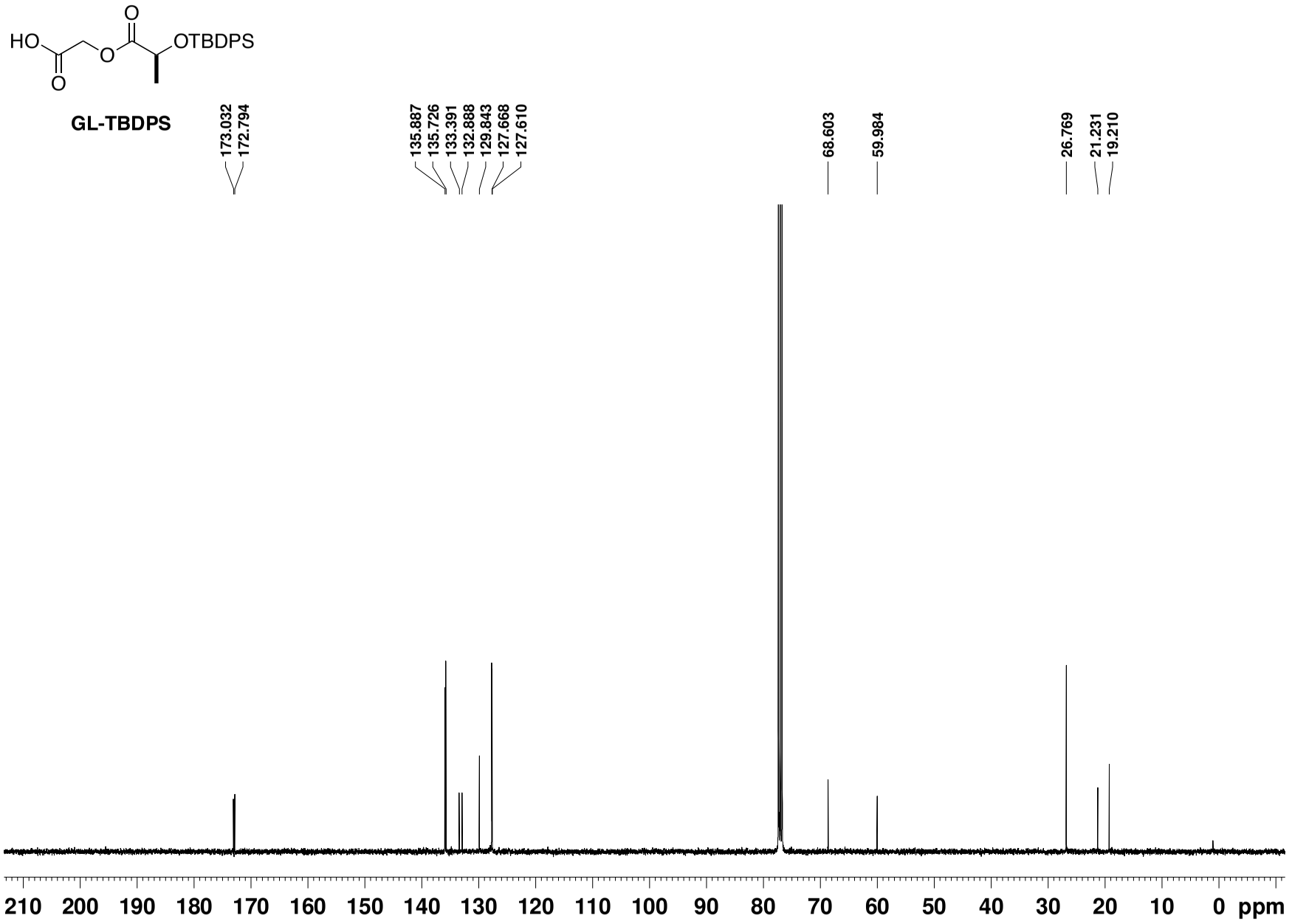
HO
O
O
O
OTBDPS
GL-TBDPS
173.032
172.794
135.887
135.726
133.391
132.888
129.843
127.668
127.610
68.603
59.984
26.769
21.231
19.210
210 200 190 180 170 160 150 140 130 120 110 100 90 80 70 60 50 40 30 20 10 0 ppm

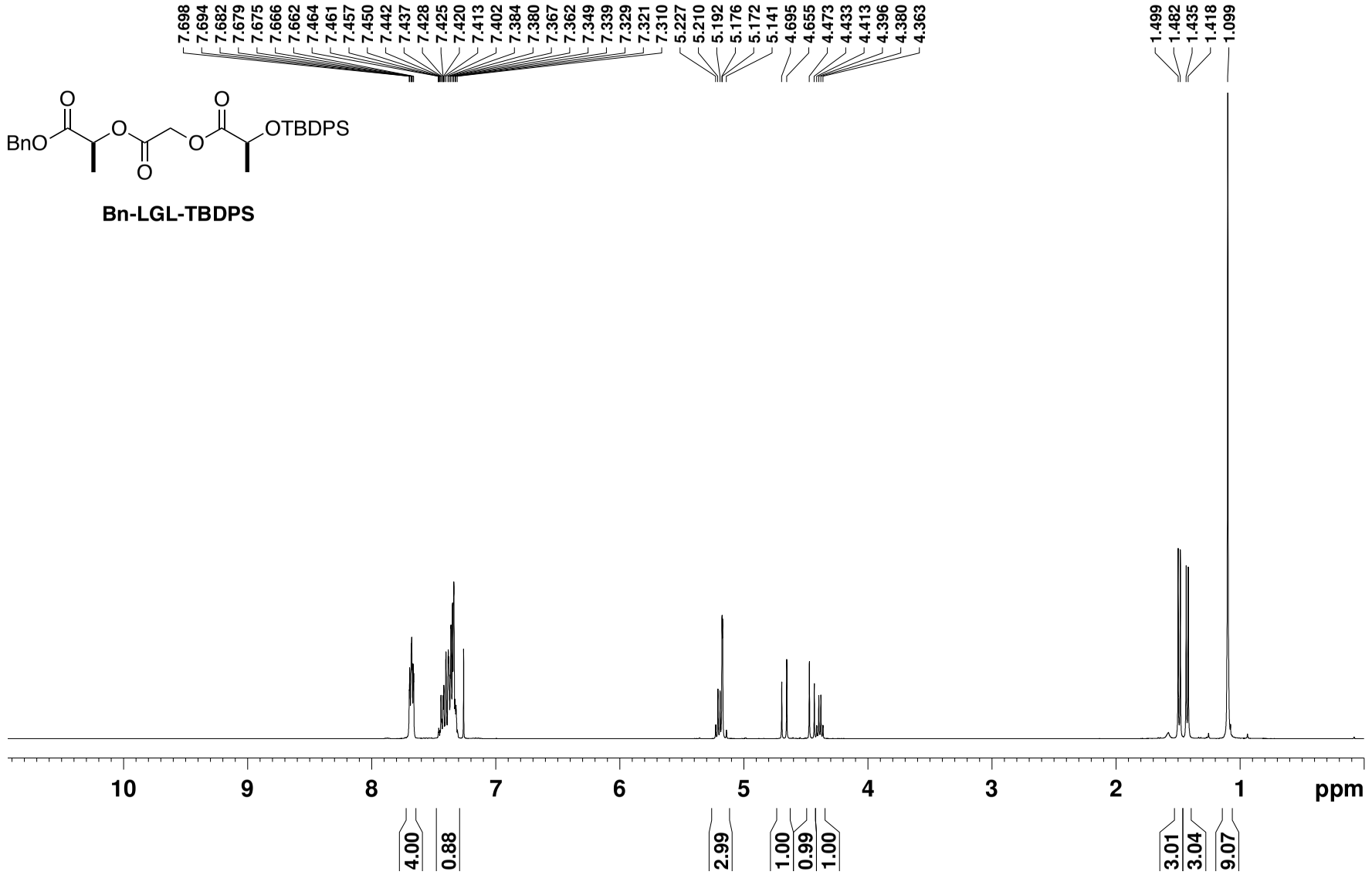
7.698
7.694
7.682
7.679
7.675
7.666
7.662
7.464
7.461
7.457
7.450
7.442
7.437
7.428
7.425
7.420
7.413
7.402
7.384
7.380
7.367
7.362
7.349
7.339
7.329
7.321
7.310
5.227
5.210
5.192
5.176
5.172
5.141
4.695
4.655
4.473
4.433
4.413
4.396
4.380
4.363
1.499
1.482
1.435
1.418
1.099
BnO
OTBDPS
Bn-LGL-TBDPS
10
9
8
7
6
5
4
3
2
1
ppm
4.00
0.88
2.99
1.00
0.99
1.00
3.01
3.04
9.07

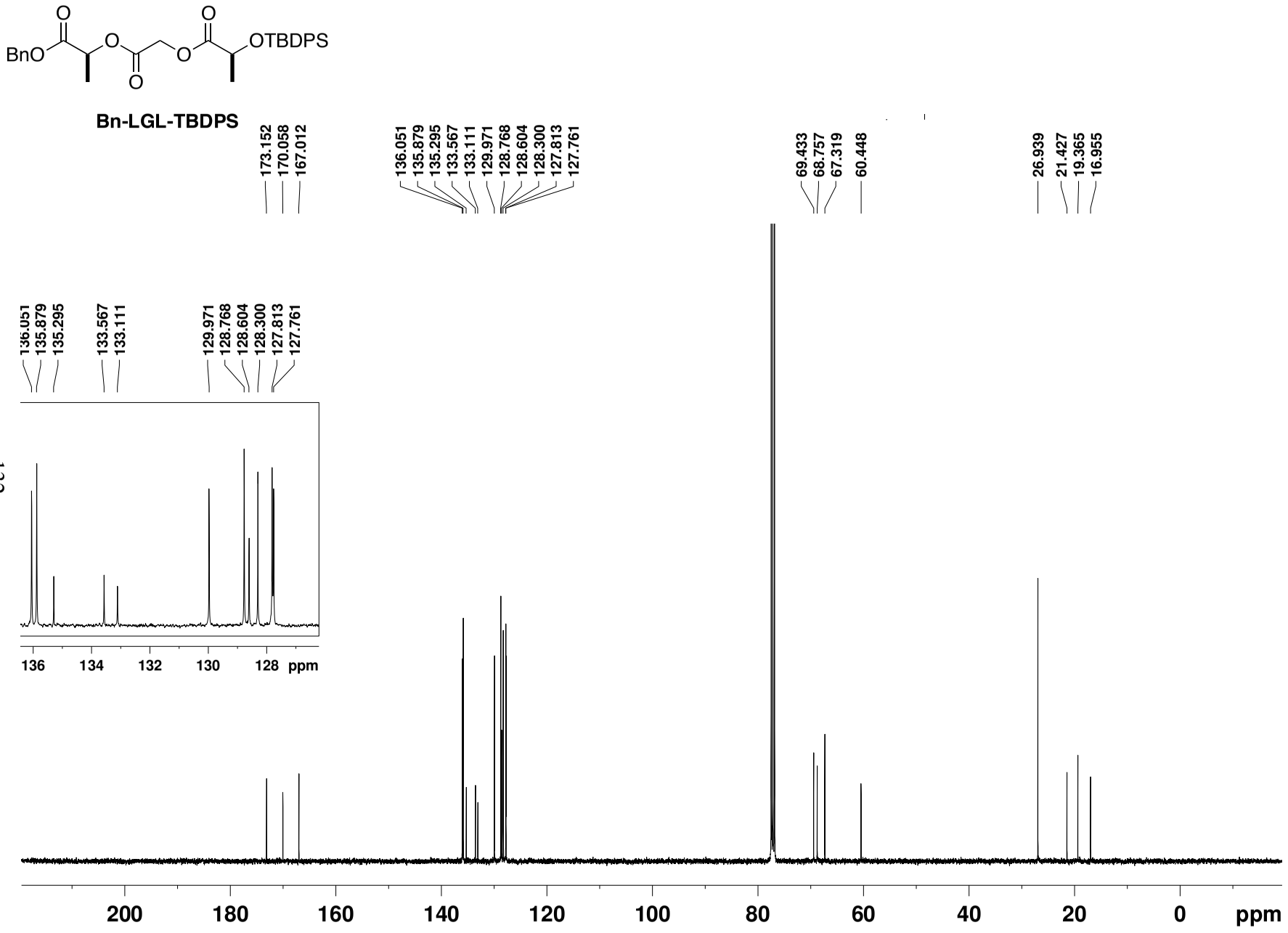
BnO
OTBDPS
Bn-LGL-TBDPS
173.152
170.058
167.012
136.051
135.879
135.295
133.567
133.111
129.971
128.768
128.604
128.300
127.813
127.761
69.433
68.757
67.319
60.448
26.939
21.427
19.365
16.955
200
180
160
140
120
100
80
60
40
20
0
ppm
136
134
132
130
128
ppm

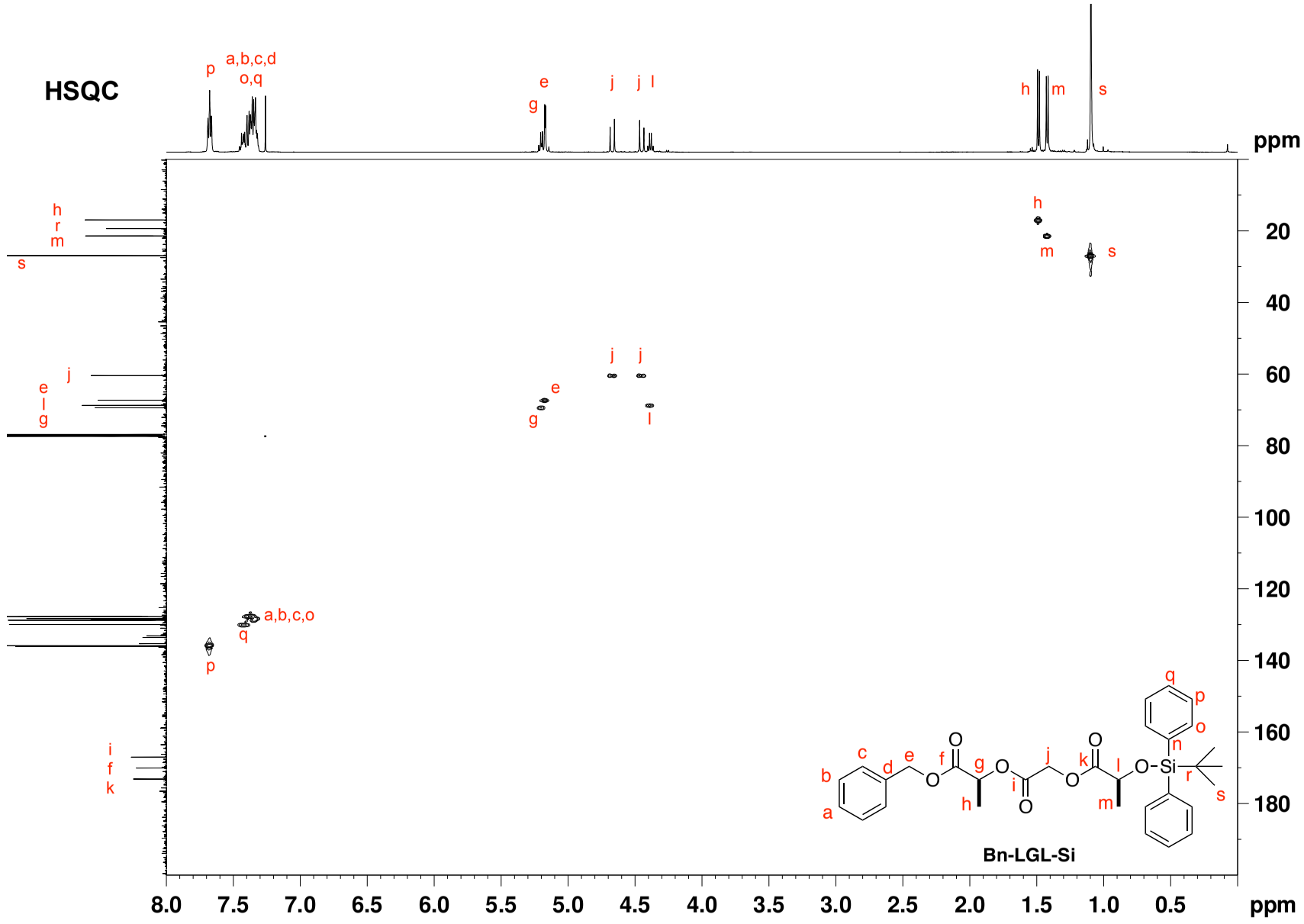
HSQC
p
a,b,c,d
o,q
e
g
j
j
l
h
m
s
ppm
h
r
m
s
j
e
l
g
a,b,c,o
q
p
i
f
k
20
40
60
80
100
120
140
160
180
8.0
7.5
7.0
6.5
6.0
5.5
5.0
4.5
4.0
3.5
3.0
2.5
2.0
1.5
1.0
0.5
ppm
Bn-LGL-Si

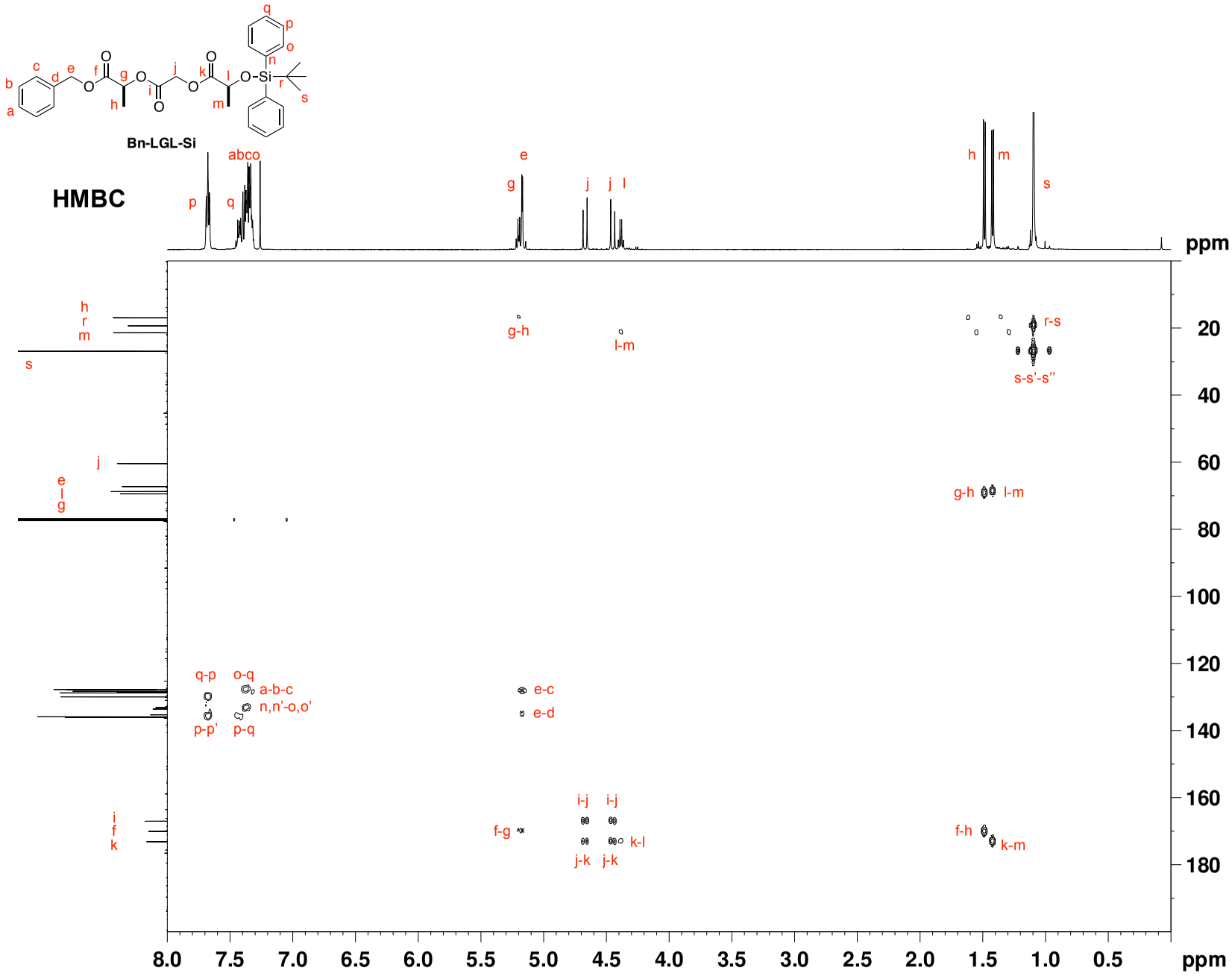
Bn-LGL-Si
HMBC
ppm
8.0
7.5
7.0
6.5
6.0
5.5
5.0
4.5
4.0
3.5
3.0
2.5
2.0
1.5
1.0
0.5
20
40
60
80
100
120
140
160
180
g-h
l-m
r-s
s-s'-s''
e-c
e-d
a-b-c
n,n'-o,o'
q-p
o-q
p-p'
p-q
f-g
i-j
k-l
j-k
f-h
k-m

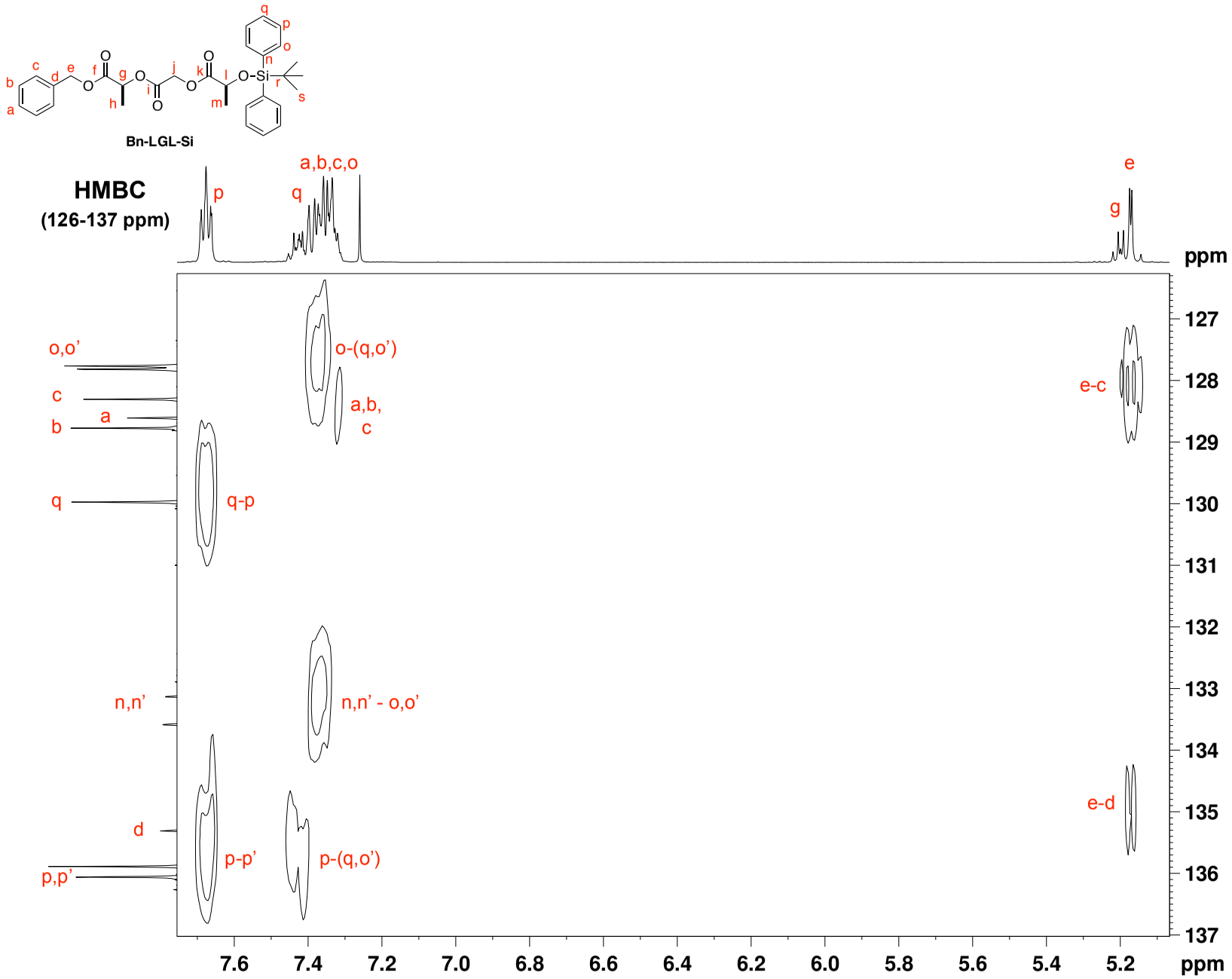
Bn-LGL-Si
HMBC
(126-137 ppm)
a,b,c,o
p
q
e
g
ppm
o,o'
c
a
b
q
n,n'
d
p,p'
o-(q,o')
a,b,
c
q-p
n,n' - o,o'
p-p'
p-(q,o')
e-c
e-d
127
128
129
130
131
132
133
134
135
136
137
7.6
7.4
7.2
7.0
6.8
6.6
6.4
6.2
6.0
5.8
5.6
5.4
5.2
ppm

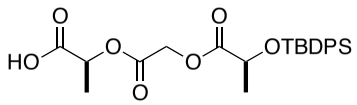

LGL-TBDPS

Ref. 21

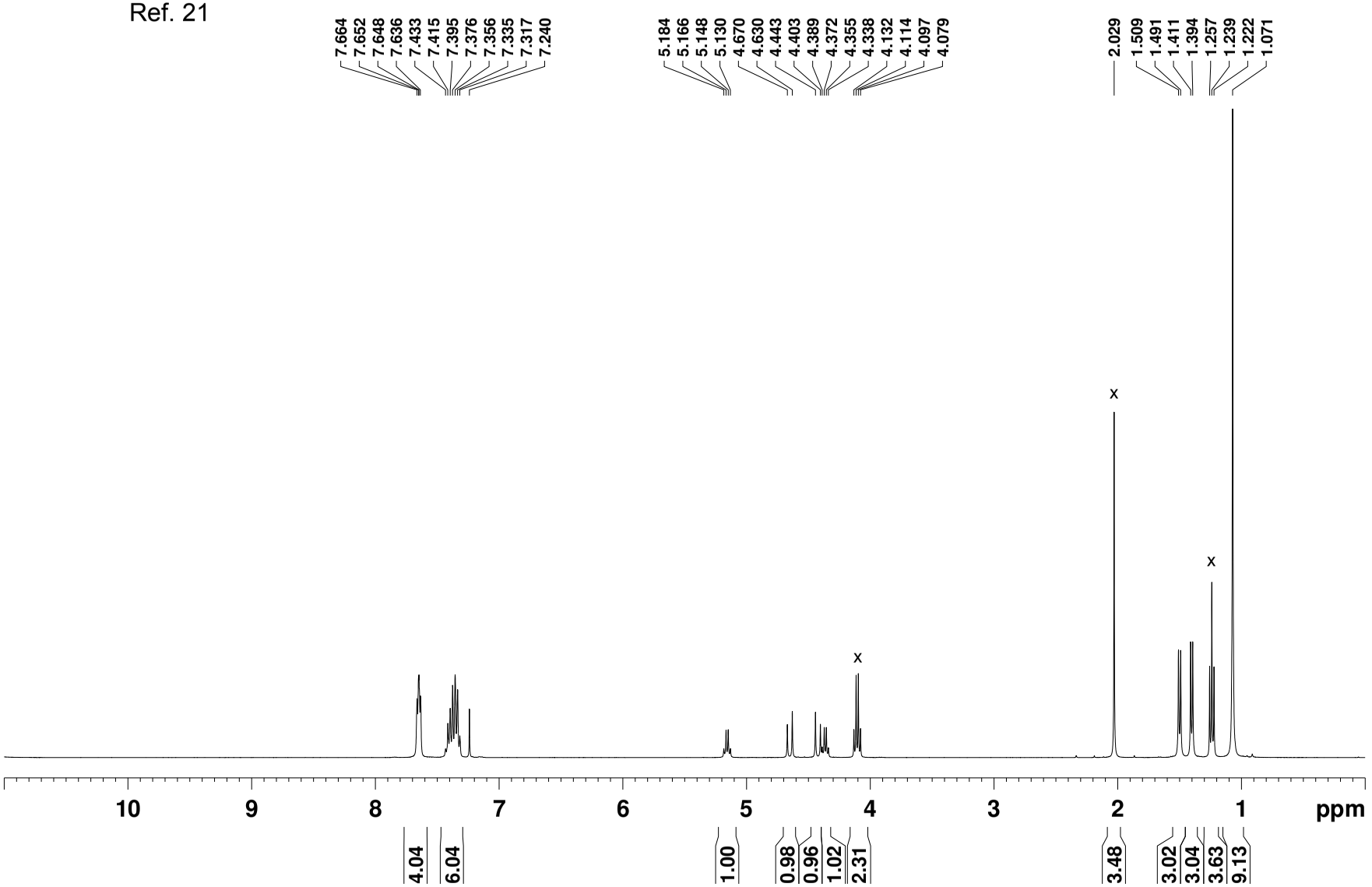

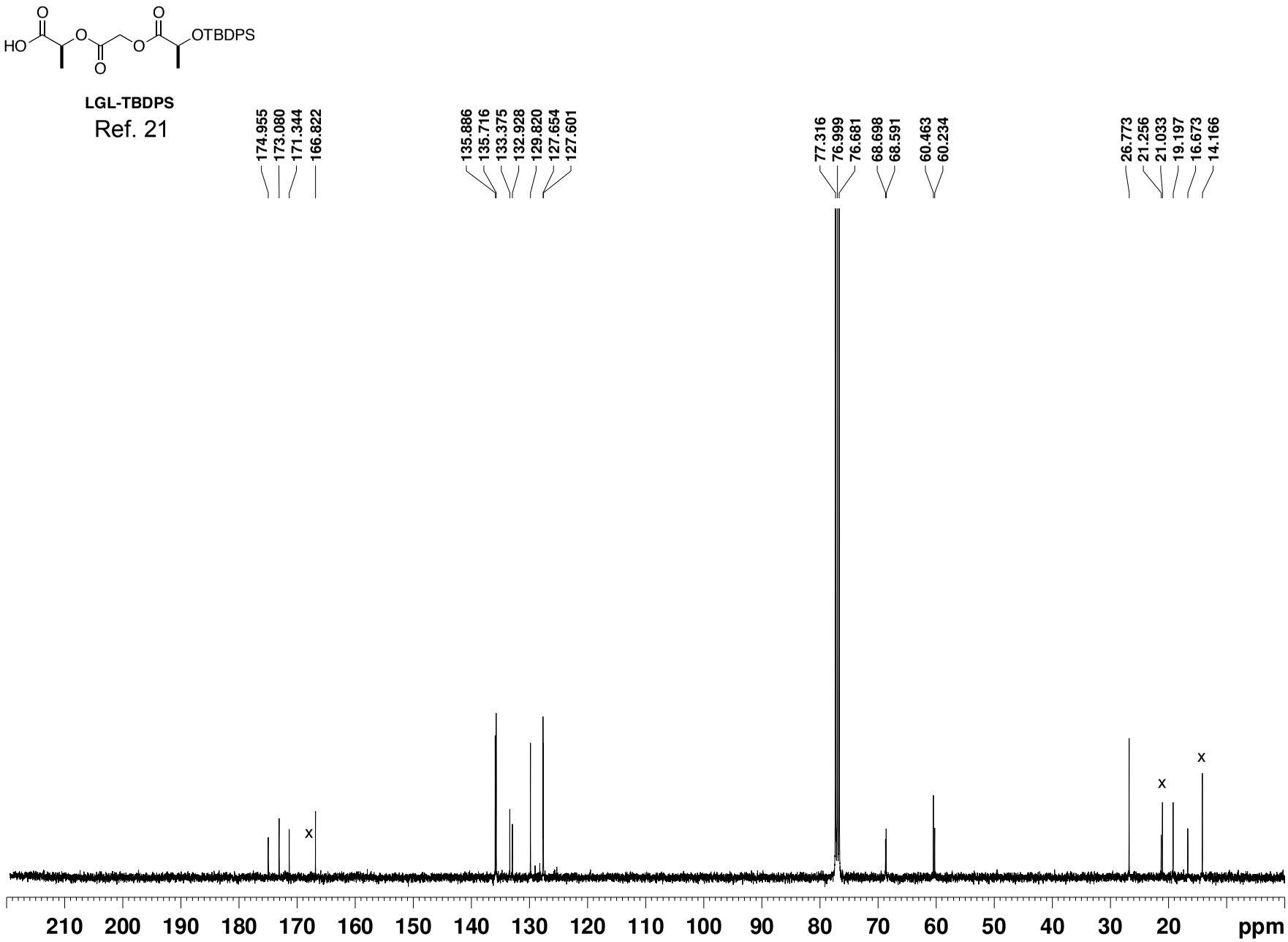
HO
O
O
O
O
O
OTBDPS
LGL-TBDPS
Ref. 21
174.955
173.080
171.344
166.822
135.886
135.716
133.375
132.928
129.820
127.654
127.601
77.316
76.999
76.681
68.698
68.591
60.463
60.234
26.773
21.256
21.033
19.197
16.673
14.166
x
x
x
210
200
190
180
170
160
150
140
130
120
110
100
90
80
70
60
50
40
30
20
ppm

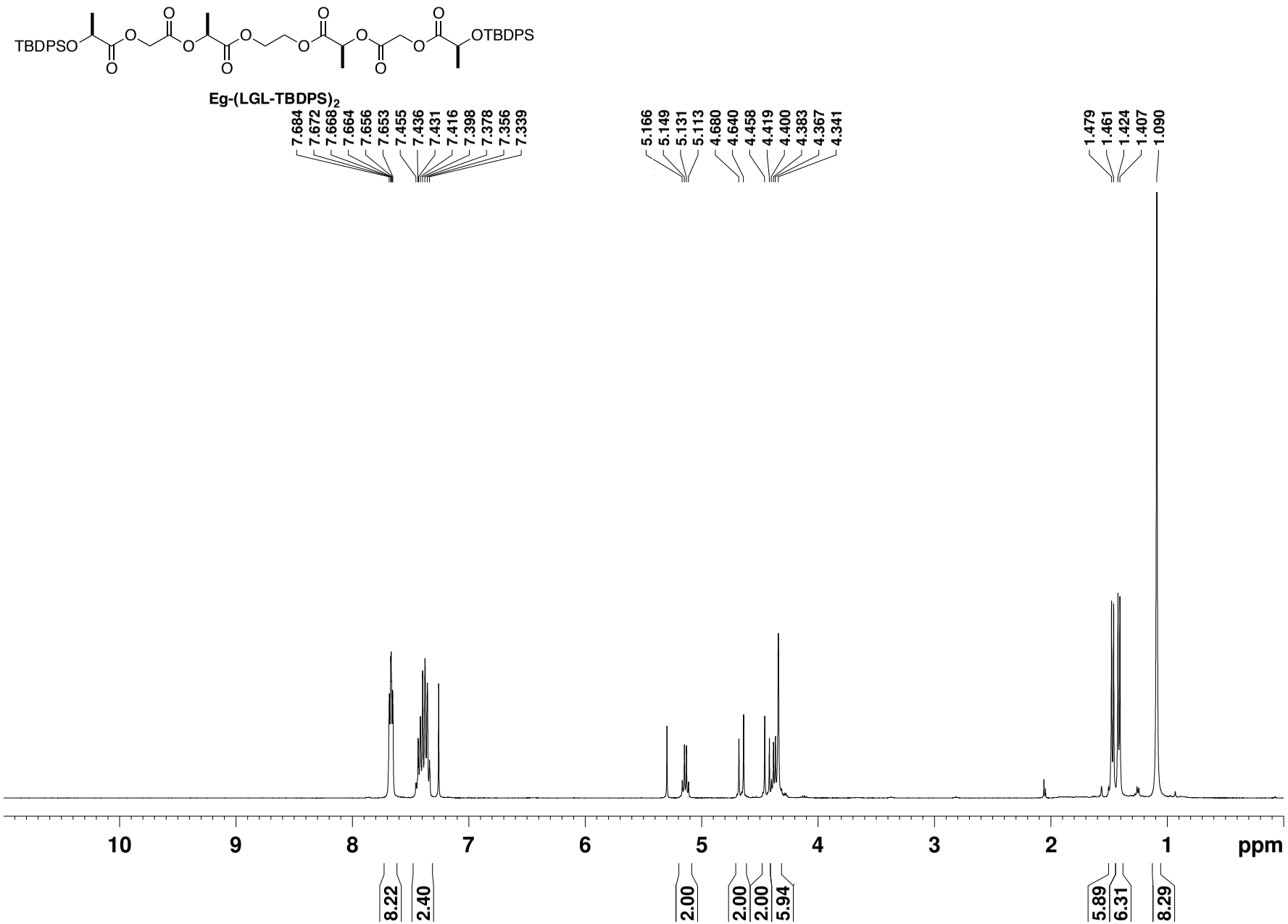
TBDPSO
OTBDPS
Eg-(LGL-TBDPS)2
7.684
7.672
7.668
7.664
7.656
7.653
7.455
7.436
7.431
7.416
7.398
7.378
7.356
7.339
5.166
5.149
5.131
5.113
4.680
4.640
4.458
4.419
4.400
4.383
4.367
4.341
1.479
1.461
1.424
1.407
1.090
10
9
8
7
6
5
4
3
2
1
ppm
8.22
2.40
2.00
2.00
2.00
5.94
5.89
6.31
8.29

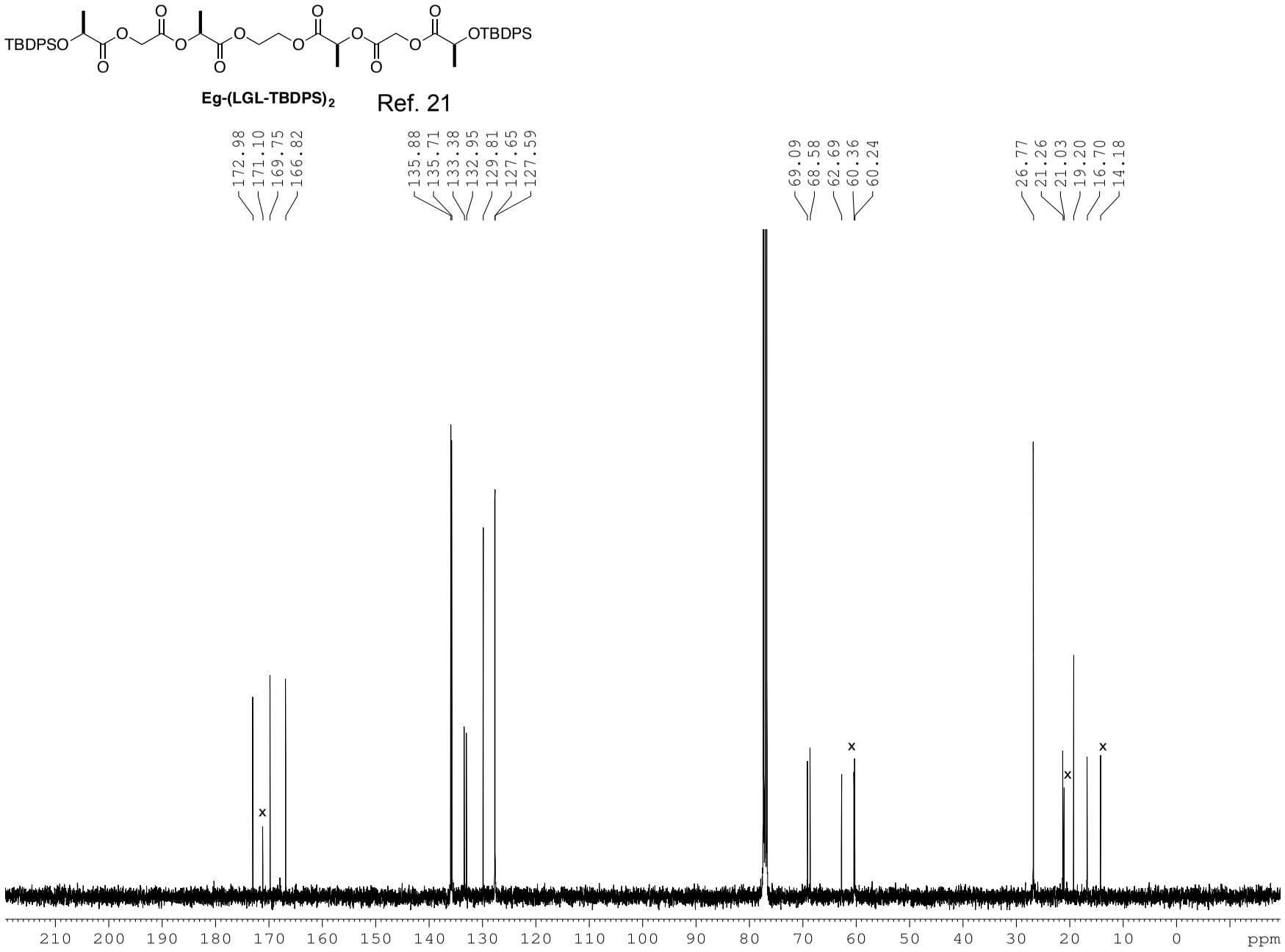
TBDPSO
OTBDPS
Eg-(LGL-TBDPS)2
Ref. 21
172.98
171.10
169.75
166.82
135.88
135.71
133.38
132.95
129.81
127.65
127.59
69.09
68.58
62.69
60.36
60.24
26.77
21.26
21.03
19.20
16.70
14.18
210 200 190 180 170 160 150 140 130 120 110 100 90 80 70 60 50 40 30 20 10 0 ppm

Eg-(LGL)2
1.486
1.500
1.524
1.538
2.879
2.890
4.347
4.354
4.355
4.357
4.365
4.373
4.375
4.377
4.385
4.391
4.398
4.400
4.413
4.415
4.420
4.427
4.435
4.440
4.730
4.762
4.813
4.845
5.175
5.189
5.203
5.217
x
6.12
6.27
1.73
6.10
1.97
2.00
1.93
ppm

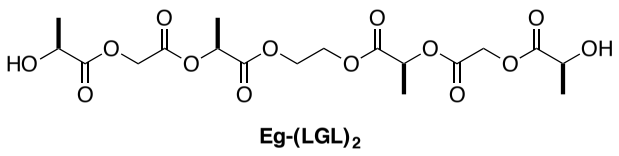
HO
O
O
O
O
O
O
O
O
O
O
O
O
OH

Eg-(LGL)$_2$

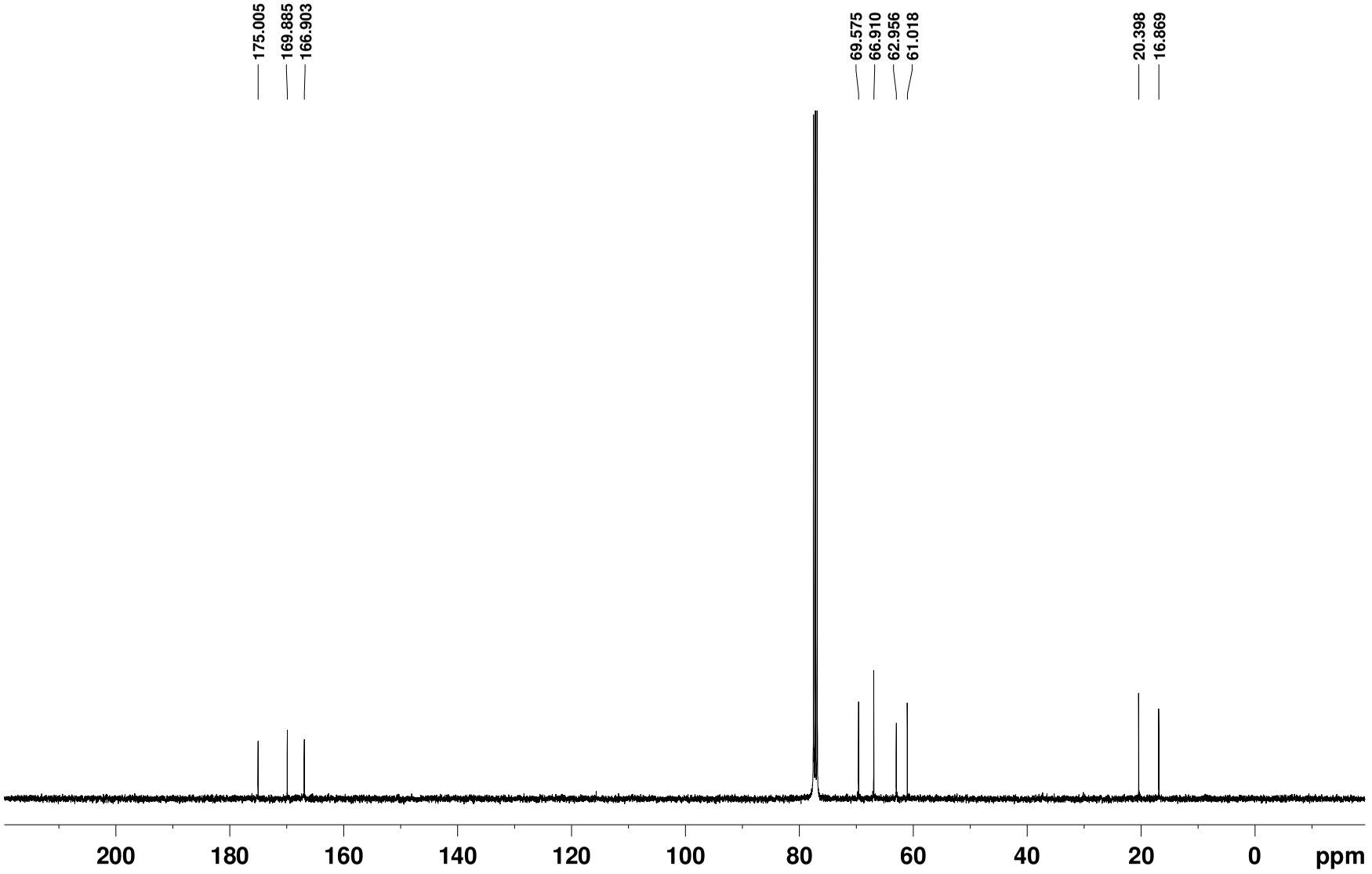
175.005
169.885
166.903
69.575
66.910
62.956
61.018
20.398
16.869
200
180
160
140
120
100
80
60
40
20
0
ppm

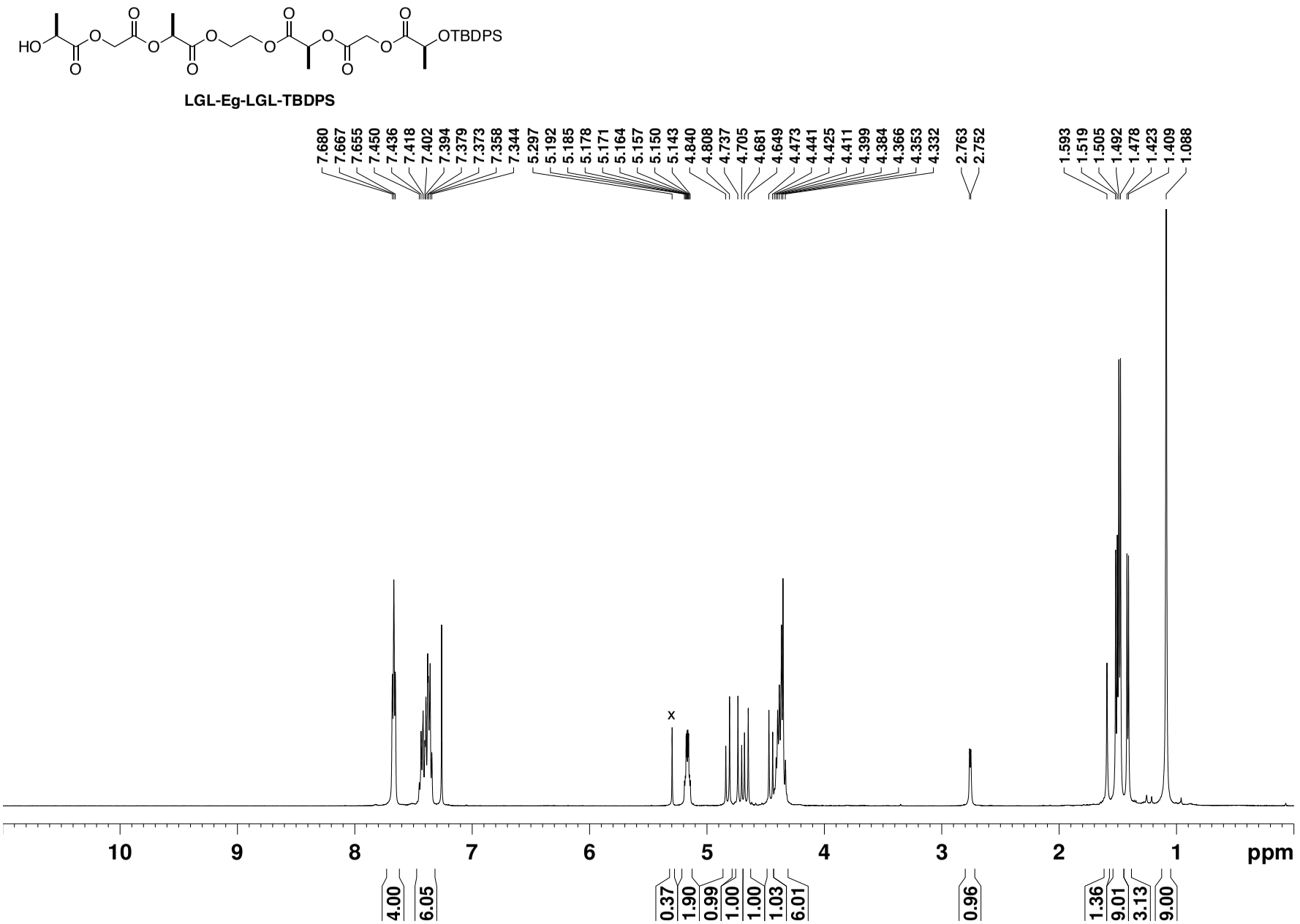
HO
OTBDPS
LGL-Eg-LGL-TBDPS
7.680
7.667
7.655
7.450
7.436
7.418
7.402
7.394
7.379
7.373
7.358
7.344
5.297
5.192
5.185
5.178
5.171
5.164
5.157
5.150
5.143
4.840
4.808
4.737
4.705
4.681
4.649
4.473
4.441
4.425
4.411
4.399
4.384
4.366
4.353
4.332
2.763
2.752
1.593
1.519
1.505
1.492
1.478
1.423
1.409
1.088
x
10
9
8
7
6
5
4
3
2
1
ppm
4.00
6.05
0.37
1.90
0.99
1.00
1.00
1.03
6.01
0.96
1.36
9.01
3.13
9.00

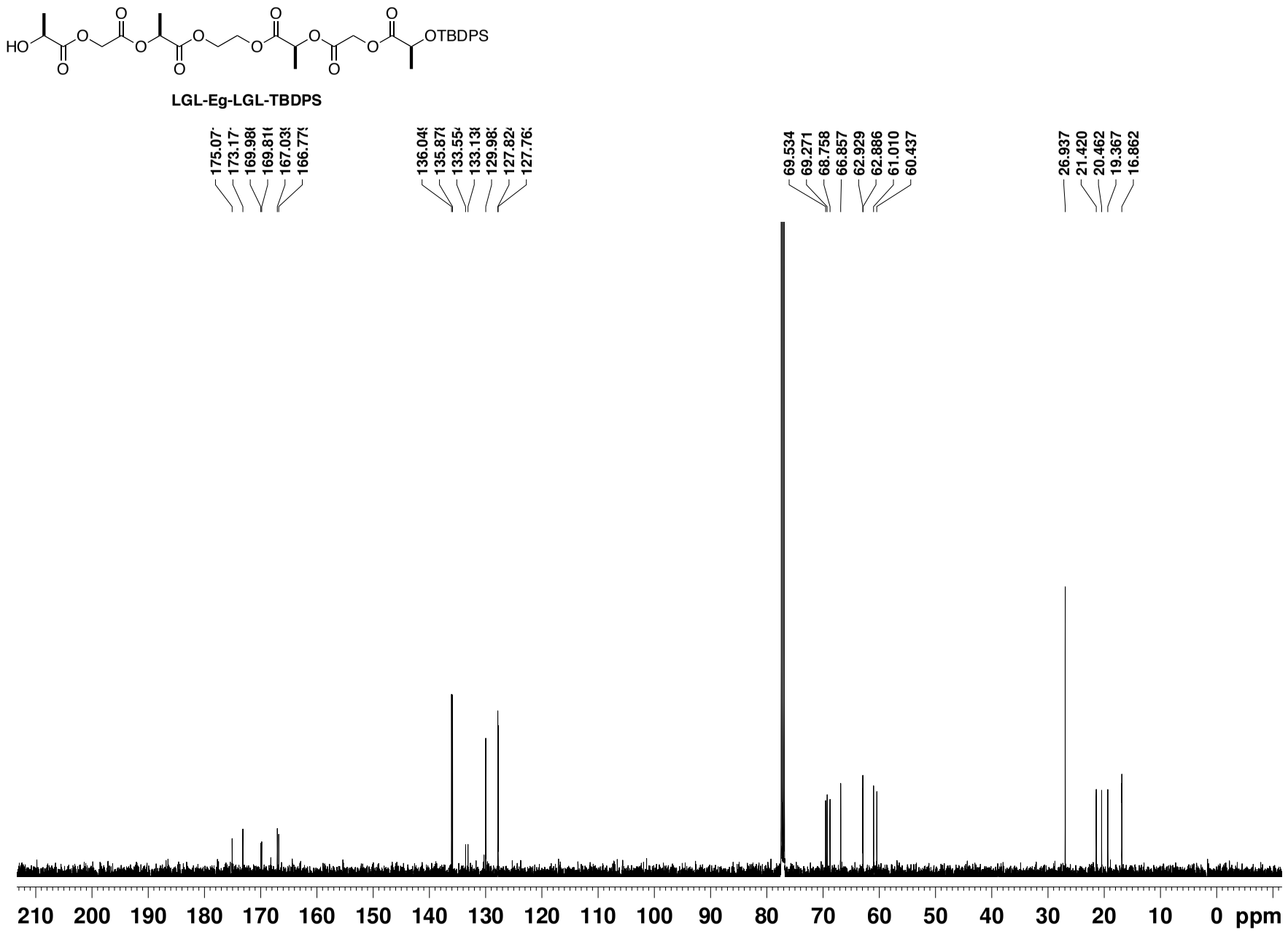
HO
O
O
O
O
O
O
O
O
O
O
O
O
O
OTBDPS
LGL-Eg-LGL-TBDPS
175.07
173.17
169.98
169.81
167.03
166.77
136.04
135.87
133.55
133.13
129.98
127.82
127.76
69.534
69.271
68.758
66.857
62.929
62.886
61.010
60.437
26.937
21.420
20.462
19.367
16.862
210 200 190 180 170 160 150 140 130 120 110 100 90 80 70 60 50 40 30 20 10 0 ppm

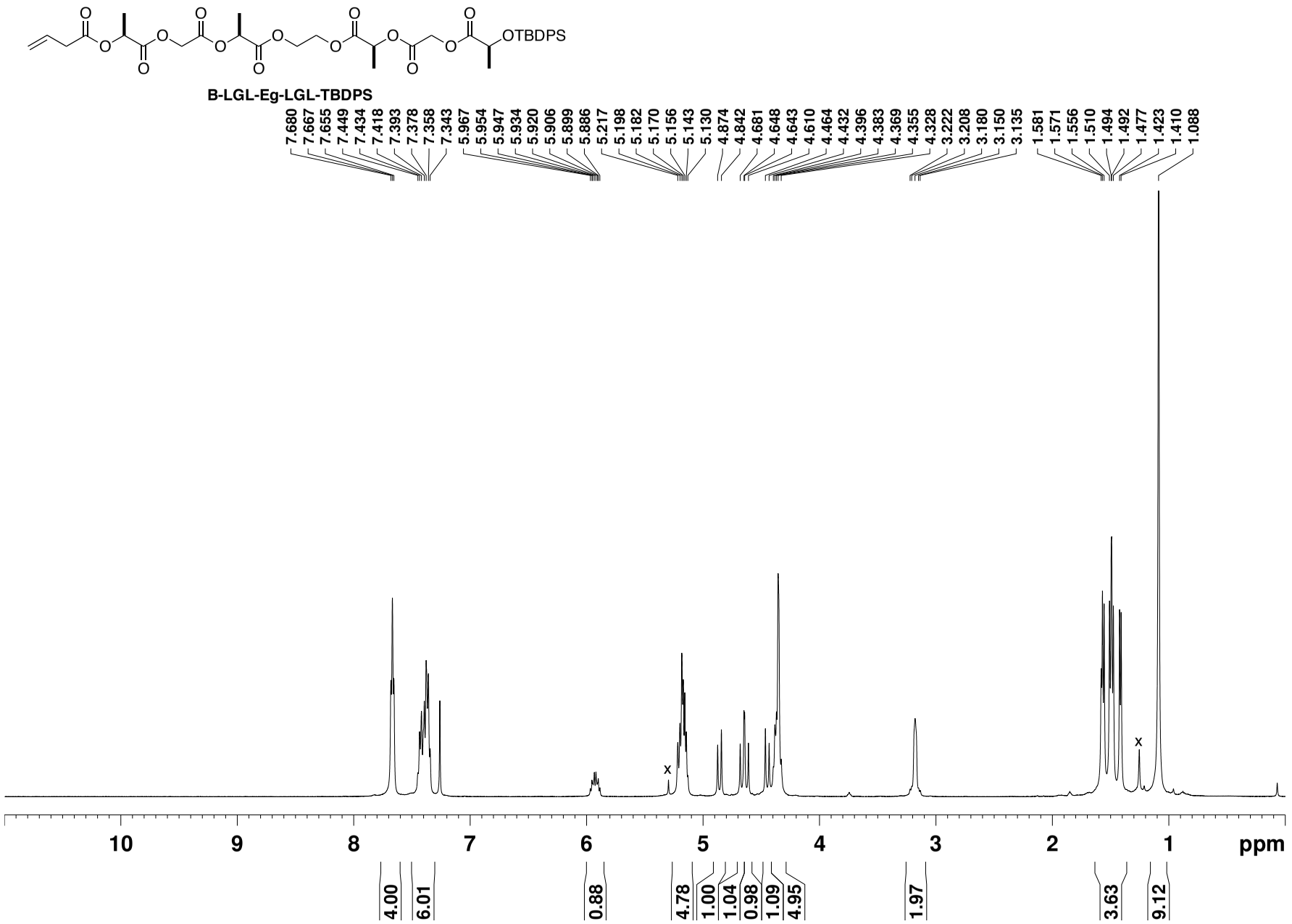
OTBDPS
B-LGL-Eg-LGL-TBDPS
7.680
7.667
7.655
7.449
7.434
7.418
7.393
7.378
7.358
7.343
5.967
5.954
5.947
5.934
5.920
5.906
5.899
5.886
5.217
5.198
5.182
5.170
5.156
5.143
5.130
4.874
4.842
4.681
4.648
4.643
4.610
4.464
4.432
4.396
4.383
4.369
4.355
4.328
3.222
3.208
3.180
3.150
3.135
1.581
1.571
1.556
1.510
1.494
1.492
1.477
1.423
1.410
1.088
x
x
10
9
8
7
6
5
4
3
2
1
ppm
4.00
6.01
0.88
4.78
1.00
1.04
0.98
1.09
4.95
1.97
3.63
9.12

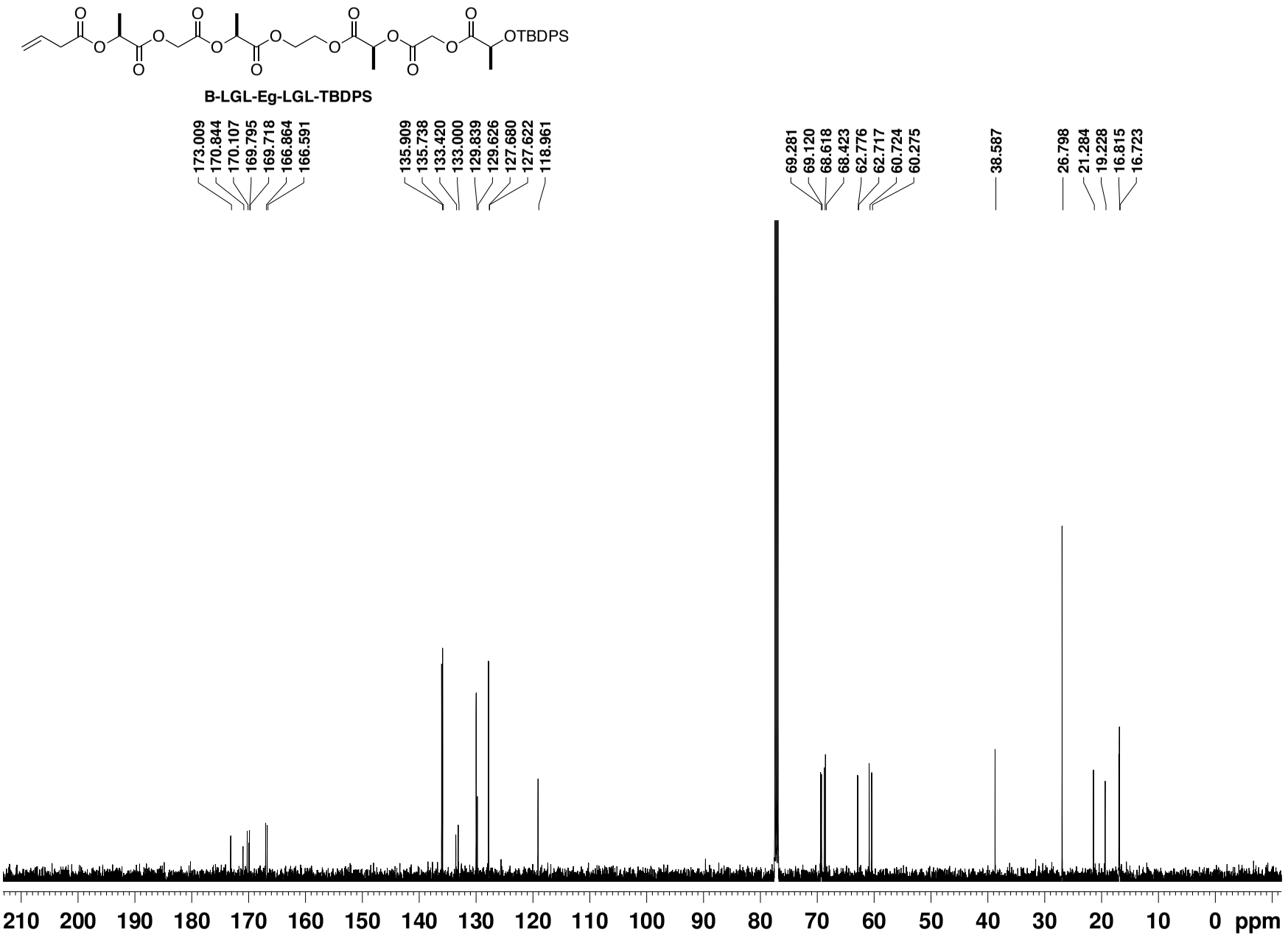
OTBDPS
B-LGL-Eg-LGL-TBDPS
173.009
170.844
170.107
169.795
169.718
166.864
166.591
135.909
135.738
133.420
133.000
129.839
129.626
127.680
127.622
118.961
69.281
69.120
68.618
68.423
62.776
62.717
60.724
60.275
38.587
26.798
21.284
19.228
16.815
16.723
210 200 190 180 170 160 150 140 130 120 110 100 90 80 70 60 50 40 30 20 10 0 ppm

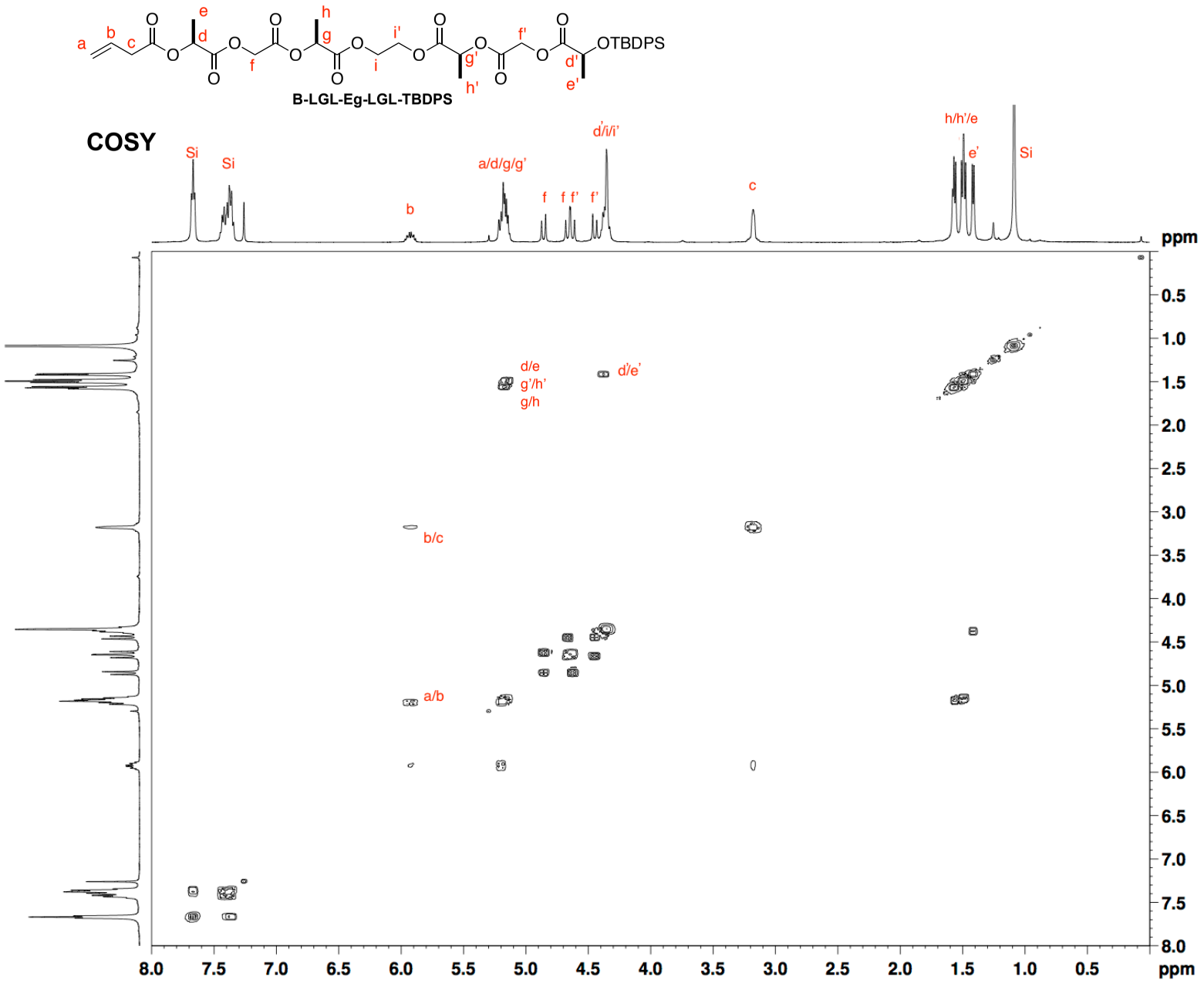
B-LGL-Eg-LGL-TBDPS
OTBDPS
COSY
Si
Si
a/d/g/g'
b
f
f
f'
f'
d'/i/i'
c
h/h'/e
e'
Si
ppm
d/e
g'/h'
g/h
d'/e'
b/c
a/b
8.0
7.5
7.0
6.5
6.0
5.5
5.0
4.5
4.0
3.5
3.0
2.5
2.0
1.5
1.0
0.5
ppm

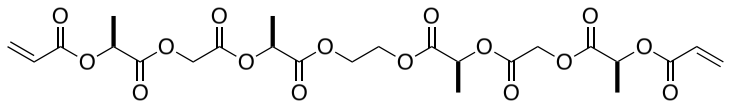

Eg-(LGL-A)$_2$

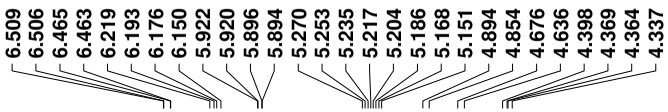
6.509
6.506
6.465
6.463
6.219
6.193
6.176
6.150
5.922
5.920
5.896
5.894
5.270
5.253
5.235
5.217
5.204
5.186
5.168
5.151
4.894
4.854
4.676
4.636
4.398
4.369
4.364
4.337
1.617
1.599
1.528
1.511

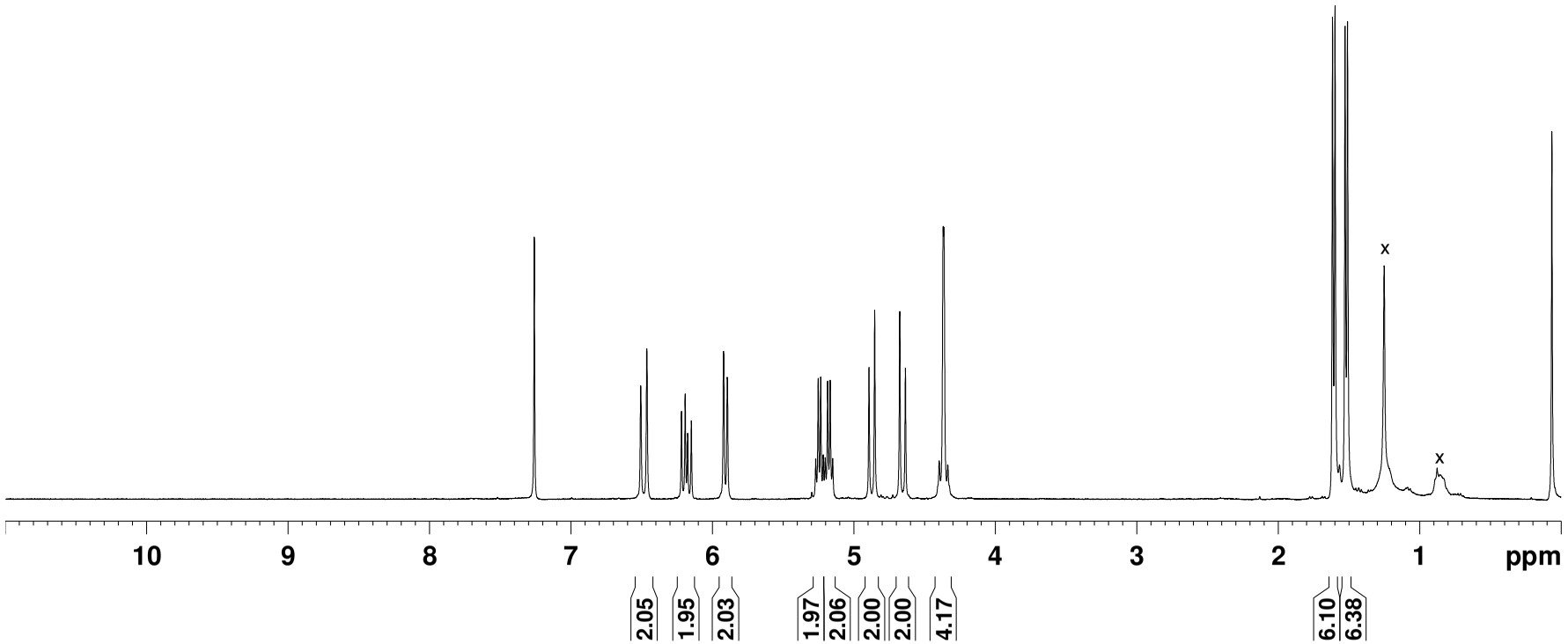
x
x
10
9
8
7
6
5
4
3
2
1
ppm
2.05
1.95
2.03
1.97
2.06
2.00
2.00
4.17
6.10
6.38

Eg-(LGL-A)2
170.235
169.840
166.731
165.411
132.221
127.603
69.380
68.482
62.875
60.830
29.801
17.010
16.829
1.126
x
ppm

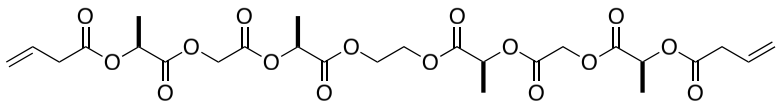

Eg-(LGL-B)$_2$

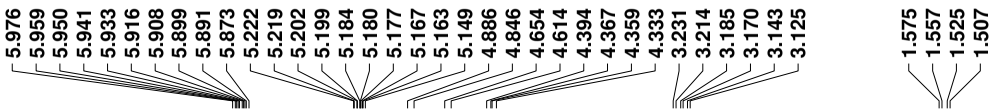
5.976
5.959
5.950
5.941
5.933
5.916
5.908
5.899
5.891
5.873
5.222
5.219
5.202
5.199
5.184
5.180
5.177
5.167
5.163
5.149
4.886
4.846
4.654
4.614
4.394
4.367
4.359
4.333
3.231
3.214
3.185
3.170
3.143
3.125
1.575
1.557
1.525
1.507

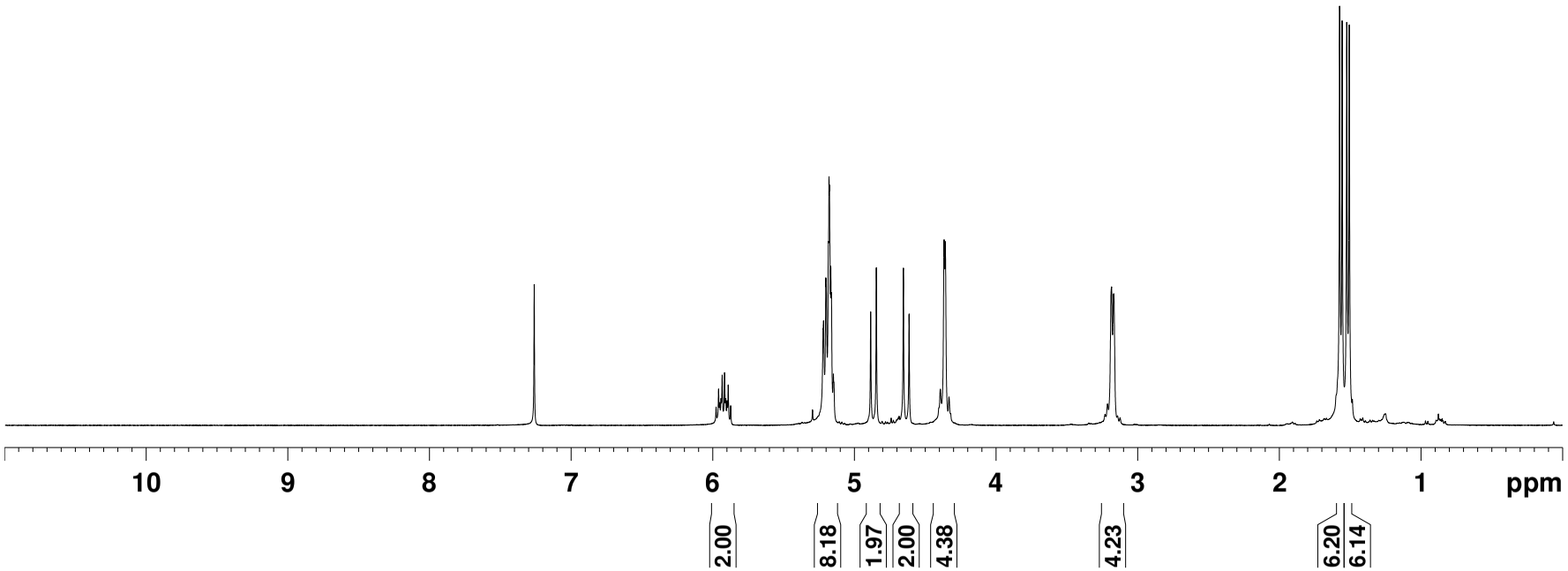
10
9
8
7
6
5
4
3
2
1
ppm
2.00
8.18
1.97
2.00
4.38
4.23
6.20
6.14

Eg-(LGL-B)2 Ref. 21
170.82
170.08
169.69
166.57
129.59
118.94
69.24
68.38
62.73
60.69
38.55
33.82
16.78
16.69
ppm

Eg-(LGL-P)2
1.510
1.527
1.551
1.569
2.370
2.373
2.391
2.408
2.425
2.436
2.450
2.475
2.486
2.491
2.503
2.508
2.524
2.543
2.564
4.323
4.335
4.361
4.370
4.396
4.408
4.421
4.613
4.653
4.848
4.888
4.996
4.999
5.022
5.024
5.044
5.048
5.087
5.090
5.144
5.147
5.161
5.165
5.179
5.182
5.197
5.200
5.781
5.797
5.807
5.813
5.823
5.839
5.850
5.856
5.865
5.881
ppm
1
2
3
4
5
6
7
8
9
10
6.34
6.20
4.27
4.31
4.19
2.01
2.01
1.97
2.14
4.15
2.00

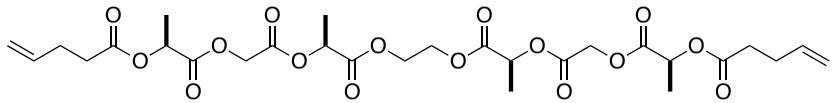

Eg-(LGL-P)$_2$

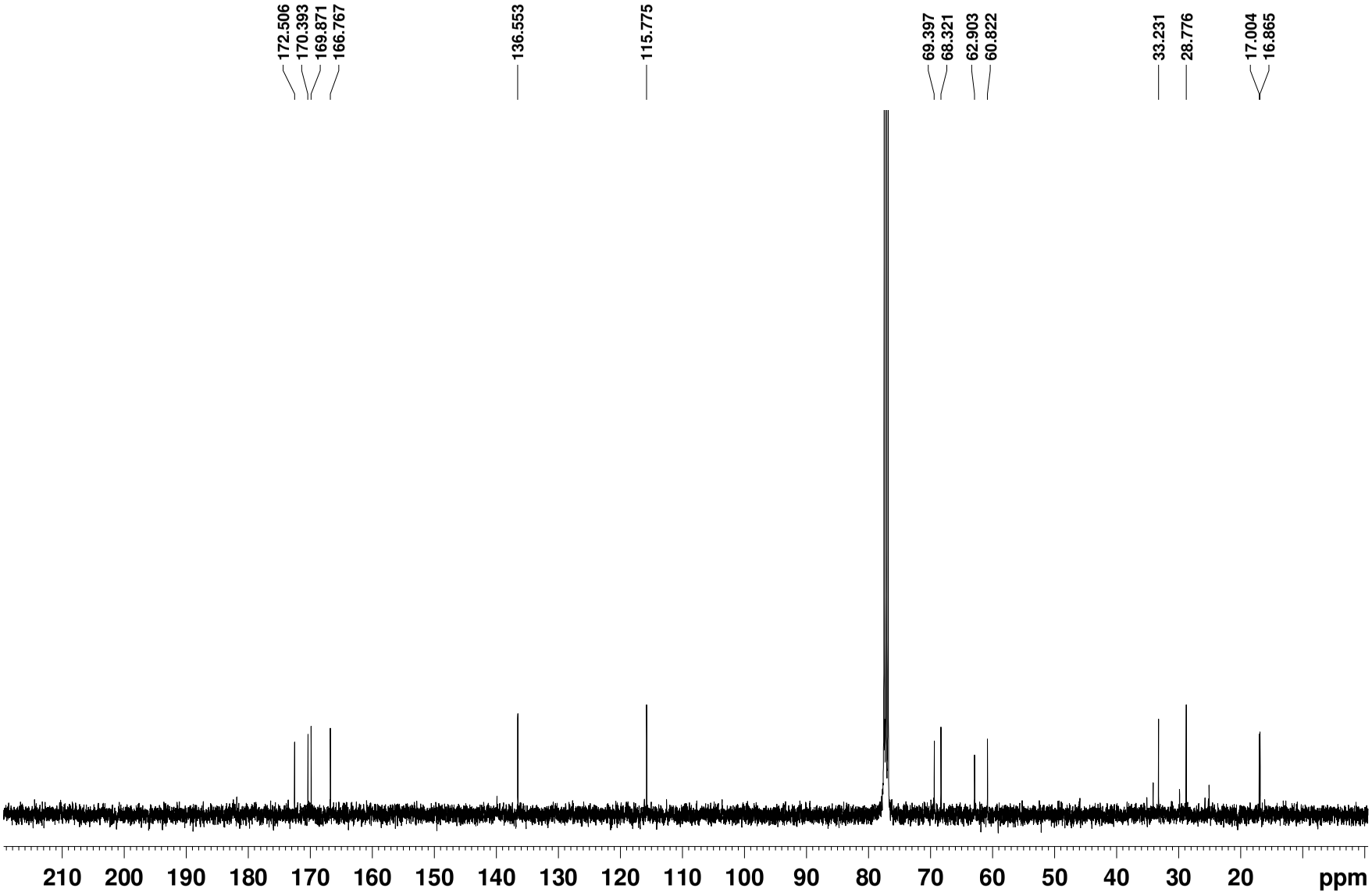
172.506
170.393
169.871
166.767
136.553
115.775
69.397
68.321
62.903
60.822
33.231
28.776
17.004
16.865
210 200 190 180 170 160 150 140 130 120 110 100 90 80 70 60 50 40 30 20 ppm

1.484
1.498
1.514
1.528
1.555
1.569
2.045
2.134
2.379
2.382
2.385
2.396
2.409
2.422
2.431
2.447
2.460
2.478
2.492
2.506
2.509
2.523
2.538
2.540
2.555
4.114
4.129
4.332
4.341
4.361
4.365
4.371
4.373
4.394
4.404
4.620
4.652
4.669
4.701
4.853
4.885
5.001
5.004
5.022
5.024
5.048
5.051
5.054
5.058
5.071
5.074
5.082
5.085
5.089
5.092
5.105
5.152
5.156
5.166
5.170
5.180
5.184
5.194
5.198
5.793
5.806
5.814
5.819
5.827
5.840
5.848
5.853
5.861
5.873
trans-cyclic-Eg-(LGL-P)2
ppm
1
2
3
4
5
6
7
8
9
10
1.79
3.54
3.77
1.80
1.80
3.75
7.81
6.00
5.62

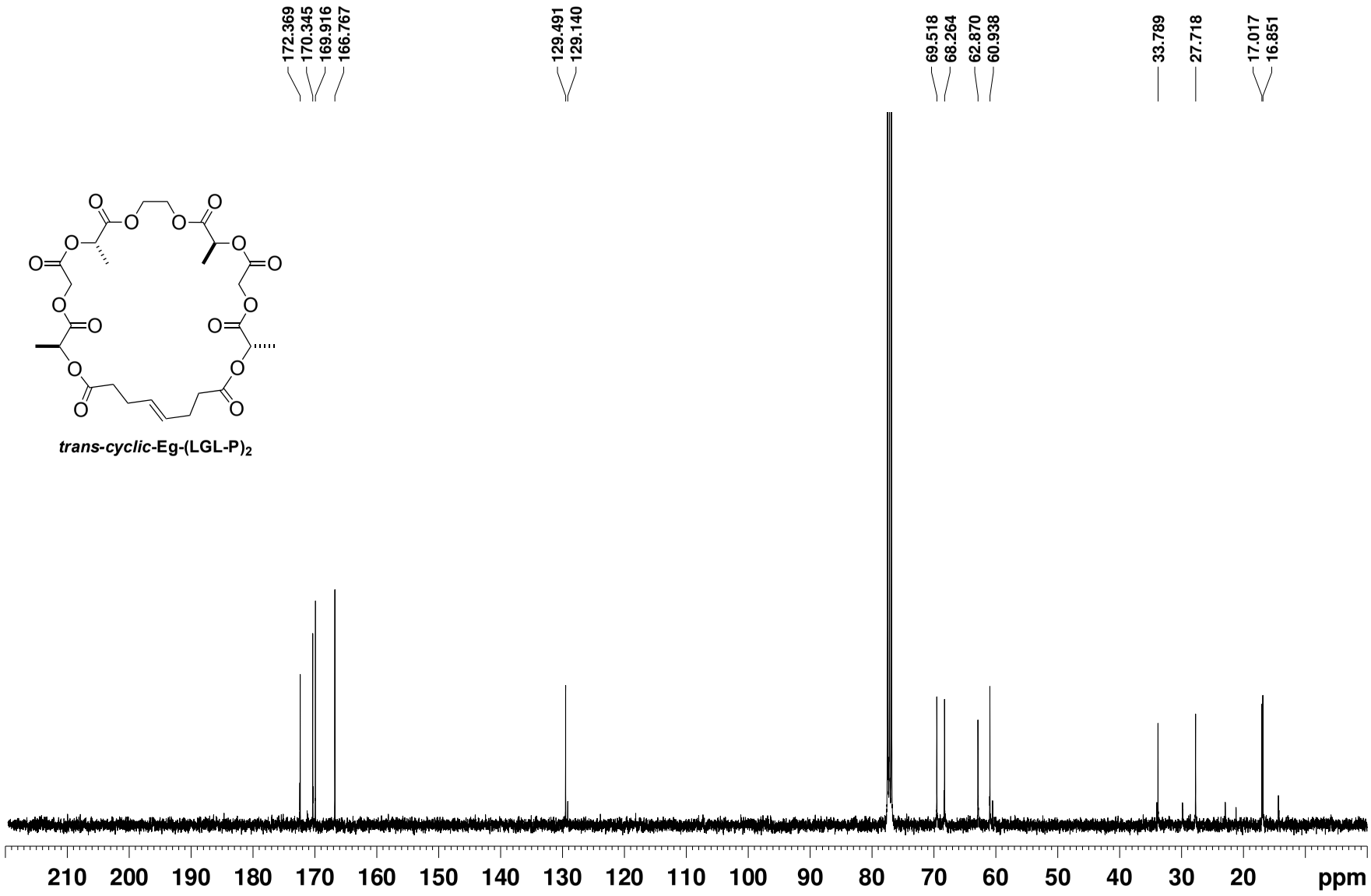

trans-cyclic-Eg-(LGL-P)$_2$

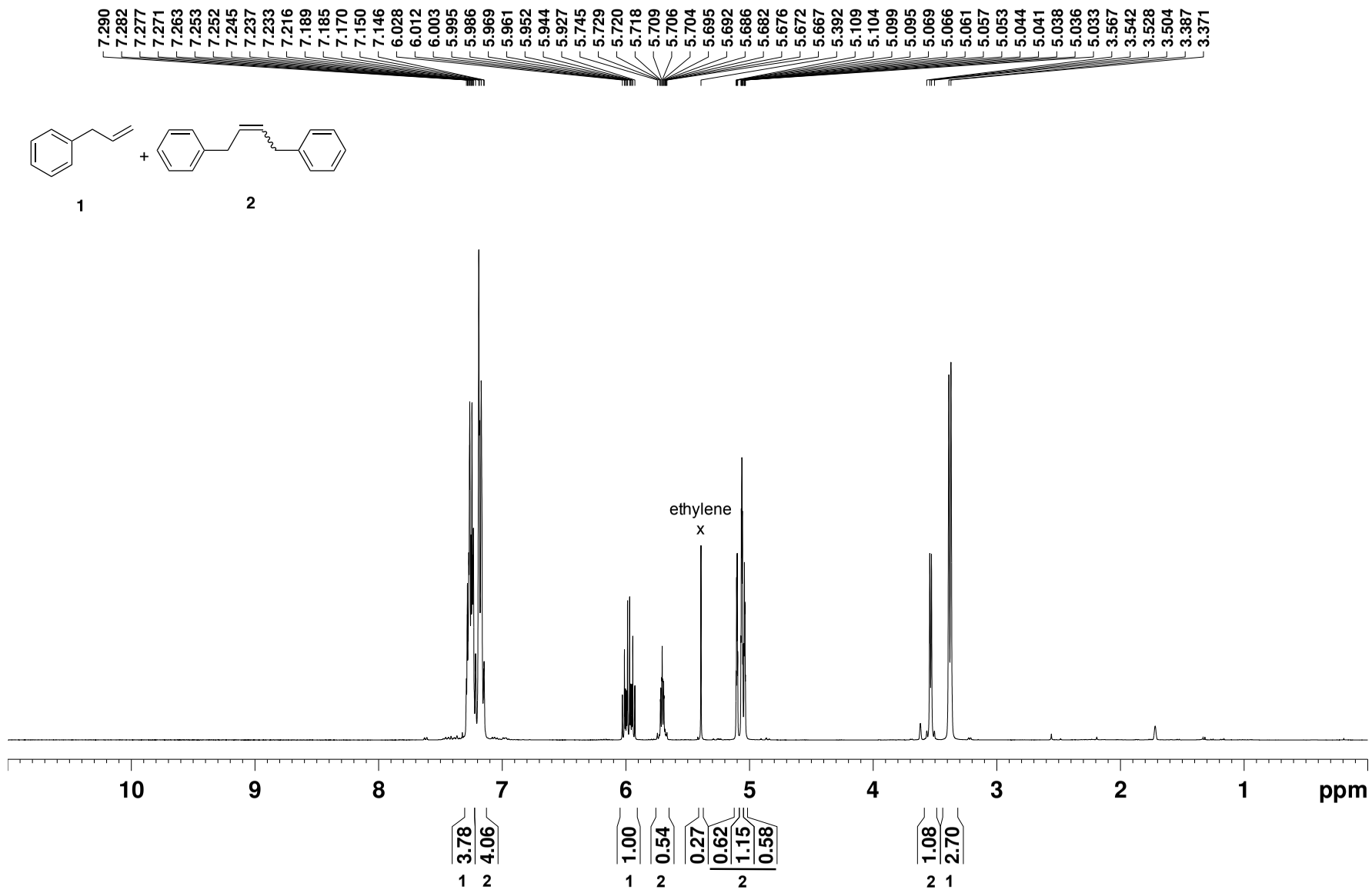
7.290
7.282
7.277
7.271
7.263
7.253
7.252
7.245
7.237
7.233
7.216
7.189
7.185
7.170
7.150
7.146
6.028
6.012
6.003
5.995
5.986
5.969
5.961
5.952
5.944
5.927
5.745
5.729
5.720
5.718
5.709
5.706
5.704
5.695
5.692
5.686
5.682
5.676
5.672
5.667
5.392
5.109
5.104
5.099
5.095
5.069
5.066
5.061
5.057
5.053
5.044
5.041
5.038
5.036
5.033
3.567
3.542
3.528
3.504
3.387
3.371
+
1
2
ethylene
x
10
9
8
7
6
5
4
3
2
1
ppm
3.78
4.06
1.00
0.54
0.27
0.62
1.15
0.58
1.08
2.70
1 2
1 2
2
2 1

cis-cyclic-Eg-(LGL-P)2
ppm
1
2
3
4
5
6
7
8
9
10
2.33
8.10
4.08
2.06
2.05
4.00
0.69
1.80
0.25
1.514
1.532
1.536
1.554
2.385
2.400
2.406
2.412
2.429
2.433
2.442
2.451
2.466
2.476
4.325
4.332
4.343
4.358
4.367
4.375
4.383
4.398
4.410
4.417
4.675
4.680
4.715
4.720
4.781
4.795
4.821
4.835
5.153
5.160
5.171
5.178
5.188
5.196
5.205
5.214
5.233
5.298
5.367
5.404
5.416
5.443
5.497
5.505
5.514

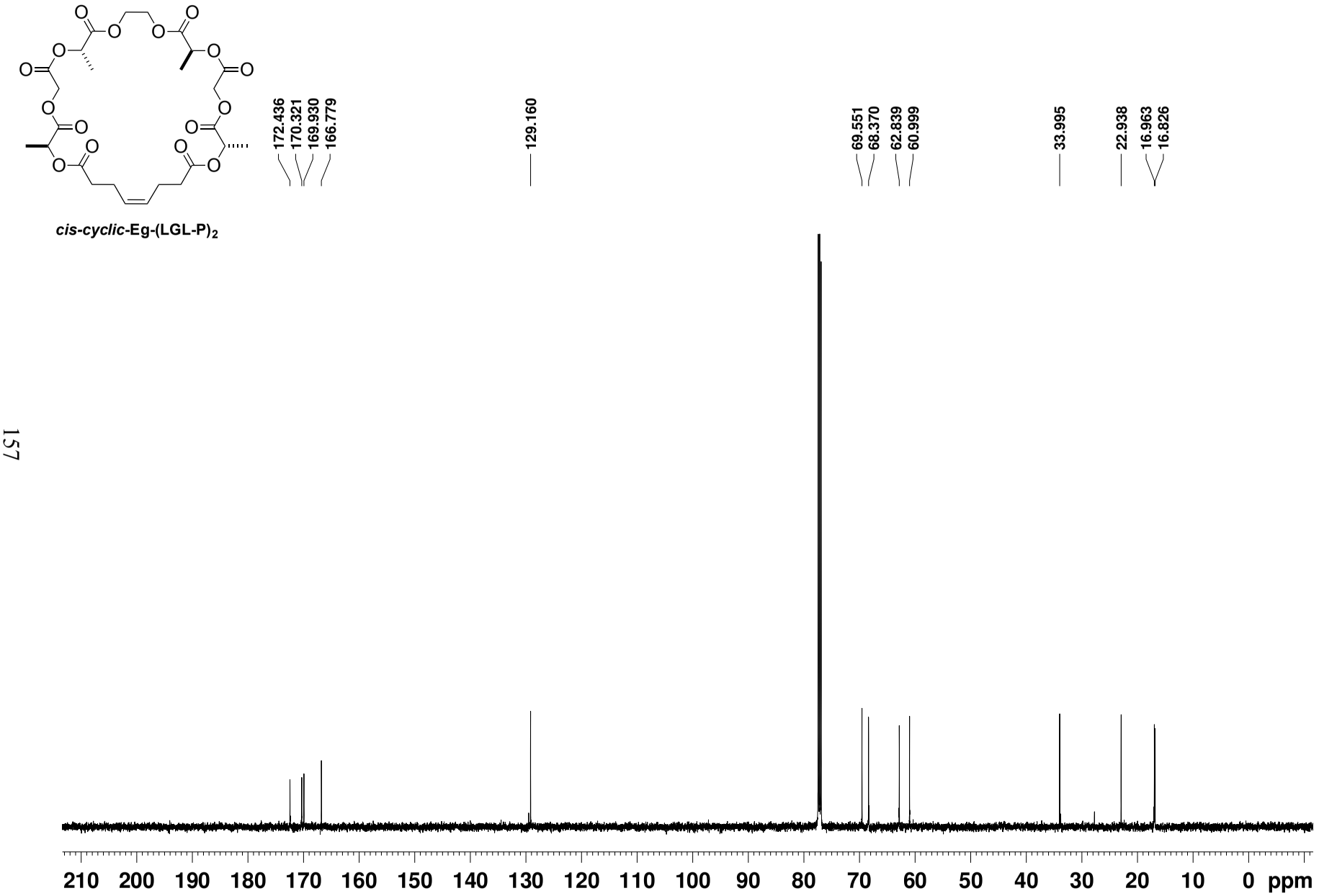

***cis-cyclic*-Eg-(LGL-P)$_2$**

cis-P_p-(LGL-Eg-LGL-P)_2
ppm
1.13
0.16
0.69
1.76
3.97
1.20
1.15
2.00
2.00
2.00
4.21
2.66
5.01
6.28
6.58
0.61

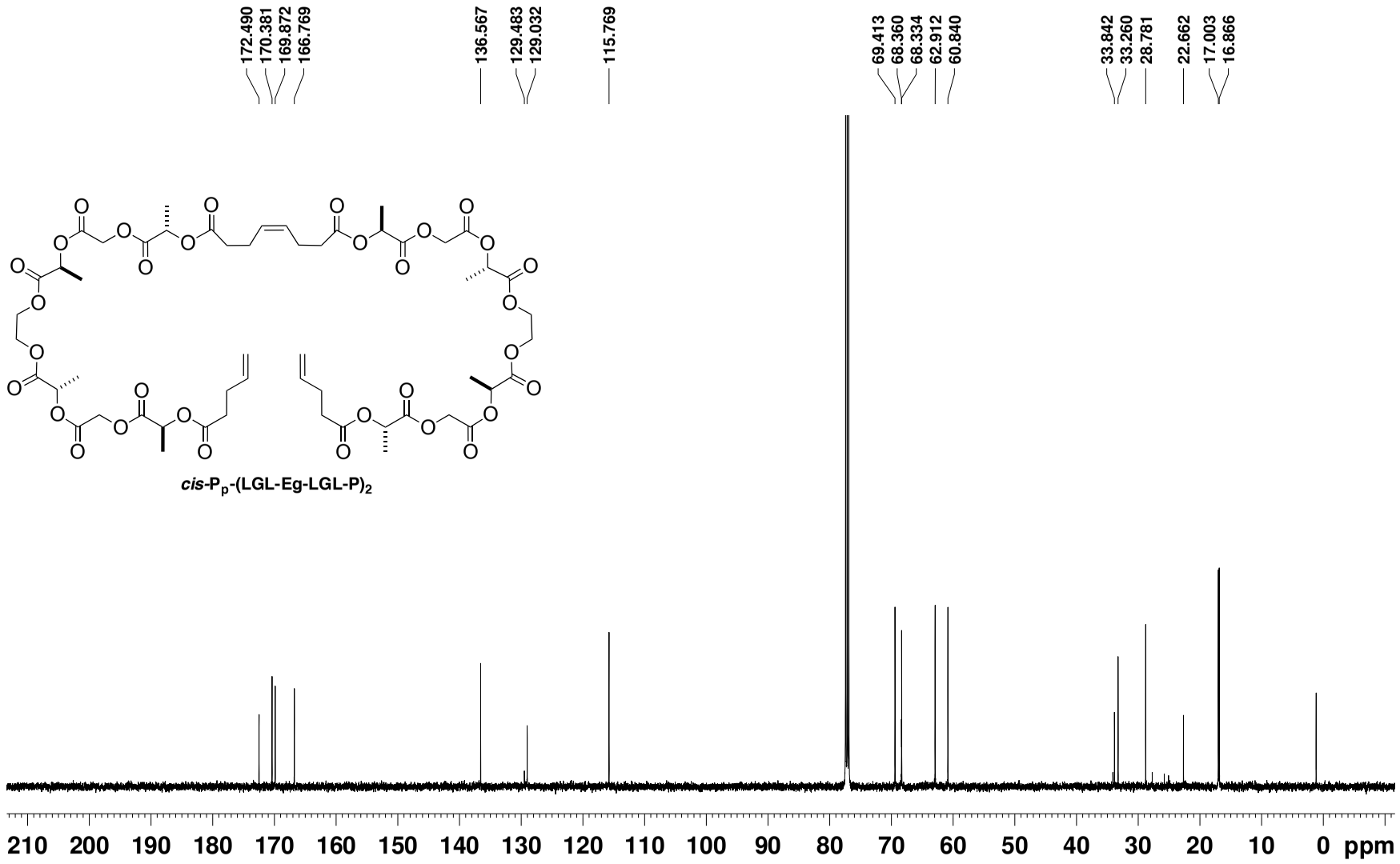
172.490
170.381
169.872
166.769
136.567
129.483
129.032
115.769
69.413
68.360
68.334
62.912
60.840
33.842
33.260
28.781
22.662
17.003
16.866
cis-P$_p$-(LGL-Eg-LGL-P)$_2$
210 200 190 180 170 160 150 140 130 120 110 100 90 80 70 60 50 40 30 20 10 0 ppm

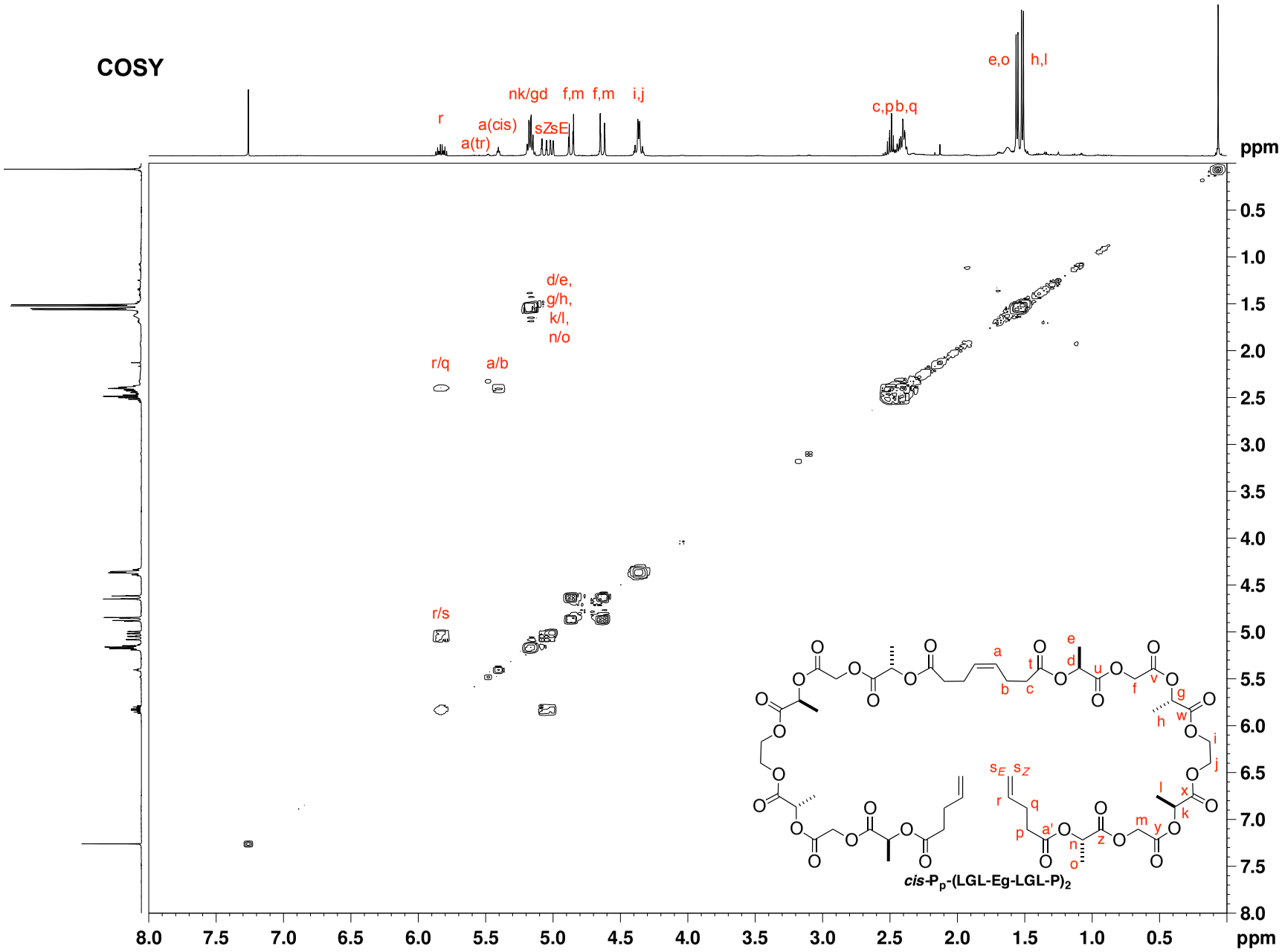
COSY
r
a(cis)
a(tr)
nk/gd
f,m
f,m
i,j
sZsE
c,p
b,q
e,o
h,l
ppm
d/e,
g/h,
k/l,
n/o
r/q
a/b
r/s
cis-P_p-(LGL-Eg-LGL-P)_2
8.0
7.5
7.0
6.5
6.0
5.5
5.0
4.5
4.0
3.5
3.0
2.5
2.0
1.5
1.0
0.5

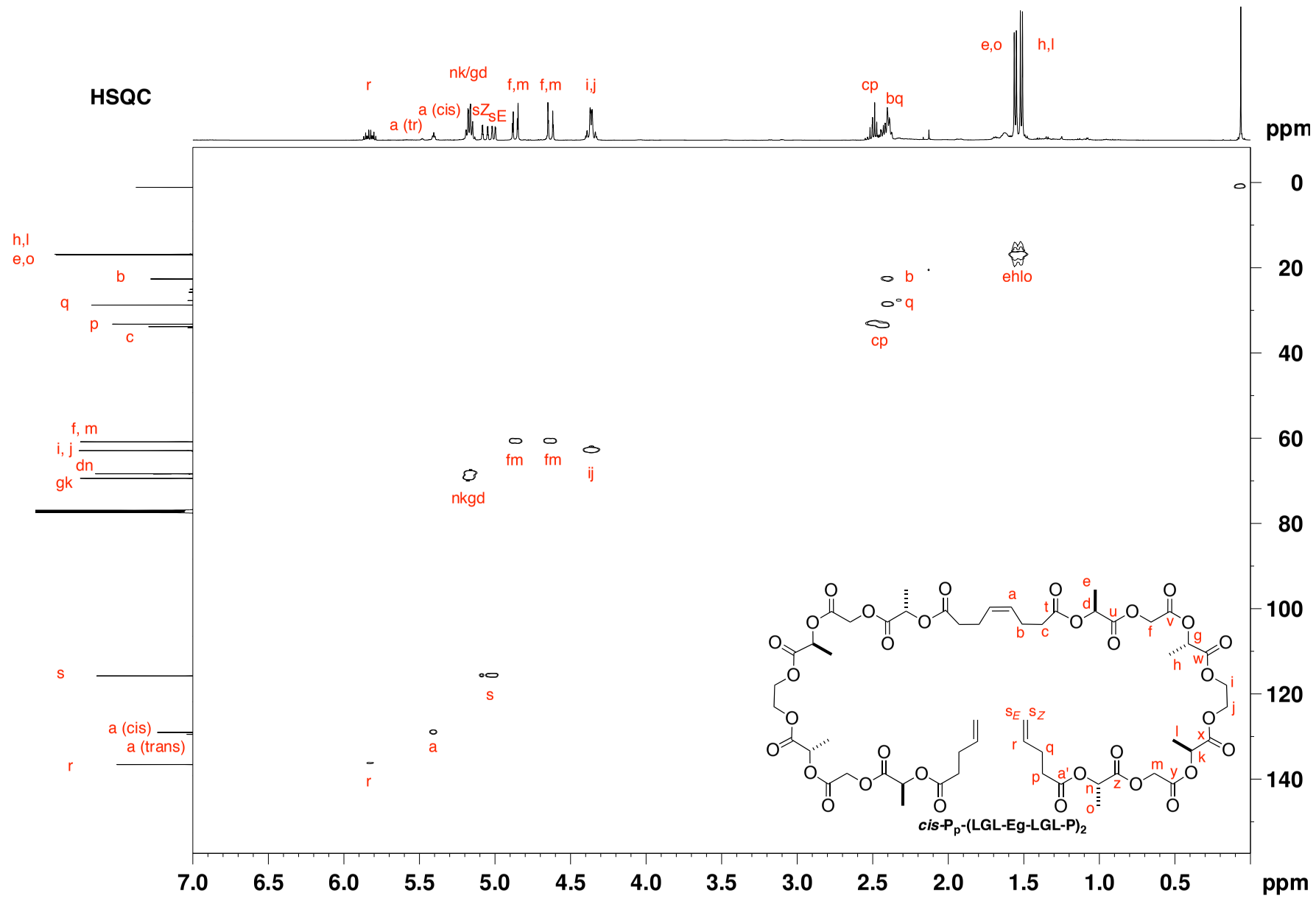
HSQC
r
a (tr)
a (cis)
nk/gd
sZ
sE
f,m
f,m
i,j
cp
bq
e,o
h,l
ppm
0
20
40
60
80
100
120
140
h,l
e,o
b
q
p
c
f, m
i, j
dn
gk
s
a (cis)
a (trans)
r
ehlo
b
q
cp
fm
fm
ij
nkgd
s
a
r
7.0
6.5
6.0
5.5
5.0
4.5
4.0
3.5
3.0
2.5
2.0
1.5
1.0
0.5
ppm
cis-Pp-(LGL-Eg-LGL-P)2

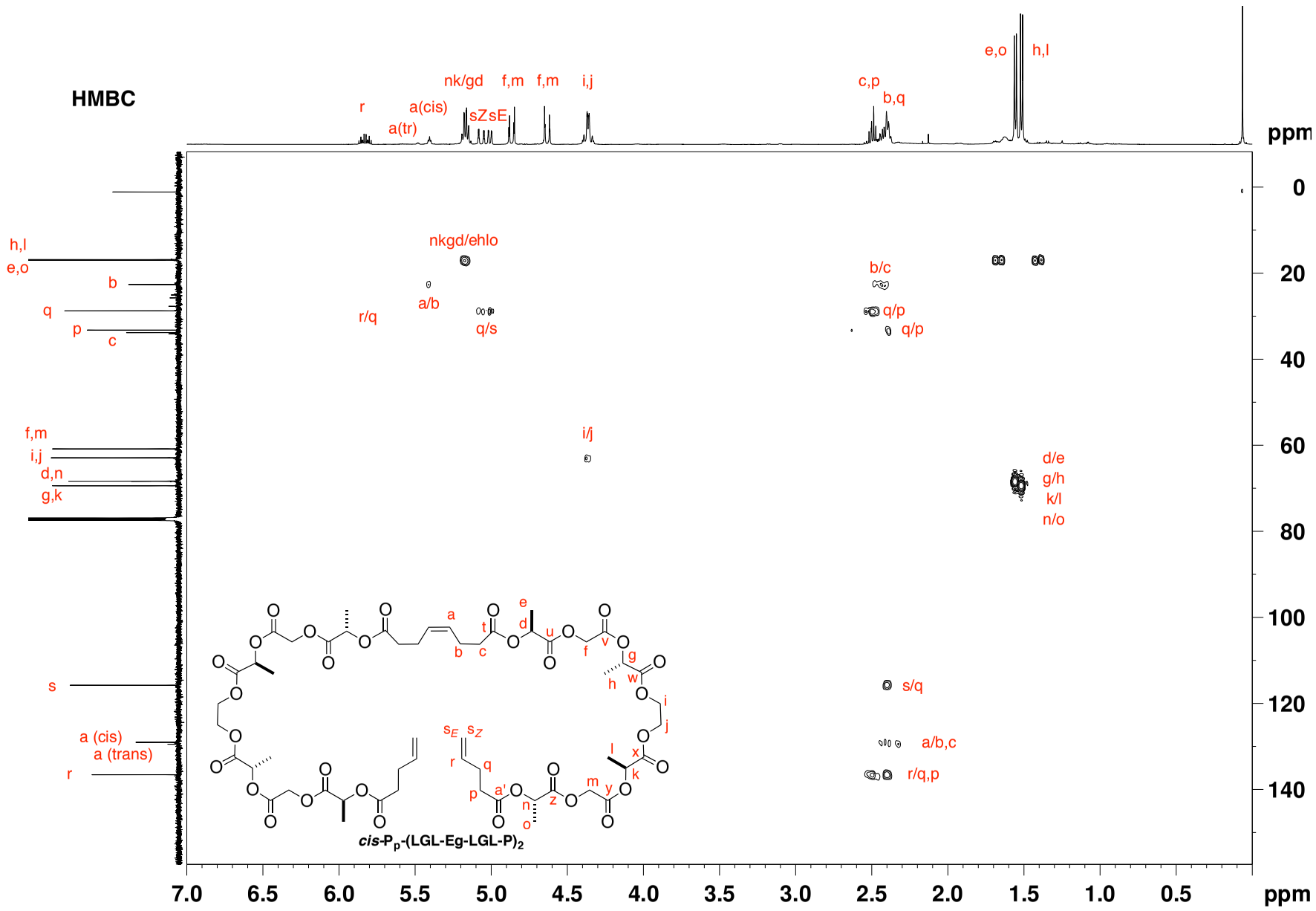
HMBC
r
a(cis)
a(tr)
nk/gd
f,m
f,m
i,j
sZsE
c,p
b,q
e,o
h,l
ppm
0
20
40
60
80
100
120
140
h,l
e,o
b
q
p
c
f,m
i,j
d,n
g,k
s
a (cis)
a (trans)
r
nkgd/ehlo
a/b
r/q
q/s
b/c
q/p
q/p
i/j
d/e
g/h
k/l
n/o
s/q
a/b,c
r/q,p
7.0
6.5
6.0
5.5
5.0
4.5
4.0
3.5
3.0
2.5
2.0
1.5
1.0
0.5
ppm
cis-Pp-(LGL-Eg-LGL-P)2

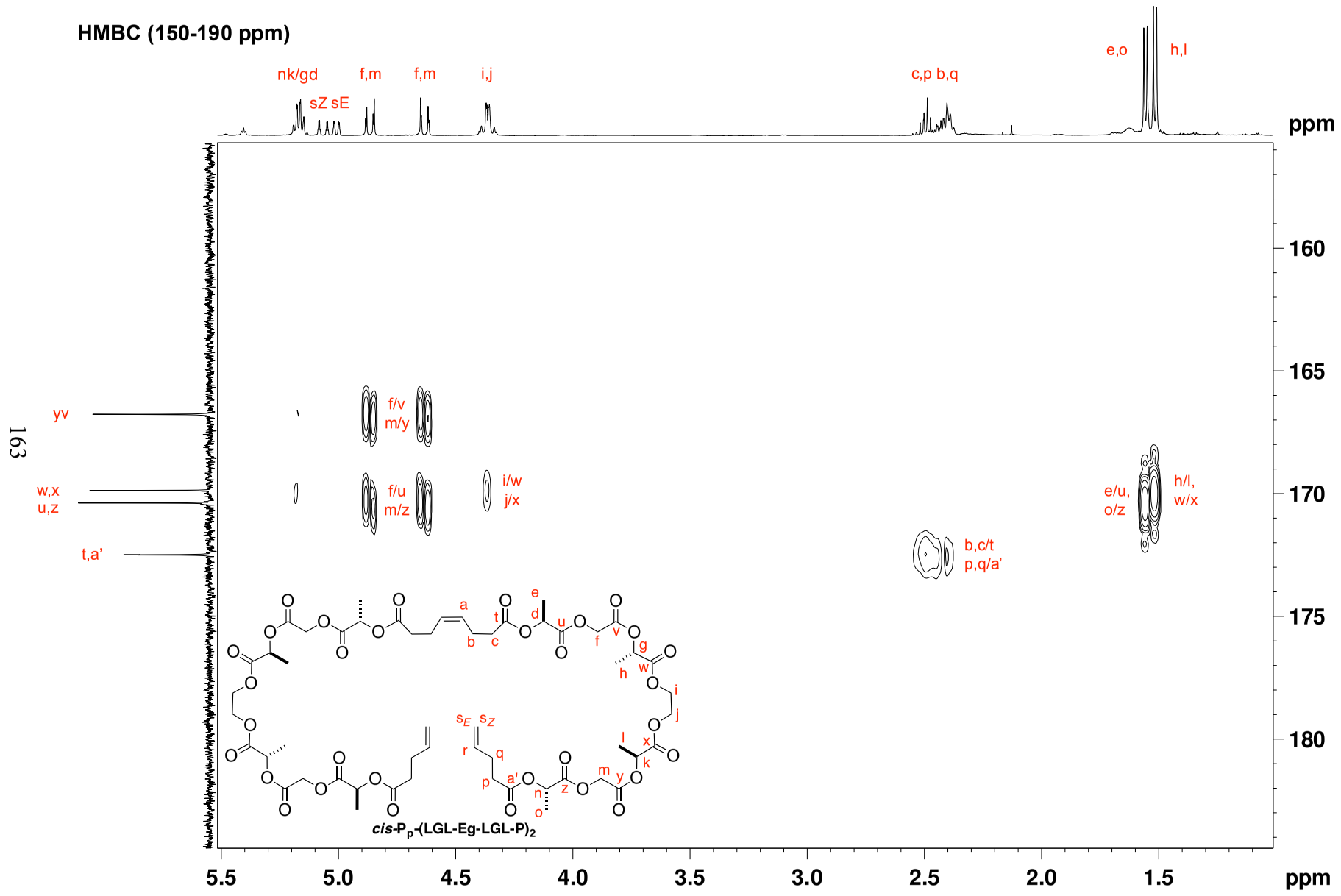
HMBC (150-190 ppm)
nk/gd
sZ sE
f,m
f,m
i,j
c,p b,q
e,o
h,l
ppm
yv
w,x
u,z
t,a'
f/v
m/y
f/u
m/z
i/w
j/x
b,c/t
p,q/a'
e/u,
o/z
h/l,
w/x
160
165
170
175
180
5.5
5.0
4.5
4.0
3.5
3.0
2.5
2.0
1.5
ppm
cis-Pp-(LGL-Eg-LGL-P)2

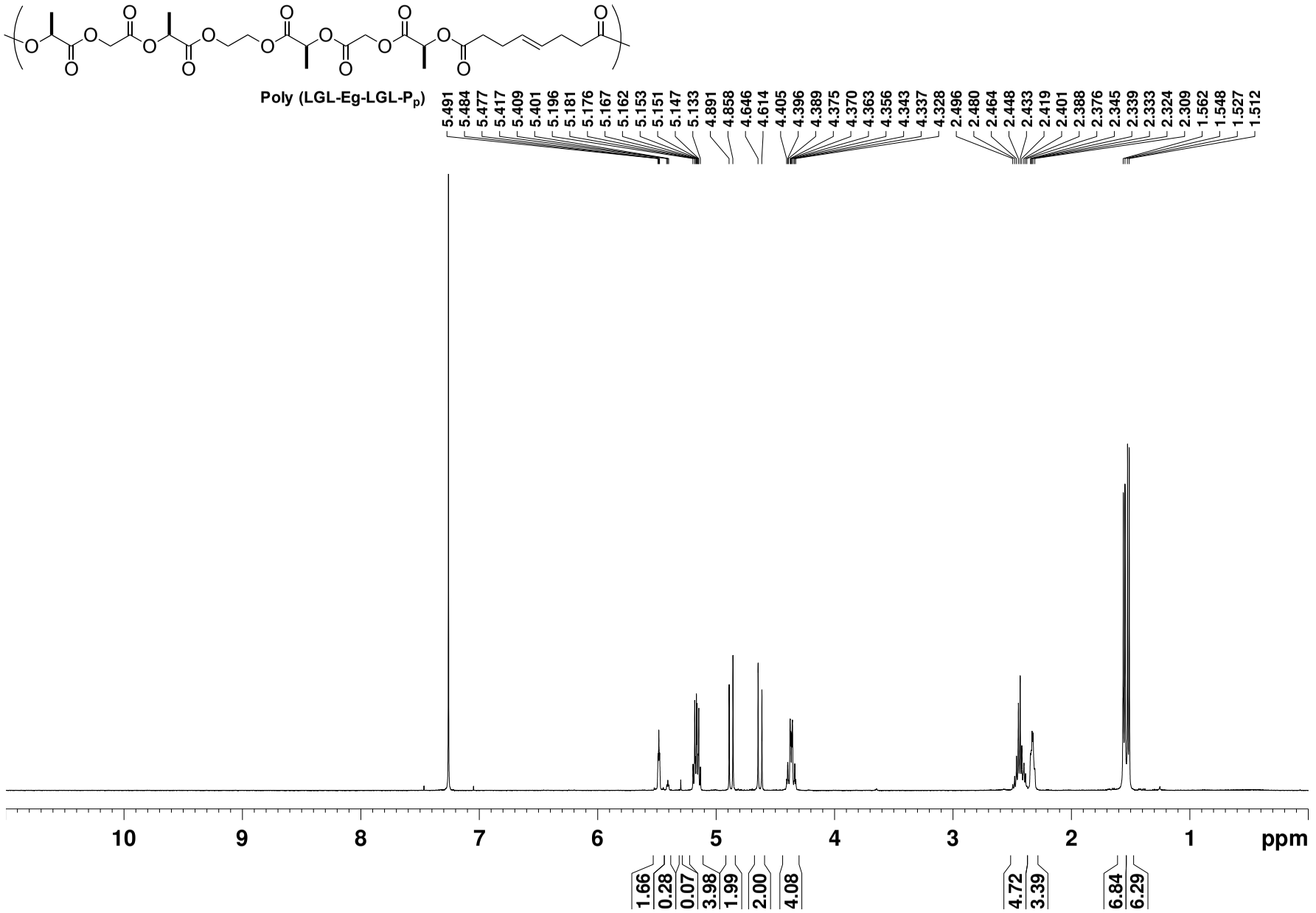
Poly (LGL-Eg-LGL-Pp)
5.491
5.484
5.477
5.417
5.409
5.401
5.196
5.181
5.176
5.167
5.162
5.153
5.151
5.147
5.133
4.891
4.858
4.646
4.614
4.405
4.396
4.389
4.375
4.370
4.363
4.356
4.343
4.337
4.328
2.496
2.480
2.464
2.448
2.433
2.419
2.401
2.388
2.376
2.345
2.339
2.333
2.324
2.309
1.562
1.548
1.527
1.512
10
9
8
7
6
5
4
3
2
1
ppm
1.66
0.28
0.07
3.98
1.99
2.00
4.08
4.72
3.39
6.84
6.29

Poly (LGL-Eg-LGL-P$_p$)
172.385
170.268
169.745
166.658
129.345
69.267
68.167
62.786
60.686
33.689
27.582
16.883
16.742
0 ppm

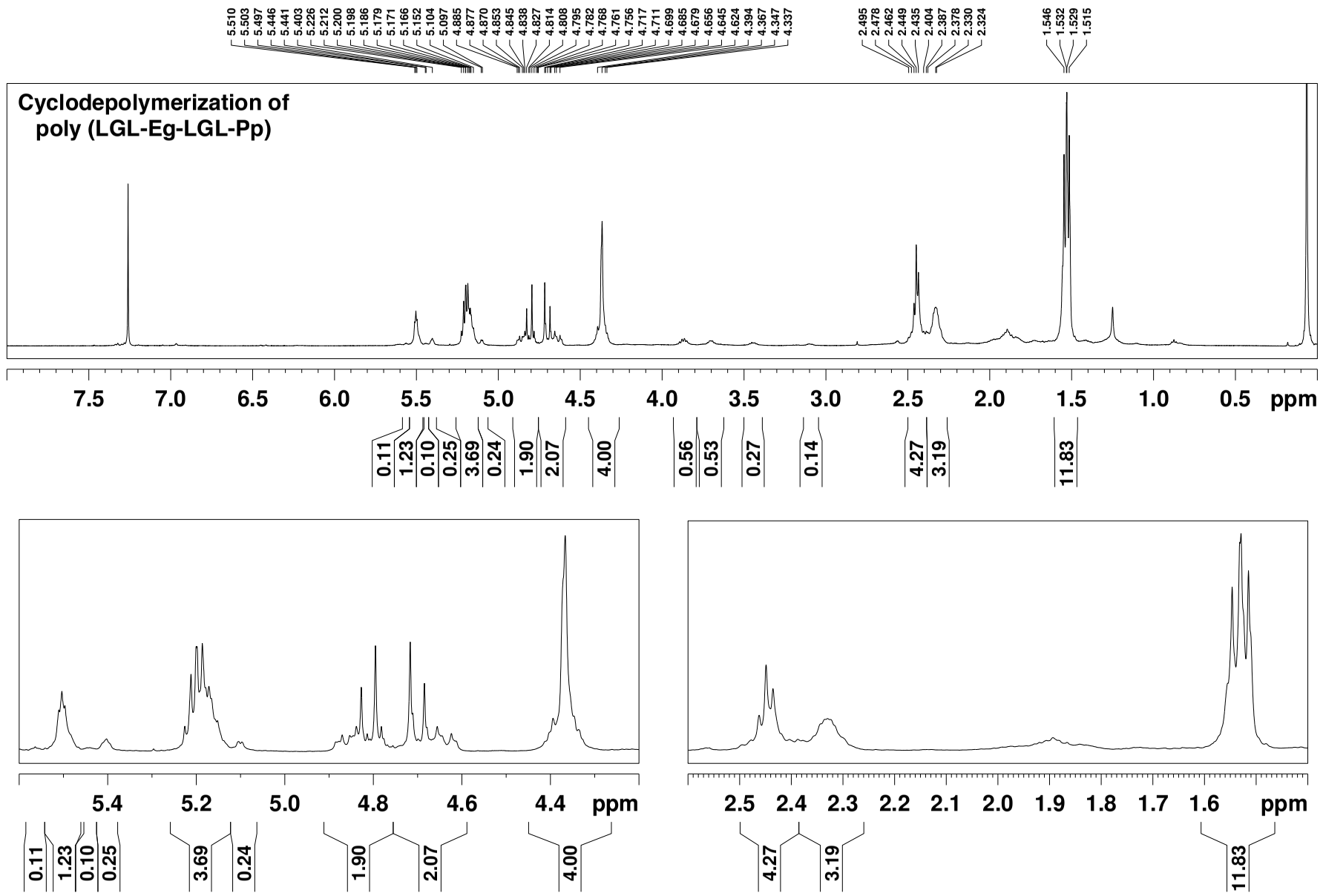
5.510
5.503
5.497
5.446
5.441
5.403
5.226
5.212
5.200
5.198
5.186
5.179
5.171
5.166
5.152
5.104
5.097
4.885
4.877
4.870
4.853
4.845
4.838
4.827
4.814
4.808
4.795
4.782
4.768
4.761
4.756
4.717
4.711
4.699
4.685
4.679
4.656
4.645
4.624
4.394
4.367
4.347
4.337
2.495
2.478
2.462
2.449
2.435
2.404
2.387
2.378
2.330
2.324
1.546
1.532
1.529
1.515
Cyclodepolymerization of
poly (LGL-Eg-LGL-Pp)
7.5
7.0
6.5
6.0
5.5
5.0
4.5
4.0
3.5
3.0
2.5
2.0
1.5
1.0
0.5
ppm
0.11
1.23
0.10
0.25
3.69
0.24
1.90
2.07
4.00
0.56
0.53
0.27
0.14
4.27
3.19
11.83
5.4
5.2
5.0
4.8
4.6
4.4
ppm
0.11
1.23
0.10
0.25
3.69
0.24
1.90
2.07
4.00
2.5
2.4
2.3
2.2
2.1
2.0
1.9
1.8
1.7
1.6
ppm
4.27
3.19
11.83

HRMS (ESI) for cyclodepolymerization study.

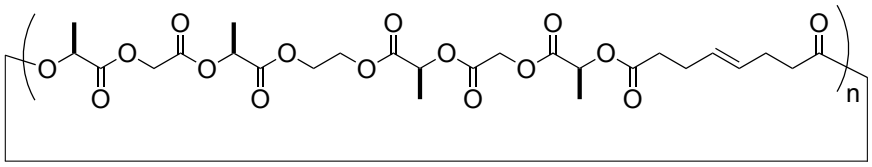

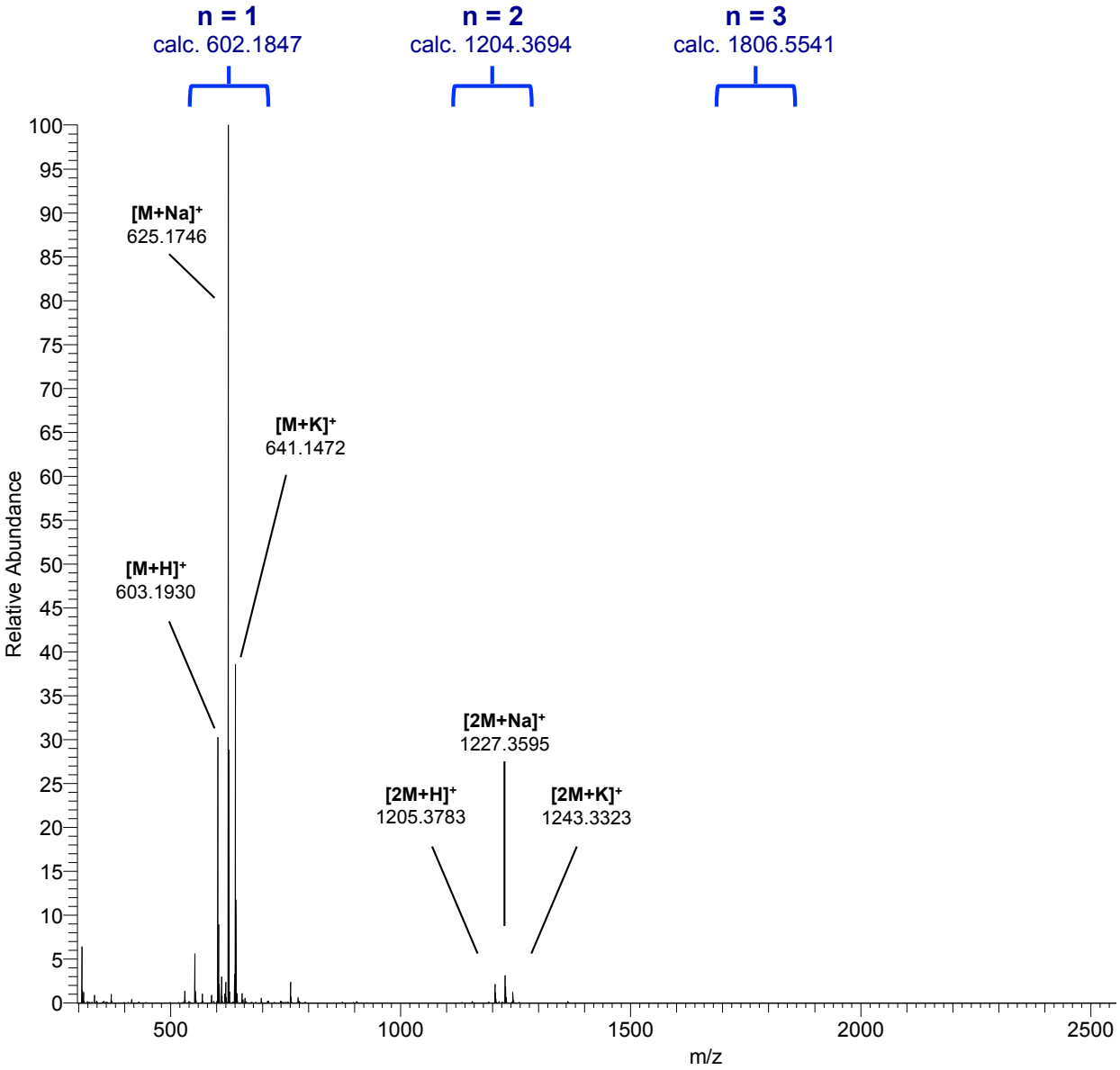

poly(NBE)
n
ppm
10
9
8
7
6
5
4
3
2
1
0.69
1.09
1.14
0.77
1.10
1.90
0.52
1.93
0.18
0.95
x
5.377
5.346
5.317
5.233
5.210
5.206
5.202
5.181
2.790
2.435
1.884
1.873
1.862
1.850
1.836
1.801
1.790
1.352
1.297
1.272
1.257
1.243
1.240
1.237
1.226
1.094
1.086
1.064
1.041

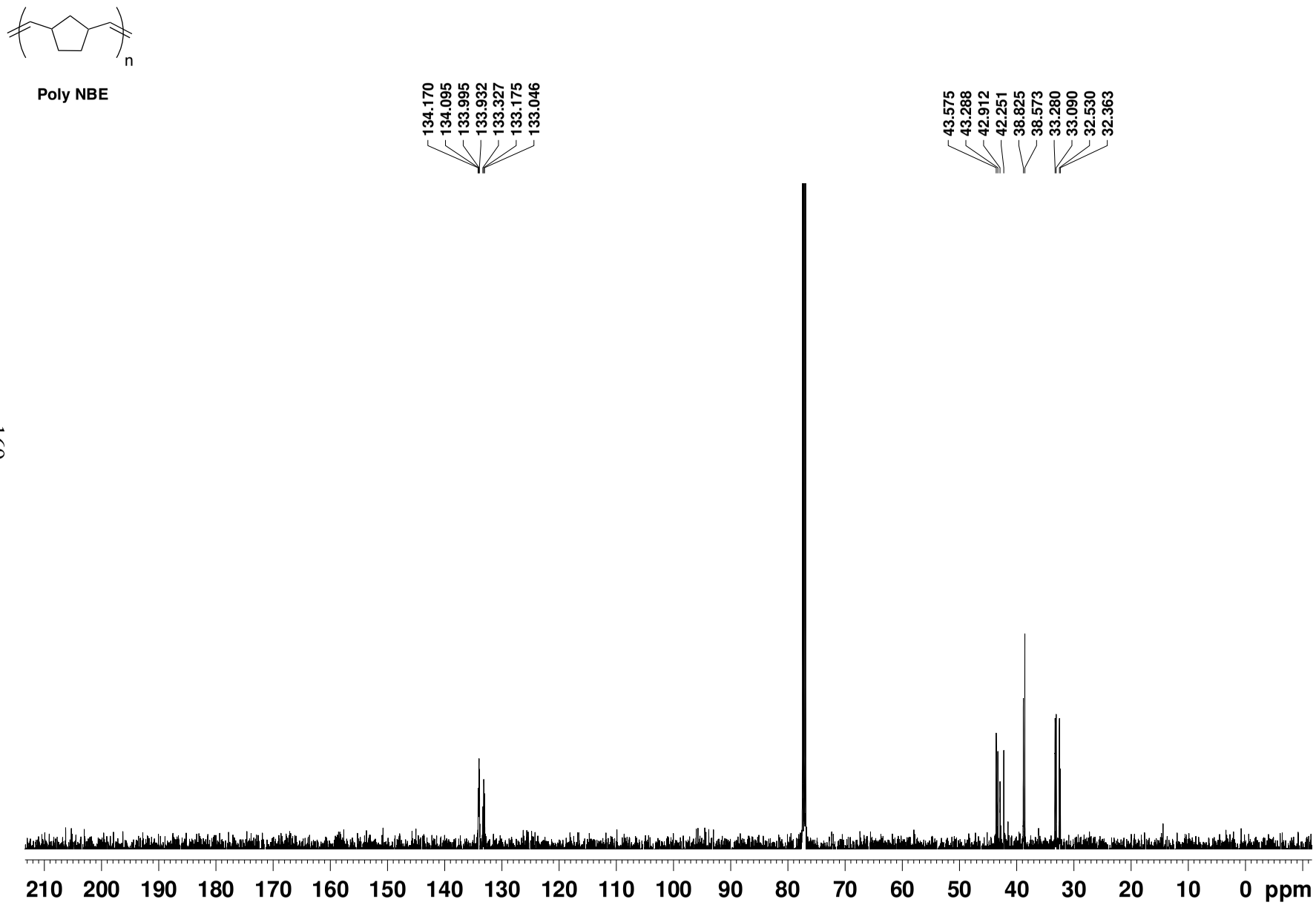
n
Poly NBE
134.170
134.095
133.995
133.932
133.327
133.175
133.046
43.575
43.288
42.912
42.251
38.825
38.573
33.280
33.090
32.530
32.363
210 200 190 180 170 160 150 140 130 120 110 100 90 80 70 60 50 40 30 20 10 0 ppm

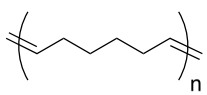
n

Poly COE

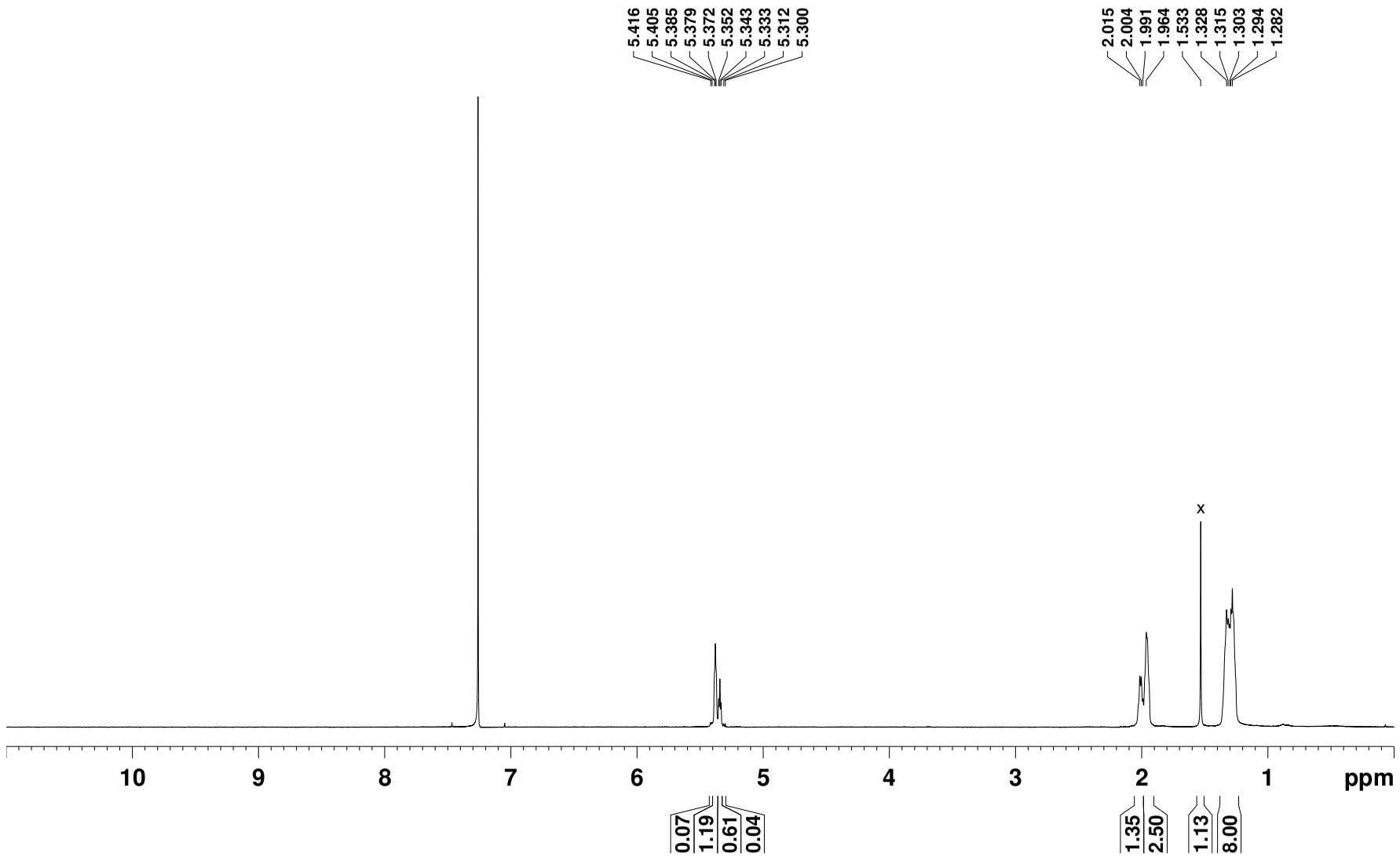
5.416
5.405
5.385
5.379
5.372
5.352
5.343
5.333
5.312
5.300
2.015
2.004
1.991
1.964
1.533
1.328
1.315
1.303
1.294
1.282
x
10
9
8
7
6
5
4
3
2
1
ppm
0.07
1.19
0.61
0.04
1.35
2.50
1.13
8.00

Poly [(LGL-Eg-LGL-P$_p$)-*block*-(NBE)]
ppm
1
2
3
4
5
6
7
8
9
10
0.10
0.17
0.10
0.22
1.81
0.50
2.18
0.20
7.90
0.25
2.22
0.09
0.09
0.15
0.12
0.44
2.00
4.91
0.20
0.17
3.29
8.96
4.32
3.63
6.31
21.24
8.08
2.93
5.63
0.994
1.015
1.040
1.065
1.085
1.351
1.513
1.519
1.527
1.536
1.548
1.563
1.790
1.797
1.849
1.861
1.874
2.324
2.333
2.389
2.402
2.420
2.434
2.448
2.465
2.480
2.495
2.790
2.847
3.684
3.698
3.751
3.757
3.772
4.328
4.337
4.358
4.363
4.370
4.376
4.396
4.405
4.614
4.647
4.683
4.688
4.715
4.721
4.786
4.800
4.818
4.831
4.859
4.891
4.947
4.985
5.134
5.148
5.162
5.167
5.176
5.182
5.197
5.205
5.210
5.346
5.401
5.409
5.417
5.478
5.485
5.491
5.508
5.991

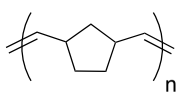

Poly NBE

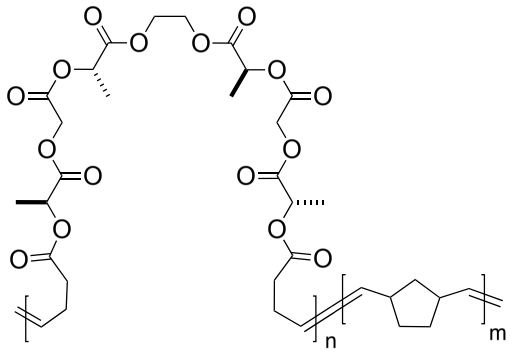

Poly [(LGL-Eg-LGL-P_p)-*block*-(NBE)]

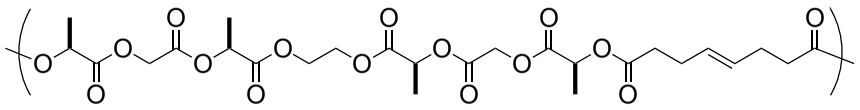

Poly (LGL-Eg-LGL-P_p)

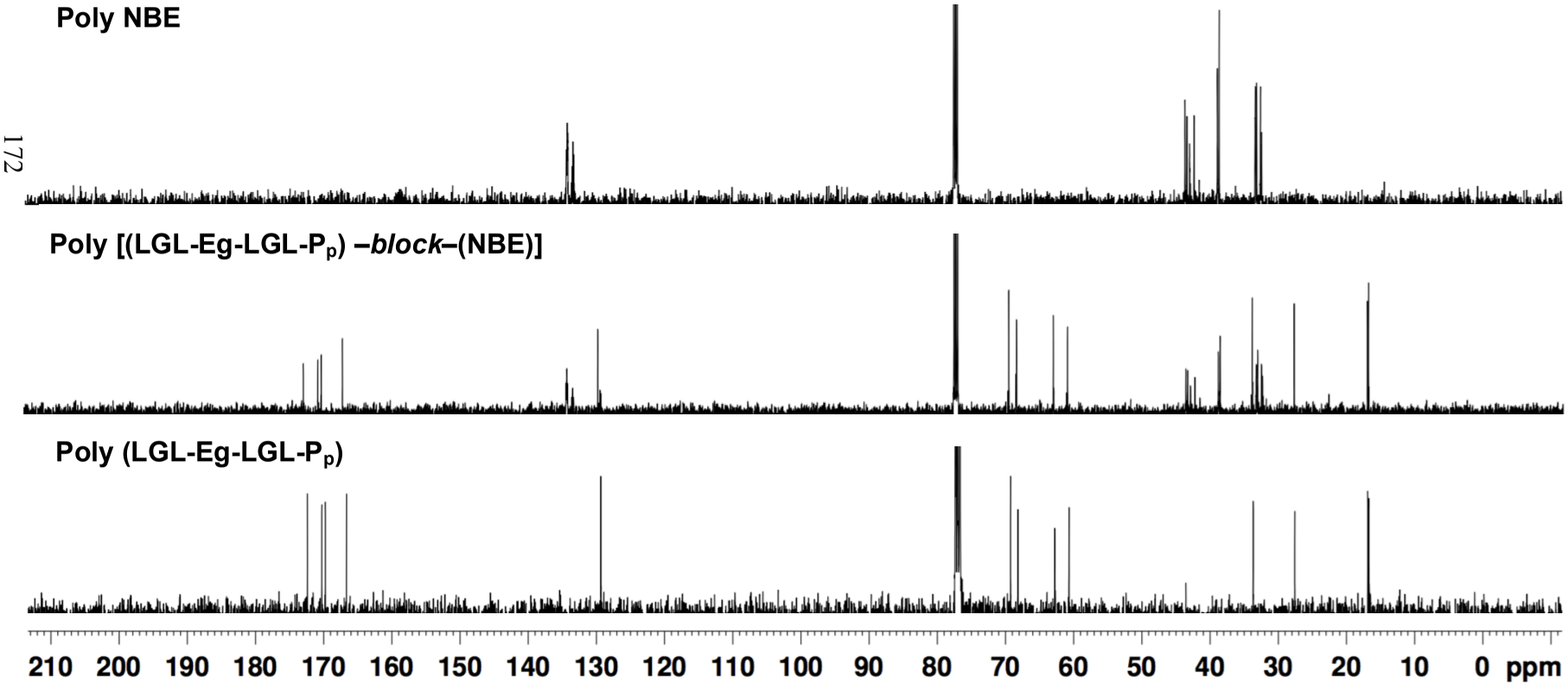

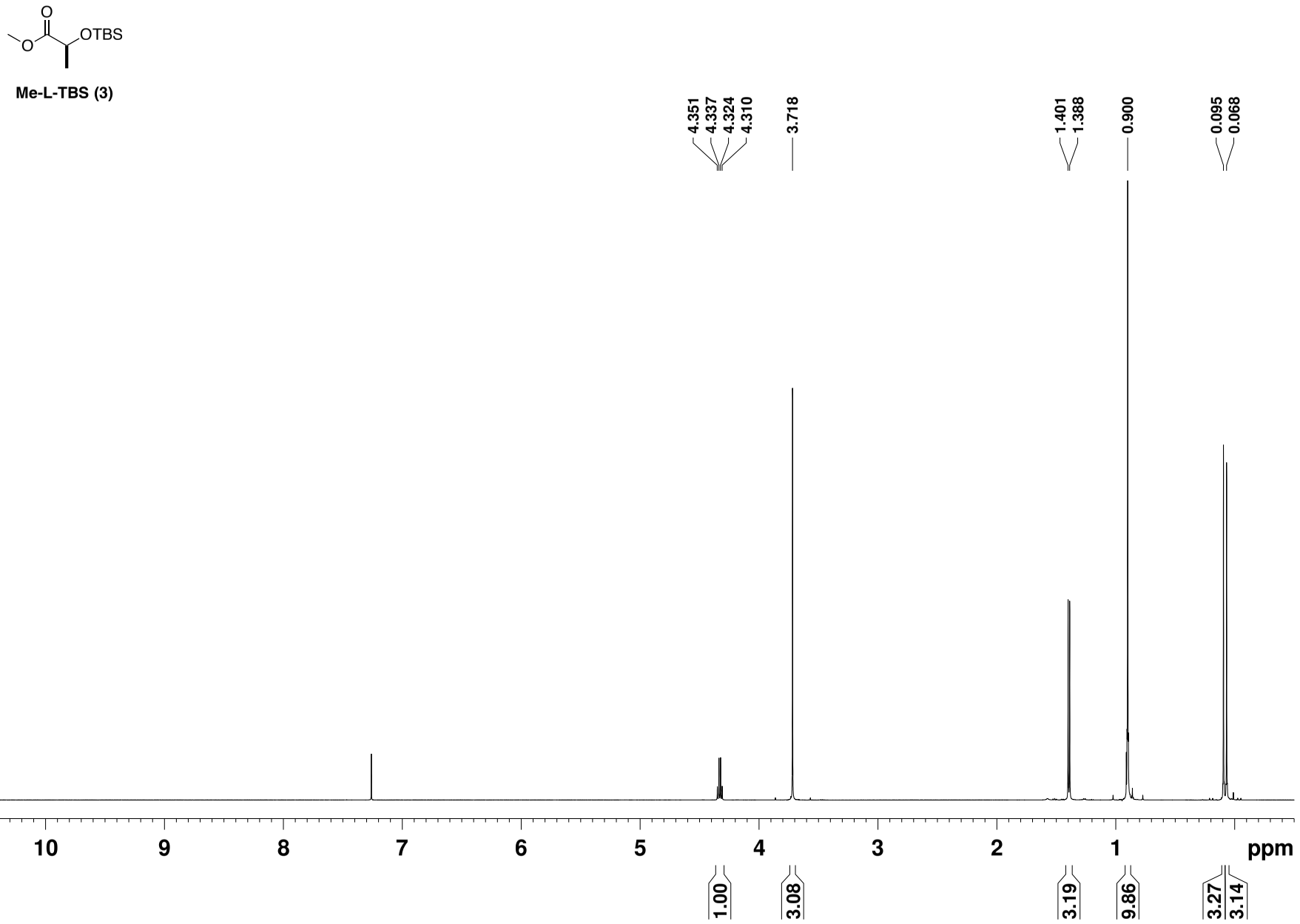
O
O
OTBS
Me-L-TBS (3)
4.351
4.337
4.324
4.310
3.718
1.401
1.388
0.900
0.095
0.068
10
9
8
7
6
5
4
3
2
1
ppm
1.00
3.08
3.19
9.86
3.27
3.14

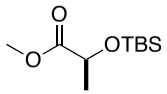
O
O
OTBS

Me-L-TBS (3)

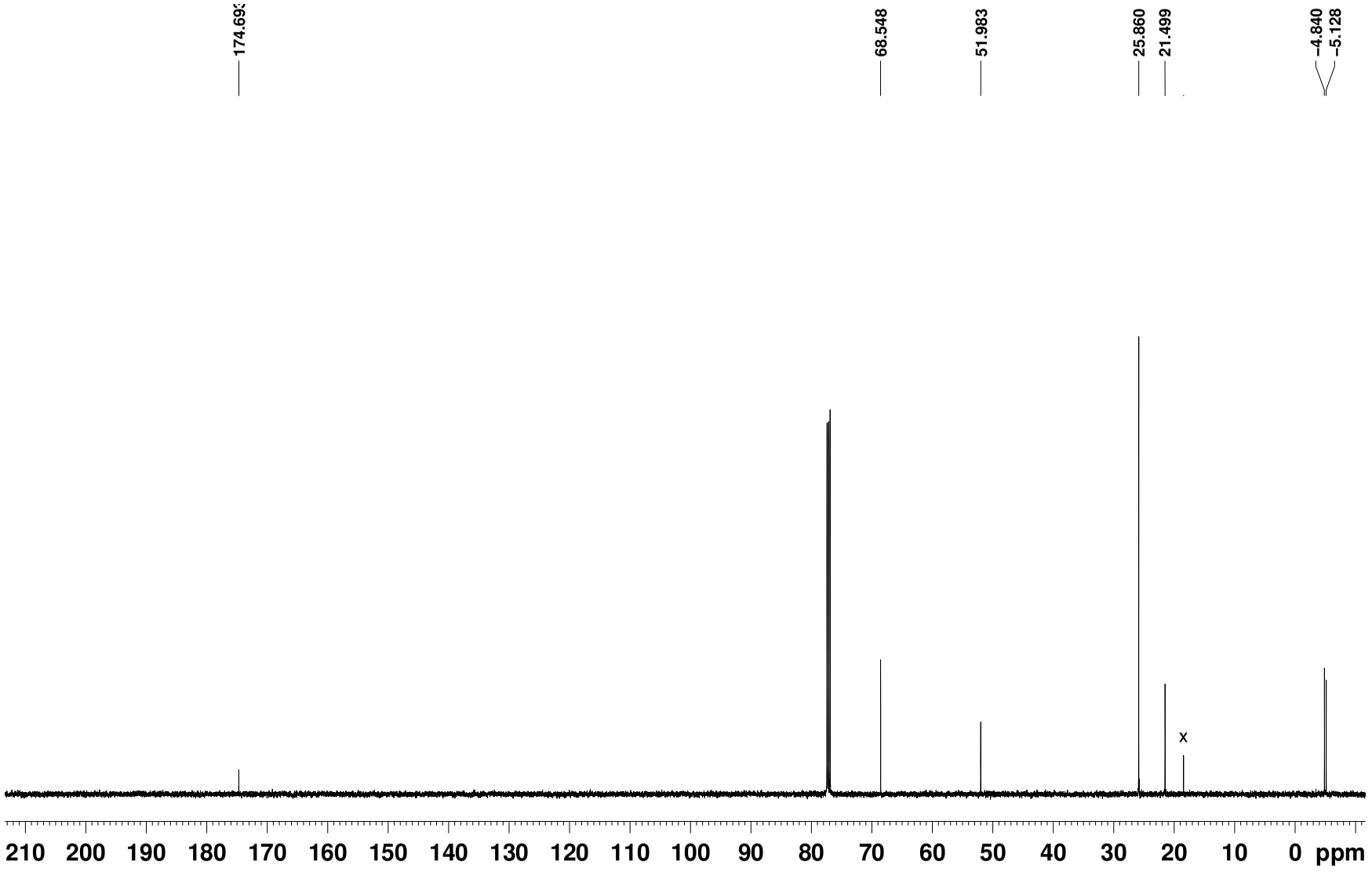
174.69
68.548
51.983
25.860
21.499
-4.840
-5.128
x
210 200 190 180 170 160 150 140 130 120 110 100 90 80 70 60 50 40 30 20 10 0 ppm

L-TBS (5)
OTBS
O
HO
ppm
10
9
8
7
6
5
4
3
2
1
0.80
1.00
3.33
9.89
6.27
4.378
4.364
4.351
4.337
1.465
1.452
0.936
0.159
0.154

OTBS
O
HO
L-TBS (5)
174.005
68.955
25.772
21.196
18.093
-4.408
-5.158
X
210 200 190 180 170 160 150 140 130 120 110 100 90 80 70 60 50 40 30 20 10 0 ppm

TBDPSO
OTBDPS
O
O
O
O
6
9
7.726
7.723
7.710
7.707
7.679
7.665
7.663
7.647
7.644
7.427
7.422
7.417
7.415
7.412
7.409
7.403
7.395
7.391
7.385
7.370
7.360
7.346
7.332
7.260
5.300
4.286
4.272
4.259
4.245
3.928
3.924
3.915
3.910
3.902
3.897
2.097
2.047
1.542
1.504
1.490
1.476
1.460
1.446
1.428
1.421
1.407
1.362
1.348
1.313
1.299
1.292
1.288
1.275
1.268
1.261
1.246
1.234
1.229
1.221
1.214
ppm
1
2
3
4
5
6
7
8
9
10
18.08
2.31
6.03
4.25
0.93
4.09
2.00
11.81
8.30

13
1.404
1.418
1.432
1.436
1.442
1.451
1.455
1.467
1.680
1.693
1.709
1.723
1.737
2.818
2.828
4.153
4.166
4.175
4.179
4.188
4.192
4.200
4.205
4.214
4.227
4.240
4.253
4.264
4.266
4.277
4.291
6.63
1.81
4.11
1.97
2.00
4.12
ppm

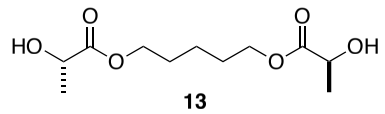
HO
O
O
O
O
OH

13

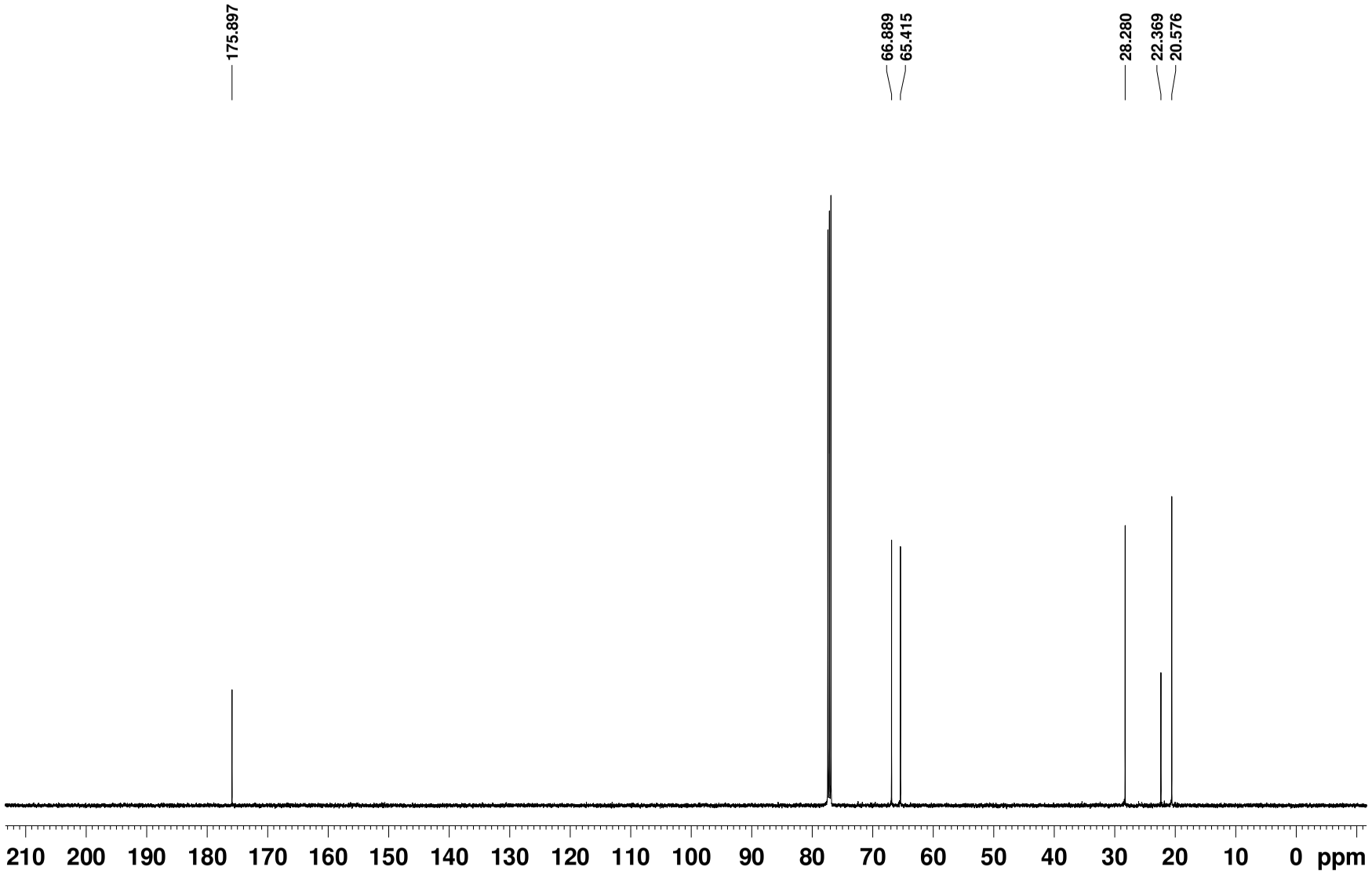
175.897
66.889
65.415
28.280
22.369
20.576
210 200 190 180 170 160 150 140 130 120 110 100 90 80 70 60 50 40 30 20 10 0 ppm

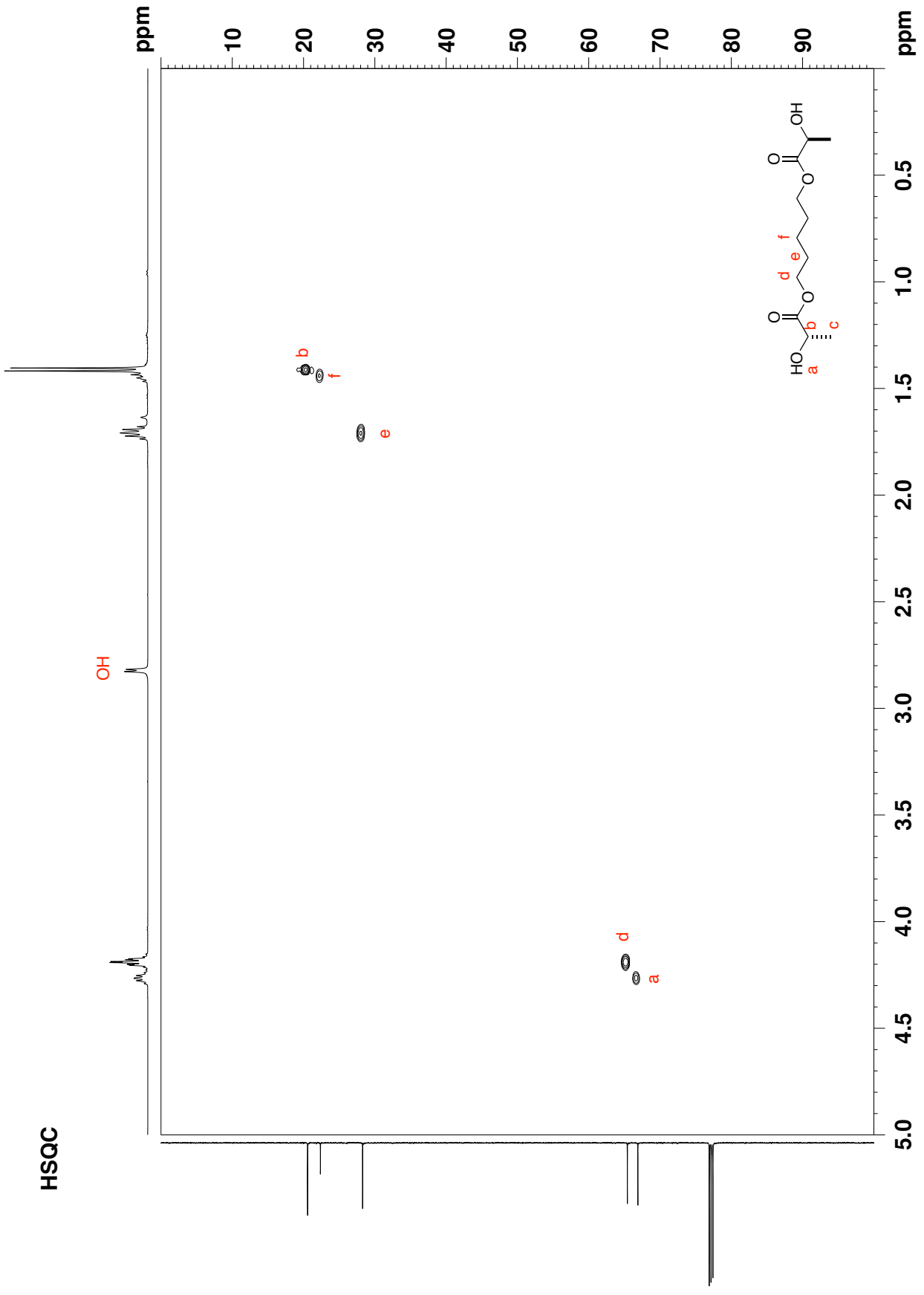
HSQC
ppm
10
20
30
40
50
60
70
80
90
ppm
0.5
1.0
1.5
2.0
2.5
3.0
3.5
4.0
4.5
5.0
OH
b
f
e
d
a
HO
O
O
O
OH
a
b
c
d
e
f

TBSO
O
O
O
O
O
O
OTBS
10
0.070
0.098
0.901
1.395
1.412
3.676
3.688
3.700
4.237
4.248
4.258
4.260
4.270
4.282
4.321
4.338
4.355
4.372
12.00
18.89
5.84
4.14
5.96
ppm
1
2
3
4
5
6
7
8
9
10

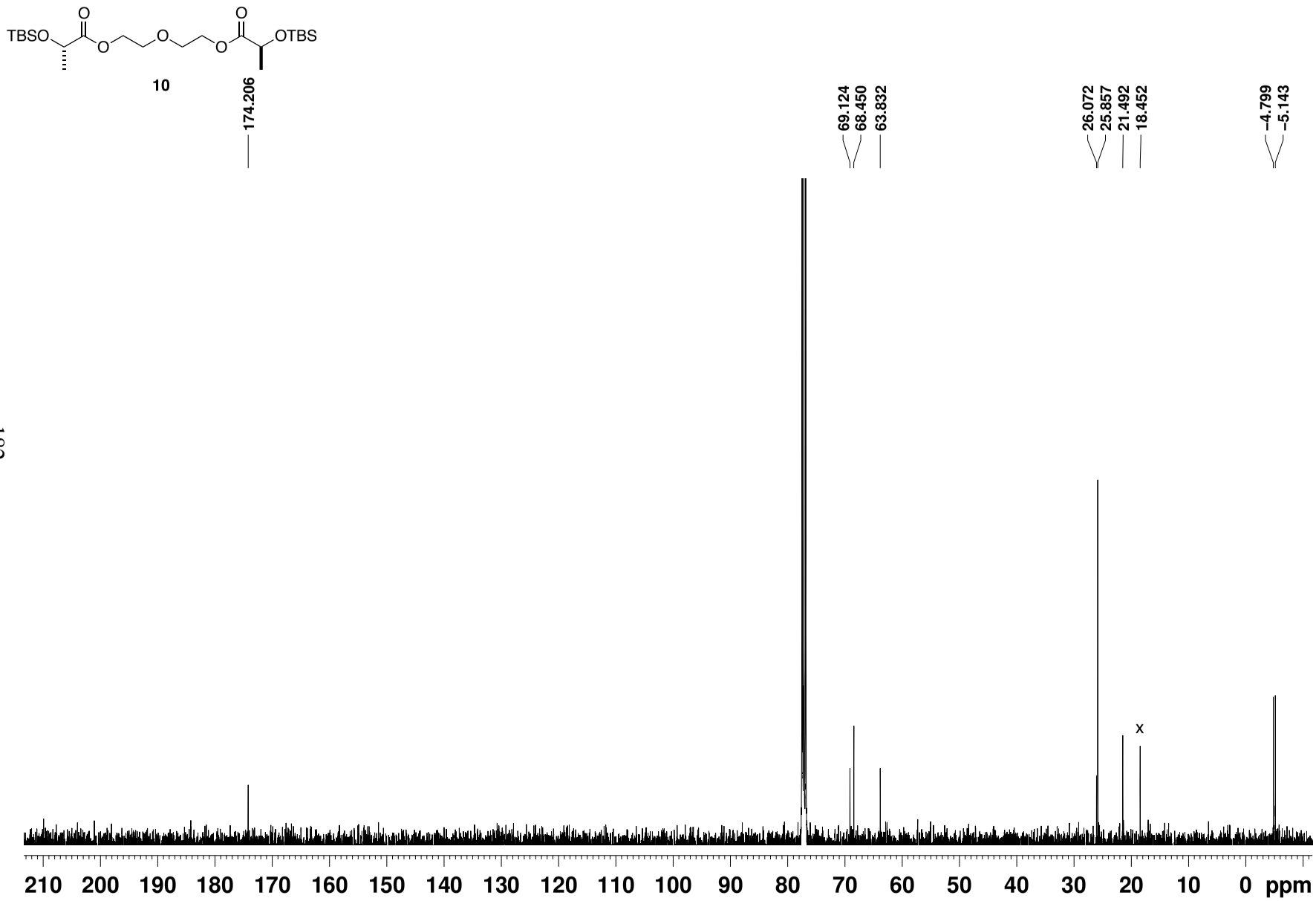
TBSO
O
O
O
O
O
OTBS
10
174.206
69.124
68.450
63.832
26.072
25.857
21.492
18.452
−4.799
−5.143
x
210 200 190 180 170 160 150 140 130 120 110 100 90 80 70 60 50 40 30 20 10 0 ppm

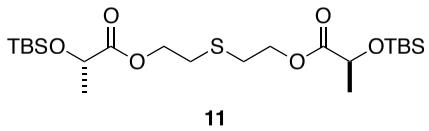
TBSO
O
O
S
O
O
OTBS

11

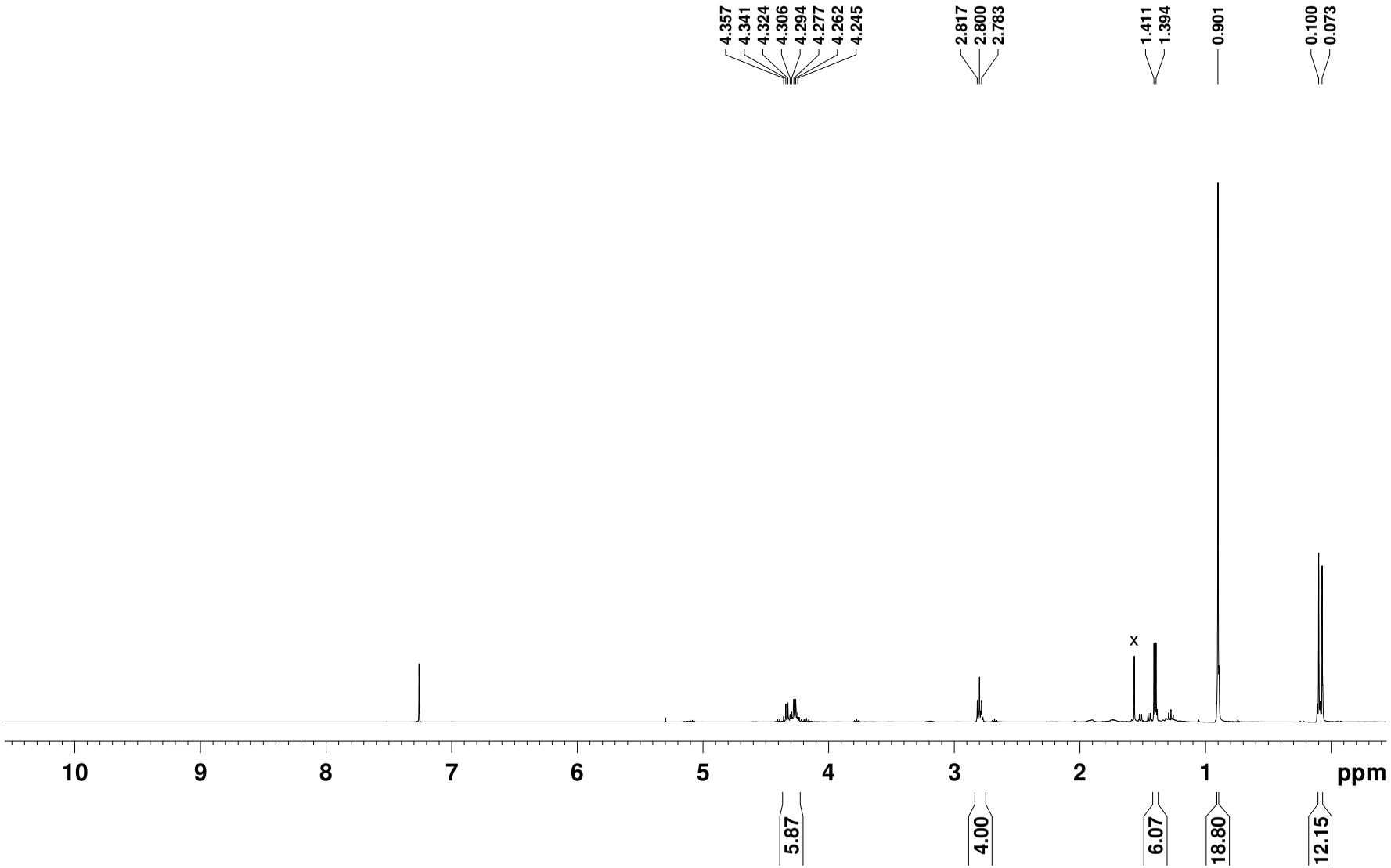
4.357
4.341
4.324
4.306
4.294
4.277
4.262
4.245
2.817
2.800
2.783
1.411
1.394
0.901
0.100
0.073
x
10
9
8
7
6
5
4
3
2
1
ppm
5.87
4.00
6.07
18.80
12.15

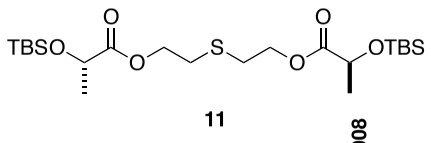
TBSO
O
O
S
O
O
OTBS

11

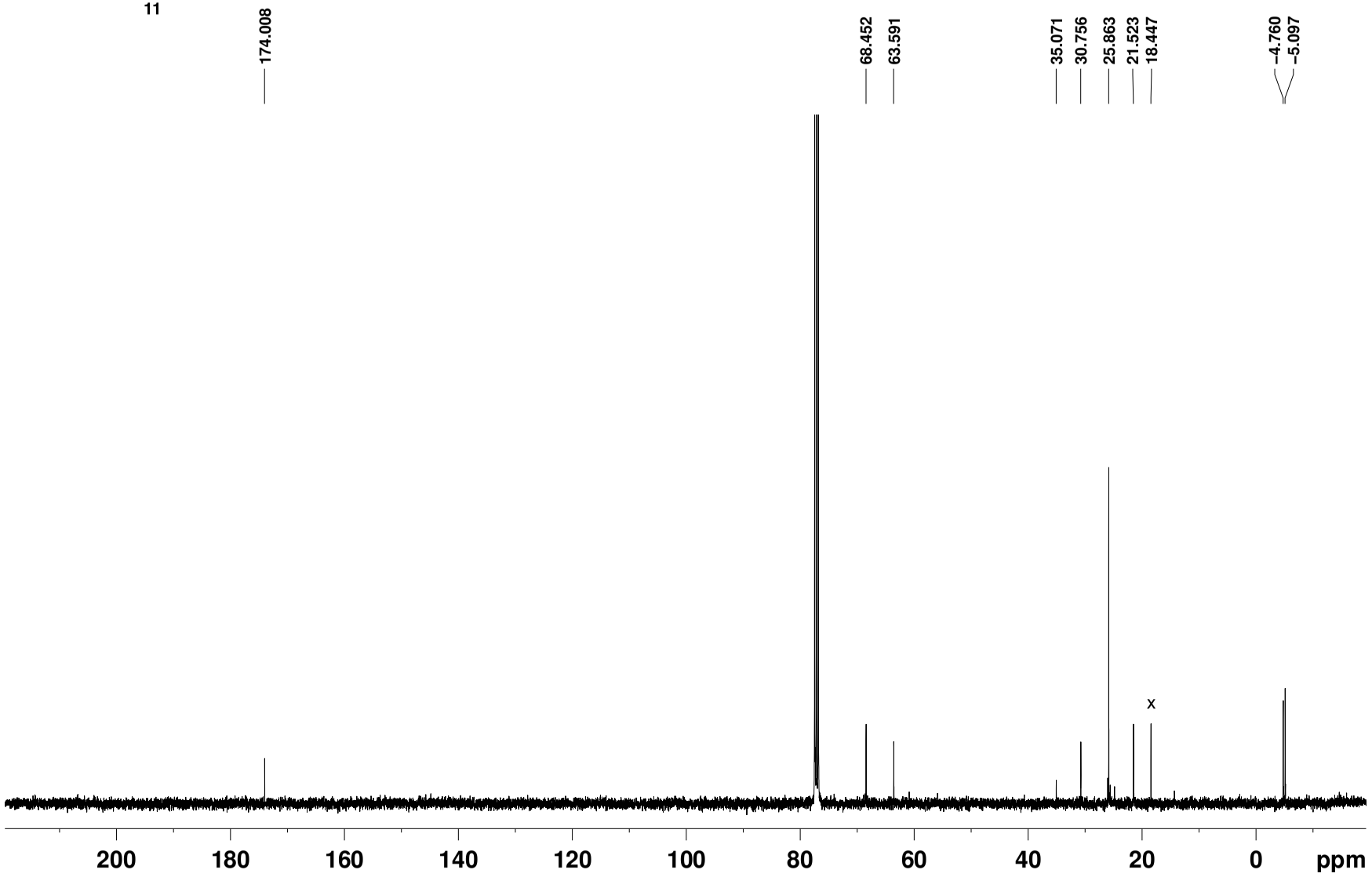
174.008
68.452
63.591
35.071
30.756
25.863
21.523
18.447
-4.760
-5.097
x
200
180
160
140
120
100
80
60
40
20
0
ppm

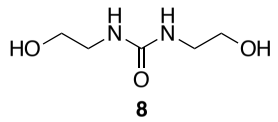
HO
H
N
H
N
OH
O

8

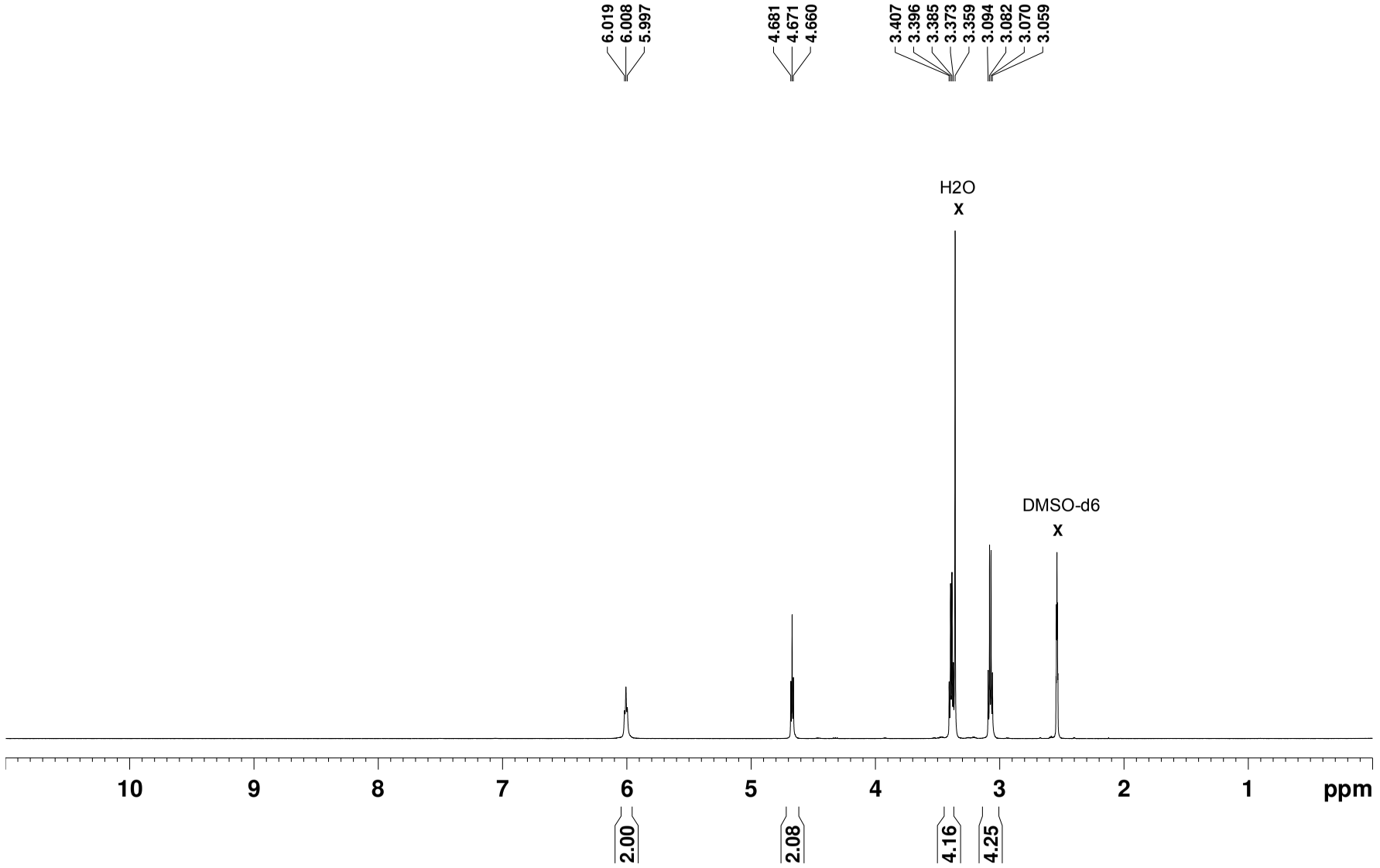
6.019
6.008
5.997
4.681
4.671
4.660
3.407
3.396
3.385
3.373
3.359
3.094
3.082
3.070
3.059
H2O
x
DMSO-d6
x
10
9
8
7
6
5
4
3
2
1
ppm
2.00
2.08
4.16
4.25

TBSO
OTBS
12
0.070
0.093
0.901
1.387
1.401
2.357
3.239
3.429
3.441
3.447
3.451
3.458
3.463
3.470
3.473
3.481
3.485
3.492
3.503
4.147
4.157
4.169
4.180
4.185
4.191
4.197
4.208
4.220
4.230
4.239
4.250
4.312
4.325
4.339
4.352
4.723
4.734
4.745
5.92
6.53
18.05
6.00
4.06
3.93
1.93
1.65
ppm

Bn-GL-TBS (14)
BnO
O
O
O
OTBS
7.388
7.383
7.382
7.380
7.375
7.371
7.368
7.363
7.357
7.349
7.343
7.340
7.335
7.324
7.320
5.190
4.736
4.705
4.682
4.650
4.455
4.441
4.428
4.414
1.447
1.433
0.903
0.101
0.079
5.00
2.10
1.06
1.08
1.02
9.61
3.21
3.04
3.18
ppm

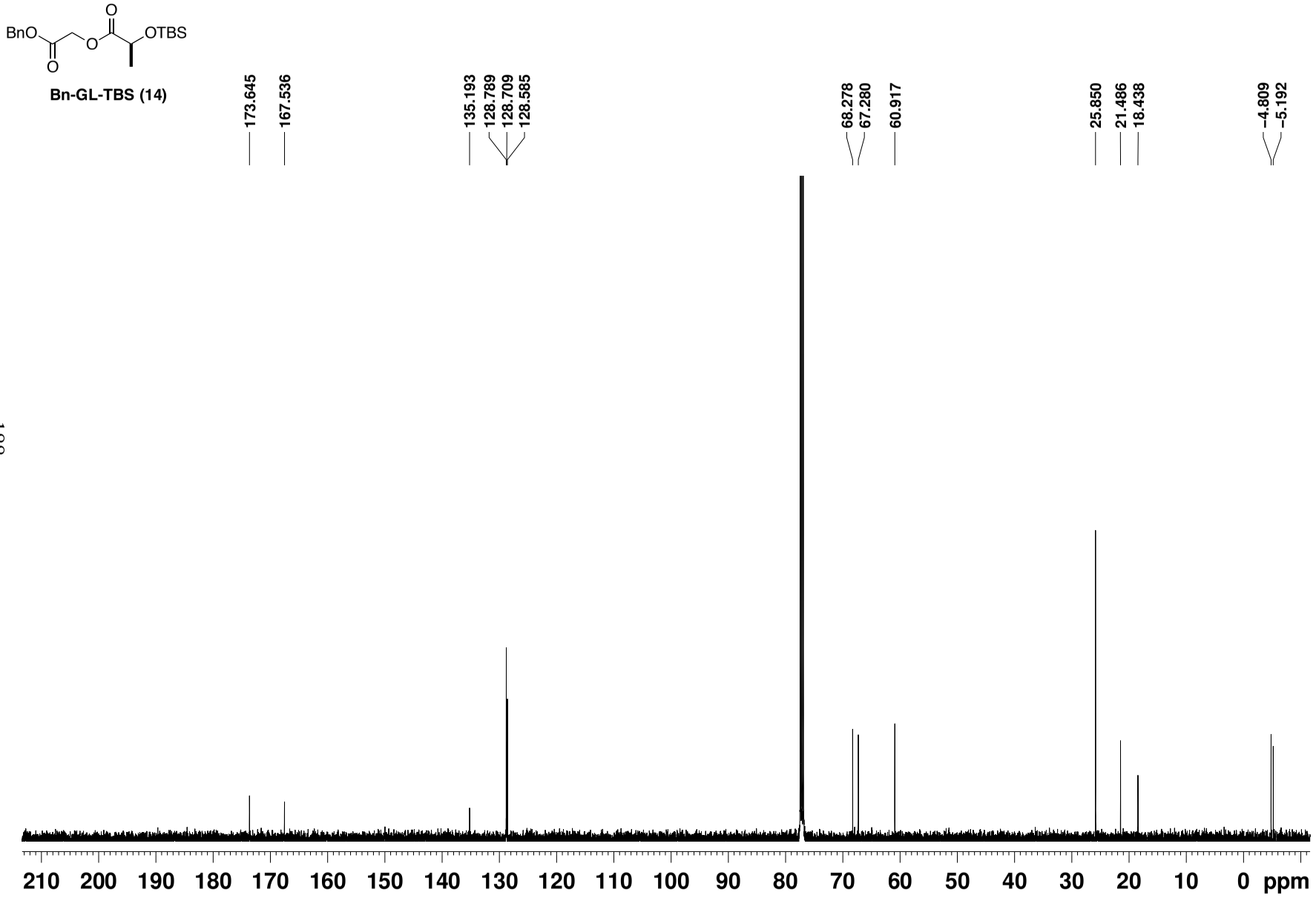
BnO
O
O
O
OTBS
Bn-GL-TBS (14)
173.645
167.536
135.193
128.789
128.709
128.585
68.278
67.280
60.917
25.850
21.486
18.438
-4.809
-5.192
210 200 190 180 170 160 150 140 130 120 110 100 90 80 70 60 50 40 30 20 10 0 ppm

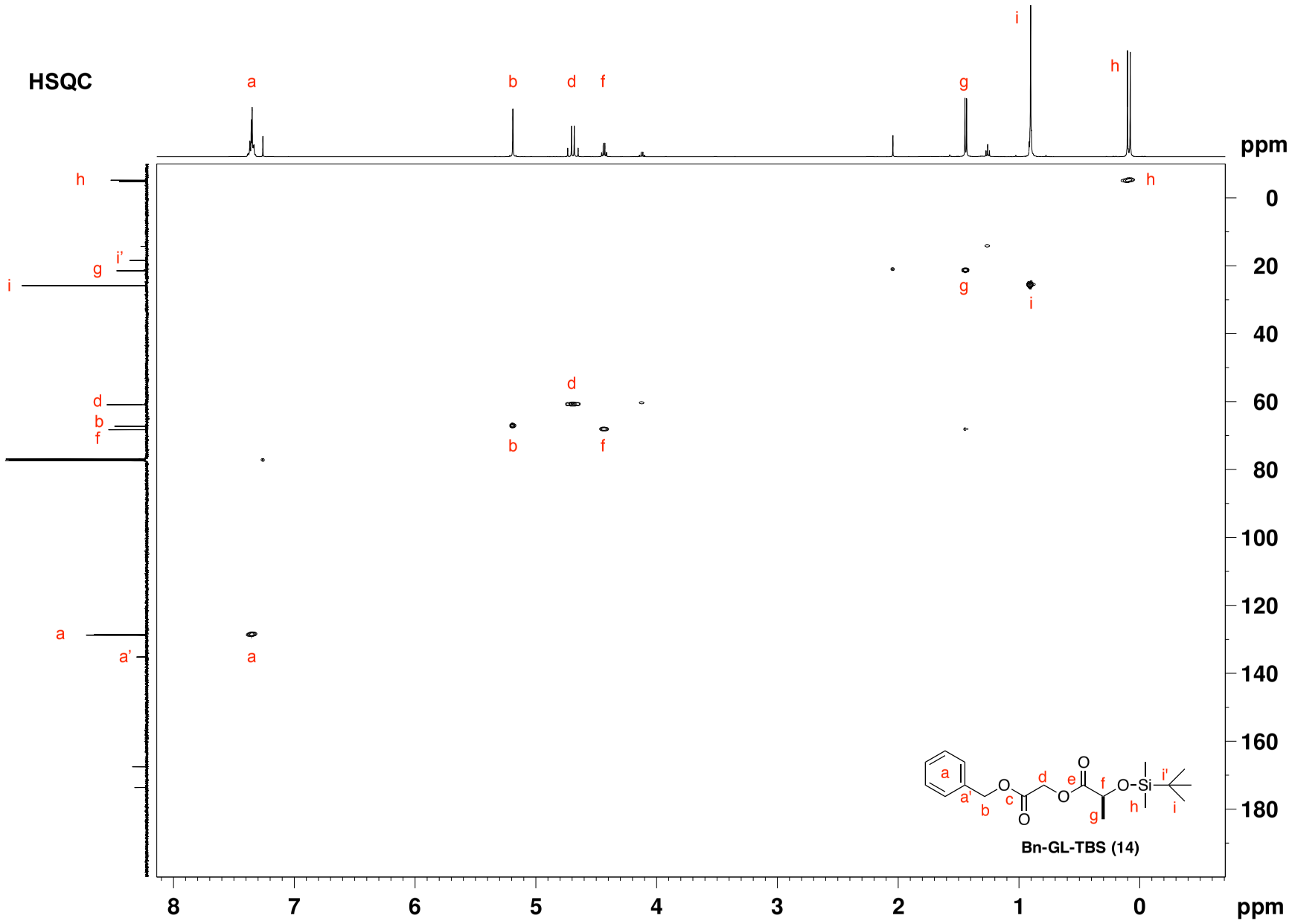
HSQC
a
b
d
f
g
i
h
ppm
0
20
40
60
80
100
120
140
160
180
8
7
6
5
4
3
2
1
0
ppm
i'
a'
Bn-GL-TBS (14)

Me-GL-TBDPS (16)
OTBDPS
O
O
O
O
O
7.729
7.725
7.710
7.706
7.695
7.692
7.686
7.682
7.676
7.672
7.666
7.662
7.459
7.456
7.441
7.434
7.423
7.419
7.402
7.398
7.384
7.366
7.349
7.345
4.592
4.553
4.458
4.418
4.401
4.384
4.367
3.730
1.431
1.414
1.098
1.073
x
ppm
1
2
3
4
5
6
7
8
9
10
3.69
9.35
3.14
3.00
0.94
1.14
1.04
8.72
5.77

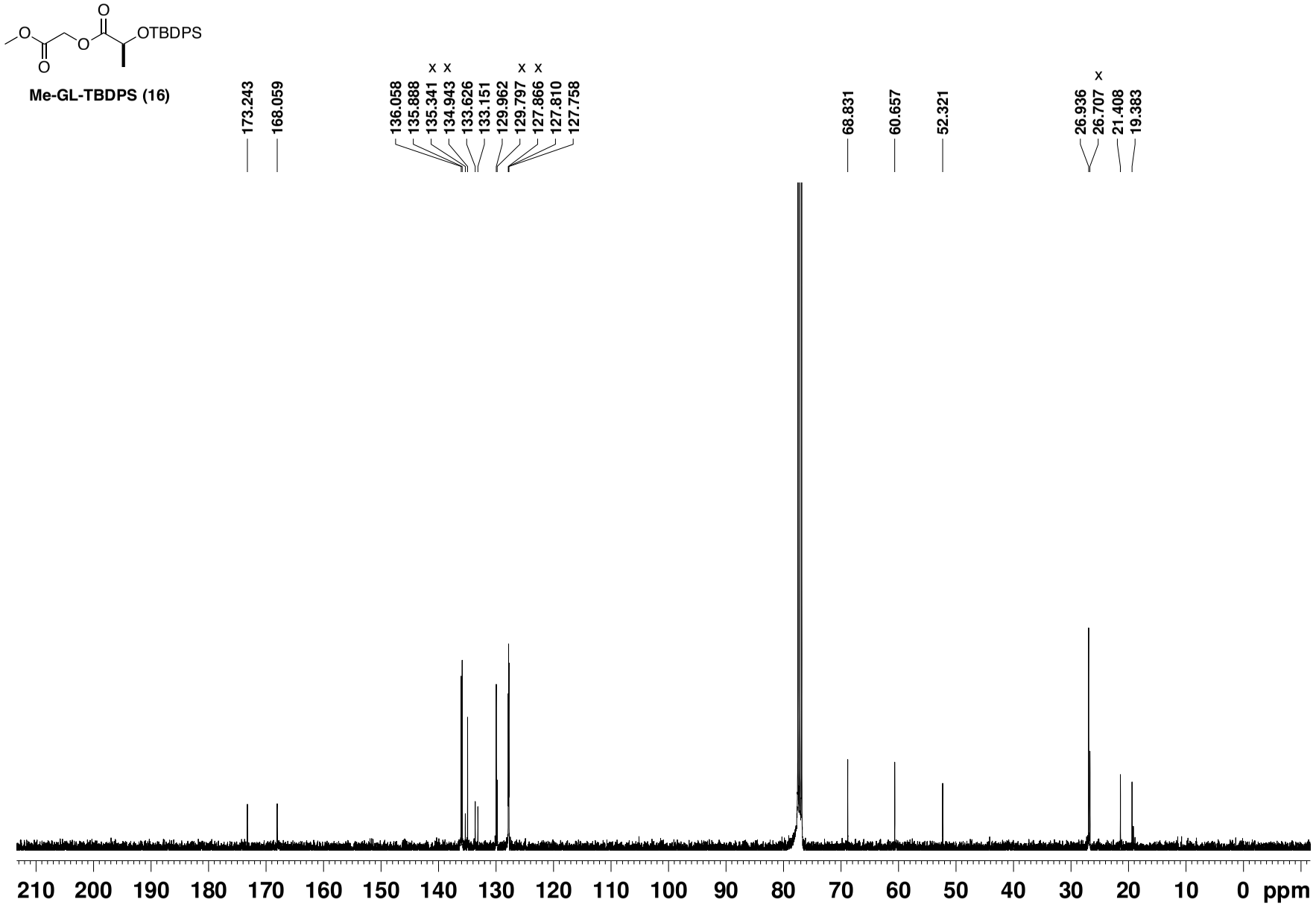
OTBDPS
Me-GL-TBDPS (16)
173.243
168.059
136.058
135.888
135.341
134.943
133.626
133.151
129.962
129.797
127.866
127.810
127.758
68.831
60.657
52.321
26.936
26.707
21.408
19.383
210 200 190 180 170 160 150 140 130 120 110 100 90 80 70 60 50 40 30 20 10 0 ppm

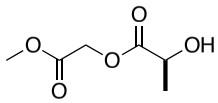

Me-GL (17)

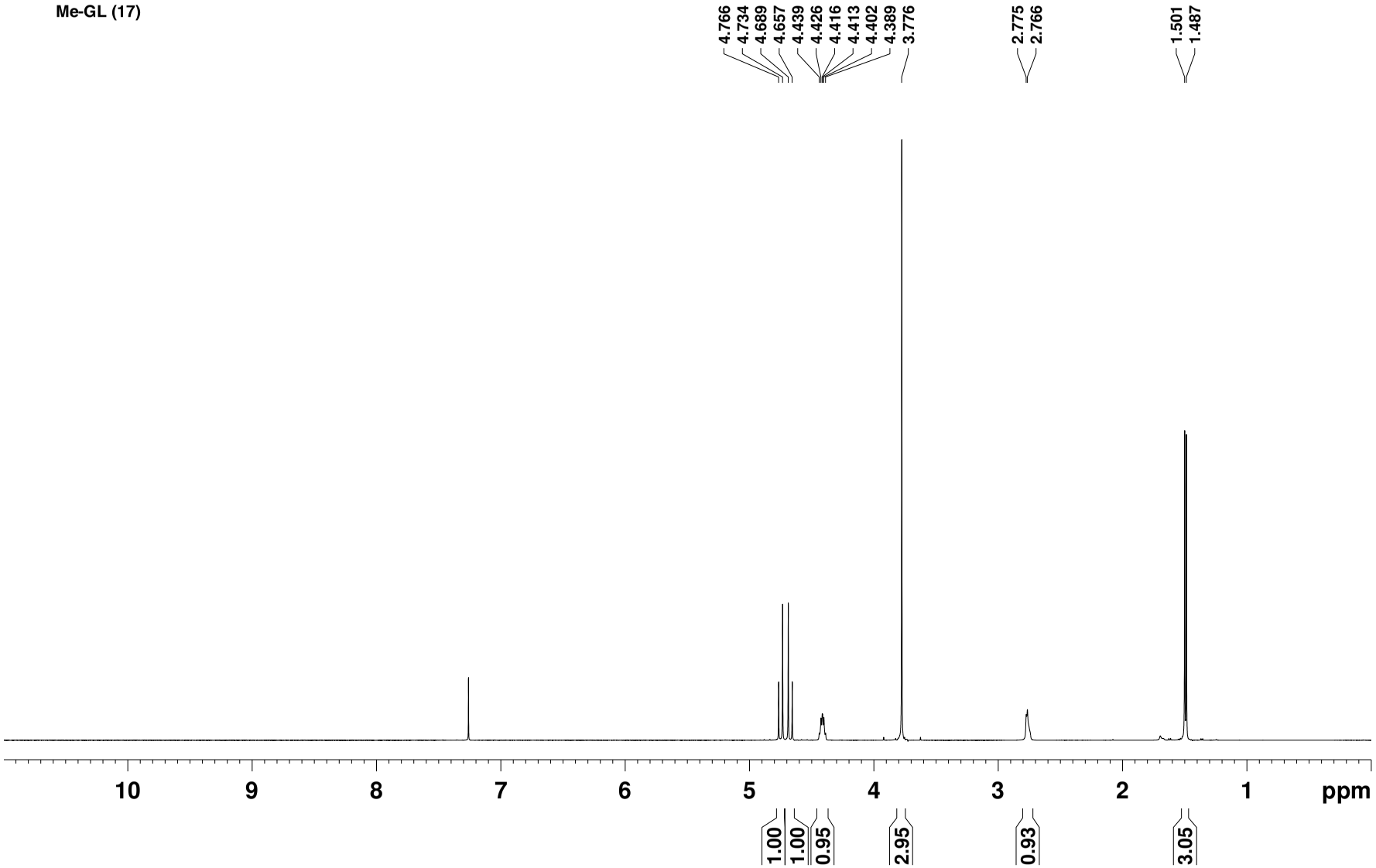
4.766
4.734
4.689
4.657
4.439
4.426
4.416
4.413
4.402
4.389
3.776
2.775
2.766
1.501
1.487
10
9
8
7
6
5
4
3
2
1
ppm
1.00
1.00
0.95
2.95
0.93
3.05

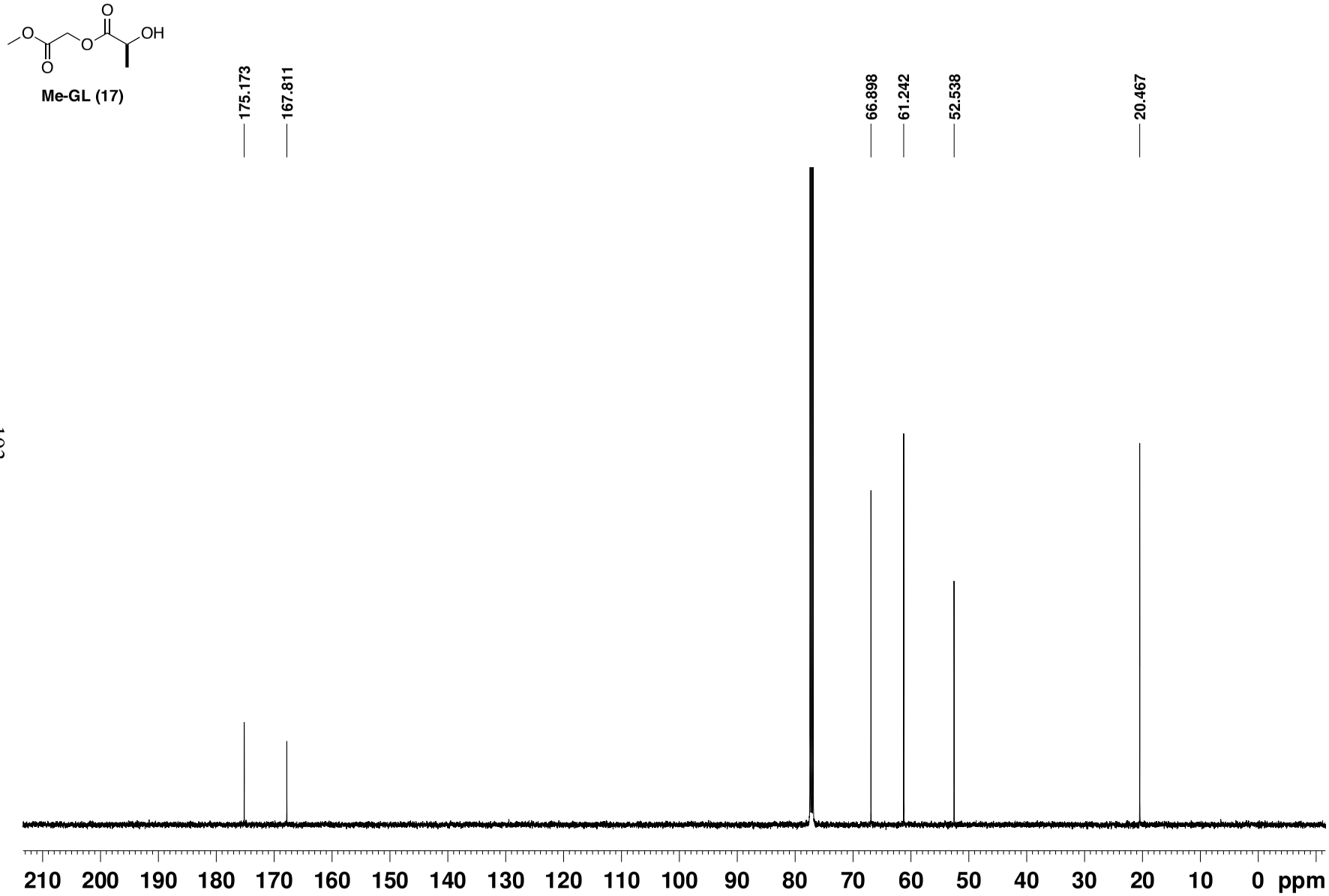
Me-GL (17)
175.173
167.811
66.898
61.242
52.538
20.467
210 200 190 180 170 160 150 140 130 120 110 100 90 80 70 60 50 40 30 20 10 0 ppm

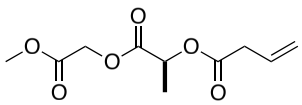

Me-GL-B (18)

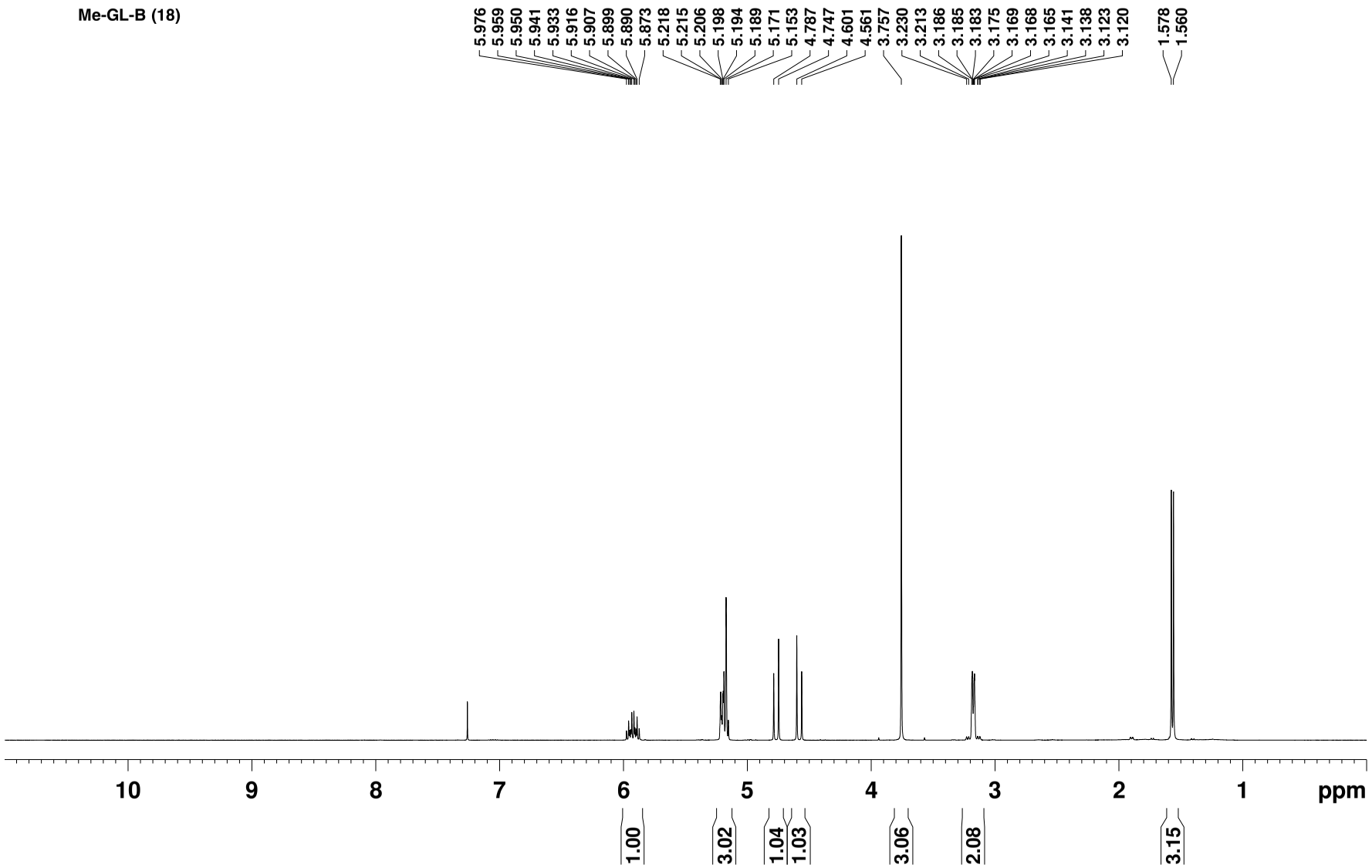
5.976
5.959
5.950
5.941
5.933
5.916
5.907
5.899
5.890
5.873
5.218
5.215
5.206
5.198
5.194
5.189
5.171
5.153
4.787
4.747
4.601
4.561
3.757
3.230
3.213
3.186
3.185
3.183
3.175
3.169
3.168
3.165
3.141
3.138
3.123
3.120
1.578
1.560
10
9
8
7
6
5
4
3
2
1
ppm
1.00
3.02
1.04
1.03
3.06
2.08
3.15

Me-GL-B (18)
170.972
170.277
167.736
129.736
119.064
68.602
61.025
52.442
38.705
16.924
ppm
200
180
160
140
120
100
80
60
40
20
0

BIBLIOGRAPHY

1. Rumbley, J.; Hoang, L.; Mayne, L.; Englander, S. W. An amino acid code for protein folding. *Proceedings of the National Academy of Sciences* **2001**, *98*, 105.
2. Guzzo, A. V. The Influence of Amino Acid Sequence on Protein Structure. *Biophys. J.*, *5*, 809.
3. Fowler, D. M.; Araya, C. L.; Fleishman, S. J.; Kellogg, E. H.; Stephany, J. J.; Baker, D.; Fields, S. High-resolution mapping of protein sequence-function relationships. *Nat Meth* **2010**, *7*, 741.
4. Lutz, J.-F.; Ouchi, M.; Liu, D. R.; Sawamoto, M. Sequence-Controlled Polymers. *Science* **2013**, *341*, 1238149.
5. Dechy-Cabaret, O.; Martin-Vaca, B.; Bourissou, D. Controlled Ring-Opening Polymerization of Lactide and Glycolide. *Chem. Rev.* **2004**, *104*, 6147.
6. Makadia, H. K.; Siegel, S. J. Poly Lactic-co-Glycolic Acid (PLGA) as Biodegradable Controlled Drug Delivery Carrier. *Polymers* **2011**, *3*, 1377.
7. Anderson, J. M.; Shive, M. S. Biodegradation and biocompatibility of PLA and PLGA microspheres. *Adv. Drug Delivery Rev.* **1997**, *28*, 5.
8. Danhier, F.; Ansorena, E.; Silva, J. M.; Coco, R.; Le Breton, A.; Préat, V. PLGA-based nanoparticles: An overview of biomedical applications. *J. Controlled Release* **2012**, *161*, 505.
9. Campolongo, M. J.; Luo, D. Drug delivery: Old polymer learns new tracts. *Nat. Mater.* **2009**, *8*, 447.
10. Jagur-Grodzinski, J. Polymers for tissue engineering, medical devices, and regenerative medicine. Concise general review of recent studies. *Polym. Adv. Technol.* **2006**, *17*, 395.
11. Jain, R. A. The manufacturing techniques of various drug loaded biodegradable poly(lactide-co-glycolide) (PLGA) devices. *Biomaterials* **2000**, *21*, 2475.
12. Malyala, P.; O'Hagan, D. T.; Singh, M. Enhancing the therapeutic efficacy of CpG oligonucleotides using biodegradable microparticles. *Adv. Drug Delivery Rev.* **2009**, *61*, 218.
13. Puranik, A. S.; Dawson, E. R.; Peppas, N. A. Recent advances in drug eluting stents. *Int. J. Pharm.* **2013**, *441*, 665.
14. Putnam, D. Drug delivery: The heart of the matter. *Nat. Mater.* **2008**, *7*, 836.
15. Li, J.; Rothstein, S. N.; Little, S. R.; Edenborn, H. M.; Meyer, T. Y. The Effect of Monomer Order on the Hydrolysis of Biodegradable Poly(lactic-co-glycolic acid) Repeating Sequence Copolymers. *J. Am. Chem. Soc.* **2012**, *134*, 16352.
16. Li, J.; Stayshich, R. M.; Meyer, T. Y. Exploiting Sequence To Control the Hydrolysis Behavior of Biodegradable PLGA Copolymers. *J. Am. Chem. Soc.* **2011**, *133*, 6910.

17. Stayshich, R. M.; Meyer, T. Y. New Insights into Poly(lactic-co-glycolic acid) Microstructure: Using Repeating Sequence Copolymers To Decipher Complex NMR and Thermal Behavior. *J. Am. Chem. Soc.* **2010**, *132*, 10920.
18. Weiss, R. M.; Jones, E. M.; Shafer, D. E.; Stayshich, R. M.; Meyer, T. Y. Synthesis of repeating sequence copolymers of lactic, glycolic, and caprolactic acids. *Journal of Polymer Science Part A: Polymer Chemistry* **2011**, *49*, 1847.
19. Weiss, R. M.; Meyer, T. Y. **2016**. *Unpublished work.*
20. Li, J.; Washington, M. A.; Bell, K. L.; Weiss, R. M.; Rothstein, S. N.; Little, S. R.; Edenborn, H. M.; Meyer, T. Y. In *Sequence-Controlled Polymers: Synthesis, Self-Assembly, and Properties*; American Chemical Society: 2014; Vol. 1170, p 271.
21. Washington, M.; Meyer, T. Y. **2016**. *Unpublished work.*
22. Weiss, R. M.; Short, A. L.; Meyer, T. Y. Sequence-Controlled Copolymers Prepared via Entropy-Driven Ring-Opening Metathesis Polymerization. *ACS Macro Letters* **2015**, *4*, 1039.
23. Szwarc, M. `Living' Polymers. *Nature* **1956**, *178*, 1168.
24. Matyjaszewski, K. Criteria for living systems with a special emphasis on living cationic polymerization of alkenes. *Journal of Polymer Science Part A: Polymer Chemistry* **1993**, *31*, 995.
25. Matyjaszewski, K. Ranking living systems. *Macromolecules* **1993**, *26*, 1787.
26. Matyjaszewski, K.; Müller, A. H. Naming of controlled, living and 'living'polymerizations. *Polym Prepr (Am Chem Soc Div Polym Chem)* **1997**, *38*, 6.
27. Jean-Louis Hérisson, P.; Chauvin, Y. Catalyse de transformation des oléfines par les complexes du tungstène. II. Télomérisation des oléfines cycliques en présence d'oléfines acycliques. *Die Makromolekulare Chemie* **1971**, *141*, 161.
28. Casey, C. P.; Burkhardt, T. J. Reactions of (diphenylcarbene)pentacarbonyltungsten(0) with alkenes. Role of metal-carbene complexes in cyclopropanation and olefin metathesis reactions. *J. Am. Chem. Soc.* **1974**, *96*, 7808.
29. Katz, T. J.; McGinnis, J. Mechanism of the olefin metathesis reaction. *J. Am. Chem. Soc.* **1975**, *97*, 1592.
30. Grubbs, R. H.; Burk, P. L.; Carr, D. D. Mechanism of the olefin metathesis reaction. *J. Am. Chem. Soc.* **1975**, *97*, 3265.
31. Grubbs, R. H.; Carr, D. D.; Hoppin, C.; Burk, P. L. Consideration of the mechanism of the metal catalyzed olefin metathesis reaction. *J. Am. Chem. Soc.* **1976**, *98*, 3478.
32. Matyjaszewski, K.; Müller, A. H. E. *Controlled and Living Polymerizations: From Mechanisms to Applications*; John Wiley & Sons, 2009.
33. Sutthasupa, S.; Shiotsuki, M.; Sanda, F. Recent advances in ring-opening metathesis polymerization, and application to synthesis of functional materials. *Polym J* **2010**, *42*, 905.
34. Ofstead, E. A.; Calderon, N. Equilibrium ring-opening polymerization of mono- and multicyclic unsaturated monomers. *Die Makromolekulare Chemie* **1972**, *154*, 21.
35. Ast, W.; Rheinwald, G.; Kerber, R. Ungesättigte Polyester und Polyester-Kautschuk-Copolymerisate durch Olefin-Metathese. *Die Makromolekulare Chemie* **1976**, *177*, 1341.
36. Höcker, H.; Reimann, W.; Reif, L.; Riebel, K. Kinetics and thermodynamic aspects of the metathesis reaction of cycloolefins considering particularly the molecular weight distribution of the products. *J. Mol. Catal.* **1980**, *8*, 191.

37. Reif, L.; Hoecker, H. Kinetics and thermodynamics of the metathesis reaction of cycloolefins. 2. Molecular weight distribution. *Macromolecules* **1984**, *17*, 952.
38. Wagener, K. B.; Marmo, J. C. Acyclic diene metathesis (ADMET) depolymerization: The synthesis of 1,4-polybutadiene telechelics. *Macromol. Rapid Commun.* **1995**, *16*, 557.
39. Hillmyer, M. A.; Nguyen, S. T.; Grubbs, R. H. Utility of a Ruthenium Metathesis Catalyst for the Preparation of End-Functionalized Polybutadiene. *Macromolecules* **1997**, *30*, 718.
40. Marsella, M. J.; Maynard, H. D.; Grubbs, R. H. Template-Directed Ring-Closing Metathesis: Synthesis and Polymerization of Unsaturated Crown Ether Analogs. *Angewandte Chemie International Edition in English* **1997**, *36*, 1101.
41. Thorn-Csányi, E.; Ruhland, K. Quantitative description of the metathesis polymerization/depolymerization equilibrium in the 1,4-polybutadiene system, 1. Influence of feed concentration and temperature. *Macromol. Chem. Phys.* **1999**, *200*, 1662.
42. Thorn-Csányi, E.; Ruhland, K. Quantitative description of the metathesis polymerization/depolymerization equilibrium in the 1,4-polybutadiene system, 2. Unusual behaviour at lower temperature. *Macromol. Chem. Phys.* **1999**, *200*, 2245.
43. Thorn-Csányi, E.; Ruhland, K. Quantitative description of the metathesis polymerization/depolymerization equilibrium in the 1,4-polybutadiene system, 3. Influence of the solvent. *Macromol. Chem. Phys.* **1999**, *200*, 2606.
44. Xue, Z.; Mayer, M. F. Entropy-driven ring-opening olefin metathesis polymerizations of macrocycles. *Soft Matter* **2009**, *5*, 4600.
45. Walker, R.; Conrad, R. M.; Grubbs, R. H. The Living ROMP of trans-Cyclooctene. *Macromolecules* **2009**, *42*, 599.
46. Choi, T.-L.; Grubbs, R. H. Controlled Living Ring-Opening-Metathesis Polymerization by a Fast-Initiating Ruthenium Catalyst. *Angewandte Chemie International Edition* **2003**, *42*, 1743.
47. Klavetter, F. L.; Grubbs, R. H. Polycyclooctatetraene (polyacetylene): synthesis and properties. *J. Am. Chem. Soc.* **1988**, *110*, 7807.
48. Bielawski, C. W.; Grubbs, R. H. Increasing the Initiation Efficiency of Ruthenium-Based Ring-Opening Metathesis Initiators: Effect of Excess Phosphine. *Macromolecules* **2001**, *34*, 8838.
49. Carnes, M.; Buccella, D.; Decatur, J.; Steigerwald, M. L.; Nuckolls, C. Helical (5Z, 11E)-Dibenzo[a,e]cyclooctatetrene: A Spring-Loaded Monomer. *Angewandte Chemie International Edition* **2008**, *47*, 2982.
50. Jacobson, H.; Stockmayer, W. H. Intramolecular Reaction in Polycondensations. I. The Theory of Linear Systems. *J. Chem. Phys.* **1950**, *18*, 1600.
51. Chen, Z.-R.; Claverie, J. P.; Grubbs, R. H.; Kornfield, J. A. Modeling Ring-Chain Equilibria in Ring-Opening Polymerization of Cycloolefins. *Macromolecules* **1995**, *28*, 2147.
52. Suter, U. W.; Höcker, H. Macrocyclization equilibria in polycycloolefins. *Die Makromolekulare Chemie* **1988**, *189*, 1603.
53. Spanagel, E. W.; Carothers, W. H. Macrocyclic Esters. *J. Am. Chem. Soc.* **1935**, *57*, 929.
54. Spanagel, E. W.; Carothers, W. H. Preparation of Macrocyclic Lactones by Depolymerization. *J. Am. Chem. Soc.* **1936**, *58*, 654.
55. Kamau, S. D.; Hodge, P.; Hall, A. J.; Dad, S.; Ben-Haida, A. Cyclo-depolymerization of olefin-containing polymers to give macrocyclic oligomers by metathesis and the

entropically-driven ROMP of the olefin-containing macrocyclic esters. *Polymer* **2007**, *48*, 6808.
56. Hodge, P. Cyclodepolymerization as a method for the synthesis of macrocyclic oligomers. *Reactive and Functional Polymers* **2014**, *80*, 21.
57. Hodge, P. Entropically Driven Ring-Opening Polymerization of Strainless Organic Macrocycles. *Chem. Rev.* **2014**, *114*, 2278.
58. Hodge, P. Recycling of condensation polymers via ring–chain equilibria. *Polym. Adv. Technol.* **2015**, *26*, 797.
59. Monfette, S.; Fogg, D. E. Equilibrium Ring-Closing Metathesis. *Chem. Rev.* **2009**, *109*, 3783.
60. Tastard, C. Y.; Hodge, P.; Ben-Haida, A.; Dobinson, M. Entropically driven ring-opening metathesis polymerization (ED-ROMP) of macrocyclic olefin-containing oligoamides. *Reactive and Functional Polymers* **2006**, *66*, 93.
61. Hill, J. W.; Carothers, W. H. Studies of Polymerization and Ring Formation. XX. Many-Membered Cyclic Esters. *J. Am. Chem. Soc.* **1933**, *55*, 5031.
62. Feng, J.; Wang, H.-f.; Zhang, X.-z.; Zhuo, R.-x. Investigation on lipase-catalyzed solution polymerization of cyclic carbonate. *Eur. Polym. J.* **2009**, *45*, 523.
63. Colquhoun, H. M.; Lewis, D. F.; Hodge, P.; Ben-Haida, A.; Williams, D. J.; Baxter, I. Ring−Chain Interconversion in High-Performance Polymer Systems. 1. [Poly(oxy-4,4‘-biphenyleneoxy-1,4-phenylenesulfonyl-1,4-phenylene)] (Radel-R). *Macromolecules* **2002**, *35*, 6875.
64. Baxter, I.; J. Williams, D.; Ben-Haida, A.; Hodge, P.; H. Kohnke, F.; M. Colquhoun, H. Cyclodepolymerisation of bisphenol A polysulfone: evidence for self-complementarity in macrocyclic poly(ether sulfones). *Chem. Commun.* **1998**, 2213.
65. L. Ruddick, C.; Hodge, P.; Zhuo, Y.; L. Beddoes, R.; Helliwell, M. Cyclo-depolymerisation of polyundecanoate and related polyesters: characterisation of cyclic oligoundecanoates and related cyclic oligoesters. *J. Mater. Chem.* **1999**, *9*, 2399.
66. Naujokas, A. A.; Ryan, K. M.; Google Patents: 1991.
67. Kamau, S. D.; Hodge, P.; Helliwell, M. Cyclo-depolymerization of poly(propylene terephthalate): some ring-opening polymerizations of the cyclic oligomers produced. *Polym. Adv. Technol.* **2003**, *14*, 492.
68. Atallah, P.; Wagener, K. B.; Schulz, M. D. ADMET: The Future Revealed. *Macromolecules* **2013**, *46*, 4735.
69. Bielawski, C. W.; Grubbs, R. H. Living ring-opening metathesis polymerization. *Progress in Polymer Science* **2007**, *32*, 1.
70. Schrock, R. R.; Hoveyda, A. H. Molybdenum and Tungsten Imido Alkylidene Complexes as Efficient Olefin-Metathesis Catalysts. *Angewandte Chemie International Edition* **2003**, *42*, 4592.
71. Maynard, H. D.; Grubbs, R. H. Synthesis of Functionalized Polyethers by Ring-Opening Metathesis Polymerization of Unsaturated Crown Ethers. *Macromolecules* **1999**, *32*, 6917.
72. Gautrot, J. E.; Zhu, X. X. Main-Chain Bile Acid Based Degradable Elastomers Synthesized by Entropy-Driven Ring-Opening Metathesis Polymerization. *Angewandte Chemie* **2006**, *118*, 7026.

73. Kamau, S. D.; Hodge, P.; Williams, R. T.; Stagnaro, P.; Conzatti, L. High Throughput Synthesis of Polyesters Using Entropically Driven Ring-Opening Polymerizations. *J. Comb. Chem.* **2008**, *10*, 644.
74. Schleyer, P. v. R.; Williams, J. E.; Blanchard, K. R. Evaluation of strain in hydrocarbons. The strain in adamantane and its origin. *J. Am. Chem. Soc.* **1970**, *92*, 2377.
75. Höcker, H.; Reimann, W.; Reif, L.; Riebel, K. Kinetics and thermodynamic aspects of the metathesis reaction of cycloolefins considering particularly the molecular weight distribution of the products. *J. Mol. Catal.* **1980**, *8*, 191.
76. Ulman, M.; Grubbs, R. H. Relative Reaction Rates of Olefin Substrates with Ruthenium(II) Carbene Metathesis Initiators1. *Organometallics* **1998**, *17*, 2484.
77. Thomas, C. M. Stereocontrolled ring-opening polymerization of cyclic esters: synthesis of new polyester microstructures. *Chem. Soc. Rev.* **2010**, *39*, 165.
78. Keitz, B. K.; Endo, K.; Herbert, M. B.; Grubbs, R. H. Z-Selective Homodimerization of Terminal Olefins with a Ruthenium Metathesis Catalyst. *J. Am. Chem. Soc.* **2011**, *133*, 9686.
79. Marinescu, S. C.; Schrock, R. R.; Müller, P.; Takase, M. K.; Hoveyda, A. H. Room-Temperature Z-Selective Homocoupling of α-Olefins by Tungsten Catalysts. *Organometallics* **2011**, *30*, 1780.
80. Vougioukalakis, G. C.; Grubbs, R. H. Ruthenium-Based Heterocyclic Carbene-Coordinated Olefin Metathesis Catalysts†. *Chem. Rev.* **2009**, *110*, 1746.
81. Eigenmann, H. K.; Golden, D. M.; Benson, S. W. Revised group additivity parameters for the enthalpies of formation of oxygen-containing organic compounds. *The Journal of Physical Chemistry* **1973**, *77*, 1687.
82. Benson, S. W.; Buss, J. H. Additivity Rules for the Estimation of Molecular Properties. Thermodynamic Properties. *J. Chem. Phys.* **1958**, *29*, 546.
83. Kim, K. O.; Shin, S.; Kim, J.; Choi, T.-L. Living Polymerization of Monomers Containing endo-Tricyclo[4.2.2.02,5]deca-3,9-diene Using Second Generation Grubbs and Hoveyda–Grubbs Catalysts: Approach to Synthesis of Well-Defined Star Polymers. *Macromolecules* **2014**, *47*, 1351.
84. Grubbs, R. H.; Wenzel, A. G.; O'Leary, D. J.; Khosravi, E. *Handbook of Metathesis, 3 Volume Set*; Wiley, 2015.
85. Love, J. A.; Morgan, J. P.; Trnka, T. M.; Grubbs, R. H. A Practical and Highly Active Ruthenium-Based Catalyst that Effects the Cross Metathesis of Acrylonitrile. *Angewandte Chemie International Edition* **2002**, *41*, 4035.
86. Sanford, M. S.; Ulman, M.; Grubbs, R. H. New Insights into the Mechanism of Ruthenium-Catalyzed Olefin Metathesis Reactions. *J. Am. Chem. Soc.* **2001**, *123*, 749.
87. Sanford, M. S.; Love, J. A.; Grubbs, R. H. Mechanism and Activity of Ruthenium Olefin Metathesis Catalysts. *J. Am. Chem. Soc.* **2001**, *123*, 6543.
88. Peng, Y.; Decatur, J.; Meier, M. A. R.; Gross, R. A. Ring-Opening Metathesis Polymerization of a Naturally Derived Macrocyclic Glycolipid. *Macromolecules* **2013**, *46*, 3293.
89. Knall, A.-C.; Slugovc, C. In *Olefin Metathesis*; John Wiley & Sons, Inc.: 2014, p 269.
90. van Lierop, B. J.; Lummiss, J. A. M.; Fogg, D. E. In *Olefin Metathesis*; John Wiley & Sons, Inc.: 2014, p 85.
91. Monfette, S.; Fogg, D. E. Equilibrium Ring-Closing Metathesis. *Chem. Rev.* **2009**, *109*, 3783.

92. Keitz, B. K.; Endo, K.; Patel, P. R.; Herbert, M. B.; Grubbs, R. H. Improved Ruthenium Catalysts for Z-Selective Olefin Metathesis. *J. Am. Chem. Soc.* **2011**, *134*, 693.
93. Keitz, B. K.; Fedorov, A.; Grubbs, R. H. Cis-Selective Ring-Opening Metathesis Polymerization with Ruthenium Catalysts. *J. Am. Chem. Soc.* **2012**, *134*, 2040.
94. Mangold, S. L.; O'Leary, D. J.; Grubbs, R. H. Z-Selective Olefin Metathesis on Peptides: Investigation of Side-Chain Influence, Preorganization, and Guidelines in Substrate Selection. *J. Am. Chem. Soc.* **2014**, *136*, 12469.
95. Herbert, M. B.; Marx, V. M.; Pederson, R. L.; Grubbs, R. H. Concise Syntheses of Insect Pheromones Using Z-Selective Cross Metathesis. *Angewandte Chemie International Edition* **2013**, *52*, 310.
96. Marx, V. M.; Herbert, M. B.; Keitz, B. K.; Grubbs, R. H. Stereoselective Access to Z and E Macrocycles by Ruthenium-Catalyzed Z-Selective Ring-Closing Metathesis and Ethenolysis. *J. Am. Chem. Soc.* **2013**, *135*, 94.
97. Liu, P.; Xu, X.; Dong, X.; Keitz, B. K.; Herbert, M. B.; Grubbs, R. H.; Houk, K. N. Z-Selectivity in Olefin Metathesis with Chelated Ru Catalysts: Computational Studies of Mechanism and Selectivity. *J. Am. Chem. Soc.* **2012**, *134*, 1464.
98. Dang, Y.; Wang, Z.-X.; Wang, X. Does the Ruthenium Nitrato Catalyst Work Differently in Z-Selective Olefin Metathesis? A DFT Study. *Organometallics* **2012**, *31*, 8654.
99. Marx, V. M.; Rosebrugh, L. E.; Herbert, M. B.; Grubbs, R. H.; Springer Berlin Heidelberg: 2014, p 1.
100. Koh, M. J.; Khan, R. K. M.; Torker, S.; Hoveyda, A. H. Broadly Applicable Z- and Diastereoselective Ring-Opening/Cross-Metathesis Catalyzed by a Dithiolate Ru Complex. *Angewandte Chemie International Edition* **2014**, *53*, 1968.
101. Khan, R. K. M.; Torker, S.; Hoveyda, A. H. Reactivity and Selectivity Differences between Catecholate and Catechothiolate Ru Complexes. Implications Regarding Design of Stereoselective Olefin Metathesis Catalysts. *J. Am. Chem. Soc.* **2014**, *136*, 14337.
102. Khan, R. K. M.; Torker, S.; Hoveyda, A. H. Readily Accessible and Easily Modifiable Ru-Based Catalysts for Efficient and Z-Selective Ring-Opening Metathesis Polymerization and Ring-Opening/Cross-Metathesis. *J. Am. Chem. Soc.* **2013**, *135*, 10258.
103. Occhipinti, G.; Hansen, F. R.; Törnroos, K. W.; Jensen, V. R. Simple and Highly Z-Selective Ruthenium-Based Olefin Metathesis Catalyst. *J. Am. Chem. Soc.* **2013**, *135*, 3331.
104. Occhipinti, G.; Koudriavtsev, V.; Tornroos, K. W.; Jensen, V. R. Theory-assisted development of a robust and Z-selective olefin metathesis catalyst. *Dalton Transactions* **2014**, *43*, 11106.
105. Ortmann, P.; Mecking, S. Long-Spaced Aliphatic Polyesters. *Macromolecules* **2013**, *46*, 7213.
106. Pepels, M. P. F.; Hansen, M. R.; Goossens, H.; Duchateau, R. From Polyethylene to Polyester: Influence of Ester Groups on the Physical Properties. *Macromolecules* **2013**, *46*, 7668.
107. Stempfle, F.; Ortmann, P.; Mecking, S. Long-Chain Aliphatic Polymers To Bridge the Gap between Semicrystalline Polyolefins and Traditional Polycondensates. *Chem. Rev.* **2016**, *116*, 4597.
108. Korshak, W. V.; Vinogradova, S. V. Macromolecular compounds. *Bulletin of the Academy of Sciences of the USSR, Division of chemical science*, *2*, 995.

109. Smith, G. D.; Ciszak, E.; Pangborn, W. A novel complex of a phenolic derivative with insulin: Structural features related to the T → R transition. *Protein Sci.* **1996**, *5*, 1502.
110. Trott, O.; Olson, A. J. AutoDock Vina: Improving the speed and accuracy of docking with a new scoring function, efficient optimization, and multithreading. *J. Comput. Chem.* **2010**, *31*, 455.
111. Morris, G. M.; Huey, R.; Lindstrom, W.; Sanner, M. F.; Belew, R. K.; Goodsell, D. S.; Olson, A. J. AutoDock4 and AutoDockTools4: Automated docking with selective receptor flexibility. *J. Comput. Chem.* **2009**, *30*, 2785.
112. Sanner, M. F. Python: a programming language for software integration and development. *J Mol Graph Model* **1999**, *17*, 57.
113. Seeliger, D.; de Groot, B. Ligand docking and binding site analysis with PyMOL and Autodock/Vina. *J. Comput.-Aided Mol. Des.* **2010**, *24*, 417.
114. Nowalk, J. A.; Meyer, T. Y. **2016**. *Unpublished work.*
115. Kobayashi, S.; Pitet, L. M.; Hillmyer, M. A. Regio- and Stereoselective Ring-Opening Metathesis Polymerization of 3-Substituted Cyclooctenes. *J. Am. Chem. Soc.* **2011**, *133*, 5794.
116. Zhang, J.; Matta, M. E.; Hillmyer, M. A. Synthesis of Sequence-Specific Vinyl Copolymers by Regioselective ROMP of Multiply Substituted Cyclooctenes. *ACS Macro Letters* **2012**, *1*, 1383.
117. Gutekunst, W. R.; Hawker, C. J. A General Approach to Sequence-Controlled Polymers Using Macrocyclic Ring Opening Metathesis Polymerization. *J. Am. Chem. Soc.* **2015**, *137*, 8038.
118. Akutsu, F.; Inoki, M.; Uei, H.; Sueyoshi, M.; Kasashima, Y.; Naruchi, K.; Yamaguchi, Y.; Sunahara, M. Synthesis of Poly(lactic acid) by Direct Polycondensation of Lactic Acid Using 1,1[prime]-Carbonyldiimidazole, N,N,N[prime],N[prime]-Tetramethylchloroformamidinium Chloride, and N,N[prime]-Dicyclohexylcarbodiimide as Condensing Agents. *Polym J* **1998**, *30*, 421.
119. Moore, J. S.; Stupp, S. I. Room temperature polyesterification. *Macromolecules* **1990**, *23*, 65.
120. Scheidt, K. A.; Chen, H.; Follows, B. C.; Chemler, S. R.; Coffey, D. S.; Roush, W. R. Tris(dimethylamino)sulfonium Difluorotrimethylsilicate, a Mild Reagent for the Removal of Silicon Protecting Groups. *The Journal of Organic Chemistry* **1998**, *63*, 6436.
121. Chatterjee, A. K.; Choi, T.-L.; Sanders, D. P.; Grubbs, R. H. A General Model for Selectivity in Olefin Cross Metathesis. *J. Am. Chem. Soc.* **2003**, *125*, 11360.
122. Chatterjee, A. K.; Morgan, J. P.; Scholl, M.; Grubbs, R. H. Synthesis of Functionalized Olefins by Cross and Ring-Closing Metatheses. *J. Am. Chem. Soc.* **2000**, *122*, 3783.
123. Ghosh, A. K.; Cappiello, J.; Shin, D. Ring-closing metathesis strategy to unsaturated γ- and δ-lactones: Synthesis of hydroxyethylene isostere for protease inhibitors. *Tetrahedron Letters* **1998**, *39*, 4651.
124. Cannon, J. S.; Grubbs, R. H. Alkene Chemoselectivity in Ruthenium-Catalyzed Z-Selective Olefin Metathesis. *Angewandte Chemie International Edition* **2013**, *52*, 9001.
125. Rosebrugh, L. E.; Herbert, M. B.; Marx, V. M.; Keitz, B. K.; Grubbs, R. H. Highly Active Ruthenium Metathesis Catalysts Exhibiting Unprecedented Activity and Z-Selectivity. *J. Am. Chem. Soc.* **2013**, *135*, 1276.

126. Miyazaki, H.; Herbert, M. B.; Liu, P.; Dong, X.; Xu, X.; Keitz, B. K.; Ung, T.; Mkrtumyan, G.; Houk, K. N.; Grubbs, R. H. Z-Selective Ethenolysis with a Ruthenium Metathesis Catalyst: Experiment and Theory. *J. Am. Chem. Soc.* **2013**, *135*, 5848.
127. Hartung, J.; Dornan, P. K.; Grubbs, R. H. Enantioselective Olefin Metathesis with Cyclometalated Ruthenium Complexes. *J. Am. Chem. Soc.* **2014**, *136*, 13029.
128. Smulik, J. A.; Diver, S. T. Terminal Alkyne−Ethylene Cross-Metathesis: Reaction of 1-Substituted Propargyl Esters at Elevated Ethylene Pressure. *The Journal of Organic Chemistry* **2000**, *65*, 1788.
129. Lysenko, Z.; Maughon, B. R.; Mokhtar-Zadeh, T.; Tulchinsky, M. L. Stability of the first-generation Grubbs metathesis catalyst in a continuous flow reactor. *J. Organomet. Chem.* **2006**, *691*, 5197.
130. van der Eide, E. F.; Romero, P. E.; Piers, W. E. Generation and Spectroscopic Characterization of Ruthenacyclobutane and Ruthenium Olefin Carbene Intermediates Relevant to Ring Closing Metathesis Catalysis. *J. Am. Chem. Soc.* **2008**, *130*, 4485.
131. *Guideline on the specification limits for residues of metal catalysts or metal reagents*, Committee for Medicinal Products for Human Use, 2008. http://www.ema.europa.eu/docs/en_GB/document_library/Scientific_guideline/2009/09/WC500003587.pdf.
132. *Q3D Elemental Impurities: Guidance for Industry*, U.S. Department of Health and Human Services, Food and Drug Administration, 2015. http://www.fda.gov/downloads/drugs/guidancecomplianceregulatoryinformation/guidances/ucm371025.pdf.
133. Borré, E.; Rouen, M.; Laurent, I.; Magrez, M.; Caijo, F.; Crévisy, C.; Solodenko, W.; Toupet, L.; Frankfurter, R.; Vogt, C.; Kirschning, A.; Mauduit, M. A Fast-Initiating Ionically Tagged Ruthenium Complex: A Robust Supported Pre-catalyst for Batch-Process and Continuous-Flow Olefin Metathesis. *Chemistry – A European Journal* **2012**, *18*, 16369.
134. Holland, M. G.; Griffith, V. E.; France, M. B.; Desjardins, S. G. Kinetics of the ring-opening metathesis polymerization of a 7-oxanorbornene derivative by Grubbs' catalyst. *Journal of Polymer Science Part A: Polymer Chemistry* **2003**, *41*, 2125.
135. Alonso-Villanueva, J.; Rodriguez, M.; Vilas, J. L.; Laza, J. M.; LeÓN, L. M. Ring-Opening Metathesis Polymerization Kinetics of Cyclooctene with Second Generation Grubbs' Catalyst. *Journal of Macromolecular Science: Pure & Applied Chemistry* **2010**, *47*, 1130.
136. Lambeth, R. H.; Moore, J. S. Light-Induced Shape Changes in Azobenzene Functionalized Polymers Prepared by Ring-Opening Metathesis Polymerization. *Macromolecules* **2007**, *40*, 1838.
137. Lebarbé, T.; More, A. S.; Sane, P. S.; Grau, E.; Alfos, C.; Cramail, H. Bio-Based Aliphatic Polyurethanes Through ADMET Polymerization in Bulk and Green Solvent. *Macromol. Rapid Commun.* **2014**, *35*, 479.
138. Fokou, P. A.; Meier, M. A. R. Studying and Suppressing Olefin Isomerization Side Reactions During ADMET Polymerizations. *Macromol. Rapid Commun.* **2010**, *31*, 368.
139. Hong, S. H.; Sanders, D. P.; Lee, C. W.; Grubbs, R. H. Prevention of Undesirable Isomerization during Olefin Metathesis. *J. Am. Chem. Soc.* **2005**, *127*, 17160.
140. Courchay, F. C.; Sworen, J. C.; Wagener, K. B. Metathesis Activity and Stability of New Generation Ruthenium Polymerization Catalysts. *Macromolecules* **2003**, *36*, 8231.

141. Schulz, M. D.; Wagener, K. B. Solvent Effects in Alternating ADMET Polymerization. *ACS Macro Letters* **2012**, *1*, 449.
142. Hodge, P.; Kamau, S. D. Entropically Driven Ring-Opening-Metathesis Polymerization of Macrocyclic Olefins with 21–84 Ring Atoms. *Angewandte Chemie International Edition* **2003**, *42*, 2412.
143. Thomas, R. M.; Keitz, B. K.; Champagne, T. M.; Grubbs, R. H. Highly Selective Ruthenium Metathesis Catalysts for Ethenolysis. *J. Am. Chem. Soc.* **2011**, *133*, 7490.
144. Lutz, J.-F. Sequence-controlled polymerizations: the next Holy Grail in polymer science? *Polymer Chemistry* **2010**, *1*, 55.
145. Bielawski, C. W.; Benitez, D.; Morita, T.; Grubbs, R. H. Synthesis of End-Functionalized Poly(norbornene)s via Ring-Opening Metathesis Polymerization. *Macromolecules* **2001**, *34*, 8610.
146. Liao, L.; Liu, J.; Dreaden, E. C.; Morton, S. W.; Shopsowitz, K. E.; Hammond, P. T.; Johnson, J. A. A Convergent Synthetic Platform for Single-Nanoparticle Combination Cancer Therapy: Ratiometric Loading and Controlled Release of Cisplatin, Doxorubicin, and Camptothecin. *Journal of the American Chemical Society* **2014**, *136*, 5896.
147. Leitgeb, A.; Wappel, J.; Slugovc, C. The ROMP toolbox upgraded. *Polymer* **2010**, *51*, 2927.
148. Madkour, A. E.; Koch, A. H. R.; Lienkamp, K.; Tew, G. N. End-Functionalized ROMP Polymers for Biomedical Applications. *Macromolecules* **2010**, *43*, 4557.
149. Ruoslahti, E.; Pierschbacher, M. New perspectives in cell adhesion: RGD and integrins. *Science* **1987**, *238*, 491.
150. Maynard, H. D.; Okada, S. Y.; Grubbs, R. H. Synthesis of Norbornenyl Polymers with Bioactive Oligopeptides by Ring-Opening Metathesis Polymerization. *Macromolecules* **2000**, *33*, 6239.
151. Maynard, H. D.; Okada, S. Y.; Grubbs, R. H. Inhibition of Cell Adhesion to Fibronectin by Oligopeptide-Substituted Polynorbornenes. *J. Am. Chem. Soc.* **2001**, *123*, 1275.
152. Biagini, S. C. G.; Parry, A. L. Investigation into the ROMP copolymerization of peptide- and PEG-functionalized norbornene derivatives. *Journal of Polymer Science Part A: Polymer Chemistry* **2007**, *45*, 3178.
153. Lodge, T. P. Block Copolymers: Past Successes and Future Challenges. *Macromol. Chem. Phys.* **2003**, *204*, 265.
154. Parry, A. L.; Bomans, P. H. H.; Holder, S. J.; Sommerdijk, N. A. J. M.; Biagini, S. C. G. Cryo Electron Tomography Reveals Confined Complex Morphologies of Tripeptide-Containing Amphiphilic Double-Comb Diblock Copolymers. *Angewandte Chemie International Edition* **2008**, *47*, 8859.
155. Förster, S.; Plantenberg, T. From Self-Organizing Polymers to Nanohybrid and Biomaterials. *Angewandte Chemie International Edition* **2002**, *41*, 688.
156. Slugovc, C. In *Olefin Metathesis*; John Wiley & Sons, Inc.: 2014, p 329.
157. Autenrieth, B.; Schrock, R. R. Stereospecific Ring-Opening Metathesis Polymerization (ROMP) of Norbornene and Tetracyclododecene by Mo and W Initiators. *Macromolecules* **2015**, *48*, 2493.
158. Slugovc, C.; Demel, S.; Riegler, S.; Hobisch, J.; Stelzer, F. The Resting State Makes the Difference: The Influence of the Anchor Group in the ROMP of Norbornene Derivatives. *Macromol. Rapid Commun.* **2004**, *25*, 475.

159. Roy, R. K.; Meszynska, A.; Laure, C.; Charles, L.; Verchin, C.; Lutz, J.-F. Design and synthesis of digitally encoded polymers that can be decoded and erased. *Nat Commun* **2015**, *6*.
160. Massad, S. K.; Hawkins, L. D.; Baker, D. C. A series of (2S)-2-O-protected-2-hydroxypropanals (L-lactaldehydes) suitable for use as optically active intermediates. *The Journal of Organic Chemistry* **1983**, *48*, 5180.
161. Zhu, H.; Xu, X.; Cui, W.; Zhang, Y.; Mo, H.; Shen, Y.-M. Synthesis and characterization of well-defined lactic acid–PEG cooligomers and its tricarbonyl rhenium conjugates. *Journal of Polymer Science Part A: Polymer Chemistry* **2011**, *49*, 1745.
162. Leroy, F.; Philippe, M.; Barbarat, P.; Blaise, C.; A61K 8/87 20060101 A61K008/87 ed.; L'OREAL: USA, 2005.